

**DOTTORATO DI RICERCA IN SCIENZE DELLA TERRA**

*Università degli Studi di Firenze*



**SILVIA DANISE**

“Modern and fossil shallow water whale fall communities”

**settore scientifico disciplinare: GEO-01**

**Tutore:** Prof. Simonetta Monechi

**Co-Tutore:** Dr. Stefano Dominici, Dr. Barbara Cavalazzi

**Coordinatore:** Prof. Federico Sani

XXIII CICLO

Firenze, 31 Dicembre 2010



## ABSTRACT

When large whales die and sink to the sea floor provide a huge and concentrated food source to the marine ecosystem. Whale falls are mainly known from the deep sea, both in the modern and in the fossil record, where they host a rich and specialized community similar to those living at other deep sea reducing habitats, like hydrothermal vents and hydrocarbon seeps. On the contrary little is known on what happens in shallow waters.

This study contributes novel data to our knowledge of shallow water whale fall communities (WFC). Fossil whale falls from the Neogene of Italy were studied in detail, together with a modern analogue ecosystem from the North Sea. A multidisciplinary approach was applied to the study of fossil shelfal WFC, based on a variety of tools, ranging from taphonomy to petrography and isotope analysis, to quantitative benthic paleoecology. Results concern different taxonomic groups that took advantage of the large quantity of energy stored in whale tissues, from the microbial consortium at the base of the food web, to benthic macro-invertebrates, to larger pelagic scavengers.

The field excavation of a 10 m long baleen-whale from the Pliocene of Tuscany is at the base of the study. Taphonomy and the position of macrofaunal whale associates with respect to the still articulated bones allowed to reconstruct the main tracts of the ecological succession at the whale fall. Sediment bulk samples collected next to whale bones and from the surrounding sediments were quantitatively analyzed for their mollusc content. Quantitative species-level data on bivalves, gastropods and scaphopods allowed to compare WFC and background communities. A similar approach was applied to the study of the mollusc community associated with a 5 m long minke whale sunk at 125 m depth in the North Sea. To further widen the field of enquiry other twenty-four, more or less complete fossil whales present in Italian museum collections were studied, guided by the experience previously gained during our own field work. The data include taphonomy of fossil bones and qualitative and partial information on the associated fauna. Petrographic microfacies techniques were applied to the study of whale bones. Taphonomy at the microscopic scale was approached through optical and scanning microscopy, Raman spectroscopy and stable isotope geochemistry in order to analyze the signature of microorganisms participating to whale bone degradation, mainly bacteria and fungi, and understand microenvironmental conditions within and around larger bones. Some of the outcrops from which museum specimens had been extracted were studied and sampled to reconstruct local environmental conditions. Bulk samples were analyzed to gather abundance data that were then compared within a larger data set of intertidal to bathyal samples from the literature. As expected, the main factor conditioning the distribution of molluscs around WFC and in other normal settings is water-depth. Absolute depth estimates and considerations based on lithology and paleoecology showed that at least seven whale falls out of twenty-four were located in open shelf settings and possibly associated with high-nutrient conditions.

The general results are consistent with the hypothesis that shallow water whale falls are different from their deep counterparts. On the shelf obligate taxa of families typical of deep sea reducing environments are small-sized and rare, possibly occurring only in offshore settings. The organic input concentrated in a large whale sunken to the bottom becomes food for generalist taxa commonly living on the shelf.

## RIASSUNTO

Una balena che dopo la morte affonda sul fondale marino costituisce un' enorme risorsa di materia organica per l'ecosistema circostante. Le comunità associate alle carcasse di balena ("whale fall communities", WFC) sono note soprattutto nei mari profondi, sia nel fossile che nell'attuale, dove sono caratterizzate da lussureggianti faune altamente specializzate simili a quelle che si trovano in altri ambienti estremi, come le sorgenti idrotermali e le fuoriuscite di metano. Al contrario si hanno poche conoscenze su cosa accade quando una carcassa affonda a basse profondità. In questo studio il record fossile dei misticeti neogenici italiani è stato analizzato per ricostruire la struttura delle WFC in ambiente di piattaforma, oltre ad un analogo attuale situato nel Mare del Nord. E' stato adottato un approccio multidisciplinare, utilizzando mezzi quali la tafonomia, la petrografia, la geochimica degli isotopi stabili fino all'analisi quantitativa delle comunità bentoniche. Di conseguenza i risultati ottenuti riguardano i diversi gruppi tassonomici che sfruttano l'enorme quantità di energia concentrata in una carcassa di balena, dalle comunità microbiche alla base della catena trofica, ai macro-invertebrati bentonici fino agli organismi pelagici come gli squali.

La base di partenza è stato il ritrovamento di un grosso misticete nei depositi marini pliocenici della Toscana. Le informazioni raccolte durante lo scavo riguardanti la tafonomia dello scheletro, ancora ben articolato, e la macrofauna associata alle ossa, hanno permesso di ricostruire le fasi principali della successione ecologica associata alla carcassa. Campioni volumetrici di terreno raccolti nelle immediate vicinanze dello scheletro e nei sedimenti circostanti sono stati analizzati per il loro contenuto di molluschi. I dati ottenuti sulle abbondanze di bivalvi, gasteropodi e scafopodi, hanno permesso di confrontare, a livello specifico la comunità associata alla carcassa con le comunità comunemente presenti sul fondo. Un approccio simile è stato applicato allo studio della comunità a molluschi associata ad una balenottera di 5 metri affondata artificialmente ad una profondità di 125 metri nel Mare del Nord. Lo studio è stato successivamente allargato a ventiquattro esemplari di balene fossili, più o meno completi, presenti nelle collezioni museali Italiane. I dati raccolti riguardano la tafonomia delle ossa e dove possibile informazioni qualitative sulla fauna associata. Le ossa fossili e le concrezioni inglobanti sono state studiate tramite un'analisi delle microfacies al microscopio ottico, e i dati integrati con l'ausilio di microscopia elettronica, Raman e analisi geochimiche degli isotopi stabili del carbonio e dell'ossigeno, in modo da ottenere informazioni sul ruolo svolto da microorganismi, quali funghi e batteri, nella degradazione delle ossa. Gli affioramenti di provenienza di alcuni degli esemplari in esame sono stati studiati in dettaglio e campionati per ricostruire le condizioni paleoambientali in cui le balene erano affondate. I campioni di sedimento sono stati analizzati per il loro contenuto a molluschi e i dati quantitativi ottenuti confrontati con un dataset più grande di campioni, desunti dalla letteratura, che spaziano da ambienti intertidali a batiali. Come previsto, il maggiore fattore che controlla la distribuzione delle comunità a molluschi sia nei campioni provenienti dalle località delle balene che negli altri è la paleo-profondità. La stima delle profondità assolute e altre informazioni ottenute dalla litologia e paleoecologia delle successioni studiate hanno permesso di osservare come almeno sette tra le balene fossili in esame provengono da un ambiente di piattaforma aperta, caratterizzato inoltre da un alto contenuto di nutrienti.

I risultati ottenuti sono concordi con l'ipotesi che le WFC in acque superficiali sono diverse da quelle tipiche degli ambienti profondi. Sulla piattaforma continentale i taxa tipici degli ambienti riducenti profondi sono rari o di piccole dimensioni, e possibilmente presenti solo nella parte più esterna della piattaforma. La grande quantità di materia organica concentrata in una carcassa di balena, sulla piattaforma, viene consumata da organismi generalisti che comunemente vivono nei sedimenti circostanti.

# INDEX

## ABSTRACT

### CHAPTER 1 — General introduction

Premise	1
1.1 Modern whale fall communities	3
1.2 Fossil whale fall communities	5
References	8

### CHAPTER 2 — Molluscs from a shallow water whale fall in the North Atlantic

2.1 Introduction	12
2.2 Study area	13
2.3 Materials and methods	14
2.4 Results	17
2.4.1 Whale fall – background community comparison	17
2.4.2 Trophism	20
2.4.3 Whale fall – methane seep comparison	21
2.5 Discussion	21
2.6 Conclusions	23
References	24

### CHAPTER 3 — Mollusc species at a Pliocene shelf whale fall (Orciano Pisano, Tuscany)

3.1 Introduction	27
3.2 General Setting	28
3.3 Materials and Methods	29
3.3.1 Stratigraphy	29
3.3.2 Sampling and analytical methods	29
3.4 Results	31
3.4.1 Paleocommunity structure	31
3.4.2 Trophic analysis	34
3.5 Discussion	36
3.5.1 General paleoenvironment	36
3.5.2 Whale fall ecological succession	36
3.5.3 Shallow water whale falls	37
3.6 Conclusions	38
References	40
Appendix	43

## **CHAPTER 4 — Taphonomy of Neogene Mediterranean fossil whales**

4.1	Introduction	46
4.2	General setting	48
4.3	Materials and methods	50
4.4	Results	51
	4.4.1 Taphonomy of the Orciano Pisano whale	51
	4.4.2 Other Italian fossil whales	53
4.5	Discussion	60
	4.5.1 Taphonomic pathways at the Orciano Pisano fossil whale	60
	4.5.2 Biostratinomy of shelf-depth fossil whales	60
	4.5.3 The fate of a whale carcass on the shelf	63
	References	65
	Appendix	70

## **CHAPTER 5 — Fossil microbial ecosystems associated with Neogene Italian fossil whales**

### *Fossil microbial ecosystem associated with a Miocene shallow-water whale fall from Northern Italy*

5.1	Introduction	74
5.2	Geological setting	75
5.3	Materials and methods	76
5.4	Results	77
	6.4.1 Fossil bone preservation	77
	6.4.2 Carbonate cements filling cancellous bones	80
	6.4.3 Microborings	82
	6.4.4 Stable isotope analyses	86
5.5	Discussion	86
5.6	Taphonomic model: an hypothesis	90
5.7	Conclusions	90

### *Two more case-studies: the Orciano Pisano and the Castelfiorentino fossil whales*

5.8	Introduction	91
5.9	Results	93
	5.9.1 The Orciano Pisano fossil whale	93
	5.9.1.1 Carbonate cements and fossil bone preservation	93
	5.9.1.2 Microborings	97
	5.9.2 The Castelfiorentino fossil whale	98
	5.9.2.1 Carbonate cements and fossil bone preservation	98
	5.9.2.2 Microborings	101
5.10	Isotope analysis	102
5.11	Discussion	103
5.12	Conclusions	105
	References	106

## **CHAPTER 6 — Whale fall communities, background communities and their controlling factors in the Neogene of Italy**

6.1	Introduction	112
-----	--------------	-----

6.2	Materials and methods	113
6.3	Results	115
	6.3.1 Outcrop evidences at whale-fall sites	115
	6.3.2 Multivariate analysis of bulk samples	122
6.4	Discussion	128
	6.4.1 Clues from sedimentary geology	128
	6.4.2 Environmental factors at whale-fall sites	128
	References	130
	<b>SHORT NOTE — Modern and fossil bathymodiolin mussels from the Mediterranean</b>	132
	References	136
	<b>GENERAL CONCLUSIONS — An ecosystem approach to the fossil record of whale falls</b>	138
	<b>Acknowledgements</b>	141
	<b>APPENDIX CHAPTER 6</b>	
	Appendix 1	143
	Appendix 2	149
	Appendix 3	173
	Appendix 4	178





# CHAPTER 1 — General introduction

---

## Premise

This is a study on modern and fossil marine communities associated with whale carcasses sunken to the sea floor in shallow water settings. Whale fall communities (WFCs) are marine benthic multispecies assemblies relying on the huge amount of organic matter associated with decaying whales, among the largest animals of all times. Present knowledge of WFCs is mainly based on deep water examples, studied in the last twenty years both in the modern and in the fossil record, but shallow marine examples are wanting.

Whales sunk in the deep sea create persistent and ecologically significant habitats that can support a diverse and highly specialized community (Smith 2006). Shark, hagfishes and other scavenging organisms remove flesh and soft tissues (“mobile scavenger stage”), polychaetes, crustaceans and other opportunistic small-sized animals thrive on whale organic remains (“enrichment opportunist stage”), while a long lasting and complex community relies on the hydrogen sulphide and other chemical compounds produced by microbial consumption of the lipid-rich bones (“sulphophilic stage”: Smith and Baco 2003). Whale falls can create thus an unusual chemosynthetic habitat in the deep sea. During the sulphophilic stage chemosynthetic bacteria - free living or in symbiosis within vesicomyids clams, bathymodiolin mussels and vestimentiferan tube worms - are at the base of a food web where organic matter is primarily produced by the oxidation of inorganic compounds, like sulphide, or methane. Chemosynthetic organisms living at whale falls have phylogenetic relationships with those occurring at other deep sea extreme environments, like hydrothermal vents, hydrocarbon seeps and organic wood falls (Baco et al. 1999, Distel et al. 2000), and whale falls could have played a key-role in the diffusion of chemosynthetic fauna among these habitats (“stepping stone hypothesis”: Smith et al. 1989). As an evidence consistent with this hypothesis molecular studies confirm that obligate taxa, specialized to live only at deep water extreme habitats, originated from shallow water ancestors living on organic falls (Distel et al. 2000, Jones et al. 2006, Samadi et al. 2007). Authors have thus looked for whale falls at shallow waters, commonly defined as 0-200 m deep, finding only anecdotal evidences on the course of the ecological succession (Smith 2006). The impact of whale carcasses in shallow water ecosystems is poorly understood and environmental conditions are extremely different respect with those of the deep sea. The sea floor is much more naturally enriched in organic carbon and the organic input given by a whale carcass may represent an insignificant contribution to the nutrient budgets of the continental shelf. However, since whale strandings, and mortality in general, are likely to be concentrated in small areas, in that places dead-whale detritus may play unusual roles in marine ecosystems (Smith 2006). Scanty findings on shelfal whale falls, where obligate taxa like the bone-eating

worm *Osedax* (Glover et al. 2005) and the bathymodiolin mussel *Idas simpsoni* (Warén 1991) have been found, confirm this hypothesis, but are in contradiction with what observed in other extreme reducing habitats. In fact in shallow water hydrocarbon seeps and hydrothermal vents, where ecosystems are fuelled by the same reduced compounds present at whale falls during the sulphophilic stage, obligate taxa are absent (Sahling et al. 2003, Tarasov et al. 2005, Dando 2010). Thus, how are whale fall communities shaped in shallow waters? What taxa are whale-fall obligate on the shelf and how are these related to the sulphophilic stage, the only one comparable to other extreme reducing habitats? Were more data available, would we find more obligate taxa in shallow marine whale falls? How are these related to deep water specialists? Can the fossil record contribute decisive evidence?

Aim of this study is to reconstruct the community structure of shallow water whale falls and to understand which biological and physical factors control their development respect to their deep water counterpart. The exceptional record of fossil whales from the Neogene of Italy, coming mainly from shallow water sediments, is a good chance to investigate the structure of WFCs. A multidisciplinary approach was applied to the analysis of museum specimens and recently excavated fossil whales from northern and central Italy, together with the study of an artificially sunken whale in the North Sea. Part of the study is focused on the analysis of the mollusc community associated with whale falls. Molluscs are among the ecologically dominant groups in whale fall ecosystems (Smith and Baco 2003) and have an excellent fossil record. **Chapter 1** introduces the general issue of whale falls and their associated biota to frame current knowledge, both in the modern and fossil record, from which the present study is based. In **Chapter 2** a species-level study of molluscs associated with a 5 m long minke whale artificially sunk at a depth of 125 m in the Kosterfjord (North Sea, Sweden) is carried out. The WFC was quantitatively compared with the community commonly living in the surrounding soft bottom sediments and with taxa from a methane seep area of the North Sea. A similar approach was used in the study of molluscs associated with a Pliocene fossil whale from Central Italy (Orciano Pisano whale) (**Chapter 3**). The mollusc fauna associated with the fossil, articulated whale fall and the surrounding sediments were bulk sampled to analyse the distribution of species abundances. The paleoecology and the trophism of each taxa was considered and the possible ecological niches associated with the fossil whale fall investigated. In **Chapter 4**, data collected during the opportunely designed excavation of the Orciano Pisano whale, served as template to the taphonomic study of twenty-four museum specimens. Information on the taphonomy of the bones, on the associated biota and on the embedding sediments allowed the reconstruction of the biostratigraphic processes dominating in shallow water environments and influencing the development of whale fall communities. Three fossil whales were selected for high spatial resolution microfacies and biosedimentological analyses through optical and scanning electron microscopy, Raman spectroscopy, and stable C and O isotope geochemistry (**Chapter 5**). Evidence of the microbial ecosystem associated with decaying whale carcasses were provided and the taphonomic processes and diagenetic history of the fossil bones have been better

understood. Finally in seven cases the original outcrop of provenance of the fossil whales was retraced, studied in detail, and bulk sampled for paleodepth and paleoenvironment estimates through statistical multivariate analysis (**Chapter 6**).

## 1.1 Modern whale fall communities

The first WFC was discovered in 1987 at 1240 m depth off California, in the Santa Catalina basin, when a rich high-diversity and high-biomass assemblage associated with a dead whale was found (Smith et al. 1989). Many of the reported species, as vesicomid clams and the extremely abundant mytilid *Idas washingtonia*, contained sulphur-oxidising chemoautotrophic endosymbionts that appeared to feed on sulphide derived from anaerobic decomposition of concentrated bone lipids (Smith et al. 1989, Deming et al. 1997). After this discovery the hypothesis that whale falls could play a role in the dispersal of species dependent on sulphide availability at the deep-sea floor was formulated. In fact, whilst other chemosynthetic habitat, like hydrothermal vents and hydrocarbon seeps are restricted to appropriate geologic settings such as mid-ocean ridges and continental margins, whale-falls may occur anywhere throughout the world's oceans (Smith et al. 1989).

WFCs are intensively sampled throughout the oceans, so data about the species adapted to live on this peculiar habitat are progressively increasing. Literature published so far concerns both whale bones trawled by fishermen, whale skeletons accidentally discovered during oceanographic explorations and carcasses experimentally sunk at different sites and depths. The most studied area is the Pacific Ocean, both on the west and on the east side (Smith et al. 1989, Bennet et al. 1994, Naganuma et al. 1996, Braby et al. 2007, Fujiwara et al. 2007, Lundstend et al. 2010). Two studied site is in the North Atlantic (Dahlgren et al. 2006, Glover et al. 2010), and one in the Sea of Japan (Pavyluk et al 2009). The studied sites range from depth of 30 m to 4037 m and are mostly concentrated in the deep sea. Remarkably no studies exist in the Mediterranean sea, apart from accidental reports of some trawled bones (Warén and Carrozza 1990, Warén 1991, Bolotin et al. 2005).

Time series studies of natural and implanted deep-sea whale falls indicate that bathyal carcasses pass through four stages of ecological succession, lasting up to several decades (Smith et al. 2002). The first is the "mobile-scavenger stage", during which soft tissues are removed from the carcass by dense aggregations of large, active necrophages, as sleeper sharks, hagfishes, amphipods and invertebrate scavengers. Then the "enrichment opportunist stage" starts, during which organically enriched sediments and exposed bones are colonised by dense assemblages of opportunistic polychaetes and crustaceans, with high population densities but low species richness. Among polychaetes the siboglinid worms *Osedax* developed peculiar adaptations to exploit whale-bone lipids. Thanks to a specialized root system *Osedax* species are able to perforate whale bones and invade the bone marrow, exploited then by heterotrophic bacteria housed within the root tissue (Rouse et al. 2004). The third stage is the "sulphophilic stage", in which

the microbial consumption of organic compounds in the lipid-rich bones and in the organically enriched sediment, sustains the production of hydrogen sulphide, which is then utilized by a chemosynthetic community (Smith and Baco 2003). The most common chemosymbiont-bearing bivalves are vesicomid clams and mytilid mussels, subfamily Bathymodioline, but also lucinid, thyasirid and solemyd bivalves have been found in minor amount (Bennet et al. 1994, Smith and Baco 2003, Fujiwara et al. 2007, Braby et al. 2007). Gastropods typical of the sulphophilic stage mainly belong to the family pyropeltids, cocclulinids and provannids (Smith 2006). The fourth stage, called “reef stage”, occurs once all the whale organic material is used up and the whale skeleton serves as hard substratum for suspension feeders exploiting flow enhancement (Smith et al. 2002).

The successional stages involve not only species turnover but also changes in faunal mobility and trophic structure, with temporal overlaps in the onset of characteristic species from different stages. (Smith and Baco 2003). A whale carcass is a complex environment and the succession is not always rigid in time, so that different parts of a carcass might simultaneously go through different succession stages (Goffredi et al. 2004, Braby et al. 2007). Comparisons of whale-fall diversity patterns with those of hydrothermal vents, cold seeps and other deep sea hard substrates show that, in the chemoautotrophic stage, whale assemblages harbour the highest local species richness of any hard substrate in the deep sea. Richness levels approach those of deep-sea soft-sediments and exceed some shallow-water hard-substrates (Baco and Smith 2003). This remarkable species richness may be explained by an unusually large number of trophic types found on whale bones, including species with chemoautotrophic endosymbionts, bacterial grazers, generalized organic-enrichment respondents, whale bones consumers and background hard substrate fauna such as suspension and deposit feeders (Baco and Smith 2003).

Whale bones are extremely rich in lipids, more than 60% lipids by wet weight (Higgs et al. 2011 and references therein). As a consequence the decomposition of bone lipids can provide sulphide to the whale-fall chemoautotrophic community for years to decades (Smith and Baco 2003, Schuller et al. 2004). The microbial sulphate reduction linked to organic carbon degradation is the key process that releases hydrogen sulphide (Allison et al. 1991). As shown in figure 1, once that the bones are skeletonised, sulphate from sea water can diffuse into them, and sulphate reduction by anaerobic bacteria starts, decomposing lipids in the lipid-rich bone core. Then sulphides diffuse outward from the bone core and concentrate both on the external surface of the bones and in the surrounding sediments. Sulphide oxidation and organic-matter synthesis, are carried out by sulphur-oxidising bacteria living on the bone surface (like members of the genus *Beggiatoa*) and within the tissues of vesicomid clams, bathymodiolin mussels and other invertebrates (Deming et al. 1997, Smith and Baco 2003). The sediments beneath and around the carcass are progressively enriched with lipids and other organic compounds (Naganuma et al. 1996, Smith et al. 1998). The organic enrichment causes anoxic conditions in the sediments, due to high microbial oxygen consumption (Allison

et al. 1991), and favours anaerobic processes such as sulphate reduction and methanogenesis (Goffredi et al. 2008). Whale falls can create thus a sedimentary reducing habitat similar to deep-sea cold seeps in terms of sulphide production, but temporally and spatially much more restricted than many seeps. Bones, on the other hand, provide sustained, low emissions of sulphide probably more similar to hydrothermal vent systems (Treude et al. 2009).

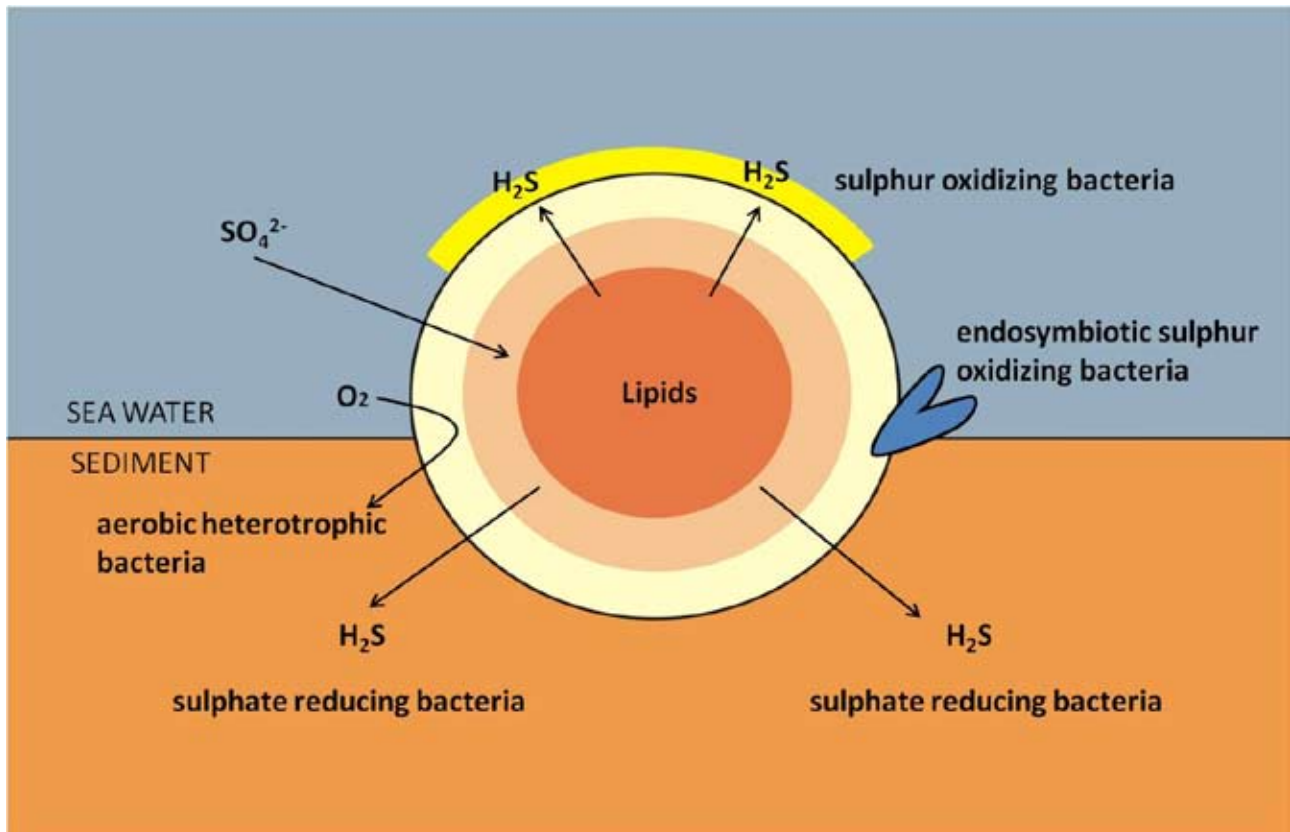


Figure 1. Schematic cross section of a whale vertebra resting at the sea floor during the sulphophilic stage of succession. The predominant decompositional processes occurring within in the bones are illustrated: (1) oxygen consumption by aerobic heterotrophic bacteria degrading whale bone lipids; (2) diffusion of sulphate from sea water into the bone; (3) sulphate reduction by anaerobic bacteria decomposing lipids in the lipid-rich bone core; (4) diffusion of sulphide outward from the bone core; (5) sulphide oxidation, and organic-matter synthesis by sulphur-oxidising bacteria living on the bone surface (e.g. *Beggiota* spp.) and within the tissues of vesicomyid clams and mytilid mussels. Modified from Smith and Baco 2003.

## 1.2 Fossil whale fall communities

WFCs are preferentially recognized in the fossil record by the presence of molluscs associated with the bones, in particular by molluscs that host chemosynthetic bacteria or graze on microbial mat at modern chemosynthetic sites. Fossil WFCs described so far belong to restricted geographical area, notwithstanding fossil cetaceans are known from many fossiliferous localities worldwide (Fordyce 2009). They belong to late Eocene and Oligocene rocks of the

Olympic Peninsula, western Washington State, USA (Squires et al. 1991, Goedert et al. 1995, Nesbitt 2005, Kiel and Goedert 2006, Kiel 2008); from the middle Miocene of California, USA (Pyenson and Haasl 2007) and from the middle Miocene of Hokkaido, Japan (Amano and Little 2005, Amano et al. 2007). All of these specimens come from deep water settings.

The earliest known fossil WFCs belong to the late Eocene and Oligocene and lack the typical vesicomid clams of modern whale falls (Goedert et al. 1995, Kiel and Goedert 2006, Kiel 2008). They are instead characterized by species typical of sulphide-rich sediments, as infaunal thyasirids and lucinids, and bathymodiolin mussels. Kiel and Goedert (2006) hypothesized thus that primitive mysticetes were not large enough or did not contained enough oil to sustain a prolonged emission of sulphide during the breakdown of bone lipids. The species associated to the early whale-falls were instead taking advantage of elevated sulphide levels in the sediments underneath and around the whale carcass, linked to the anaerobic degradation of the whale organic matter material. Kiel and Goedert (2006) called this stage of the ecological succession “chemosymbiotic opportunist” stage, instead of the “sulphophilic stage” of modern whale-falls. The absence of vesicomids at the earliest whale-falls sheds doubt on the hypothesis that whale-falls were evolutionary stepping stones for taxa now inhabit hydrothermal vents and seeps, especially because vesicomids were present at cold-seeps in the same formations (Kiel and Goedert 2006). Mollusc communities resembling modern whale falls were found in middle Miocene sediments of Japan and California, where vesicomid clams of the genus *Calyptogena* and *Vesicomys* occur (Amano and Little 2005, Amano et al. 2007, Pyenson and Hassl 2007). In particular, the finding of vesicomids also on a very small specimen, smaller than the adult individuals of any living mysticete species, partially contradicts the hypothesis of Kiel and Goedert (2006), according to which the origin of modern WFCs was associated with the evolution of extremely large mysticetes, which provided sufficient biomass and oil to sustain the modern complement of whale-fall invertebrates (Pyenson and Hassl 2007).

Chemosynthetic communities have an evolutionary history that goes further back the origin of cetaceans (Taylor and Glover 2000). Mesozoic oceans were inhabited by large marine reptiles, and after the discovery of WFCs scientists have long speculated on the role of mosasaurids, ichthyosaurids or plesiosaurids as benthic islands in the deep sea floor and as stepping stones in the dispersal of chemosynthetic faunas (Martill et al. 1991, 1995; Hogler 1994). Kaim et al. (2008) described for the first time a chemosynthesis-based association on plesiosaurid bones, with the finding of micro-grazing provannid gastropods and ataphrid-like vetigastropods associated with two plesiosaurid skeletons in the upper Cretaceous deposits of Hokkaido, northern Japan. This is the only finding described so far, and no chemosymbiotic bivalves have been found associated with Mesozoic marine reptile bones.

Most recent studies on fossil WFCs focus on the fossil record left by free-living bacteria and archaea at base of the food web, linked to the anaerobic decay of bone lipids (Amano and Little 2005, Kiel 2008, Shapiro and Splanger 2009). Microborings, authigenic pyrite, botryoidal cements, and micropeloids have been described so far from deep water fossil bones and their

enclosing Ca-carbonate concretions (Amano and Little 2005, Amano et al. 2007, Kiel 2008, Shapiro and Splanger 2009). Such features, similar to those found in analogous reducing environment, like fossil hydrocarbon seeps, are interpreted as the product of microbial activity (Shapiro and Splanger 2009). However, the role played by depositional and diagenetic processes in preserving the traces left these microbial ecosystems still remains to be elucidated (e.g., Kiel 2008, Shapiro and Spangler 2009).

## References

- Allison P.A., Smith C.R., Kukert H., Deming J.W. and Bennett B.A. 1991. Deep-water taphonomy of vertebrate carcasses: A whale skeleton in the bathyal Santa Catalina Basin. *Paleobiology* 17, 78–89.
- Amano K. and Little C.T.S. 2005. Miocene whale-fall community from Hokkaido, northern Japan. *Palaeogeography, Palaeoclimatology, Palaeoecology* 215, 345–356.
- Amano K., Little C.T.S. and Inoue K. 2007. A new Miocene whale-fall community from Japan. *Palaeogeography, Palaeoclimatology, Palaeoecology* 247, 236–242.
- Baco A.R. and C.R. Smith. 2003. High biodiversity levels on deep-sea whale skeletons. *Marine Ecology Progress Series* 260, 109–114.
- Bennett B.A., Smith C.R., Glaser B. and Maybaum H.L. 1994. Faunal community structure of a chemoautotrophic assemblage on whale bones in the deep northeast Pacific Ocean. *Marine Ecology Progress Series* 108, 205–223.
- Bolotin J., Hrs-Brenko M., Tutman P., Glavic N., Kožul V., Skaramuca B., Lucic D. and Lucic J. 2005. First record of *Idas simpsoni* (Mollusca: Bivalvia: Mytilidae) in the Adriatic Sea. *Journal of the Marine Biological Association of the UK* 85, 977–978.
- Braby C.E., Rouse G.W., Johnson S.B., Jones W.J. and Vrijenhoek R.C. 2007. Bathymetric and temporal variation among *Osedax* boneworms and associated megafauna on whale-falls in Monterey Bay, California. *Deep-Sea Research I* 54, 1773–1791.
- Dahlgren T.G., Wiklund H., Källström B., Lundälv T., Smith C.R. and Glover A. 2006. A shallow-water whale-fall experiment in the north Atlantic. *Cahiers de Biologie Marine* 47, 385–389.
- Dando P.R. 2010. Biological communities at marine shallow-water vent and seep sites. In: S. Kiel (Ed.), *The Vent and Seep Biota*, Springer, pp. 333–378.
- Danise S., Dominici S. and Betocchi U. 2010. Mollusk species at a Pliocene shelf whale fall (Orciano Pisano, Tuscany). *Palaios* 25, 449–556.
- Deming J.W., Reysenbach A.L., Macko S.A. and Smith C.R. 1997. Evidence for the microbial basis of a chemoautotrophic invertebrate community at a whale fall on the deep seafloor: bone-colonizing bacteria and invertebrate endosymbionts. *Microscopy Research and Technique* 37, 162–170.
- Distel D.L., Baco A.R., Chuang E., Morrill W., Cavanaugh C. and Smith C.R. 2000. Do mussels take wooden steps to deep-sea vents? *Nature* 403, 725–726.
- Dominici S., Cioppi E., Danise S., Betocchi U., Gallai G., Tangocci F., Valleri G. and Monechi S. 2009. Mediterranean fossil whale falls and the adaptation of mollusks to extreme habitats. *Geology* 37, 815–818.
- Fordyce R.E. 2009. Cetacean fossil record. In: Perrin W.F., Würsig B. and Thewissen J.G. (Eds), *Encyclopedia of Marine Mammals*. Academic press. pp. 207–215.
- Fujiwara Y., Kawato M., Yamamoto T., Yamanaka T., Sato-Okoshi W., Noda C., Tsuchida S., Komai T., Cubelio S.S., Sasaki T., Jacobsen K., Kubokawa K., Fujikura K., Maruyama T., Furushima Y., Okoshi K., Miyake H., Miyazaki M., Nogi Y., Yatabe A., and Okutani T. 2007. Three-year investigations into sperm whale-fall ecosystems in Japan. *Marine Ecology* 28, 219–232.



Glover A.G., Kallstrom B., Smith C.R. and Dahlgren T.G. 2005. World-wide whale worms? A new species of *Osedax* from the shallow North Atlantic. *Proceedings of the Royal Society of London, Series B* 272, 2587–2592.

Glover A.G., Higgs N.D., Bagley P.M., Carlsson R., Davies A.G., Kemp K.M., Last K.S., Norling K., Rosenberg R., Wallin K., Källström B. and Dahlgren T.G. 2010. A live video observatory reveals temporal processes at a shelf-depth whale-fall. *Cahiers de Biologie Marine* 51, 375-381.

Goedert J.L., Squires R.L. and Barnes L.G. 1995. Paleocology of whale-fall habitats from deep-water Oligocene rocks, Olympic Peninsula, Washington State. *Palaeogeography, Palaeoclimatology, Palaeoecology* 118, 151–158.

Goffredi S.K., Paull C.K., Fulton-Bennett K., Hurtado L.A. and Vrijenhoek R.C. 2004. Unusual benthic fauna associated with a whale fall in Monterey Canyon, California. *Deep-Sea Research, Part I* 51, 1295–1306.

Goffredi S.K., Wilpiseski R., Lee R. and Orphan V.J. 2008. Temporal evolution of methane cycling and phylogenetic diversity of archaea in sediments from a deep-sea whale-fall in Monterey Canyon, California. *The International Society for Microbial Ecology Journal* 2, 204–220.

Higgs N.D., Little C.T.S. and Glover A.G. 2011. Bones as biofuel: a review of whale bone composition with implications for deep-sea biology and palaeoanthropology. *Proceedings of the Royal Society B* 278, 9–17.

Hogler J. A. 1994. Speculations on the role of marine reptile deadfalls in Mesozoic deep-sea paleoecology. *Palaios* 9, 42–47.

Jones W.J., Won Y.J., Maas P.A.Y., Smith P.J., Lutz R.A. and Vrijenhoek R.C. 2006. Evolution of habitat use by deep-sea mussels. *Marine Biology* 148, 841–851.

Kaim A., Kobayashi Y., Echizenya H., Jenkins R.G. and Tanabe K. 2008. Chemosynthesis based associations on Cretaceous plesiosaurid carcasses. *Acta Palaeontologica Polonica* 53, 97–104.

Kiel S. 2008. Fossil evidence for micro- and macrofaunal utilization of large nektonfalls: examples from early Cenozoic deep-water sediments in Washington State, USA. *Palaeogeography, Palaeoclimatology, Palaeoecology* 267, 161–174.

Kiel S. and Goedert J.L. 2006. Deep-sea food bonanzas: Early Cenozoic whale-fall communities resemble wood-fall rather than seep communities. *Proceedings of the Royal Society B* 273, 2625–2631.

Levin L.A., James D.W., Martin C.M., Rathburn A.E., Harris L.H. and Michener R.H. 2000. Do methane seeps support distinct macrofaunal assemblages? Observations on community structure and nutrition from the northern California slope and shelf. *Marine Ecology Progress Series*, 208, 21–39.

Lundsten L., Paull C.K., Schlining K.L., Mc Gann M., Ussler III W. 2010. Biological characterization of a whale-fall near Vancouver Island, British Columbia, Canada. *Deep Sea Research I* 57, 918–922

Martill D.M., Cruickshank A. R.I. and Taylor M.A. 1991. Dispersal via whale bones. *Nature* 351, 193.

Martill D.M., Cruickshank A. R.I. and Taylor M.A. 1995. Speculations on the role of marine reptile deadfalls in Mesozoic deep-sea paleoecology: comment and replay. *Palaios* 10, 96–97.

Naganuma, T., Wada, H. and Fujioka, K., 1996. Biological community and sediment fatty acids associated with the deep-sea whale skeleton at the Torishima Seamount. *Journal of Oceanography* 52, 1–15.

Nesbitt E.A. 2005. A novel trophic relationship between cassid gastropods and mysticete whale carcasses. *Lethaia* 38, 17–25.

Pavlyuk O.N., Trebukhova Y.A. and Tarasov V.G. 2009. The impact of implanted whale carcass on Nematode communities in shallow water area of Peter the Great Bay (East Sea). *Ocean Science Journal* 44, 181–188.

Pyenson N.D. and Haasl D.M. 2007. Miocene whale-fall from California demonstrates that cetacean size did not determine the evolution of modern whale-fall communities. *Biology Letters (Palaeontology)* 3, 709–711.

Rouse G.W., Goffredi S.K. and Vrijenhoek R.C. 2004. *Osedax*: Bone-eating marine worms with dwarf males. *Science* 305, 668–671.

Sahling H., Galkin S.V., Salyuk A., Greinert J., Foerstel H., Piepenburg D. and Suess E. 2003. Depth-related structure and ecological significance of cold-seep communities—A case study from the Sea of Okhotsk. *Deep-Sea Research Part I* 50, 1391–1409.

Samadi S., Quemere E., Lorion J., Tillier A., Cosel R., Lopez P., Cruaud C., Couloux A. and Boisselier-Dubayle M.-C. 2007. Molecular phylogeny in mytilids supports the wooden steps to deep-sea vents hypothesis. *Comptes Rendus Biologies* 330, 446–456.

Shapiro R.S. and Spangler E. 2009. Bacterial fossil record in whale-falls: Petrographic evidence of microbial sulfate reduction. *Palaeogeography, Palaeoclimatology, Palaeoecology* 274, 196–203.

Schuller D., Kadko D. and Smith C. 2004. Use of <sup>210</sup>Pb/<sup>226</sup>Ra disequilibria in the dating of deep-sea whale falls. *Earth Planet Science Letters* 218, 277–289.

Sahling H., Galkin S.V., Salyuk A., Greinert J., Foerstel H., Piepenburg D. and Suess E. 2003. Depth-related structure and ecological significance of cold-seep communities—a case study from the Sea of Okhotsk. *Deep Sea Research I* 50, 1391–1409.

Smith C.R. 2006. Bigger is better: The role of whales as detritus in marine ecosystems. In: Estes J.(Ed.), *Whales, Whaling and Ocean Ecosystems*. Berkeley, University of California Press. pp. 284–299.

Smith C.R., Kukert H., Wheatcroft R.A., Jumars P.A. and Deming J.W. 1989. Vent fauna on whale remains. *Nature* 341, 27–28.

Smith C.R., Maybaum H.L., Baco A.R., Pope R.H., Carpenter S.D., Yager P.L., Macko S.A. and Deming J.W. 1998. Sediment community structure around a whale skeleton in the deep Northeast Pacific: macrofaunal, microbial and bioturbation effects. *Deep-Sea Research II* 45, 335–364.

Smith C.R., Baco A.R. and Glover A. 2002. Faunal succession on replicate deep-sea whale falls: time scales and vent-seep affinities. *Cahiers de Marine Biologie* 43, 293–297.

Smith C.R. and Baco A.R. 2003. Ecology of whale falls at the deep-sea floor. *Oceanography and Marine Biology Annual Review* 41, 311–354.

Squires R.L., Goedert J.L. and Barnes L.G. 1991. Whale carcasses. *Nature* 349, 574.

Tarasov V.G., Gebruk A.V., Mironov A.N. and Moskalev L.I. 2005. Deep-sea and shallow-water hydrothermal vent communities: Two different phenomena? *Chemical Geology* 224, 5–39.

Taylor J.D. and Glover E.A. 2000. Functional anatomy, chemosymbiosis and evolution of the Lucinidae. In: Harper E.M., Taylor J.D., Crame J.A. (Eds), *The Evolutionary Biology of the Bivalvia*. Geological Society of London Special Publication 177, pp. 207–225.

Treude T., Smith C.R., Wenzhöfer F., Carney E., Bernardino A.F., Hannides A.K., Krüger M. and Boetius A. 2009. Biogeochemistry of a deep-sea whale fall: sulphate reduction, sulfide efflux and methanogenesis. *Marine Ecology Progress Series* 382, 1–21.

Warén A. 1991. New and little known Mollusca from Iceland and Scandinavia. *Sarsia* 76, 53–124.

Warén A. and Carrozza F. 1990. *Idas ghisotti* sp. n., a new mytilid bivalve associated with sunken wood in the Mediterranean. *Bollettino Malacologico* 26, 19–24.

# CHAPTER 2 — Molluscs from a shallow water whale fall in the North Atlantic

---

## 2.1 Introduction\*

The study of modern whale falls is biased toward the deep sea where whale carcasses produce organic-rich “islands” at the food-poor deep-sea floor for extended time periods, supporting highly specialized and diverse assemblage of animals. Some of these animals are restricted to whale falls, including the gutless bone-eating worm *Osedax*, while others are also found at vents and seeps, such as vesicomid clams, bathymodiolin mussels and vestimentiferan tube worms (Smith 2006, Dutilleul et al. 2008). Little is known with regard the ecosystem response in shallow water (<200 m), where the flux of organic carbon to the sea floor in the form of whale detritus makes a much less significant contribution to the nutrient budgets and where primary production is almost always dominated by phototrophy in contrast to chemoautotrophy (Dutilleul et al. 2008, Dando 2010).

Natural whale-falls appear to be rarely encountered on the shelf, possibly due to resurfacing after decomposition (Allison 1991) or because they are easily decomposed by biological activities at relatively higher water temperatures or they are quickly buried in sediments transported from shore (Fujiwara et al. 2007). Artificial sinking of whale carcasses on the shelf and the subsequent monitoring of ecological succession can thus be a useful tool to analyze the changes through time in community structure and to understand the relationships with other shallow and deep-water reducing environments. Time-series studies carried out so far on modern shallow-water whale falls show the presence of some obligate taxa even on the shelf, like the siboglinid worm *Osedax mucofloris* and several new species of dorvilleid polychaetes (Glover et al. 2005, Dahlgren et al. 2006, Wiklund et al. 2009). Low diversity assemblage of nematodes have been also found (Pavlyuk et al. 2009), but no quantitative data are available so far concerning molluscs. Artificial whale falls sunken just below the threshold of 200 m depth (219–254 m: Fujiwara et al. 2007) show a general composition similar to that of deep-water reducing habitats, with a chemosynthesis-based fauna mainly represented by bathymodiolin mussels.

Here we present a species-level study of molluscs associated with a 5 m long minke whale (*Balaenoptera acutorostrata*) experimentally implanted at a depth of 125 m in the Kosterfjord (Skagerrak, Sweden). Our sampling was carried out five years after the implantation of the carcass. Time series studies carried out previously at the same site have

---

\* This study is in collaboration with Thomas Dahlgren (Department of Zoology, Göteborg University, Göteborg, Sweden; current address: Uni Environment, Bergen, Norway) and Adrian Glover (Zoology Department, The Natural History Museum, London, United Kingdom).

shown that within five weeks of implantation the Atlantic hagfish (*Myxine glutinosa*), sharks and other scavenging organisms consumed the flesh and exposed the bones, and the carcass was completely skeletonised after six months on the sea floor (Dahlgren et al. 2006). Nine months after sinking the bones were colonized by *Osedax mucofloris*, the first species of *Osedax* known from a shelf-depth whale-fall, and the first from the Atlantic Ocean (Glover et al. 2005, Dahlgren et al. 2006). In this study we also compare the collected samples from the whale fall and the surrounding sediments with quantitative data measured by Dando et al. (1994) from a methane seep area in the Skagerrak.

Our primary objective was to analyze the community structure of the sediment dwelling mollusc fauna associated with a shallow-water whale-fall. Secondly our aim was to evaluate the differences in taxonomic composition and community structure of the whale fall community with the surrounding background community and with the macrofaunal community related to a different ephemeral, sulphide-rich habitat in the same area.

## 2.2 Study area

The Kosterfjord is situated in the north eastern part of the Skagerrak, the major gateway between the north Atlantic and the Baltic Sea. It is a 250 meter deep, 62 km long, submarine trench parallel to the coastline of Sweden to the east and sheltered by the Koster islands to the west (Figure 1). The trench is a fault fissure connected with the north-west to the Norwegian Trough which in turn is connected to the deep North Atlantic. As a consequence of its connection

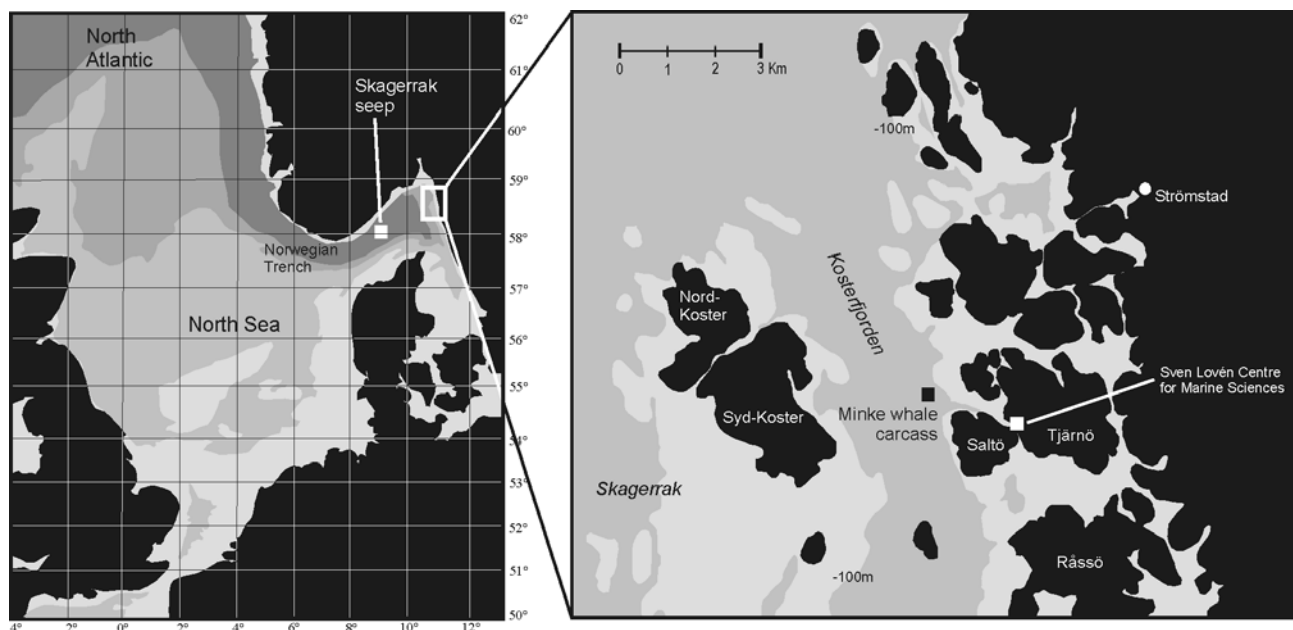


**Figure 1.** Map of the North Sea, showing the methane seep in the Skagerrak, and the location of the experimental Kosterfjord whale-fall site, next to the Sven Lovén Centre for Marine Sciences. Modified from Dahlgren et al. 2006.

with the North Atlantic the Kosterfjord is not a fjord in its proper meaning, because of the prevailing of marine conditions, i.e. high salinity (Palm et al. 2004).

The Skagerrak sedimentary environment is characterized by muddy bottoms and a high content of organic material (about 2% of organic carbon), with sedimentation rates in the Northern sector of 0.20 cm/year (Josefson 1985, Van Weering et al. 1987). The overall oceanographic regime is driven by a counter clockwise circulation pattern, where dense, saline (30–35 psu) and oxygenated oceanic water underflows the more brackish (8–30 psu) surface water outflow of the Baltic Sea. The main surface currents entering the area are the Jutland Current from the North Sea (south-west) and the Baltic Current from south-east. The mixing between these two currents forms the Norwegian Coastal Current, with a predominating northern heading, which flows out of the Skagerrak on the Norwegian side. This surface circulation is compensated by a deep counter current that brings the saline Atlantic water through the 700 m deep Norwegian Trench into the Skagerrak (Whissak 2005). However, the temperature and salinity of the surface waters are subject to strong seasonal fluctuations; in deeper waters the fluctuation is present with lower amplitude. Measurements of bottom water temperature at 125 m depth in the Kosterfjord indicate only small variations during the year of 4.8–7.5 °C, with salinity 34.3–34.7 psu.

## 2.3 Materials and methods

For the present study four sediment samples (W1, B1, B2, B3) were collected and analyzed for their mollusc composition. Sample W1 was taken in May 2008 from the minke whale skeleton (125 m depth), samples B1, B2 and B3 (background samples) were collected in January 2009 at the same depth but at a distance from whale bones, respectively 18 m South, 13 and 55 m North from the whale. Sampling at the whale fall was conducted with a ROV (Remotely Operated Vehicle) equipped with a forward-mounted sampling scoop (16 cm long, diameter of 8,4 cm). We used the latter to collect soft sediments close to the bones and we stored them in a sample basket (size of the sample basket: 34X26.5X25 cm, volume of collected sediment: 4420 cm<sup>3</sup>). Background sediments were collected using a Van Veen grab, able to sample 0.1 m<sup>2</sup> of sediments

**Table 1. Basic data for the studied samples.**

Sample	Name	Volume	Depth	Latitude	Longitude	Distance from the whale	Sampling date	References
		(cm <sup>3</sup> )	(m)	(N)	(E)	(m)		
Kosterfjord whale fall	W1	4420	125	58° 52,968'	11° 05,728'	0	May 2008	This study
Kost. backgorund sediments	B1	15500	125	58° 52,963'	11° 05,719'	18	January 2009	This study
Kost. backgorund sediments	B2	15500	125	58° 52,973'	11° 05,725'	13	January 2009	This study
Kost. backgorund sediments	B3	15500	126	58° 52,991'	11° 05,705'	55	January 2009	This study
Skagerrak seep	SEEP	50x50 cm <sup>2</sup>	330	58° 1.3'	9° 34.6' E	–	July 1991	Dando et al. 1994
Seep background sediments	NON-SEEP	50x50 cm <sup>2</sup>	330	58° 1.3'	9° 34.6' E	–	July 1991	Dando et al. 1994

(volume 1.5 litres), and that would have penetrated the bottom sediments on average 5 cm (Table 1). The ROV was equipped with digital video and with digital still cameras.

The sediment samples were wet sieved through a 0.5 mm screen and preserved in a solution with ethanol ( $\approx 80\%$ ) before identification. The residue was washed with hydrogen peroxide and sorted under a binocular microscope for all recognizable hard shelled biogenic components. The latter includes molluscs, serpulids, echinoids, bryozoans, decapods, ostracods, brachiopods, fishes and whale bone fragments. Molluscs were determined at the species level and used for quantitative comparisons. Both live and dead specimens have been included. Bivalve number was counted as the highest number of right or left valves and half of the remaining, the latter roughly corresponding to the number of unmatchable valves. Gastropods were equated to the number of apices. Used nomenclature follows Hansson (1998).

The Kosterfjord dataset, including 1.575 specimens belonging to 45 mollusc species forms the basis for sample diversity study and trophic structure analysis. Diversity indices were calculated for each sample. Each diversity index provides different information on the community structure. The Simpson index is affected by the 2-3 most abundant species and represents the probability that 2 individuals chosen at random from a sample belong to the same species (Hayek and Buzas 1997). Shannon's index ( $H$ ) provides a measure of uncertainty in the identity of an individual pulled randomly from a sample (Hayek and Buzas 1997), with low  $H$  indicating a fairly high certainty of outcome (i.e. low diversity).  $H$  is thus insensitive to rare (especially singleton) species. Fisher's  $\alpha$  is a number close to that of species expected to be represented by only a single (i.e. rare) individual (Hayek and Buzas 1997).

The four samples ( $n=1575$ ) were used for trophic analysis. Seven trophic categories are distinguished consistently following the Molluscan Life Habits Databases (Todd 2000), using abbreviations appropriate for the present study: chemosymbiotic deposit feeders (DC), suspension feeders (SU), subsurface deposit feeders (DU), surface deposit feeder (DS), herbivores, including herbivores on fine-grained substrates, herbivores on rock, rubble or coral substrates and herbivores on plant or algal substrates (HE) and predatory carnivores, including scavengers (CP). Comparisons were expressed through percent of number of specimens ( $n$ , abundance) and number of species ( $S$ , richness) for each category.

Two quantitative samples from the literature were added to the Kosterfjord dataset for multivariate analysis. They were collected in the Skagerrak area at 330 m depth by Dando et al. (1994). One is from a methane seep (called here "SEEP" sample) and the other is from the seep background sediments (called here "NON-SEEP" sample) (Dando et al. 1994). The combined dataset, which includes the Kosterfjord and the Skagerrak seep-non seep samples, consists of 3.744 specimens and 47 taxa (Table 2). From this dataset species occurring in only one sample were removed and abundances square-root transformed to de-emphasize the influence of the most abundant taxa. Percentage data were used for statistical analysis because differing volumes of sediment were sampled and the absolute numbers of individuals are not comparable between samples (Clarke and Warwick, 1994). A matrix of similarity was calculated with the

**Table 2. Quantitative species composition of the studied samples and trophism category of each species. For trophic categories abbreviations see text (material and methods section). The SEEP and NON-SEEP samples are from Dando et al. 1994.**

FAMILY	SPECIES	W1	B1	B2	B3	SEEP	NON-SEEP	TROPHISM
Lottidae	<i>Testudinalia testudinalis</i>	0	0	5	1	0	0	HE
Lepetidae	<i>cf. Lepeta caeca</i>	0	0	6	0	0	0	HE
Fissurellidae	<i>Emarginula fissura</i>	0	1	3	0	0	0	HE
Fissurellidae	<i>Puncturella noachina</i>	0	0	4	2	0	0	HE
Trochidae	<i>Jujubinus miliaris</i>	0	0	3	0	0	0	HE
Rissoidae	<i>Rissoa lilacina</i>	2	0	0	0	0	0	HE
Rissoidae	<i>Alvania punctura</i>	10	0	0	1	0	0	HE
Rissoidae	<i>Alvania subsoluta</i>	0	0	2	0	0	0	HE
Rissoidae	<i>Pusillina sarsii</i>	19	0	0	0	0	0	HE
Iravadiidae	<i>Hyalia vitrea</i>	0	0	2	2	0	0	HE
Cerithiidae	<i>Bittium reticulatum</i>	0	0	1	2	0	0	HE
Turritellidae	<i>Turritella cf. communis</i>	2	0	0	0	0	0	SU
Littorinidae	<i>Littorina sp.</i>	0	0	1	1	0	0	HE
Littorinidae	<i>Littorina saxatilis</i>	0	0	1	0	0	0	HE
Capulidae	<i>Capulus hungaricus</i>	1	0	0	0	0	0	SU
Naticidae	indet.	0	0	0	4	0	0	CP
Cylichnidae	<i>Cylichna cylindracea</i>	13	2	0	2	0	0	CP
Nuculidae	<i>Nucula sulcata</i>	4	23	16	21	0	0	DU
Nuculidae	<i>Ennucula tenuis</i>	24	49	44	57	0	0	DU
Nuculidae	<i>Nucula sp.1</i>	0	0	1	0	0	0	DU
Nuculidae	<i>Nucula sp.2</i>	0	0	0	0	33	0	DU
Nuculanidae	<i>Nuculana pernula</i>	1	6	14	25	0	0	DU
Nuculanidae	<i>Nuculana minuta</i>	4	4	15	14	0	0	DU
Yoldiidae	<i>Yoldiella cf. philippiana</i>	9	30	83	61	0	0	DU
Mytilidae	<i>Mytilus edulis</i>	25	5	4	6	0	0	SU
Mytilidae	<i>Musculus cf. discors</i>	5	0	0	0	0	0	SU
Ostreidae	<i>Ostrea sp.</i>	0	0	1	0	0	0	SU
Pectinidae	<i>Pdseudamussium septemradiatum</i>	0	0	3	1	0	0	SU
Pectinidae	<i>Palliolium striatum</i>	0	2	3	4	0	0	SU
Pectinidae	<i>Delectopecten vitreus</i>	0	0	3	1	0	0	SU
Pectinidae	indet.1	0	0	0	2	0	0	SU
Pectinidae	indet.2	0	0	0	2	0	0	SU
Pectinidae	indet.3	0	0	5	0	0	0	SU
Anomiidae	<i>Anomia ephippium</i>	0	0	13	5	0	0	SU
Thyasiridae	<i>Thyasira sarsi</i>	262	0	0	0	133	0	DC
Thyasiridae	<i>Thyasira equalis</i>	0	128	88	106	300	750	DC
Thyasiridae	<i>Axinulus eumiaris</i>	0	0	0	0	0	83	SU
Montacutidae	<i>Tellymia ferruginosa</i>	41	3	3	0	0	0	SU
Astartidae	<i>Astarte sulcata</i>	0	0	0	3	0	0	SU
Astartidae	<i>Astarte sp.</i>	0	0	2	0	0	0	SU
Cardiidae	<i>Parvicardium minimum</i>	3	12	12	8	0	0	SU
Hiatellidae	<i>Hiatella arctica</i>	3	0	5	0	0	0	SU
Semelidae	<i>Abra nitida</i>	83	30	38	45	567	303	DS
Cuspidariidae	<i>Cuspidaria cf. cuspidata</i>	0	1	0	0	0	0	CP
Dentaliidae	<i>Antalis entalis</i>	0	0	2	1	0	0	DU
Dentaliidae	indet.	1	1	0	2	0	0	DU
Entalinidae	<i>Entalina quinquangularis</i>	0	0	2	2	0	0	DU
	<b>TOTAL</b>	<b>512</b>	<b>297</b>	<b>385</b>	<b>381</b>	<b>1033</b>	<b>1136</b>	<b>3744</b>



Bray–Curtis coefficient, commonly used in ecological studies (Clarke and Warwick 1994). Non-metric multidimensional scaling (NMDS; Clarke and Warwick 1994), one of the best ordination techniques available in ecological analyses (Kenkel and Orłóci 1986, Clarke and Warwick, 1994), was used to analyze the dataset, and a map of the samples was produced wherein points that plot close together represent samples that are very similar in taxonomic composition. Diversity indices and NMDS analysis were performed with the software PAST (Hammer et al. 2001).

## 2.4 Results

### 2.4.1 Whale fall – background community comparison

During the ROV survey at the whale fall site, five years after implantation, the skull, one mandible and some ribs were still visible on the sea floor. No macro-invertebrates were seen lying directly over or around the bones, which were found to be densely covered in a coat of blackish sulphides and/or muddy sediments (Figure 2A). Algal debris were trapped within the bones (*e.g. Fucus serratus*) and the decapod *Hyas araneus* was frequently observed close to the skeleton (Figure 2B). Bones were highly bioeroded and specimens of the bone eating worm *Osedax mucofloris* were recorded living on collected bone samples.

The sieving residue includes molluscs, regular and irregular echinoids (*Brissopsis lyrifera* and *Spatangus purpureus*), brachiopods (*Crania* sp. and terebratulids), benthic foraminifers, ostracods, serpulids, bryozoans, decapods, fish fragments and teeth, and myxinid dental plates.

Sample W1 is dominated by the bivalve *Thyasira sarsi* (51% of the total), followed by *Abra nitida* (16.2%), *Tellymia ferruginosa* (8%), *Mytilus edulis* (4.9%) and the nuculanid *Ennucula tenuis* (4.7%) (Figure 3). Among the gastropods the most abundant are *Pusillina sarsii* (3.7%), *Cylichna cylindracea* (2.5%) and *Alvania punctura* (2%). Specimens of *Thyasira sarsi* (Figure 4A), *Abra nitida* (Figure 4B) and *Mytilus edulis* were observed alive during sieving operations, for the others no certain information are available. Juveniles of *Mytilus edulis* were directly attached by byssus to bone fragments. *Thyasira equalis* is the most abundant species in B1, B2 and B3, accounting respectively for the 43.1%, 22.9% and 27.8% of the total (Figure 3). *Thyasira sarsi* is absent from the background samples, whereas *T. equalis* was not found in the sediments associated with the whale fall. Besides *T. equalis*, the background samples contain many protobranchiate bivalves, such as *Ennucula tenuis*, *Yoldiella philippiana*, *Nucula sulcata*, *Nuculana minuta* and *N. pernula* (Figure 3). The semelid *Abra nitida* and the cardiid *Parvicardium minimum* are represented in significant quantities in the background sediments.

The Simpson index of Dominance and the Shannon-Wiener index indicate that W1 has the highest dominance and the lowest diversity. B2 and B3 instead have the highest evenness, as also shown by the Fisher's  $\alpha$  index. B2 and B3 have the highest values of Fisher's  $\alpha$ , they have in fact a higher number of rare species (singletons and doubletons) in respect to the other two samples. B1, the sample with the lower number of individuals, has intermediate values (Table 3).

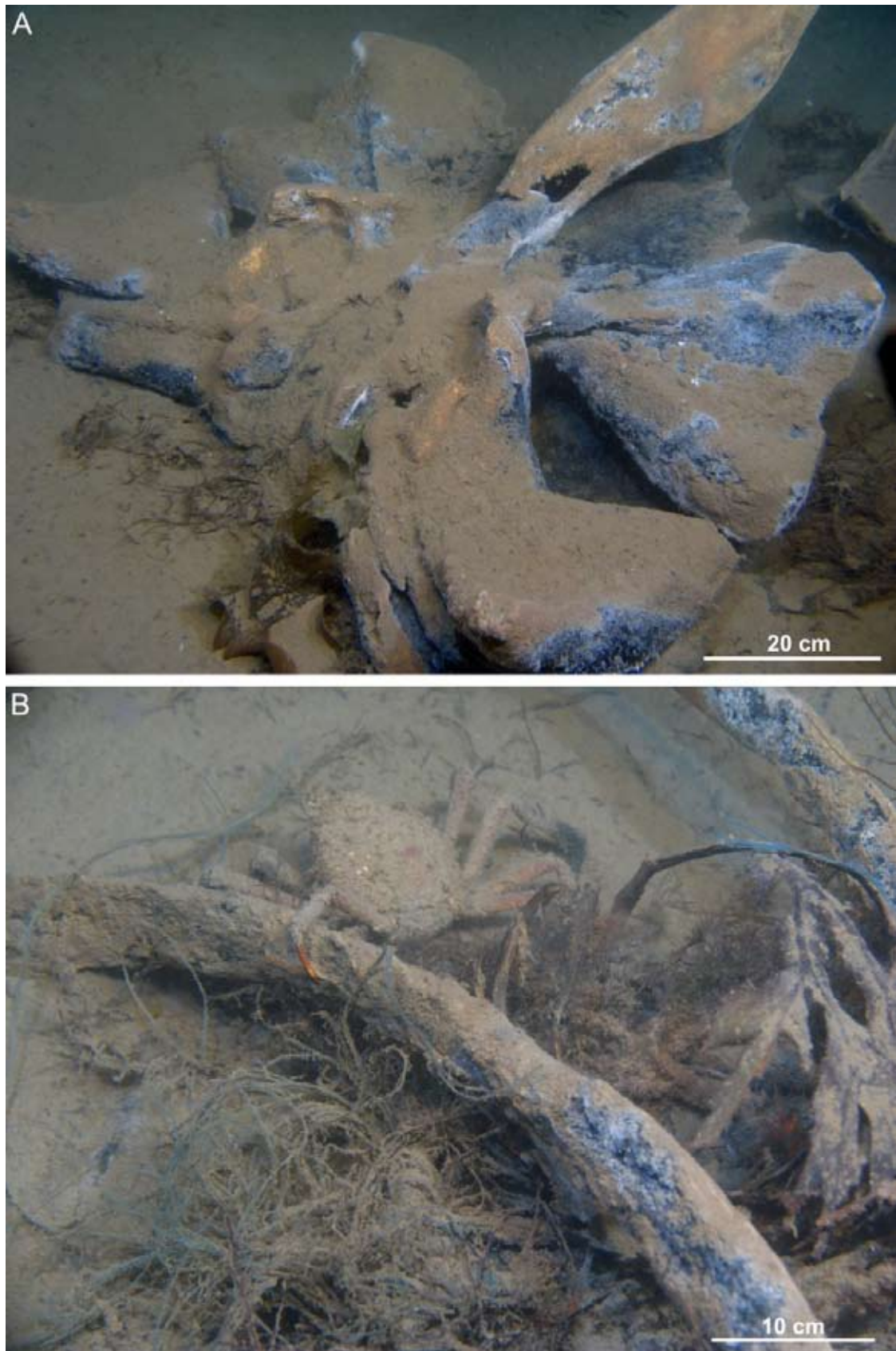


Figure 2. Remotely operated vehicle (ROV) video stills showing the minke whale skeleton 5 years after implantation. A. Minke whale skull covered by muddy sediment and sulphides. B. Minke whale ribs partially covered by sediments and sulphides, showing signs of intense bioerosion. The decapod *Hyas araneus* in the upper part of the figure, algal debris (*Fucus serratus* on the right) trapped within whale bones.

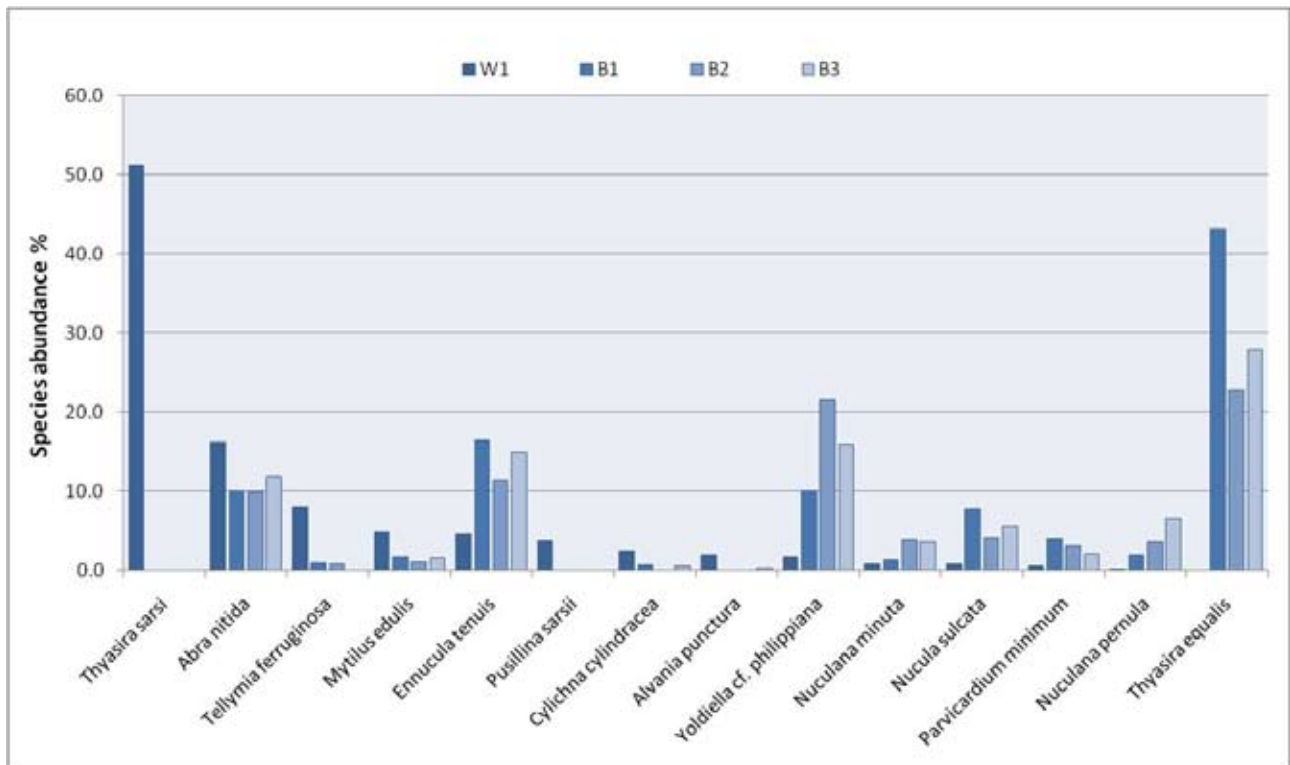


Figure 3. Abundances (%) of the quantitatively important species (>2%) in each of the four samples (W1, B1, B2, B3).

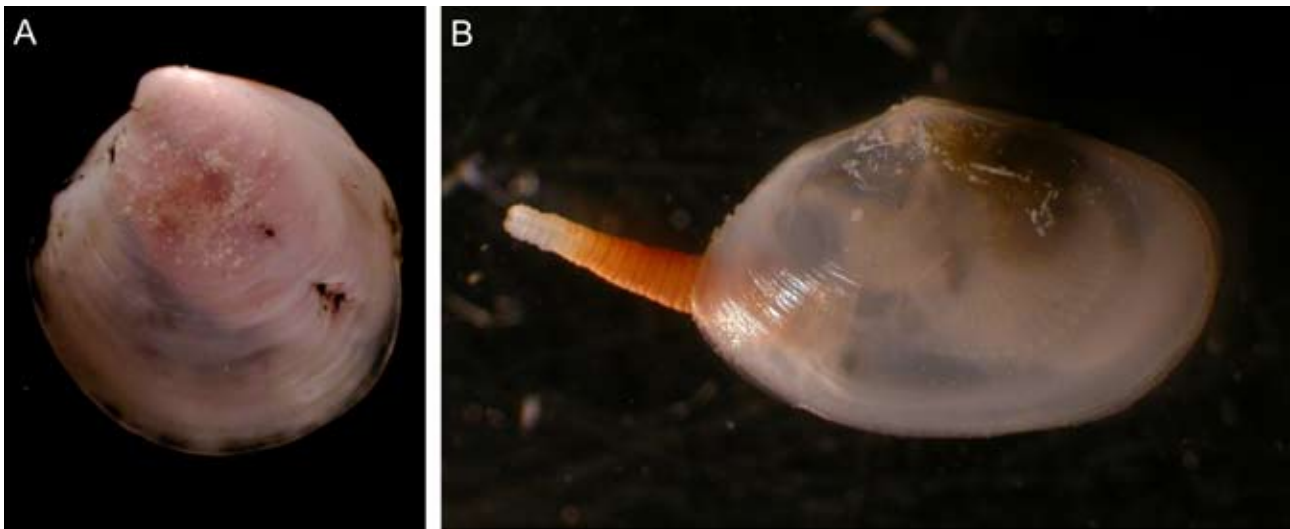


Figure 4. Living specimens of *Thyasira sarsi* (A) and *Abra nitida* (B) from the whale fall sample (W1).

Table 3. Species abundance, number of individuals and diversity indices of the studied samples.

Sample	N° of species	N° of individuals	Simpson index of Dominance (D)	Shannon-Wiener index (S)	Fisher's $\alpha$ index ( $\alpha$ )
W1	19	512	0.3022	1.755	3.887
B1	15	297	0.2421	1.828	3.332
B2	31	385	0.1297	2.516	7.947
B3	27	381	0.1495	2.297	6.638
SEEP	4	1033	0.4032	1.062	0.5277
NON-SEEP	3	1136	0.5124	0.8178	0.3741

## 2.4.2 Trophism

The two predominant thyasirids, *T. sarsi* (W1) and *T. equalis* (B1, B2, and B3), are infaunal chemosymbiotic deposit feeders, containing symbiotic sulphur-oxidizing bacteria in their gill tissue (Southward 1986). Studies on the nutritional dependence of the two bivalves on chemoautotrophic symbiotic bacteria show that *T. equalis* has fewer symbiotic bacteria in its gills compared to *T. sarsi*, indicating that the nutritional importance of carbon fixed by the bacteria is less in *T. equalis* (Dando and Spiro 1993, Dufour 2005). Chemosymbiotic taxa, as a trophic group, have the higher abundance in all the four samples, but the lower species richness (Figure 5). Like chemosymbiotic deposit feeders, surface deposit feeders have a high overall abundance but a low species richness, being represented by only one species, the semelid *Abra nitida*, which is more abundant in W1 than in the background community. Subsurface deposit feeders (nuculids, nuculanids, yoldiids and dentaliids) are abundant and diverse in B1, B2 and B3 (38%, 46% and 47.9% respectively), whereas in W1 occur the same species but with a lower abundance (8.4%). Suspension feeders have a high species richness, both in the whale fall and in the background fauna. The mytilids (*Mytilus edulis* and *Musculus discors*) and the montacutid *Tellymia feruginosa*, occur in W1, whereas pectinids, anomiiids and cardiids are typical of B1, B2 and B3. Herbivores are diverse but rare in all samples. Those associated with the whale fall, as the rissoids *Rissoa violacea*, *Alvania punctura*, and *Pusillina sarsii*, are typical of shallower settings where they are associated to algae (*Laminaria*) and seagrass (*Zostera*) (Warén 1996).

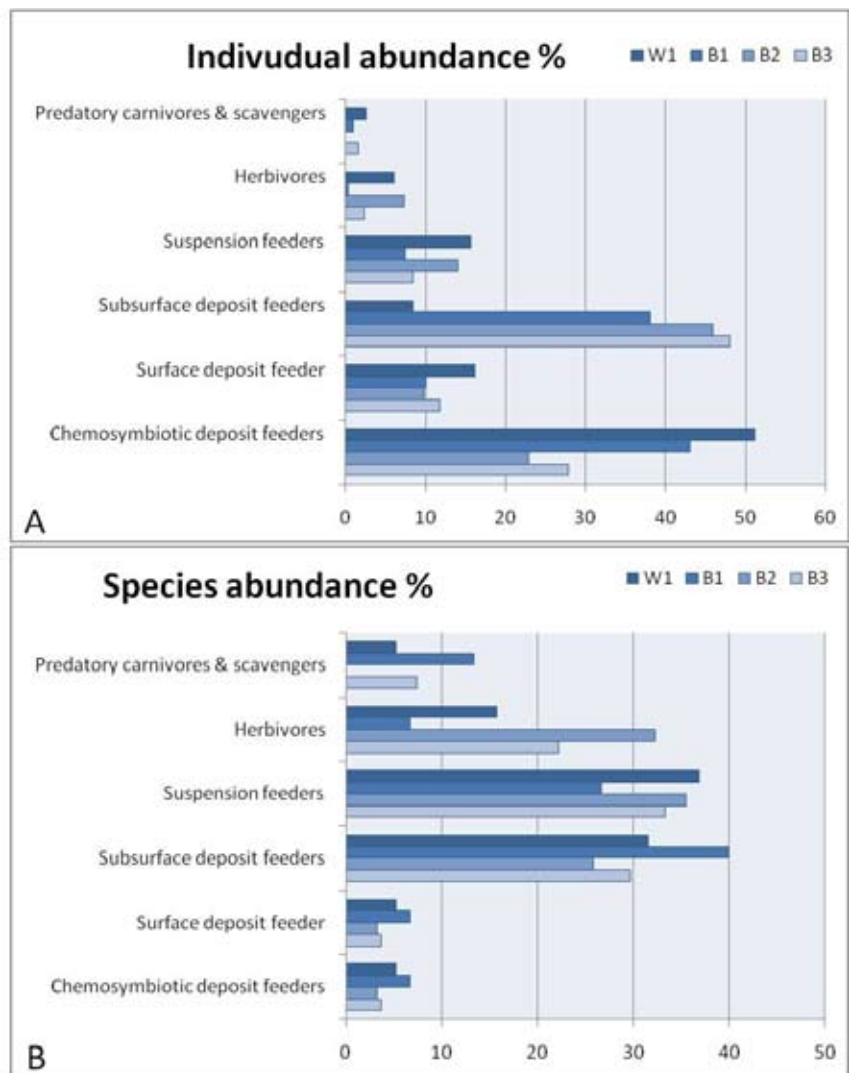
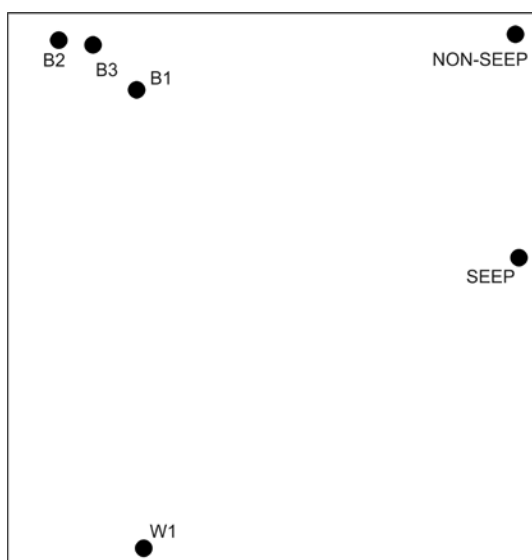


Figure 5. Trophic analysis expressed through percent of number of individuals (abundance) and number of species (richness). Trophic categories: chemosymbiotic deposit feeders, suspension feeders, subsurface deposit feeders, surface deposit feeder, herbivores and predatory carnivores, including scavengers.

Carnivores are the least represented among trophic categories, the only carnivore in the whale fall sample being the burrowing *Cylichna cylindracea*.

### 2.4.3 Whale fall – methane seep comparison

The two samples included for multivariate analysis, one from a methane seep (SEEP sample) in the Skagerrak and the other from its surrounding sediments (NON-SEEP samples), are characterized by low diversity and high dominance (Table 2, 3). The SEEP sample contains four species: *Abra nitida* (55%), *Thyasira equalis* (29%), *T. sarsi* (12.9%) and *Nucula sp.* (3.2%). The NON-SEEP sample contains three species: *T. equalis* (66%), *Abra nitida* (26.7%) and *Axinulus eumiaris* (7.3%) (Table 3). In the plot resulting from NMDS analysis the six samples of the combined



dataset form an irregular quadrilateral (Figure 6). B1, B2 and B3 group together and are on the same side of the diagram than NON-SEEP sample; W1 rests in the lower part of the diagram, at the same distance from B1, B2, B3 and the SEEP sample. A depth gradient follows the direction of the horizontal axis of the diagram, with shallower sites on the left side, represented by the whale fall and the background samples, and the deeper seep sites on the right. The vertical axis, on the other hand, corresponds to an oxygenation gradient, with samples from reducing soft bottoms in the lower part of the diagram and normal bottoms at the top.

Figure 6. Multidimensional scaling ordination of samples belonging to the whale fall (W1), the whale-fall background sediments (B1, B2 and B3), the Skagerrak seep site (SEEP) and the seep background sediments (NON-SEEP).

## 2.5 Discussion

The quantitative analysis of the Kosterfjord samples shows that the presence of the minke whale carcass on the sea floor still influences the community structure five years after its implantation. Although many species are shared between the whale fall and the background community, with changes in their relative abundance, the whale fall community clearly shows a lower diversity in its species composition, with the dominance of the chemosymbiotic bivalve *Thyasira sarsi*. The high abundance of *T. sarsi* in the sediments associated with the skeleton suggests that the Kosterfjord whale fall has reached a sulphophilic stage of the ecological succession (Smith et al. 2002). Specialized whale-fall forms, such as bathymodiolin mussels and vesicomysids clams, were not recovered during the survey, although the presence of the bathymodiolin *Idas simpsoni* has been previously reported in the North Sea even at shallow depth (Warén 1991).

The species *T. sarsi* is generally found in association with organic rich sediments with high total sulphide concentrations and is widely distributed in the NE Atlantic (Dando and Southward 1986). In the North Sea and in the Skagerrak *T. sarsi* is found at sewage-polluted fjords and active methane seeps (Dando et al. 1991, Dando and Spiro 1993, Dando et al. 1994), with a depth range of 50-340 m (Dufour 2005). On the other hand, the dominant species in the background sediments, *T. equalis*, is the most common thyasirid on the North European continental shelf, and is able to survive in less organic-rich sediments than *T. sarsi* (Dando and Southward 1986).

The opportunist species *Abra nitida*, common along the Northern part of the Swedish west coast, is a density dependent species normally occurring in turbid environments (Josefson 1982). Its high abundance at the whale fall site can be linked to the high organic sediment content, as observed in fish farm areas with increased food supply (Kutti et al. 2008). The abundance of *Tellymia feruginosa* in the whale fall sample, a small bivalve that typically lives symbiotically in the burrow of the echinoid *Echinocardium cordatum* (Gillan and De Ridder 1997), is an indirect evidence of the presence of the echinoid itself, not found during this study. *Echinocardium cordatum*, burrowing below or at the level of the oxidized-reduced interface and ingesting both surface and deep reduced sediments, hosts ectosymbiotic sulphide-oxidizing bacteria, *Thyothrix* like, in its intestinal caecum. This symbiosis opens an access for *E. cordatum* to sulphide rich habitats (Temara et al. 1993, Brigmon and De Ridder 1998) and adds further evidence to the presence of a chemosynthetic ecological niche at this shallow water whale fall site (Bromely et al. 1995).

Both the whale fall and the surrounding sediment communities record the presence of species typical of shallower water settings, probably transported down-slope by bottom currents, as the mytilids *Mytilus edulis* and *Musculus cf. discors* and littorinid gastropods. However it is worth noting that juvenile specimens of *Mytilus edulis* were found directly attached to the bones by byssus. Rissoids, which are known to live commonly on sea weeds, are much more abundant at the whale fall than in the background samples. They could have been transported together with drifting algae and concentrated around the bones, which acted as obstacle for near bottom currents. However, rissoids are occasionally found at deep water wood-falls (Warén, personal communication), and at relatively shallow vents (~550m) in the North Atlantic (Schander et al. 2010). The species associated with the Kosterfjord whale fall could have fed directly on the bacterial mat covering the bones, as hypothesized for those found associated with *Beggiatoa*-like bacteria at hydrothermal vents (Schander et al. 2010).

Judging from our limited data set, a methane seep area of the Skagerrak is dominated by the same species as the Kosterfjord whale fall community: the seepage zone with high dissolved sulphide hosts the bivalve *T. sarsi*, whereas the surrounding sediments, with a lower sulphide concentration, host the congeneric *T. equalis*. Despite the species overlap between taxa hosting chemoautotrophic endosymbionts, the whale fall and the seep samples differ by their species richness, the methane seep community being characterized by a very low number of mollusc

species. The higher species richness at the whale fall site can be related both to the higher habitat complexity encountered around whale falls (Smith and Baco 2003) and to the presence of drifted taxa from shallower areas.

Our analysis of patterns of chemosynthesis and habitat specialization in the molluscs of the Kosterfjord whale fall is in agreement with data available from the fossil record. In a Pliocene whale fall from an outer shelf setting, the sulphophilic stage was characterized by lucinids, which are generalist chemosymbiotic molluscs that occupy a broad range of reducing habitats from deep- to shallow-water settings (Taylor and Glover 2006) and by rare bathymodiolins (Dominici et al. 2009, Danise et al. 2010: CHAPTER 3). Similarly, in the Kosterfjord, no obligate molluscs were found in sediments associated with whale bones. The Pliocene and the Kosterfjord examples suggest thus that shallow-water whale fall communities differ from those of the deep sea for the absence of trophic specialization among infaunal molluscs, as observed for hydrothermal vent and seep shallow water macrofaunal assemblages (Levin et al. 2000, Sahling et al. 2003, Tarasov 2005).

## 2.6 Conclusions

According to the Kosterfjord study, in which we report for the first time the mollusc composition of a whale-fall community on a modern shelf, we can conclude that the organic rich sediments around whale bones are not a different habitat in respect to other shallow water reducing environments. This is in contrast with the observations of a specialized fauna found on the whale bones raising on the sea floor, including the bone eating worm *Osedax mucofloris* and dorvilleid polychaetes.

## References

- Brigmon R.L. and De Ridder C. 1998. Symbiotic Relationship of *Thiothrix* spp. with an Echinoderm. *Applied and Environmental Microbiology* 64, 3491–3495.
- Bromley R.G., Jensen M. and Asgaard U. 1995. Spatangoid echinoids: deep-tier trace fossils and chemosymbiosis. *Neues Jahrbuch für Geologie und Paläontologie, Abhandlungen* 195, 25–35.
- Clarke K.R. and Warwick R.M. 1994. Changes in marine communities: An approach to statistical analysis and interpretation. Plymouth Marine Laboratory, Plymouth, UK, p 144.
- Dahlgren T.G., Wiklund H., Källström B., Lundälv T., Smith C.R. and Glover A. 2006. A shallow-water whale-fall experiment in the North Atlantic. *Cahiers de Biologie Marine* 47, 385–389.
- Dando P.R. and Southward A.J. 1986. Chemoautotrophy in bivalve molluscs of the genus *Thyasira*. *Journal of the Marine Biological Association of the United Kingdom* 66, 915–929.
- Dando P.R., Austen M.C., Burke R.J., Kendall M.A., Kennicutt M.C., Judd A.G., Moore D.C., Schmaljohann R. and Southward A.J. 1991. Ecology of a North Sea pockmark with an active methane seep. *Marine Ecology Progress Series* 70, 49–63.
- Dando P.R. and Spiro B. 1993. Varying nutritional dependence of the thyasirid bivalves *Thyasira sarsi* and *T. equalis* on chemoautotrophic symbiotic bacteria, demonstrated by isotope ratios of tissue carbon and shell carbonate. *Marine Ecology Progress Series* 92, 151–158.
- Dando P.R., Bussmann I., Niven S.J., O'Hara S.C.M., Schmaljohann R. and Taylor L.J. 1994. A methane seep area in the Skagerrak, the habitat of the pogonophore *Siboglinum poseidoni* and the bivalve mollusc *Thyasira sarsi*. *Marine Ecology Progress Series* 107, 157–167.
- Dando P.R. 2010. Biological communities at marine shallow-water vent and seep sites. In: S. Kiel (Ed.), *The Vent and Seep Biota*, Springer, p.333–378.
- Danise S., Dominici S., Betocchi U. 2010. Mollusk species at a Pliocene shelf whale fall (Orciano Pisano, Tuscany). *Palaios* 25, 449–556.
- Dominici S., Cioppi E., Danise S., Betocchi U., Gallai G., Tangocci F., Valleri G. and Monechi S. 2009. Mediterranean fossil whale falls and the adaptation of mollusks to extreme habitats. *Geology* 37, 815–818.
- Dubilier N., Bergin C. and Lott C. 2008. Symbiotic diversity in marine animals: The art of harnessing chemosynthesis. *Nature Review* 6, 725–740.
- Dufour S.C. 2005. Gill Anatomy and the Evolution of Symbiosis in the Bivalve Family Thyasiridae. *Biological Bulletin* 208, 200–212.
- Gillan C. and De Ridder C. 1997. Morphology of a ferric iron-encrusted biofilm forming on the shell of a burrowing bivalve (Mollusca). *Aquatic Microbial Ecology* 12, 1–10.
- Glover A.G., Kallstrom B., Smith C.R. and Dahlgren T.G. 2005. World-wide whale worms? A new species of *Osedax* from the shallow North Atlantic. *Proceedings of the Royal Society of London, Series B* 272, 2587–2592.
- Hammer Ø., Harper D.A.T. and Ryan P.D. 2001. PAST: Paleontological statistics software package for education and data analysis: *Palaeontologia Electronica* 4: 1–9. [https://palaeo-electronica.org/2001\\_1/past/issue1\\_01.htm](https://palaeo-electronica.org/2001_1/past/issue1_01.htm).
- Hansson H.G. 1998. NEAT (North East Atlantic Taxa): Scandinavian marine Mollusca Check-List. Internet Ed., Aug. 1998. <http://www.tmbi.gu.se>.



- Hayek L.A. and Buzas M.A. 1997. Surveying natural populations. Columbia University Press, New York.
- Josefson A.B. 1982. Regulation of population size, growth, and production of a deposit-feeding bivalve: a long-term field study of three deep-water populations off the Swedish west coast. *Journal of Experimental Marine Biology and Ecology* 59, 125–150.
- Josefson A.B. 1985. Distribution of diversity and functional groups of marine benthic infauna in the Skagerrak (eastern North Sea) – Can larval availability affect diversity? *Sarsia* 70, 229–249.
- Kenkel N.C., and Orlóci L. 1986. Applying metric and nonmetric multidimensional scaling to ecological studies: Some new results. *Ecology* 67, 919–928.
- Kutti T., Ervik A. and Høisæter T. 2008. Effects of organic effluents from a salmon farm on a fjord system. III. Linking deposition rates of organic matter and benthic productivity. *Aquaculture* 282, 47–53.
- Levin L.A., James D.W., Martin C.M., Rathburn A.E., Harris L.H. and Michener R.H. 2000. Do methane seeps support distinct macrofaunal assemblages? Observations on community structure and nutrition from the northern California slope and shelf. *Marine Ecology Progress Series* 208, 21–39.
- Palm A., Cousins I., Gustafsson O., Axelman J., Grunder K., Broman D. and Brorström-Lunden E. 2004. Evaluation of sequentially-coupled POP fluxes estimated from simultaneous measurements in multiple compartments of an air–water–sediment system. *Environmental Pollution* 128, 85–97.
- Pavlyuk O.N., Trebukhova Y.A. and Tarasov V.G. 2009. The impact of implanted whale carcass on nematode communities in shallow water area of Peter the Great Bay (East Sea). *Ocean Science Journal* 44, 181–188.
- Sahling H., Galkin S.V., Salyuk A., Greinert J., Foerstel H., Piepenburg D. and Suess E. 2003. Depth-related structure and ecological significance of cold-seep communities—A case study from the Sea of Okhotsk. *Deep-Sea Research Part I* 50, 1391–1409.
- Schander C., Rapp H.T., Kongsrud J.A., Bakken T., Berge J., Cochrane S., Oug E., Byrkjedal I., Todt C., Cedhagen T., Fosshagen A., Gebruk A., Larsen K., Levin L., Obst M., Pleijel F., Stöhr S., Warén A., Mikkelsen N.T., Hadler-Jacobsen S., Keuning R., Heggøy Petersen K., Thorseth I.H. and Pedersen R.B. 2010. The fauna of hydrothermal vents on the Mohn Ridge (North Atlantic). *Marine Biology Research* 6, 155–171.
- Smith C.R. 2006. Bigger is better: The role of whales as detritus in marine ecosystems. In: Estes J. (Ed.), *Whales, Whaling and Ocean Ecosystems*. Berkeley, University of California Press, pp. 284–299.
- Smith C.R., Baco A.R. and Glover A. 2002. Faunal succession on replicate deep-sea whale falls: Time scales and vent-seep affinities. *Cahiers de Biologie Marine* 43, 293–297.
- Smith C.R. and Baco A.R. 2003. Ecology of whale falls at the deep-sea floor. *Oceanography and Marine Biology an Annual Review* 41, 311–354.
- Southward E.C. 1986. Gill symbionts in thyasirids and other bivalve molluscs. *Journal of the Marine Biological Association of the United Kingdom* 66, 889–914.
- Tarasov V.G., Gebruk A.V., Mironov A.N. and Moskalev L.I. 2005. Deep-sea and shallow-water hydrothermal vent communities: Two different phenomena? *Chemical Geology* 224, 5–39.
- Taylor J.D. and Glover E.A. 2006. Lucinidae (Bivalvia)—The most diverse group of chemosymbiotic molluscs. *Zoological Journal of the Linnean Society* 148, 421–438.
- Temara A., De Ridder C., Kuenen J.C. and Robertson L.A. 1993. Sulfide oxidizing bacteria in the burrowing echinoid, *Echinocardium cordatum* (Echinodermata). *Marine Biology* 115, 179–185.
- Todd J.A. 2000. Introduction to molluscan life habits databases, updated March 27, 2001. <http://>

eusmilia.geology.uiowa.edu/database/mollusc/mollusclifestyles.htm.

Van Weering T.C.E., Berger G.V. and Kalf J. 1987. Recent sediment accumulation in the Skagerrak, northeastern North Sea. *Netherlands Journal of Sea Research* 21, 177–189.

Warén A. 1991. New and little known Mollusca from Iceland and Scandinavia. *Sarsia* 76, 53–124.

Warén A. 1996. Ecology and systematics of the northern European species of *Rissoa* and *Pusillina* (Prosobranchia: Rissoidae). *Journal of the Marine Biological Association of the United Kingdom* 76, 1013–1059.

Wiklund H., Glover A.G., Johannessen P. and Dahlgren T.G. 2009. Cryptic speciation at organic-rich marine habitats: a new bacteriovore annelid from whale-fall and fish farms in the North East Atlantic. *Zoological Journal of the Linnean Society* 155, 774–785.

Wisshak M., Gettidis M., Freiwald A. and Lundalv T. 2005. Bioerosion along a bathymetric gradient in a cold temperate setting (Kosterfjord, SW Sweden): an experimental study. *Facies* 51, 93–117.

# CHAPTER 3 — Mollusc species at a Pliocene shelf whale fall (Orciano Pisano, Tuscany)

---

## 3.1 Introduction\*

Since their first discovery in the deep sea, whale falls have attracted scientists for the exceptional fauna they host, largely based on chemoautotrophic pathways fuelled by lipid-rich whale skeletons (Smith et al. 1989, Bennett et al. 1994). Time series studies of natural and implanted deep-sea whale falls indicate that bathyal carcasses pass through four stages of ecological succession: a mobile-scavenger, an enrichment-opportunist, a sulphophilic and lastly a reef stage (Smith et al. 2002). Experimental studies have once yielded evidence of the fourth stage (Fujiwara et al. 2007), whereas the third, sulphophilic stage has been found going on also on very old carcasses (Smith and Baco 2003). Successional stages involve species turnover and changes in faunal mobility and trophic structure, with temporal overlaps in the onset of characteristic species from different stages. For these reasons, diversity in whale-bone faunal communities varies with successional stages, the sulphophilic stage harboring the greatest number of species (Smith and Baco 2003).

While research programs concentrate on the deep sea, remarkably little is known about ecosystem response to whale falls at shallow depth, where the flux of organic carbon to the bottom is already high and constant, and different degree, if not type, of resource exploitation is expected. Natural shelf occurrences are probably rare, due to re-floating of carcasses by decay gas (Allison et al. 1991, Smith 2006), however artificially sunken carcasses show the presence of obligate whale fall taxa even at shallow depth (Dahlgren et al. 2006).

Paleontological reports of fossil whale fall communities, ranging from the Palaeogene (Goedert et al. 1995, Kiel and Goedert 2006, Nesbitt 2005, Kiel 2008) to the early Neogene (Amano and Little, 2005, Pyenson and Haasl 2007), are similarly unbalanced towards deep sea paleosettings.

Fossil whales are not rare in the Mediterranean Pliocene, and their taphonomy was approached in the early days of palaeontology (*e.g.*, Cortesi 1819). However, no quantitative study of the associated biota has been undertaken until the recent finding of a whole and articulated skeleton of a large mysticaete in the Pliocene of Tuscany, with a mollusc fauna testifying to the sulphophilic stage (Dominici et al. 2009). This is particularly interesting since it enables the study of a whale fall community at shelf depth.

In the present study the distribution of mollusc abundances and the trophic structure of the Orciano fossil community are discussed at the species level, with a comparison with

---

\* This chapter consists of a paper by S. Danise, S. Dominici and U. Betocchi, "Mollusk species at a Pliocene shelf whale fall (Orciano Pisano, Tuscany)" published in volume 25 of *Palaios* (2010), except for Figure 4 which is unpublished.

the background fauna. Species-level comparisons allow us to interpret the paleoecology at a finer resolution on uniformitarian grounds, many Pliocene species still being alive. Moreover, new samples were analyzed with respect to the previous family-level study (Dominici et al. 2009), allowing the discovery of new chemosymbiotic forms. Mollusc species from sediments in contact with whale bones have been compared with assemblages from the sediments below and around the whale fall, in order to reconstruct the paleoenvironmental conditions before and during the permanence of the carcass on the sea floor. The results will be discussed in terms of faunal adaptations to exploit whale carcasses at shelf depths, where competition is keen.

### 3.2 General setting

The fossil whale was found at Orciano Pisano, in Southern Tuscany, a locality known for its rich marine vertebrate fauna including fishes, cetaceans, pinnipeds and chelonids (Bianucci and Landini 2005). Orciano is located in the Fine Basin (Figure 1), on the Tyrrhenian side of the northern Apennines, a structure filled by 1000 m of Tortonian-Pleistocene, mostly marine deposits. The depositional environment rapidly shifts from deltaic to bathyal depths at the start of the Pliocene (Carnevale et al. 2008 and references therein), at the onset of deposition of grey-blue marls. The skeleton was found in the middle part of the regressive deposits overlaying the grey-blue marls, within silty fine-grained sandstones marking the regression to shelf depths. Planktonic foraminifers and fossil nanoplankton indicate that the age of the whale fall ranges from the upper Piacenzian to the lower Gelasian (3.19-2.82 Ma interval) (Dominici et al. 2009).

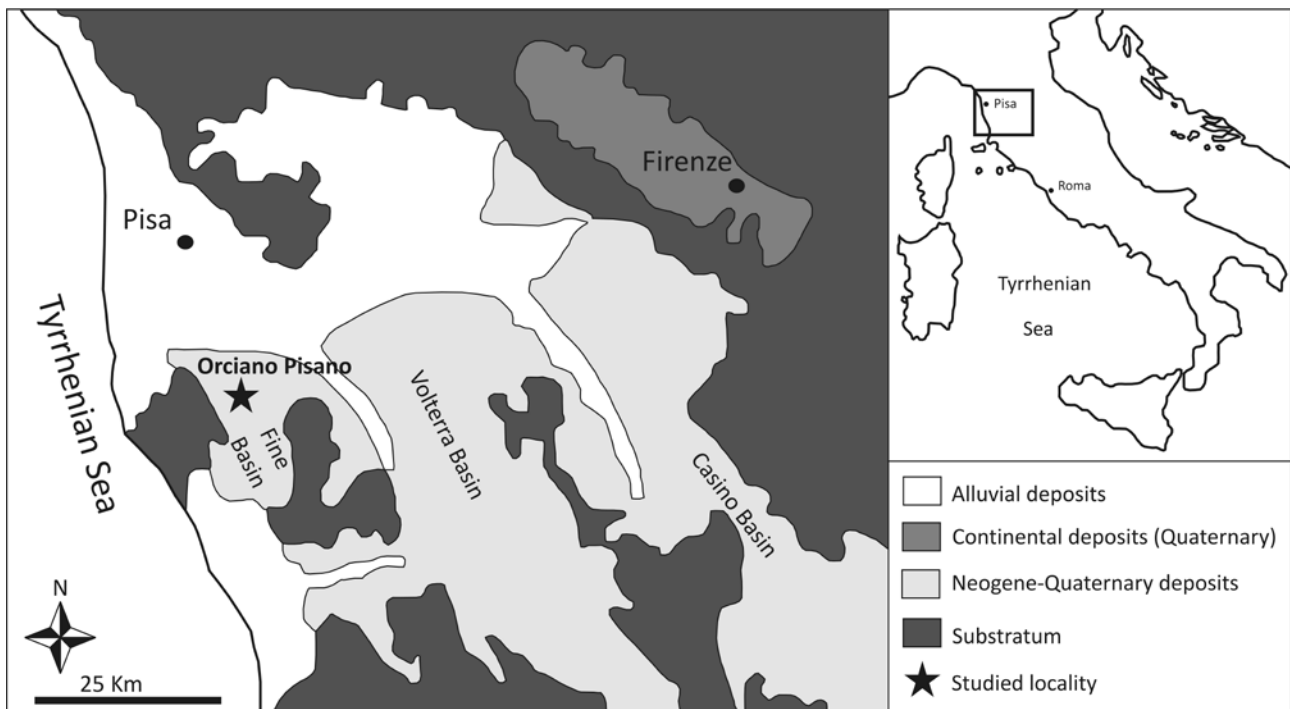
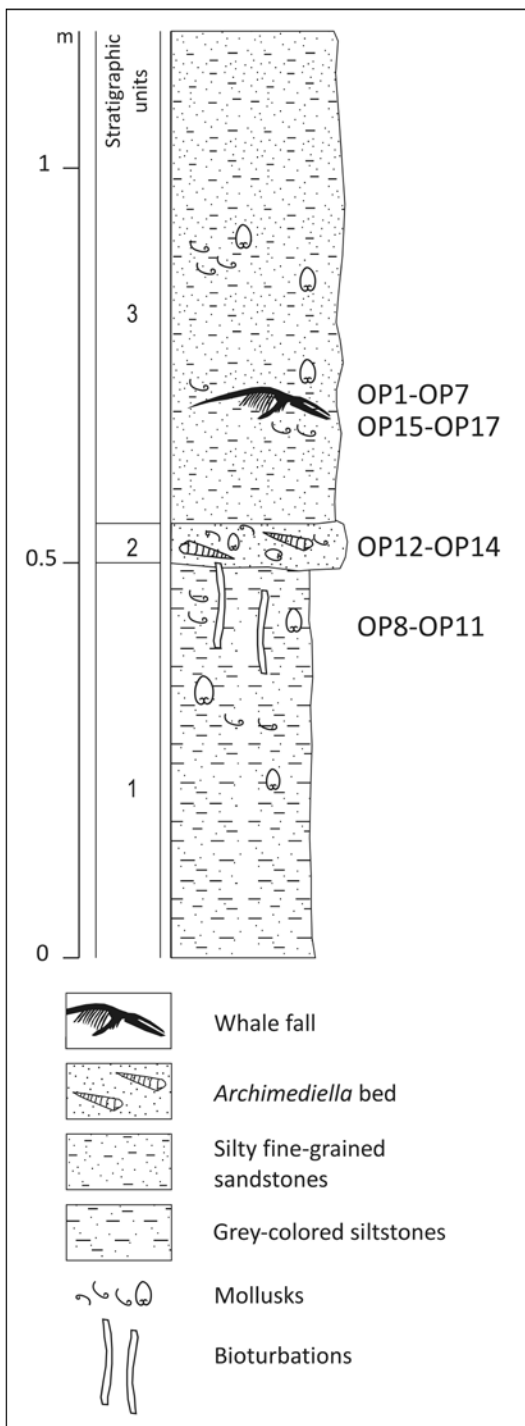


Figure 1. Location of the study area at Orciano Pisano, Italy and schematic geological map (modified after Carnevale et al. 2008).

### 3.3 Materials and methods



#### 3.3.1 Stratigraphy

The local succession is formed by the following units, from bottom to top (Figure 2): (1) bioturbated grey-colored siltstones (thickness 50 cm) with sparse macrofauna; (2) a 4-5 cm thick, densely-packed *Archimediella spirata* shell pavement (Turritlella bed in the sense of Allmon 1988) regularly continuous in all the area; bivalves are typically articulated, *Archimediella* shells are empty or partially filled with clay; fragments of fossil wood are abundant and up to 15 cm long; remains of marine vertebrates are abundant (sharks, teleosts, marine mammals, chelonids); (3) massive silty fine-grained sandstones, more than 1 m thick, with sparse to loosely-packed macrofauna; adults of the highly mobile epifaunal *Amusium cristatum* and other bivalves (*e.g.*, *Anadara diluvii*, *Corbula gibba*, *Tellina planata*) are in life position. *Archimediella spirata*, *Aporrhais uttingeriana*, spatangoid echinoderms, trace fossils (Ophiomorpha, Thalassinoides) and vegetal debris are abundant throughout the outcrop. The whale was lying in unit 3 about 20 cm above the *Archimediella* bed and parallel to it.

Figure 2. Studied Pliocene section subdivided into three stratigraphic units (unit 1, unit 2, unit 3). Sample locations are marked by OP.

#### 3.3.2 Sampling and analytical methods

A total of 17 bulk samples can be subdivided in 4 groups depending on their relative position with respect to the whale bones; these a priori groups are used in between-samples comparisons. The first group (whale fall community: wfc) is represented by the seven samples representative of the whale fall fauna (OP1-OP7) collected above the bones and positioned on a grid of 1 m-sized

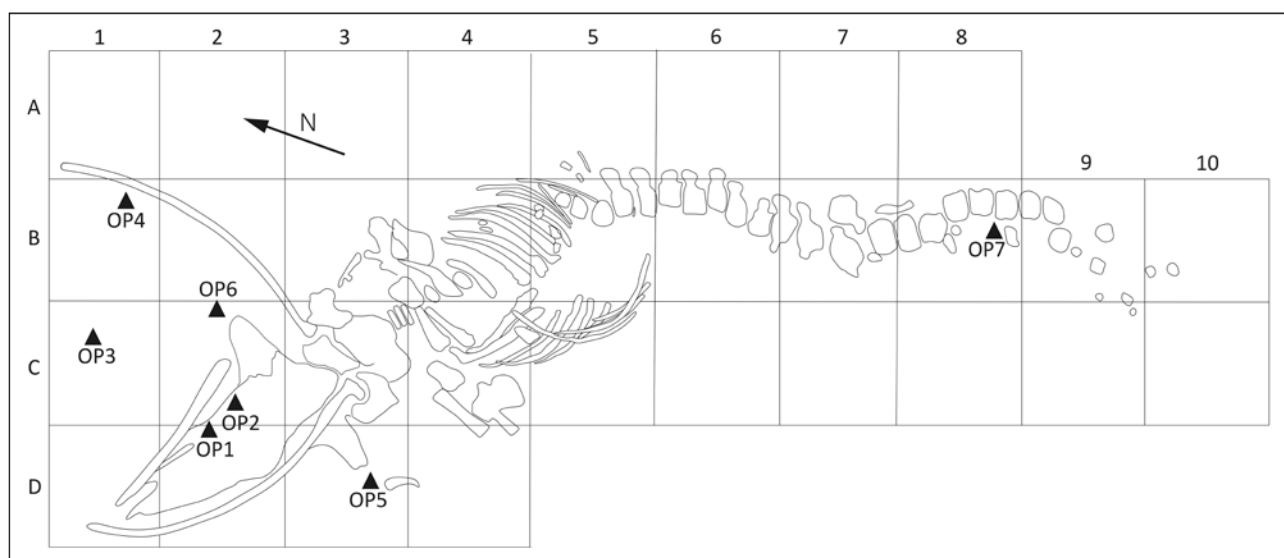


**Figure 3.** Plane view of the Orciano Pisano whale skeleton on a grid of 1 m squares. Triangles indicate the position of whale-fall samples (OP1–OP7).

squares (Figure 3). Ten additional samples were collected from background sediments: four from unit 1 (below-wfc: OP8–OP11) three from the *Archimediella* bed (*Archimediella* bed: OP12–OP14) and three from unit 3 at 1–2 m from the closest bone (lateral-wfc: OP15–OP17) (Figure 2, Table 1). The data set includes 17 samples. All samples, ranging 0.5–1 litres, were wet sieved through a 1 mm screen and the residue sorted under a binocular microscope for all recognizable biogenic components. The latter includes molluscs, polychaetes, echinoids, decapods and fishes. Molluscs were determined at the species level and used for quantitative comparisons. Bivalve number was counted as the highest number of right or left valves and half of the remaining, the latter roughly corresponding to the number of unmatched valves. Gastropods were equated to the number of apices. Each unit was scoured for large-sized species, which are likely to be underrepresented in bulk samples, and a species was added as present to the data matrix where appropriate.

**Table 1.** Basic data for the studied samples.

Stratigraphic unit	Group of samples	Sample number	Volume (liter)	Number of individuals	Number of species
Unit 3	wfc	OP1	1 l	257	37
		OP2	1 l	228	41
		OP3	0.5 l	241	41
		OP4	0.5 l	116	27
		OP5	0.5 l	150	34
		OP6	0.5 l	204	29
		OP7	0.5 l	72	25
Unit 1	below-wfc	OP8	0.5 l	56	22
		OP9	0.5 l	61	20
		OP10	0.5 l	92	24
		OP11	0.5 l	61	18
Unit 2	<i>Archimediella</i> bed	OP12	0.5 l	282	43
		OP13	0.5 l	172	27
		OP14	0.5 l	188	30
Unit 3	lateral-wfc	OP15	0.5 l	54	22
		OP16	0.5 l	75	22
		OP17	1 l	140	28
		All samples	12 l	2449	97

The data set, including 2449 specimens belonging to 97 mollusc species (Appendix), formed the basis for a multivariate comparison and for trophic structure analysis. For multivariate elaboration, species occurring in only one sample were removed, resulting in a data set with 62 species and 2409 specimens (98,4% of the original specimens). Abundances were standardized and square-root transformed to de-emphasize the influence of most abundant taxa.

A similarity percentage analysis (SIMPER, see Clarke and Warwick 1994) was performed to determine which species were responsible for similarity within groups of sample. Those species for which the ratio of mean similarity to standard deviation of similarity is  $>1$  typify the sample group and were listed in the comparison. Then a matrix of square-root transformed data was obtained based on the Bray-Curtis similarity coefficient, one of the most widely used in ecological studies (Bray and Curtis 1957, Clarke and Warwick 1994). Analysis of similarity (ANOSIM) was carried out to test the degree of differences between a priori groups of samples considering stratigraphic and taphonomic information. The important message of the pair-wise tests of the ANOSIM analysis is the pair-wise R-values; the latter give an absolute measure of how separated the groups are, on a scale of zero (indistinguishable) to one (all similarities within groups are less than any similarity between groups). With R-values  $>0.75$ , groups are well separated; with R-values  $>0.5$ , groups are overlapping but clearly different; with R-values  $>0.25$ , groups strongly overlap; and with R-values  $<0.25$ , groups are barely separable.

Non-metric multidimensional scaling (nMDS) was performed (Clarke and Warwick 1994), producing a map of the samples where points that plot close together represent samples very similar in taxonomic composition. All statistical analyses were performed with the software PRIMER (Clarke and Warwick 1994) except for ANOSIM that was performed with PAST (Hammer et al. 2001).

The whole data set ( $n=2449$ ), subdivided into the a priori groups, was used for trophic analysis by considering trophism of modern molluscs genera or families. Seven trophic categories are distinguished following the Molluscan Life Habits Databases (Todd 2000): suspension feeders (SU), deposit feeders (DE), predatory carnivores, including scavengers (CP), browsing carnivores (CB), herbivores (HE), parasites (PA) and chemosymbiotic forms (CH). Comparisons were expressed through percent of number of specimens ( $n$ , abundance) and number of species ( $S$ , richness) for each category.

## 3.4 Results

### 3.4.1 Paleocommunity structure

The full dataset includes 42 species of gastropods, 50 bivalves, 5 scaphopods, bony fishes, sharks and rays (*Carcharhinus* sp., *Hexanchus griseus*, *Raja* cf. *clavata*) (Figure 4), decapods, barnacles, regular and irregular echinoids, serpulids (*Ditrupa cornea* and others) and foraminifers. The quantitatively important species of the mollusc dataset, contributing at least 1% to the total

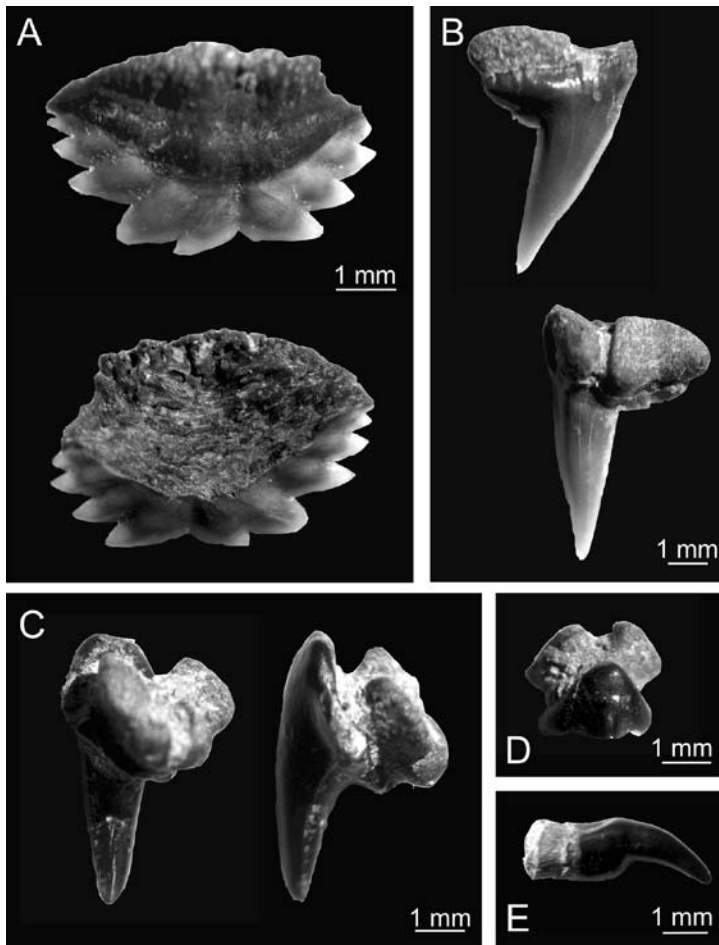


Figure 4. Chondricthe and fish teeth associated with the studied samples. A. *Hexanchus griseus*. B. *Carcharhinus* sp. C. and D. *Raja* cf. *clavata*. E. Teleosteus fish.

assemblage, are all represented in the four groups of samples, with minor exceptions. Species rank changes between the a priori groups (Figure 5). The most abundant species is the bivalve *Corbula gibba*, dominant in wfc, below-wfc and lateral-wfc samples, with a mean abundance ranging 39-41%. The turritellid *Archimediella spirata* largely predominates in the *Archimediella* bed group (average 31%), being rare in wfc and lateral-wfc groups (average 1%) (Figure 5). SIMPER analysis shows that *Archimediella* bed samples have the highest similarity, with an average value of 70%, followed by wfc (67%) and below-wfc samples (62%). The most heterogeneous group is the lateral-wfc, with an average similarity of 57% (Table 2). Characteristic species within each group of samples are mainly shared between all groups, with the exception of *Natica* sp. and *Hiatella rugosa*, characteristic respectively of *Archimediella* bed and lateral-wfc groups, and the mytilid *Modiolula phaseolina* and the lucinid *Megaxinus incrassatus*, only typical of the whale fall. *M.*

*rugosa*, characteristic respectively of *Archimediella* bed and lateral-wfc groups, and the mytilid *Modiolula phaseolina* and the lucinid *Megaxinus incrassatus*, only typical of the whale fall. *M.*

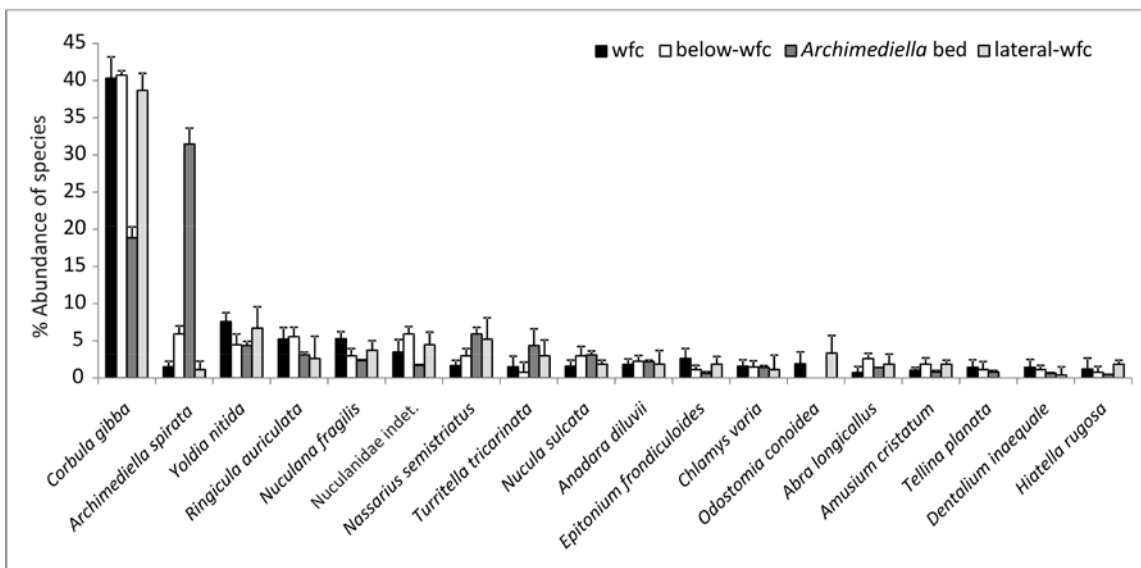


Figure 5. Percentage abundances in each of the four a priori groups of the quantitatively important species (>1%) in the total data set. Mean percentage abundances shown with the upper limit of 95% confidence intervals; wfc = whale-fall community.



**Table 2. Characteristic species of each group of samples, calculated for standardized data set and square-root transformed abundances using similarity percentage analysis (SIMPER, Clarke and Warwick 1994). Underlined species are characteristic taxa not shared among the four groups.**

Species	Av.Abund.	Av.Sim.	Sim/SD	Contrib.%
<b>"wfc" samples</b>				
<b>Average similarity: 67.30</b>				
<i>Corbula gibba</i>	39.95	13.20	9.19	19.62
<i>Yoldia nitida</i>	8.03	5.58	6.49	8.29
<i>Nuculana fragilis</i>	5.41	4.74	10.73	7.04
<i>Ringicula auriculata</i>	5.10	3.92	5.47	5.83
<u><i>Modiolula phaseolina</i></u>	1.58	2.54	6.27	3.78
<i>Anadara diluvii</i>	1.95	2.54	6.02	3.77
<i>Nassarius semistriatus</i>	1.75	2.48	4.20	3.68
Nuculanidae indet.	3.14	2.34	1.41	3.48
<u><i>Megaxinus incrossatus</i></u>	1.71	2.19	3.73	3.26
<i>Archimediella spirata</i>	1.77	2.18	2.66	3.23
<i>Epitonium frondiculoides</i>	2.74	2.09	1.42	3.11
<i>Amusium cristatum</i>	1.18	2.03	9.27	3.02
<i>Nucula sulcata</i>	1.68	1.95	1.47	2.90
<i>Chlamys varia</i>	1.82	1.88	1.48	2.79
<i>Dentalium inaequale</i>	1.23	1.58	1.52	2.35
<i>Limea strigilata</i>	1.14	1.54	1.37	2.29
<i>Anomia ephippium</i>	0.78	1.28	1.51	1.90
<i>Aporrhais uttingeriana uttingeriana</i>	1.25	1.24	1.25	1.84
<b>"below-wfc" samples</b>				
<b>Average similarity: 61.97</b>				
<i>Corbula gibba</i>	43.04	16.81	19.15	27.13
Nuculanidae indet.	5.93	6.02	41.60	9.72
<i>Archimediella spirata</i>	5.88	5.71	7.85	9.22
<i>Ringicula auriculata</i>	5.42	4.96	3.32	8.00
<i>Abra longicallus</i>	2.58	3.75	7.21	6.05
<i>Nuculana fragilis</i>	2.93	3.73	5.43	6.01
<b>"Archimediella bed" samples</b>				
<b>Average similarity: 70.45</b>				
<i>Archimediella spirata</i>	32.35	12.41	37.34	17.62
<i>Corbula gibba</i>	19.48	9.29	14.94	13.18
<i>Nassarius semistriatus</i>	5.81	5.10	22.00	7.24
<i>Yoldia nitida</i>	4.83	3.93	7.63	5.58
<i>Ringicula auriculata</i>	3.18	3.62	6.94	5.15
<i>Nuculana fragilis</i>	2.40	3.44	23.57	4.88
<i>Nucula sulcata</i>	3.13	3.41	3.76	4.83
<i>Anadara diluvii</i>	2.26	3.06	69.92	4.34
Nuculanidae indet.	1.86	2.73	4.56	3.88
<i>Abra longicallus</i>	1.49	2.58	7.63	3.66
<i>Chlamys varia</i>	1.36	2.40	21.43	3.41
<i>Chlamys pesfelis</i>	1.11	2.38	28.32	3.38
<u><i>Natica sp.</i></u>	1.35	2.14	6.28	3.04
<i>Chlamys glabra cf. flexuosa</i>	1.77	2.10	7.75	2.99
<i>Aporrhais uttingeriana uttingeriana</i>	1.22	2.08	3.91	2.96
<i>Dentalium sexangulum</i>	0.87	1.72	2.88	2.45
<i>Dentalium inaequale</i>	0.62	1.69	22.39	2.41
<b>"lateral-wfc samples"</b>				
<b>Average similarity: 56.68</b>				
<i>Corbula gibba</i>	41.08	14.79	9.41	26.10
<i>Yoldia nitida</i>	5.55	4.17	3.19	7.35
Nuculanidae indet.	4.11	4.10	3.45	7.23
<i>Nassarius semistriatus</i>	4.17	3.61	10.01	6.37
<i>Nuculana fragilis</i>	4.17	3.46	3.66	6.10
<i>Limea strigilata</i>	2.64	3.34	4.32	5.90
<i>Amusium cristatum</i>	2.01	3.11	8.33	5.49
<i>Epitonium frondiculoides</i>	1.80	3.04	13.01	5.36
<i>Nucula sulcata</i>	2.19	2.90	33.85	5.11
<u><i>Hiatella ruqosa</i></u>	2.40	2.78	2.20	4.90

*incrossatus* is found exclusively in whale fall samples, whereas *Modiolula phaseolina* abundance is statistically significant here with respect to the other settings (Kruskal-Wallis test:  $p=0,006$ ).

ANOSIM points out that the largest difference is observed between whale fall and *Archimediella* bed samples, the two groups being well-separated ( $R=0.81$ ) and the difference statistically highly significant ( $p=0.0078$ ). Whale fall samples overlap but are still distinguishable from below-wfc samples ( $R=0.66$ ;  $p=0.0033$ ). Whale fall samples record the smallest difference when compared with samples from surrounding sediments of the same unit, a difference that is clear ( $R=0.56$ ), but statistically less significant ( $p=0.0402$ ), due to the small size of lateral-wfc samples (Table 1). Even lower is the statistical significance while comparing lateral-wfc with all other groups. Finally, a strong overlap is encountered between below-wfc and *Archimediella* bed samples (Table 3).

Non-metric multidimensional scaling allows us to visualize compositional differences between samples and their a priori groups. This underlines no overlap between groups and a slightly larger distance of wfc samples from below-wfc and *Archimediella* bed samples (Figure 6). The three lateral-wfc samples appear scattered, consistently with their small size and unreliable character for comparisons. On the other hand, wfc samples and *Archimediella* bed samples form tight clusters, depending on their inner similarities

and sufficiently large size for comparisons. As a matter of fact, samples with fewer than 80 specimens tend to be more scattered, whereas samples with 100 specimens or more tend to plot closer. Multivariate analysis overall show that mollusc assemblages living by the whale

carcass are different from those that lived on the same bottom before the fall of the carcass. Even samples collected at a distance from the bones, but within the same unit, appear different.

**Table 3. Results of ANOSIM (analysis of similarity) among the four identified groups of samples. Statistical decisions are based on R-values, which give an absolute measure of the separation of the groups; s = significant, ns = not significant.**

group of samples	R	description (based on R-values)	p	statistical decision
total	0.5569	groups overlapping but clearly different	< 0.0001	s
wfc v below-wfc	0.6614	groups overlapping but clearly different	0.0033	s
wfc v <i>Archimediella</i> bed	0.8135	groups well separated	0.0078	s
wfc v lateral-wfc	0.5556	groups overlapping but clearly different	0.0402	s
below-wfc v <i>Archimediella</i> bed	0.3333	groups strongly overlap	0.0857	s
below-wfc v lateral-wfc	0.2593	groups strongly overlap	0.117	ns
<i>Archimediella</i> bed v lateral-wfc	0.6667	groups overlapping but clearly different	0.1015	ns

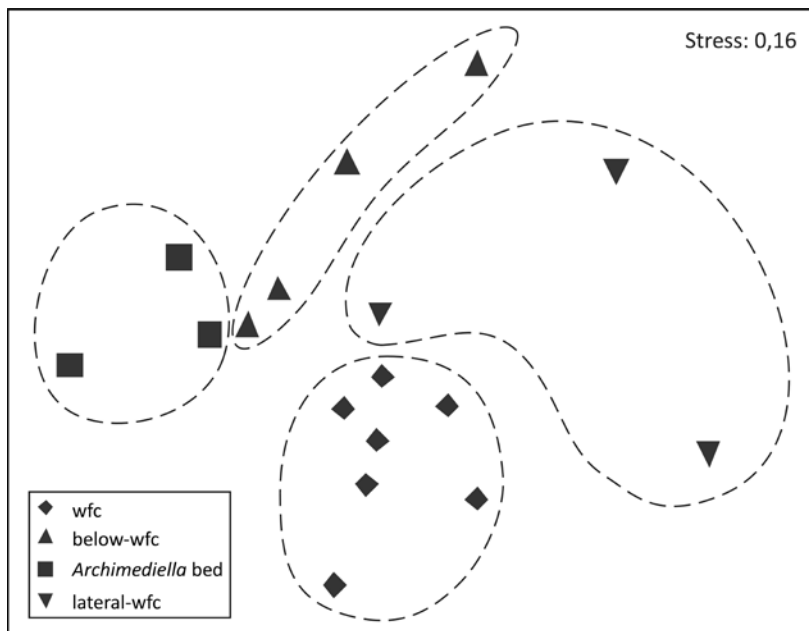


**Figure 6. Multidimensional scaling ordination of samples belonging to the four identified a priori groups; wfc = whale-fall community.**

### 3.4.2 Trophic analysis

Trophic structure was analyzed after cumulating individual samples into the four a priori groups (Figure 7). Suspension feeders dominate in both richness (40-50%) and abundance (56-66%) in all groups. In below-wfc, lateral-wfc and wfc groups *Corbula gibba* is the most important suspension feeder, whereas the *Archimediella* bed is dominated by the turritelids (*Archimediella spirata*, *Turritella tricarinata*). Other common suspension feeders shared between all samples are the pectinids *Chlamys varia* and *Amusium cristaum* and the arcid *Anadara diluvii*. The whale fall assemblage shows a significant higher abundance of the mussel *Modiolula phaseolina*. The second most important group is the deposit feeders (S=20,0-25,5%, n=17,0-24,3%), particularly nuculids and nuculanids (*Yoldia nitida*, *Nuculana fragilis*, *Nucula sulcata* and *Nuculanidae* indet.) followed by the tellinoidea (*Abra longicallus*, *Tellina planata*) and scaphopods. Concerning

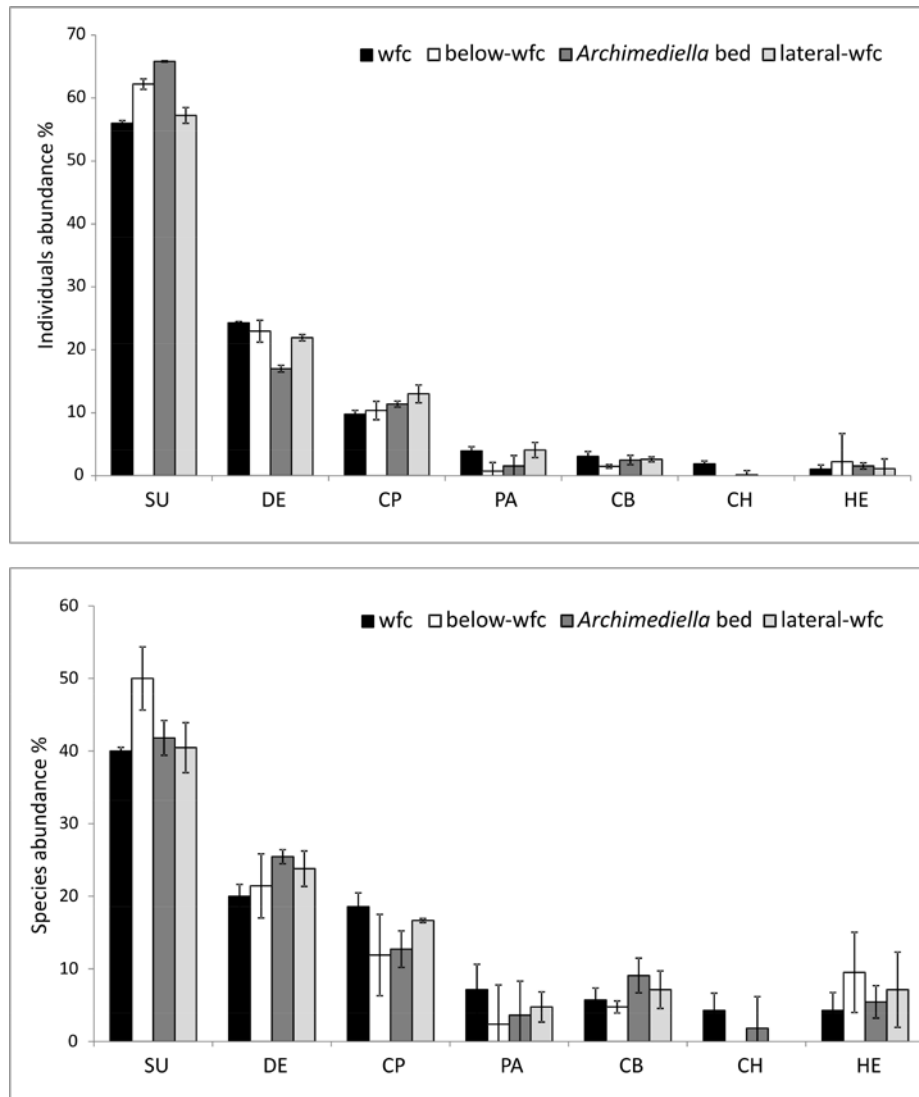
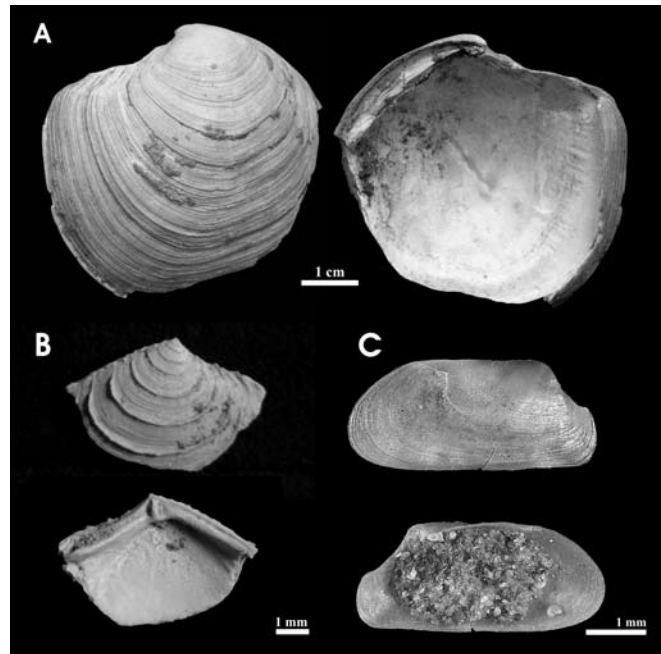


Figure 7. Trophic analysis expressed through percent of number of individuals (abundance) and number of species (richness). Trophic categories: suspension feeders (SU), deposit feeders (DE), predatory carnivores, including scavengers (CP), parasites (PA), browsing carnivores (CB), chemosymbiotic forms (CH) and herbivores (HE). Data shown with 95% confidence intervals; wfc = whale-fall community.

carnivores and scavengers, abundance data show comparable percentages, while whale fall samples show a higher species richness. Ringiculids (*Ringicula auriculata* and *R. ventricosa*) and nassarids (*Nassarius semistriatus*) are the most common, the first feeding mainly of small copepods (Fretter 1960), the latter being secondarily an active predator on polychaetes and small crustaceans (Britton and Morton 1994). Naticids (*Euspira helicina* and *Natica sp.*) are quite common, feeding mainly on bivalves and crustaceans (Taylor 1980). Parasites are represented mainly by the ectoparasite pyramidellids in all assemblages, with a higher diversity in whale fall samples. The browsing carnivores, i.e., predators which feed on sedentary and typically clonal animals without killing them, are poorly represented overall. This category include the epitonids (*Epitonium frondiculoides*, *E. turtoni*) and the trochids (*Calliostoma granulatum*). Chemosymbiotic bivalves occur just in wfc and *Archimediella* bed samples, with

a low overall diversity. They are significantly more abundant in wfc samples, represented by the lucinid *Megaxinus incrassatus*, followed by the lucinid *Myrtea spinifera* and by two specimens of the previously unreported, bathymodiolin mytilid *Idas sp.* (Figure 8). All the *M. incrassatus* specimens found associated with whale bones are 3,5 to 5,5 cm wide, juveniles being absent. In the *Archimediella* bed samples chemosymbiotic bivalves are represented exclusively by *Myrtea spinifera*. Herbivores are rare in all the samples and less represented in the whale fall.

Figure 8. Chemosynthetic bivalves from the Pliocene whale fall at Orciano Pisano. A) *Megaxinus incrassatus*. B) *Myrtea spinifera*. C) *Idas sp.*



### 3.5 Discussion

#### 3.5.1 General paleoenvironment

Studied mollusc species are generally indicative of a marine outer shelf setting, as previously demonstrated by a family-level study (Dominici et al. 2009). The predominance of suspension feeders is consistent with the general composition of benthic communities at shelf depths, whereas the high diversity and abundance of deposit feeders is typical of the deeper parts of the shelf (Rhoads 1974). The high frequency of *Corbula gibba*, a small infaunal species inhabiting soft bottoms, is indicative of stressed conditions, either through high turbidity or low oxygen values (references in Hrs-Brenko 2006). The dominance of turritellids in the *Archimediella* bed is consistent with high content of particulate organic matter, usually associated with coastal upwelling (Allmon 1988). The abundance of fossil wood suggests instead that nutrients were of fluvial origin. The hypothesis of meso- or eutrophic conditions in the Fine Basin during the Pliocene is in accordance with modern conditions in the Ligurian Sea, facing the study region. Here high nutrient contents are met with both in coastal areas and offshore. Modern coastal upwelling and high productivity in the Ligurian Sea sustain an abundant and diverse cetacean fauna (Notarbartolo Di Sciara et al. 2008), conditions that would explain the general abundance and diversity of marine vertebrates at Orciano Pisano.

#### 3.5.2 Whale fall ecological succession

Due to time averaging, fossil assemblages generally do not allow the positive subdivision of stages within an ecological succession (Miller 1986). The following discussion is to be taken

therefore as a hint to possible ecological pathways within a shallow water whale fall, relying on both observed fossil data and known modern examples.

Chondrichthyes that might have scavenged the carcass include, in addition to *Prionace glauca* and *Carcharodon carcharias* collected during field excavation, the sharks *Carcharhinus* sp., *Hexanchus griseus* and rays (*Raja* cf.). Higher richness of predatory gastropods in whale fall samples with respect to the others suggests a general high quantity of prey species and trophic niches that could interest more than one ecological stage. These, together with decapods and echinoids not considered in the quantitative analysis, give a clue to the later parts of the scavenger stage (e.g. amphipods and copepods ultimate flesh consumption: Smith 2006). However, carnivore molluscs could also have been preying on species of the enrichment opportunistic stage, one chiefly characterized by the polychaetes (Smith et al. 2002, Dahlgren et al. 2004, Goffredi et al. 2004). Whether or not whale fall polychaetes can be a food item for species such as *Natica tigrina*, *Ringicula auriculata* or *Nassarius semistriatus* is presently unknown. High diversity of parasites, dominated by pyramidellids, could also pertain to the opportunistic stage through their possible hosts, such as polychaetes, gastropods and bivalves (Robertson and Mau-Lastovicka 1979). Smith and Baco (2003) report a great abundance of the pyramidellid *Eulimella lomana* from a recent California whale fall community during the sulphophilic stage, which also suggests that pyramidellids belong to the third successional stage.

The sulphophilic stage, fuelled by the anaerobic breakdown of bone lipids, is well represented by the lucinid *Megaxinus incrassatus* and by the occurrence of the mytilid *Idas* sp.

Finally, even though suspension feeders are not more abundant in whale fall samples with respect to the background fauna, field data evidence the presence of many suspension feeders in life position directly in contact with the bones, as the pectinid *Amusium cristatum* and the arcid *Anadara diluvium*. They could testify to the occurrence of the reef stage, commonly recognized at shelf depths.

Smith and co-workers (2002) hypothesized that the ecological succession at lower latitudes and shallower depths runs faster than in deep water whale fall. In Japan, whale fall successional stages at shallow depths suggest that higher water temperature enhances bacterial activity at the carcass, shortening the duration of the sulphophilic stage (Fujiwara et al. 2007). In accordance with this hypothesis, the absence of juveniles among the paleopopulation of *M. Incrassatus* suggests the presence of a single cohort.

### 3.5.3 Shallow water whale falls

Paleoecology and trophic analysis allow us to understand the effect of an episodic introduction of a large organic particle in the form of a whale carcass on the biota commonly inhabiting this area. The bulk of mollusc species found on the whale fall were already present at the site before the sinking of the carcass. The only meaningful difference concerns the introduction of two chemosymbiotic species, *Megaxinus incrassatus* and *Idas* sp., directly related to the whale carcass, the second with negligible abundance. These species allow us to recognize

the final stages of ecological succession typical of whale falls, but with a completely different overall composition compared to deep-water analogues. Mollusc species at outer shelf depths were thus tolerant of high organic and presumably low oxygen content around the carcass, and the study area may have experienced a generally high nutrient flux and eutrophic conditions. As a consequence, the studied outer shelf species largely out-competed whale fall specialists of the sulphophilic stage, notwithstanding the fact that the Orciano whale fall could still be reached by the larvae of deep water chemosymbiotic bivalves.

The paleoenvironmental distribution of the diagnostic, but extinct, bivalve *Megaxinus incrassatus* is not sufficiently known to understand its specificity to geologically ephemeral reducing habitats. It should also be considered that lucinids are more generalist than deep water vesicomysids and bathymodilinids, and occupy a broad range of reducing habitats from deep to shallow water settings (Taylor and Glover 2006 and reference therein).

In the Mediterranean Neogene, *Idas* has been previously found only at a deep water woodfall (Bertolaso and Palazzi 1993). Modern distributions of the genus include species *Idas simpsoni*, *I. ghisotti* and *I. dalmasi* found associated with sunken-wood and whale carcasses at depths of 170-430 m in the western Mediterranean (Bolotin et al. 2005, Warén and Carrozza 1990, Warén 1991). The species *Idas modiolaeformis* instead appears to be relatively ubiquitous in cold seep communities of the deep eastern Mediterranean Sea (Olu-Le Roy et al. 2004). Recent molecular studies single out genus *Idas* as a distinct clade in Bathymodiolinae mussels, with putative origins in shallow water, and emphasise that *Idas* species have the ability to live on various organic substrates (Jones et al. 2006, Lorion et al. 2009). This supports the stepping stone hypothesis which assumes that carcasses of whales, and Mesozoic marine reptiles before them, facilitated the dispersal of chemosynthetic-based communities down to the continental slope and into deep-sea vent and seep habitats (Smith et al. 1989, Distel et al. 2000, Kaim et al. 2008). In this scenario, outer shelf settings, such as Orciano Pisano, would have an intermediate character between deep and shallow bottoms, and a sufficiently developed island character, so as to reduce competition for space and resources to a minimum and favour speciation within small populations of coastal-dwelling species like the mussels. Outer shelf conditions are the most common place for the development of shallow water species peripheral isolates (Mayr 1963, Frey 1993), such as the suspension feeding ancestors of bathymodiolins (Jones et al. 2006). These populations, therefore, experienced sufficiently high competition as to suffer high pressure selection.

### **3.6 Conclusions**

The species-level comparison of the mollusc assemblages sampled from fine-grained sediments at Orciano Pisano, some of which represent the community that had lived by the carcass of a large whale, suggests that the localized reducing habitat had an intermediate character with respect to similar environments found at shallow and deep settings. In coastal

bottoms the sulphophilic stage has never been encountered, whereas in bathyal bottoms it is always one of the end stages of the ecological succession.

The Orciano Pisano whale fall community is recognizable thanks to the presence of the two chemosymbiotic bivalves *Megaxinus incrassatus* and *Idas sp.* The first is abundant, the second very rare, but both their occurrences are suggestive for the sulphophilic stage of the ecological succession. This is the first case of a fully developed whale fall community at shelf depths, and the first overall in the Mediterranean Sea. Other aspects of the whale fall mollusc community, however, make it impossible to statistically recognize this from the fauna commonly living at the same depth in more normal conditions. High organic content at the whale fall is largely exploited by shelf species already tolerant of dysoxic conditions.

Neogene whale skeletons sunken at shelf depths, not unusual in the Mediterranean record, can serve as important sites to test the hypothesis according to which very large organic particles, like whales which have sunk on the bottom, served as evolutionary stepping stones. Outer shelf settings would preferably show an island character, as at the Orciano study site, best suited for speciation within small population of species commonly inhabiting coastal areas.

## References

- Allison P.A., Smith C.R., Kukert H., Deming J.W. and Bennett B.A. 1991. Deep-water taphonomy of vertebrate carcasses: A whale skeleton in the bathyal Santa Catalina Basin. *Paleobiology* 17, 78–89.
- Allmon W.D. 1988. Ecology of recent turritelline gastropods (Prosobranchia, Turritellidae): current knowledge and paleontological implications. *Palaios* 3, 259–284.
- Amano K. and Little C.T.S. 2005. Miocene whale-fall community from Hokkaido, northern Japan. *Palaeogeography, Palaeoclimatology, Palaeoecology* 215, 345–356.
- Bennett B.A., Smith C.R., Glaser B. and Maybaum H.L. 1994. Faunal community structure of a chemoautotrophic assemblage on whale bones in the deep northeast Pacific Ocean. *Marine Ecology Progress Series* 108, 205–223.
- Bertolaso L. and Palazzi S. 1993. La posizione sistematica di *Delphinula bellardii* Michelotti, 1847. *Bolletino Malacologico* 29, 291–302.
- Bianucci G. and Landini W. 2005. I paleositi a vertebrati fossili della Provincia di Pisa. *Atti della Società Toscana di Scienze Naturali, Memorie, Serie A* 110, 1–21.
- Bolotin J., Hrs-Brenko M., Tutman P., Glavic N., Kožul V., Skaramuca B., Lucic D. and Lucic J. 2005. First record of *Idas simpsoni* (Mollusca: Bivalvia: Mytilidae) in the Adriatic Sea. *Journal of the Marine Biological Association of the UK* 85, 977–978.
- Bray J.R. and Curtis J.T. 1957. An ordination of the upland forest communities of southern Wisconsin. *Ecological Monographs* 27, 325–349.
- Britton J.C. and Morton B. 1994. Marine carrion and scavengers. *Oceanography and marine biology, An annual review* 32, 369–434.
- Carnevale G., Longinelli A., Caputo D., Barbieri M. and Landini W. 2008. Did the Mediterranean marine reflooding precede the Mio–Pliocene boundary? Paleontological and geochemical evidence from upper Messinian sequences of Tuscany, Italy. *Palaeogeography, Palaeoclimatology, Palaeoecology* 257, 81–105.
- Clarke K.R. and Warwick R.M. 1994. Changes in marine communities: An approach to statistical analysis and interpretation. Plymouth Marine Laboratory, Plymouth, UK, 144 pp.
- Cortesi G. 1819. Saggi geologici degli stati di Parma e Piacenza. Torchj del Majno, Piacenza, 165 pp.
- Dahlgren T.G., Wiklund H., Källström B., Lundälv T., Smith C.R. and Glover A. 2006. A shallow-water whale-fall experiment in the north Atlantic. *Cahiers de Biologie Marine* 47, 385–389.
- Dahlgren T.G., Glover A.G., Baco A. and Smith C.R. 2004. Fauna of whale falls: systematics and ecology of a new polychaete (Annelida: Chrysopetalidae) from the deep Pacific Ocean. *Deep-Sea Research Part I* 51, 1873–1887.
- Distel D.L., Baco A.R., Chuang E., Morrill W., Cavanaugh C. and Smith C.R. 2000. Do mussels take wooden steps to deep-sea vents? *Nature* 403, 725–726.
- Dominici S., Cioppi E., Danise S., Betocchi U., Gallai G., Tangocci F., Valleri G. and Monechi S. 2009. Mediterranean fossil whale falls and the adaptation of mollusks to extreme habitats.



Geology 37, 815–818.

Fujiwara Y., Kawato M., Yamamoto T., Yamanaka T., Sato-Okoshi W., Noda C., Tsuchida S., Komai T., Cubelio S.S., Sasaki T., Jacobsen K., Kubokawa K., Fujikura K., Maruyama T., Furushima Y., Okoshi K., Miyake H., Miyazaki M., Nogi Y., Yatabe A., and Okutani T. 2007. Three-year investigations into sperm whale-fall ecosystems in Japan. *Marine Ecology* 28, 219–232.

Fretter V. 1960. Observations on the tectibranch *Ringicula buccinea* (Brocchi). *Proceedings of the Zoological Society of London* 135, 537–549.

Frey J.K. 1993. Modes of peripheral isolates formation and speciation. *Systematic Biology* 42, 373–281.

Goedert J.L., Squires R.L. and Barnes L.G. 1995. Paleocology of whale-fall habitats from deep-water Oligocene rocks, Olympic Peninsula, Washington State. *Palaeogeography, Palaeoclimatology, Palaeoecology* 118, 151–158.

Goffredi S.K., Paull C.K., Fulton-Bennett K., Hurtado L.A. and Vrijenhoek R.C. 2004. Unusual benthic fauna associated with a whale fall in Monterey Canyon, California. *Deep-Sea Research, Part I* 51, 1295–1306.

Hammer Ø., Harper D.A.T. and Ryan P.D. 2001. PAST: Paleontological statistics software package for education and data analysis: *Palaeontologia Electronica* 4, 1–9. [https://palaeo-electronica.org/2001\\_1/past/issue1\\_01.htm](https://palaeo-electronica.org/2001_1/past/issue1_01.htm). Checked January 2009.

Hrs-Brenco M. 2006. The basket shell, *Corbula gibba* Olivi, 1792 (Bivalve Mollusks) as a species resistant to environmental disturbances: A review. *Acta Adriatica* 47, 49–64.

Jones W.J., Won Y.J., Maas P.A.Y., Smith P.J., Lutz R.A. and Vrijenhoek R.C. 2006. Evolution of habitat use by deep-sea mussels. *Marine Biology* 148, 841–851.

Kaim A., Kobayashi Y., Echizenya H., Jenkins R.G. and Tanabe K. 2008. Chemosynthesis-based associations on Cretaceous plesiosaurid carcasses. *Acta Palaeontologica Polonica* 53, 97–104.

Kiel S. 2008. Fossil evidence for micro- and macrofaunal utilization of large nektonfalls: examples from early Cenozoic deep-water sediments in Washington State, USA. *Palaeogeography, Palaeoclimatology, Palaeoecology* 267, 161–174.

Kiel S. and Goedert J.L. 2006. Deep-sea food bonanzas: Early Cenozoic whale-fall communities resemble wood-fall rather than seep communities. *Proceedings of the Royal Society of London, Series B* 273, 2625–2631.

Lorion J., Duperron S., Gros O., Cruaud C. and Samadi S. 2009. Several deep-sea mussels and their associated symbionts are able to live both on wood and on whale falls. *Proceedings of the Royal Society B* 276, 177–185.

Myer E. 1963. *Animal Species and Evolution*. The Belknap Press of Harvard University Press, Cambridge, Massachusetts, 795 pp.

Miller-III W. 1986. Paleocology of benthic community replacement. *Lethaia* 19, 225–231.

Nesbitt E.A. 2005. A novel trophic relationship between cassid gastropods and mysticete whale carcasses. *Lethaia* 38, 17–25.

Notarbartolo di Sciara G., Agardy T., Hyrenbach D., Scovazzi T. and Van Klaveren P. 2008. The Pelagos sanctuary for Mediterranean marine mammals. *Aquatic Conservation. Marine and Freshwater Ecosystems* 18, 367–391.

Olu-Le Roy K., Sibuet M., Fiala-Medioni A., Gofas S., Salas C., Mariotti A., Foucher J.-P. and Woodside J. 2004. Cold seep communities in the deep eastern Mediterranean Sea: Composition, symbiosis and spatial distribution on mud volcanoes. *Deep-Sea Research I* 51, 1915–1936.

Pyenson N.D. and Haasl D.M. 2007. Miocene whale-fall from California demonstrates that cetacean size did not determine the evolution of modern whale-fall communities. *Biology Letters (Palaeontology)* 3, 709–711.

Rhoads D.C. 1974. Organism-sediment relations on the muddy sea floor. *Oceanography and Marine Biology* 12, 263–300.

Robertson R. and Mau-Lastovicka T. 1979. The ectoparasitism of *Boonea* and *Fargoa* (Gastropoda: Pyramidellidae). *The Biological Bulletin* 157, 320–333.

Smith C.R. 2006. Bigger is better: The role of whales as detritus in marine ecosystems. In: Estes J. (Ed.), *Whales, Whaling and Ocean Ecosystems*. Berkeley, University of California Press, pp. 284–299.

Smith C.R., Kukert, H. Wheatcroft R.A., Jumars P.A. and Deming J.W. 1989. Vent fauna on whale remains. *Nature* 34, 27–28.

Smith C.R., Baco A.R. and Glover A. 2002. Faunal succession on replicate deep-sea whale falls: time scales and vent-seep affinities. *Cahiers de Marine Biologie* 43, 293–297.

Smith C.R. and Baco A.R. 2003. Ecology of whale falls at the deep-sea floor. *Oceanography and Marine Biology Annual Review* 41, 311–354.

Taylor J.D. 1980. Diets and habitats of shallow water predatory gastropods around Tolo Channel, Hong Kong. In: Morton B. (Ed.), *The Malacofauna of Hong Kong and Southern China*. Hong Kong University Press, Hong Kong, pp. 163–180.

Taylor J.D. and Glover E.A. 2006. Lucinidae (Bivalvia) – the most diverse group of chemosymbiotic mollusks. *Zoological Journal of the Linnean Society* 148, 421–438.

Todd J.A. 2000. Introduction to molluscan life habits databases, updated March 27, 2001, <http://eusmilia.geology.uiowa.edu/database/mollusc/mollusclifestyles.htm>. Checked February 2009.

Warén A. and Carrozza F. 1990. *Idas ghisotti* sp. n., a new mytilid bivalve associated with sunken wood in the Mediterranean. *Bollettino Malacologico* 26, 19–24.

Warén A. 1991. New and little known Mollusca from Iceland and Scandinavia. *Sarsia* 76, 53–124.

## Appendix

Orciano Pisano data base: absolute abundances of mollusk species within samples.

FAMILY	SPECIES	OP1	OP2	OP3	OP4	OP5	OP6	OP7	OP8	OP9	OP10	OP11	OP12	OP13	OP14	OP15	OP16	OP17	tot
<b>GASTROPODA</b>																			
Trochidae	<i>Gibbula sp.1</i>	0	0	0	0	0	0	0	0	0	0	0	0	0	0	0	0	0	1
Trochidae	<i>Gibbula sp.2</i>	0	0	0	0	0	0	0	0	0	0	1	0	0	0	0	0	0	1
Trochidae	<i>Calliostoma granulatum</i>	0	1	0	0	1	0	0	0	0	0	0	4	0	2	0	1	0	9
Trochidae	<i>Calliostoma sp.</i>	0	0	1	1	0	0	0	0	0	0	0	0	1	0	0	0	0	3
Trochidae	indet.	0	0	0	0	0	0	0	0	0	0	0	0	0	0	0	0	1	1
Skeneidae	<i>Skenea sp.</i>	0	0	0	0	0	0	0	0	0	0	0	0	0	0	0	1	0	1
Iravadiidae	<i>Hyala vitrea</i>	0	0	0	0	0	0	0	1	0	0	0	1	0	0	0	1	0	3
Cerithiidae	<i>Cerithium vulgatum</i>	0	0	0	0	0	0	0	0	0	0	0	1	0	0	0	0	0	1
Cerithiidae	<i>Bittium lacteum</i>	0	0	0	0	1	0	0	0	0	0	0	0	0	0	0	0	0	1
Potamididae	<i>Potamides tricintus</i>	1	0	0	0	0	0	0	0	0	0	0	0	0	0	0	0	0	1
Turritellidae	<i>Turritella tricarinata</i>	0	0	5	1	6	7	0	0	0	0	2	28	0	0	2	0	6	57
Turritellidae	<i>Archimediella spirata</i>	5	4	1	4	2	1	2	2	3	7	4	80	50	72	0	2	1	240
Vermetidae	<i>Petalocochnus intortus</i>	0	0	1	0	0	1	0	0	0	0	0	0	0	0	0	0	0	2
Vermetidae	<i>Serpulorbis arenarius</i>	0	1	0	0	0	0	0	0	0	0	0	0	0	0	0	0	0	1
Vermetidae	<i>Vermetus sp.</i>	0	0	0	0	0	0	0	0	0	2	0	0	0	0	0	0	0	2
Calipteridae	<i>Crepidula sp.</i>	0	1	0	0	0	0	0	0	0	2	0	0	0	0	0	0	0	3
Aporrhaidae	<i>Aporrhais uttingeriana uttingeriana</i>	1	2	1	4	1	0	2	1	2	0	0	4	1	3	0	0	1	23
Naticidae	<i>Euspira helicina</i>	0	0	2	0	1	1	0	3	0	0	0	0	0	0	0	0	4	11
Naticidae	<i>Natica tigrina</i>	0	0	0	2	0	0	0	0	0	0	0	0	0	0	0	0	0	2
Naticidae	<i>Natica sp.</i>	1	3	2	0	0	0	0	0	0	0	1	2	2	4	0	1	0	16
Cassidae	<i>Galeodea echinophora</i>	0	0	0	2	0	0	0	1	0	0	0	0	0	0	0	0	0	3
Triphoridae	<i>Triphora perversa</i>	0	0	1	0	0	0	0	0	0	0	0	0	0	0	0	0	0	1
Epitonidae	<i>Epitonium frondiculoideis</i>	7	3	3	0	12	6	2	1	1	0	1	1	0	3	1	1	3	45
Epitonidae	<i>Epitonium turtoni</i>	0	0	0	1	0	1	0	0	0	0	0	2	0	0	0	0	0	4
Epitonidae	<i>Epitonium sp.</i>	0	0	0	0	0	0	0	0	0	1	0	0	0	0	0	0	0	1
Muricidae	<i>Ocenebrina aciculata</i>	0	1	0	0	0	0	0	0	0	0	0	0	0	0	0	0	0	1
Buccinidae	<i>Phos cf. polygonus</i>	1	1	0	0	0	0	0	0	0	0	0	0	0	0	0	0	0	2
Nassariidae	<i>Nassarius costulatus</i>	0	0	0	0	0	0	0	0	0	0	0	0	1	0	0	0	0	3
Nassariidae	<i>Nassarius semistriatus</i>	2	2	6	3	3	4	1	3	0	3	2	20	9	9	1	2	11	81
Cancellariidae	<i>Sveltia tribulus</i>	0	0	0	0	0	0	0	0	0	0	0	3	0	0	0	0	0	3
Turridae	<i>Stenodrillia bellardii</i>	0	0	0	0	0	0	0	0	0	0	0	1	0	0	0	0	0	1
Turridae	<i>Gemmula contigua</i>	1	1	3	1	0	1	0	0	0	0	0	0	0	0	0	0	0	8

FAMILY	SPECIES	OP1	OP2	OP3	OP4	OP5	OP6	OP7	OP8	OP9	OP10	OP11	OP12	OP13	OP14	OP15	OP16	OP17	tot
Conidae	<i>Comarmondia</i> sp.	0	0	0	0	1	0	0	0	0	0	0	0	0	0	0	0	0	1
Pyramidellidae	<i>Pyramidella plicosa</i>	0	0	3	0	0	0	0	0	0	0	0	1	0	2	1	0	1	8
Pyramidellidae	<i>Odostomia acuta</i>	4	9	2	0	1	0	2	0	0	0	0	0	0	0	0	0	0	18
Pyramidellidae	<i>Odostomia conoidea</i>	5	0	10	0	2	7	0	0	0	0	0	0	0	0	0	2	7	33
Pyramidellidae	<i>Odostomia</i> sp.	0	0	0	0	0	0	0	1	1	0	0	0	0	7	0	0	0	9
Pyramidellidae	<i>Turbonilla lactea</i>	0	1	3	0	0	0	0	0	0	0	0	0	0	0	0	0	0	4
Ringiculidae	<i>Ringicula auriculata</i>	8	13	20	2	14	6	3	1	3	7	4	9	7	4	0	0	7	108
Ringiculidae	<i>Ringicula ventricosa</i>	5	0	0	0	4	0	0	0	0	0	0	0	0	0	4	3	0	16
Cyllichnidae	<i>Scaphander lignarius</i>	0	0	0	0	0	0	0	0	0	0	0	1	0	0	0	0	0	1
Cyllichnidae	<i>Cyllichnina</i> sp.	0	0	0	1	0	0	0	0	0	0	0	0	0	0	0	0	0	1
<b>BIVALVIA</b>																			
Nuculidae	<i>Nucula placentina</i>	0	0	0	0	0	0	0	0	0	0	0	1	0	0	0	1	2	4
Nuculidae	<i>Nucula jeffersi</i>	1	0	0	0	0	0	0	0	0	0	0	0	0	0	0	0	0	1
Nuculidae	<i>Nucula sulcata</i>	3	4	3	2	0	6	2	1	0	4	3	10	7	3	2	1	2	53
Nuculanidae	<i>Nuculana concava</i>	0	0	0	0	0	0	0	0	0	0	0	1	0	0	0	0	0	1
Nuculanidae	<i>Nuculana hoernesii</i>	0	0	0	0	0	0	0	0	0	0	0	2	0	0	0	0	0	2
Nuculanidae	<i>Nuculana fragilis</i>	15	13	11	9	8	8	3	2	1	4	1	6	4	5	4	1	5	100
Nuculanidae	indet.	10	16	9	0	5	2	2	3	3	7	3	3	4	4	1	4	7	83
Yoldiidae	<i>Yoldia nitida</i>	24	15	17	14	12	8	6	0	2	6	4	7	14	7	1	4	13	154
Yoldiidae	<i>Yoldia mendax</i>	0	0	3	0	2	6	0	0	2	0	0	6	0	0	1	2	0	22
Arcoideae	<i>Arca tetragona</i>	0	0	0	0	0	0	0	1	0	0	0	0	0	0	0	0	0	1
Arcoideae	<i>Anadara dilatavi</i>	6	2	4	5	2	3	1	0	2	2	2	5	3	6	1	0	4	48
Limopsidae	<i>Limopsis aurita</i>	0	0	0	0	0	1	0	0	1	1	2	1	0	2	0	0	1	9
Limopsidae	<i>Limopsis minuta</i>	2	1	2	1	1	0	0	0	0	0	0	0	0	0	2	0	0	9
Mytilidae	<i>Modiolula phaseolina</i>	4	2	5	2	2	4	1	0	0	0	0	0	0	2	0	0	1	23
Mytilidae	<i>Modiolus adriaticus</i>	0	0	0	0	0	0	0	0	0	0	0	1	0	0	0	0	0	1
Mytilidae	<i>Idas</i> sp.	1	1	0	0	0	0	0	0	0	0	0	0	0	0	0	0	0	2
Limidae	<i>Linea strigilata</i>	1	4	3	2	2	0	1	1	0	0	0	0	2	0	2	2	2	22
Pectinidae	<i>Chlamys glabra</i> cf. <i>flexuosa</i>	2	3	3	0	1	0	1	0	0	1	0	2	6	2	0	0	3	24
Pectinidae	<i>Chlamys pesfelis</i>	3	3	1	0	0	1	2	0	2	0	0	3	2	2	1	1	0	21
Pectinidae	<i>Chlamys varia</i>	0	4	5	1	2	5	3	0	1	1	2	5	2	2	0	0	3	36
Pectinidae	<i>Chlamys</i> sp.	0	0	0	0	1	0	0	1	0	0	0	1	0	0	0	0	0	3
Pectinidae	<i>Aequipecten opercularis</i>	2	0	0	0	0	0	0	0	0	0	0	1	0	0	0	0	0	3
Pectinidae	<i>Pecten</i> sp.1	1	0	0	0	0	0	0	1	0	0	0	0	1	0	0	0	0	3
Pectinidae	<i>Pecten</i> sp.2	0	0	0	0	0	0	0	0	0	0	0	0	0	0	1	0	0	1
Pectinidae	<i>Propeamussium duodecylamellatum</i>	0	0	0	0	0	0	0	0	0	0	0	2	0	0	0	0	0	2
Pectinidae	<i>Amusium cristatum</i>	3	2	2	1	1	2	2	2	1	2	0	0	3	2	1	2	2	28



# CHAPTER 4 — Taphonomy of Neogene Mediterranean fossil whales

---

## 4.1 Introduction\*

Since great whales are the largest animals living, and possibly that have ever lived, it is no wonder that in the course of becoming part of the fossil record many things can occur. Large size conditions the causes of death of large whales, which can easily escape predation and naturally die in most cases of disease. Given poor nutritional conditions upon death, most dead whales are negatively buoyant and sink to the sea floor (Smith 2006 and references therein). The following destiny of the carcass depends then in large part on water depth. Actualistic studies indicate that if a carcass sinks to relatively deep bottoms, hydrostatic pressure will limit the generation of buoyant decompositional gases through reduction of gas volume and increased gas solubility (Allison et al. 1991). At depths greater than 1.000 m the soft tissue of a carcass will be removed by scavengers or consumed by microbial decomposers long before positive buoyancy can be generated. The carcass will thus remain on the sea floor (Allison et al. 1991). At shallower depths, gas generation will refloat whale carcasses (Schäfer 1972), depending on the rate of decomposition by microbes. High levels of scavenging may prevent high rates of decomposition, so that not all shallow water carcasses will refloat (Allison et al. 1991). A floating carcass will continue to decay, removal of supportive soft tissues promoting disarticulation of skeletal elements (Schäfer 1972).

In the shelf taphonomic pathways are complex and natural whale falls extremely rare (Smith 2006), partly justifying why most time series studies on natural or artificially implanted carcasses have focused on the deep sea (Allison et al. 1991, Smith and Baco 2003, Goffredi et al. 2004, 2008, Lundsten et al. 2010), only some dealing also with whale falls close to the shelf edge (Braby et al. 2007, Fujiwara et al. 2007). In the deep sea carcasses are more unlikely to refloat and naturally rest on the sea floor for several decades (Allison et al. 1991). Deep sea whale falls have been known to pass through four main stages of ecological succession: the mobile scavenger stage, the enrichment opportunist stage, the sulphophilic stage and the reef stage, during which all the whale organic matter is gradually consumed by a highly specialized fauna (Smith et al. 2002). Specialization occurs at more than one level, depending on the clade. For example, whale fall bivalves belong to chemosymbiotic families exclusive of extreme reducing environments such as cold seeps and hydrothermal vents, whereas polychaetes genera show more pronounced specialization to life on whale bones, as is the case with the bone-eater

---

\* Part of this chapter consists of a paper by Dominici S., Cioppi E., Danise S., Betocchi U., Gallai G., Tangocci F., Valleri G. and Monechi S., "Mediterranean fossil whale falls and the adaptation of mollusks to extreme habitats" published in volume 37 of *Geology* (2009). The rest is unpublished.

*Osedax* (Rouse et al. 2004). Biological and physical processes at whale carcass on the shelf are little known. Apart from anecdotal knowledge from the rare natural occurrences (Smith 2006), modern data are available only from the three artificial experiments performed so far in cold temperate seas (Dahlgren et al. 2006, Pavyluck et al. 2009, Glover et al. 2010). These suggest the development of successional stages, with some differences with respect to the deep sea. In general, the carcasses are consumed by generalist mobile scavengers commonly living in the same area, and rate of decomposition expressed in terms of time taken to remove all the flesh is significantly slower compared to deep-water analogs (Glover et al. 2010). Obligate whale-fall species thrive also on the shelf, like the siboglinid eating-bone *Osedax* (Glover et al. 2005, Dahlgren et al. 2006). Chemosymbiotic bivalves in modern shallow water settings are known only from rare reports not focusing on whale fall ecosystems (Marshall 1900, Wären 1991) and from one instance reported here (Chapter 2).

If modern whale fall literature is skewed towards the deep sea, paleontological research has done so far the same. One reason for this is the interest that paleontologists have for whale fall hard-shelled invertebrates, with a relatively good fossil record, such as the chemosymbiotic bivalves. Since these live in practice only below the shelf break (Dando 2010), all published paleontological papers deal with deep water whale fall molluscs (Squires et al. 1991, Goedert et al. 1995, Amano and Little 2005, Nesbitt et al. 2005, Kiel and Goedert 2006, Amano et al. 2007, Pyenson and Haas 2007). Quite the opposite approach was made available from the recovery in 2007 of the first natural shallow water whale fall ever studied, both modern or fossil (Dominici et al. 2009; Danise et al. 2010: Chapter 3). Paleontologists working with large marine vertebrates are accustomed at understanding the serial stages which have preceded the final burial (biostratinomic processes: Kauffman 1981, Martill 1985, 1987, Lancaster 1986) and have easily switched their attention after the news coming from marine biologists, taking modern whale falls as viable analogs for the fossil record of Mesozoic reptiles (Hogler 1994, Martill et al. 1995). The feedback between paleontology and marine biology has narrowed the focus to whale carcasses with the 2007 recovery of an articulated 10 m mysticete (Dominici et al. 2009), when it became clear that the taphonomic analysis of the fossil marine vertebrate and its associated fauna could bring new insights to the understanding of physical and biological processes at whale falls on a time scale not available in modern time series studies. That finding also meant a reconsideration of a rich record of Italian fossil whales, in search for missed hints at extreme and often complex interactions between large carcasses and specialized marine invertebrates.

Fossil cetaceans are abundant in marine Neogene shallow marine sediments of Italy, particularly in the central and northern regions of Piedmont, Emilia Romagna and Tuscany (Bianucci and Landini 2005, Bisconti 2009). Many discoveries of fossil mysticetes, including almost complete skeletons, date back to the early 19<sup>th</sup> century, when the first excavations were reported within taxonomic monographs by Italian paleontologists. The first important monograph on Italian fossil mysticetes was written by Giuseppe Cortesi (Cortesi 1819). In his book Cortesi described three fossil mysticetes, and he focused not only on the morphology of

the specimens, but also on the taphonomic context and the geological setting. Its first, true taphonomic work on marine vertebrate remains, inspired other important paleontologists, like Giovanni Capellini, Pellegrino Strobel, and Alessandro Portis that wrote large monographs on Italian fossil whales (Capellini 1865, Strobel 1881, Portis 1885). In the 20th century and in the first decade of the 21st further excavations were carried out (Caretto 1970, Sarti and Gasparri 1996, Chicchi and Scacchetti 2001) increasing museum collections.

In the present work, data obtained from the case study on the 10 m long baleen whale from the Pliocene of Tuscany (Dominici et al. 2009) served as a template for the analysis of twenty-four analogs hosted in northern and central Italy museum collections. Not all the taphonomical data that can be gathered following a modern approach in the excavation and study of a large fossil vertebrate are available when studying a museum specimen, but some are. Among the latter, the degree of bone articulation, the completeness of the skeleton, and the lithology of the embedding sediments can give information on water depth, current intensity and rate of burial of the bones (Martill 1985, 1987, Lancaster 1986, Allison et al. 1991). Shark teeth in close association with the bones, which past researchers seem to have not missed (Bianucci et al. 2002), and hard shelled invertebrates with a necrophagous diet, occasionally reported in records of past excavations, testify scavenging. Fossil bone bioerosion, cementation, and hard shelled organisms in the proximity of the remains can inform on past biological activity around the bones at the micro- and mesoscale (Martill 1987, Allison et al. 1991).

## 4.2 General setting

The fossil skeletons here under study are twenty-five fossil mysticetes, numbered from W1 to W25. Twenty-four are from the Pliocene, one from the middle Miocene (Serravallian) (Appendix).

The studied specimens are from two different paleogeographic domains of the Italian peninsula, the paleo-Adriatic and the paleo-Tyrrhenian domain, both related to the tectonic evolution of the northern Apennines. The northern Apennine fold-thrust belt was formed by collision between the European plate (Corsica-Sardinia block) and the Adriatic microplate (related to the African plate). The thrust imbrication includes the formation of an Upper Cretaceous–Cenozoic polyphase accretionary wedge characterized by the migration of the foredeep depocenters towards the foreland, actually located in the Adriatic Sea. Successively, during the Neogene, the Apennine thrust belt was interested by a NNE-migrating pattern, with a compressional regime in the front of the chain (paleo-Adriatic domain) and extension in the hinterland area (paleo-Tyrrhenian domain) (Carmignani et al. 2001).

Specimens W2-W4 belong to the Pliocene Asti Basin, the North-Western extension of the paleo-Adriatic sea (Figure 1). The basin is filled by a regressive sedimentary succession of circalitoral mudstones of Zanclean age at the base, followed by Piacentian shallow-marine sandstones (Ferrero and Pavia 1996, Polino and Clari 2003). Specimens W5-W16 come from the



Pliocene portion of late Eocene to early Pleistocene satellite basins cropping out in the northern Apennines. These satellite, piggy-back basins are mostly filled by terrigenous, diachronous deposits, originated during the NE migration of the Apennine thrust belt (Ricci Lucchi 1987). In particular, specimens W5-W13 come from the Castell'Arquato basin, whereas specimens W14-W16 are from the Pliocene Intra-Apenninic Basins of the Bologna and Modena Apennines. Specimens W1, W17-W24 belong to the Pliocene portion of Neogene hinterland basins located on the Tyrrhenian side of the northern Apennines. They are part of the paleo-Tyrrhenian domain and originated in the internal portion of the chain, when important extensional tectonic events were superposed upon existing compressional structures (Carmignani et al. 2001). The sedimentary fill of Tyrrhenian basins typically consists of Tortonian continental deposits at the base, covered by brackish, evaporitic, and marine sediments of Messinian to Pleistocene age (Bossio et al. 1992). The older Miocene whale (W25) comes from the earlier filling of piggy-back basins of the Northern Apennines, belonging to the Epiligurid succession. It comes from the Monte Vallassa Formation, which ranges in age from the Serravallian to the Tortonian, and is an approximately 400 m thick sequence forming a marine transgressive cycle going from coastal settings to inner and outer shelf deposits (Bellinzona et al. 1971).

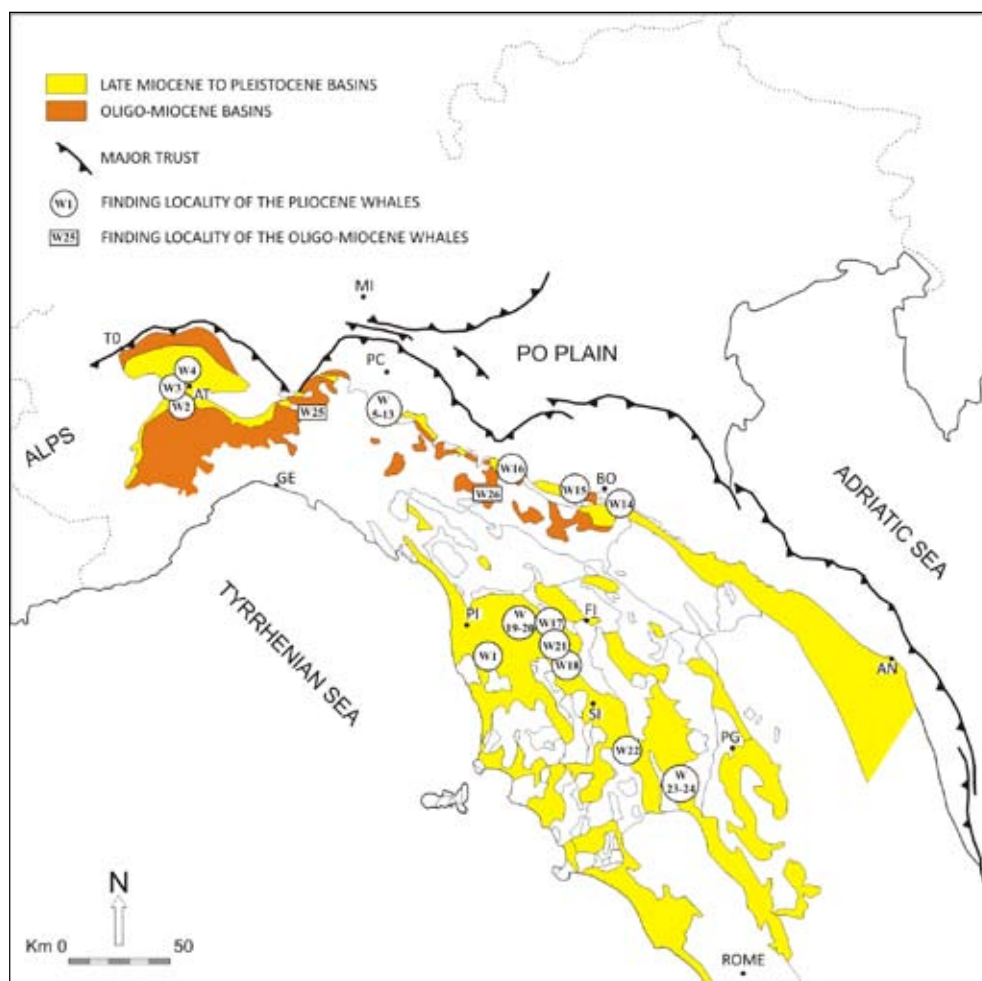


Figure 1. Location map of the localities of recovery of the studied fossil whales and schematic geological map. Modified from Vai (2001).

### 4.3 Materials and methods

During the excavation and the museum preparation of the Orciano Pisano fossil whale (W1) information on the taphonomy of the bones and the position of the associated macrofauna respect to the whale skeleton were recorded. To evaluate the level of generality of the Orciano Pisano finding, Italian Neogene collections were surveyed for large more or less complete whale skeletons that could have hosted a whale fall community (n=20, including W1). We have included large skulls in the absence of postcranial bones (n=2) and articulated vertebral columns in the absence of the skull (n=3). We have not considered isolated bones, which were however abundant in some collections. A total of twenty four museum specimens were tested for the taphonomic variables recognized in W1 (Appendix). For each specimen information on the taphonomy of the fossil bones and on the associated biota were gathered (Table 1). Taphonomic data on the bones concerns (a) the articulation, (b) the completeness of the skeleton, the preservation of (c) cortical bones and (d) vertebral processes and (e) the cementation. Information on the associated biota include presence/absence of (f) shark teeth, (g) chemosynthetic bivalves, (h) encrusting epibionts or (i) other invertebrates associated with the bones, identified at the highest taxonomic level possible. Bone articulation is “high” when all the bones lie in positions, showing true bone-to-bone relationships with adjacent elements of the skeleton; “medium” when the bones are slightly displaced from their original position and the original skeleton outline is still recognizable; “low” when the skeletons are completely disarticulated. Skeletal completeness is “high” when all the main constituent of the skeleton were recovered (skull, jaws, arms, ribs, vertebrae); “low” when one or more skeletal element is missing. Cortical bone preservation can be “high”, “medium” or “low” if the outer cortical bone is still in place, or if it is partially removed or absent, respectively. Vertebral process preservation is “high” when spinous processes are well preserved; “medium” when they are partially preserved; “low” when they are absent. Cementation was considered “high” when large part of the skeleton are enclosed in a carbonate concretion (*e.g.*, the whole thoracic region); “medium” if cements occur in localized areas, otherwise “absent”. Encrusting epibionts were recorded when observed directly on the bone surface. Data on the presence/absence of shark teeth were considered reliable, since these fossils particularly attracted palaeontologists (*e.g.*, Bianucci et al. 2002) during excavations and have possibly never escaped recovery. On the other hand the absence of chemosymbiotic bivalves and other invertebrates from museum collections was interpreted as a missing datum (“n.d.”).

All these variables were recorded from different sources, including the direct observation of museum specimens, literature data on the excavations, oral interviews to people who have participated to excavations, and in rare occurrences from samples collected in the field. Additional data gathered from the literature concerned the age and taxonomy of each fossil whale and the lithology of the embedding sediments. In seven cases (W1, W14-W16, W21-W23) the original outcrop of provenance was retraced, studied in detail, and bulk sampled for

paleoenvironmental estimates (see Chapter 6). All the collected information are summarized in the Appendix, and the results displayed and compared in synthetic histograms.

**Table 1. List of the main taphonomic and paleoecologic variables considered in this study.**

<b>TAPHONOMY OF THE BONES</b>		
a	Bone articulation	high, medium, low
b	Completeness of the skeleton	high, low
c	Cortical bone preservation	high, medium, low
d	Vertebral process preservation	high, medium, low
e	Bone cementation	high, medium, absent
<b>BIOTA ASSOCIATED WITH THE BONES</b>		
f	Shark teeth	present, absent
g	Chemosymbiotic bivalves	present, absent , n.d.
h	Encrusting epibionts	present, absent
i	Other invertebrates	present, absent , n.d.

The analyzed fossil whales are hosted in the following museums are: MGPT: Museo di Geologia e Paleontologia, Torino (TO); MPSC: Museo Paleontologico San Pietro in Consavia (AT); CMSNV: Civico Museo di Scienze Naturali di Voghera (PV), MPP: Museo Paleontologico Parmense (PR); MGC: Museo Geologico, Castell'Arquato (PC); MGCB: Museo "G. Capellini", Bologna (BO); MCRE: Musei Civici di Reggio Emilia (RE); MSNT: Museo di Storia Naturale e del Territorio, Università di Pisa, Calci (PI); MSNF: Museo di Storia Naturale, Firenze (FI); MCPG: Museo Civico di Palazzo Guicciardini, Montopoli in Valdarno (PI); CVB: Castello di Villa Banfi (SI); MCGA: Museo dei cicli geologici, Allerona (TR).

## 4.4 Results

### 4.4.1. Taphonomy of the Orciano Pisano whale

W1 was found lying on its ventral side in a massive silty fine grained sandstone, about 20 cm above a shell bed dominated by the gastropod *Archimediella spirata*. Spatangoid echinoderms, large decapods, and most bivalves (Figure 2A–E) occur in life position, all of which are consistent with a low-energy setting below storm-weather wave base. W1 bones maintain their original relative position and are only slightly displaced (Figure 2H–H'), but they are not pristine. Possibly all caudal vertebrae are present, but they lack dorsal processes and are frequently cemented one to the other in the lowermost part. Their cortical bone layer is corroded, exposing a fragile "spongy" bone tissue, increasingly so as the chest region is approached. Thoracic vertebrae are lacking, and cervical bones are cemented. Costae, symmetrical around the vertebral column,

preserve a large part of their cortical layer. One tympanic bulla bears bite marks (Figure 2G). The skull is heavily worn. Macrofossils directly associated with W1 include remains of pelagic (white and blue sharks; Figure 2F) and benthic predators and scavengers (gastropods, decapods) and many other heterotrophs (Figure 3). Articulated specimens of the chemosymbiotic lucinid *Megaxinus incrassatus* (for adaptations in lucinids, see Williams et al., 2004) and large specimens of the bivalve *Glossus humanus* were recovered in life position by the chest and the skull (Figure 2A, E).

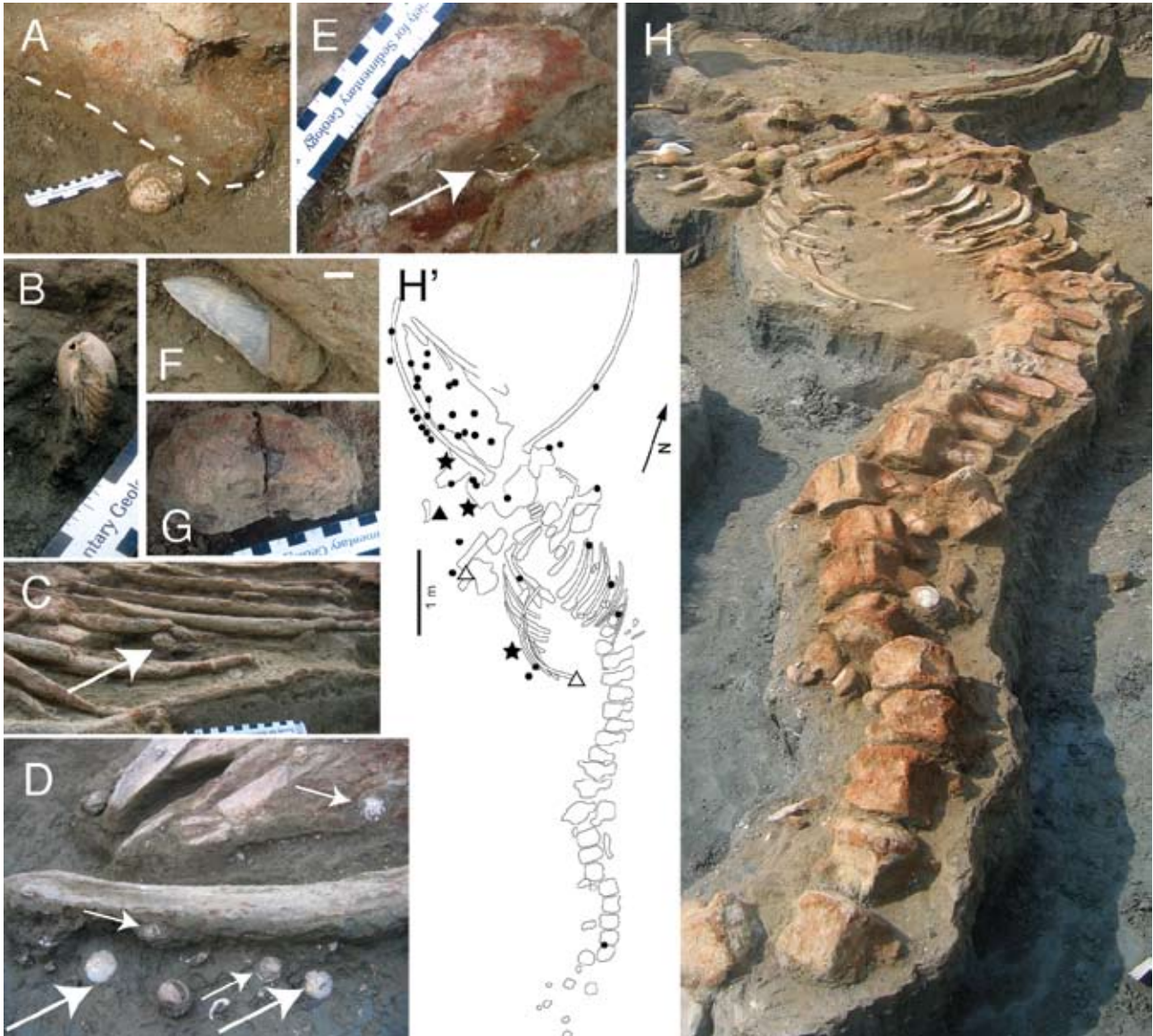


Figure 2. Taphonomy and paleoecology of Orciano Pisano fossil whale (W1; IGF 9299V). A. *Glossus humanus* (IGF 14635E) in life position below neurocranium (dashed line outlines scapula). B. *Megaxinus incrassatus* (IGF 14634E) in vertical position near left humerus. C. *M. incrassatus* in horizontal position below a costa (arrow). D. Tip of skull, with *Amusium cristatum* (long arrows) and *M. incrassatus* (short arrow). E. Articulated *M. incrassatus* below heavily damaged large bones. F. Large tooth of *Carcharodon carcharias* (IGF 9314V). G: Tympanic bulla with deeply cut marks. H: Field view of W1 showing articulated, but damaged caudal vertebrae and lacking dorsal vertebrae. H'. Orthogonal sketch of W1 with position of *M. incrassatus* (circles), *G. humanus* (stars), and teeth of white shark (*Carcharodon carcharias*—open triangles) and blue shark (*Prionace glauca*—black triangle). Scale bars are in cm in A, C, and E–G, inches in B, and m in H; D is 90 cm wide.



Figure 3. Macrofauna associated with the Orciano Pisano whale (W1). A. The gastropod *Aporrhais uttingeriana*. B. *Ostrea* sp. attached to a caudal vertebra. C. The carnivore gastropod *Fusinus longiroster* next to caudal vertebrae.

#### 4.4.2 Other Italian fossil whales

The twenty five analyzed specimens of the full dataset (n=25) are evenly distributed between sandy sediments (52%) and mudstones (48%). 28% are fully articulated skeletons, 24% have the bones slightly displaced from their original position, 36% are disarticulated, for the rest (12%) no data are available (Figure 4A, 7). Most of the disarticulated skeletons were embedded in sandstones (67%), the rest in mudstones, whereas well articulated specimens come from sandstones in the 43% of the cases (Figure 5A). W22, an highly disarticulated specimen, shows a bivariate orientation of the bones (Figure 7D). It was recovered from silty sandstones associated with a shell bed made by disarticulated and nestling bivalves, clues of reworking (see Chapter 6). Half of the fossil skeletons are complete (Figure 4A). Among incomplete skeletons four are acephalous, and two conserve only the skull (Appendix). 67% of low articulated specimens are also incomplete, whereas most of the well articulated skeletons (86%) have a high degree of completeness (Figure 5B). More than half of the specimens preserve the external cortical bone tissue (60%), which is partially preserved or absent in the 36%. Vertebral processes are pristine in the 32% of the fossil whales, partially damaged in the 24%, totally absent in the 20%, no available data in the 24% (Figure 4A, 8A-C). The 20% of the fossil whales are highly cemented (Figure 4A). The thoracic region, which includes cervical and thoracic vertebrae and the ribs, is the most interested by cementation (Figure 8D). Highly cemented specimens have in most of the cases a good degree of cortical bone preservation (80%) and most of them come

from muddy sediments (Figure 6A-B). A medium degree of cementation was observed in the 36% of the specimens, e.g. Figure 8E, where isolated ribs are cemented. The rest shows no cementation or there are no available data (Figure 4A).

Shark teeth associated with fossil bones are documented for almost half of the fossil whales (40%) (Figure 4B). They come more frequently from articulated (71%) than disarticulated skeletons (44%) (Figure 5C). They are found directly in contact with the bones, as in W1, or in the nearest sediments (Figure 9A). The identified species are *Carcharodon Charcarias* (W1, W15, W17, W22), *Prionace glauca* (W1), *Carcharinus cf. brachyurus* (W22), *Odontaspis* sp. (W17), *Isurus oxyrhincus* (W3), *Galeorhinus galeus* (W7), and cf. *Galeorhinus galeus* (W15). Cemented epibionts directly attached to the external surface of the bones were found on the 44% of the specimens (Figure 4B). They consist mostly of molluscs of the family Ostreidae, with specimens up to 10 cm in length (Figure 9C-D) and balanid barbacles, solitary (Figure 9B) or gregarious (Figure 9E-F). Bioencrustation was recovered both from sandy and muddy sediments (Figure 6C).

No data are available for chemosymbiotic bivalves associated with the fossil bones, except for W1 (Figure 4A). Other invertebrates were recovered in the 40% of the cases (Figure 4B). These are molluscs in most cases, and decapods reported in W16 and W17. Within the molluscs the most represented trophic category is the suspension feeders, including bivalves of the family Glossidae, Pectinidae, Veneridae and Mytilidae (Figure 10). Tens of specimens of *Glossus humanus* were found in life position next to intervertebral disks of W8 (Figure 10A). Pectinids were associated with specimens W3, W5, W17, W20 and W21, and are represented by the species *Amusium cristatum*, *Chlamys opercularis* and cf. *Chlamys varia* (Figure 10D). The venerid *Pelecypora brocchi* is associated with specimens W15 (Figure 10C) and W24 (Figure 10E). Unidentified mytilids are associated with W5 and W21, *Mytilus* sp. with W14 and *Modiolus* sp. with W16. Deposit feeders were found at W3 (*Aporrhais uttingeriana uttingeriana*, *Tellina compressa*) and W17 (*Aporrhais uttingeriana uttingeriana*, *Dentalium fossile*). Predatory carnivores are represented by naticid gastropods at W5, W15 and W20 (Figure 10E), and by *Ficus* sp. (W14, Appendix). Among scavenging gastropods, nassarids were found (*Nassarius italicus*: W3; W20).

**Next page:**

**Figure 4. Histograms summarizing collected data on the 25 fossil whales. A. Taphonomic data: bone articulation, cortical bone preservation, vertebral process preservation, bone cementation. B. Biota associated with the bones: shark teeth, encrusting epifauna, chemosynthetic bivalves, other molluscs. All data expressed in per cent.**

**Figure 5. Bar diagrams in which bone articulation is compared with other taphonomic and paleoecologic variables. A. Comparison between the degree of bone articulation and the litology of the embedding sediments. B. Bone articulation compared with skeletal completeness. C. Comparison between bone articulation and the presence/absence of shark teeth. vs: versus.**

**Figure 6. Bar diagrams comparing some of the measured taphonomic and paleoecologic variables. A. Degree of bone cementation respect to cortical bone preservation. B. Changing of degree of cementation with litology. C. Distribution of encrusting epibionts respect to litology.**

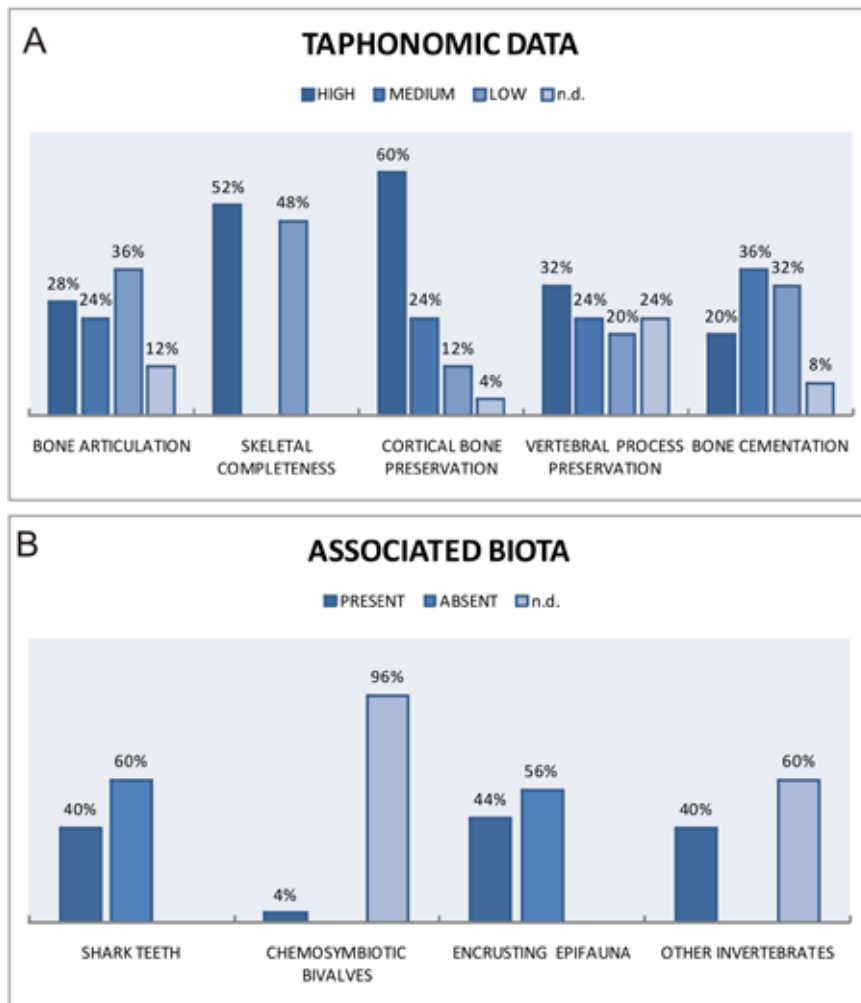


Figure 4

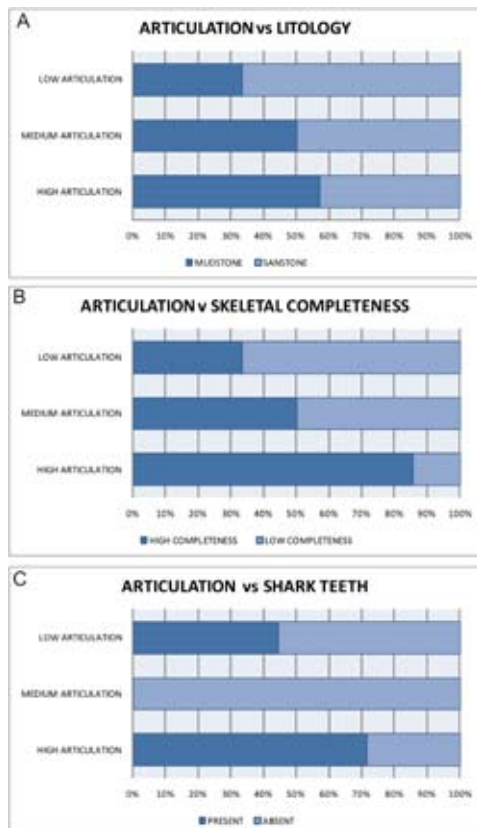


Figure 5

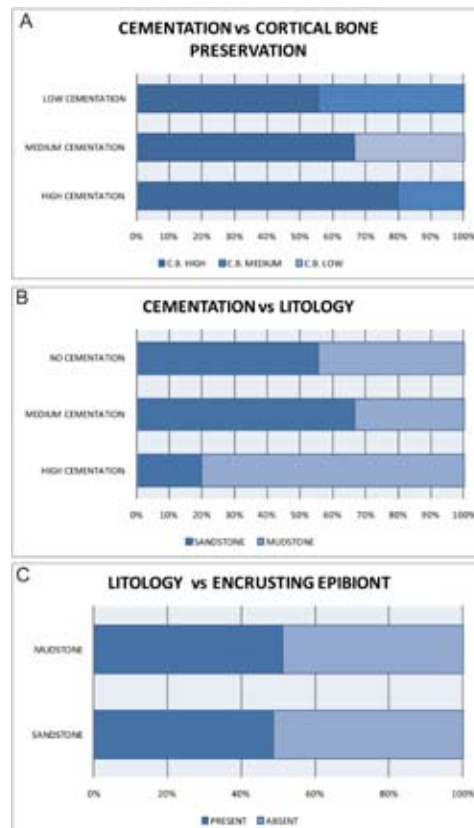


Figure 6



**Figure 7. Taphonomic data from fossil whale bones: different degrees of skeletal articulation. A. W10 with highly articulated bones and well preserved vertebral processes. B. W16 in fine grained silty sandstones, with a medium degree of bone articulation; note the ribs in anatomical position whereas vertebrae are displaced. C. Acephalous W18 in sandy sediments; like in the former specimen (W16), ribs are in true position and vertebrae missing or displaced. D. W22, Highly disarticulated specimen; note the bimodal distribution of the bones.**





Figure 8. Taphonomic data from fossil whale bones: cortical bone and vertebral process preservation, and cementation. A. W15 with highly bioeroded vertebra and badly preserved compact bone tissue. B. W13 with partially preserved spinous processes and partially preserved compact bone. C. W11 with intact spinous processes and well preserved outer compact bone. D. Articulated skeleton with pristine costae, heavily cemented to thoracic vertebrae in unconsolidated muds (W17). E. Isolated ribs partially enclosed in a carbonate concretion.



Figure 9. Shark teeth and encrusting epifauna associated with fossil whale bones. A. W17 with *Carcharodon carcharias* tooth next to the bones (see Bianucci et al. 2002). B. Large solitary balanid barnacle on one vertebral process (W22). C and D. Ribs and mandibles with encrusting oysters(W16). E. W11 highly preserved vertebrae encrusted with balanid barnacles (arrow). F. Detail of figure E showing a small naticid gastropod next to the barnacles.

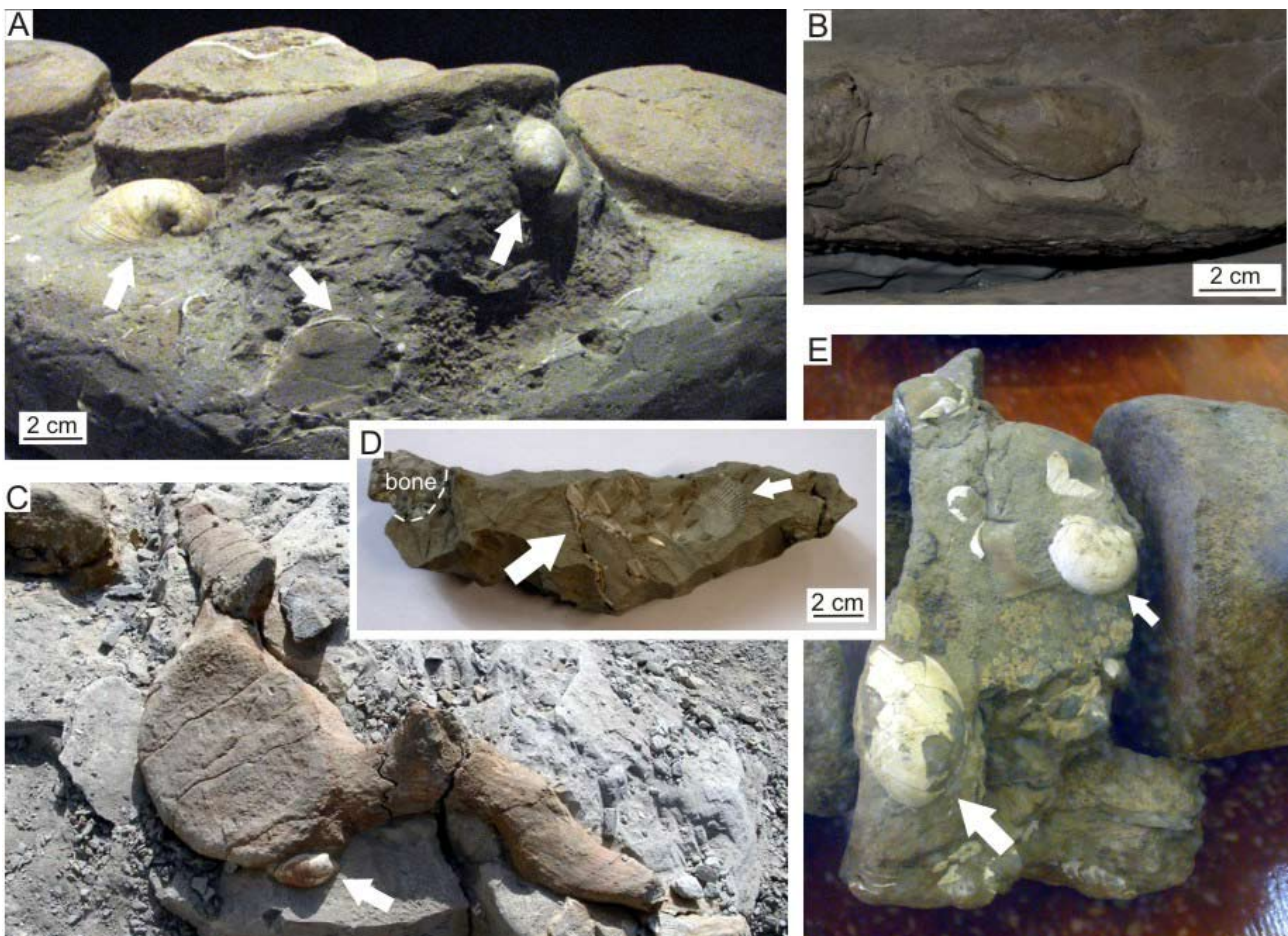


Figure 10. Molluscs associated with fossil whale bones. A. Three articulated specimens of *Glossus humanus* (arrows) next to intervertebral disks of a large whale (W8) embedded in muddy sediments B. Mytilid on one vertebra (W11). C. *Pelecypora brocchi* ? attached to a vertebra of W24. D. Mytilid (large arrow) and pectinid cf. *Chlamys varia* (small arrow) enclosed in the carbonate concretion around W21. E. *Pelecypora brocchi* ? (large arrow) and naticid gastropod (small arrow) on lumbar vertebra of W15.

## 4.5 Discussion

### 4.5.1 Taphonomic pathways at the Orciano Pisano fossil whale

The detailed study of the Orciano Pisano fossil whale (W1) is here discussed separately from the others, because used as a template for all the other specimens. Shark teeth and bite marks suggest scavenging, consistent with the habits of white sharks, which attack whales in pelagic waters, and blue sharks, which dive up to 80–100 m depths (Fergusson 1996, Kubodera et al. 2007). White sharks were large (Figure 2F), but the high degree of W1 articulation suggests that they had a limited role in stripping soft tissues away. Successive steps were deduced from taphonomic pathways in some modern deep-water analogs that show analogies with W1 (Allison et al. 1991, Goffredi et al. 2004, Fujiwara et al. 2007). Some modern, heavily downgraded carcasses show badly preserved or missing thoracic vertebrae and corroded skulls, while ribs and lumbar and caudal vertebrae are retained (Fujiwara et al. 2007). Costae, tail bones, and jawbones seem to be the first part of the skeleton to be exposed and collapse (Goffredi et al. 2004), whereas soft tissues in the skull remain available for months to years (Fujiwara et al. 2007). Biotic activity is thus expected to be more intense around the chest and the head. High sedimentation rates could explain early burial and low corrosion of the ribs that lay lowest in the pile (Allison et al. 1991, Fujiwara et al. 2007). We infer early exposition of W1 tail bones, ribs, and jaws, and costae undergoing early burial in a soft muddy bottom. Aerobic and anaerobic decomposition followed at the chest and head regions, where bones underwent a prolonged exposure and destruction possibly by bone-eating worms (genus *Osedax*, hosting heterotroph bacteria; Dubilier et al. 2008) active on the shelf (Glover et al. 2005, Dahlgren et al. 2006). The subsequent sulfophilic stage is inferred from the abundant lucinids, and their uneven distribution along the carcass suggests that higher nutrient content at the chest and the skull fuelled a more intense and prolonged chemosynthetic activity (Figure 2H-H'). At the end of the succession, large bones still lying on the bottom offered enhanced flow conditions ("reef" stage) to the suspension feeders found on the skull (Figure 2D).

### 4.5.2 Biostratinomy of shelf-depth fossil whales

Since water depth correlates with several environmental parameters that are important factors of biostratinomic processes, we first estimated the water depth from grain size of the sediments associated with the fossil whales. Muddy sediments settle in fact, on average, at greater depth than sandy sediments (Thorson 1957). According to this general rule, we approximated depth with grain size, and considered that fossil whales excavated from sandstones come from shallower waters than those from mudstones. Accordingly, we have a positive correlation between lithology and degree of skeletal articulation, i.e. well articulated specimens occur more frequently in muddy sediments, whereas disarticulated in sandstones (Figure 5A), as observed in a similar study for Jurassic marine vertebrates in the Lower Oxford Clay of central England

(Martill 1985). This implies lower bottom energy for mudstones and thence deeper settings. Our data suggest thus that in outer shelf areas with soft substrates and low sedimentation rate marine vertebrate skeletons are preserved preferentially more articulated than in onshore position, where reworking is higher.

We know from actualistic data that disarticulation, especially if related to skeletal incompleteness, can be also linked to carcass flotation after resurfacing (Allison et al. 1991). In shallow waters, floating carcasses resurfaced by the production of decay gasses in the abdominal cavity continue to decay, and the removal of supportive soft tissues promotes the disarticulation of skeletal elements. The skull is usually the first part lost, and the mandibles are soon separated from the cranium (Schäfer 1972). Flotation in shallow waters, may be prevented by scavenging if soft parts are stripped before decay, or by catastrophic burial, if a sufficient overburden of sediment is deposited on the carcass (Allison et al. 1991). Six fossil whales here under study, which miss either the trunk or the head, are good candidates to refloatation before final settling. All other cases have been possibly prevented from refloatation by scavenging or catastrophic burial. In cemented specimens, carbonate concretions probably precipitated by microbial processes linked to the decay of the whale organic matter, which favours carbonate precipitation increasing poor fluid alkalinity (Coleman and Raiswell 1993). Cementation is thus an indirect evidence of rapid burial before all the organic matter is consumed.

The abundance and diversity of shark teeth in close association with the bones indicates an interaction between pelagic sharks and whales. In the modern Mediterranean, cetaceans represent a significant component of the diet of large size white sharks, either through scavenging or predation on living animals (Mojetta et al. 1997). Considering the body size of Pliocene white sharks, Bianucci et al. (2002) hypothesized that active predation was possible only on small Mysticeti, as some cetotheriids and baleanids (*eg.*, *Balaenula*), whereas in all other instances concerning larger specimens, the association with shark teeth must have been true scavenging. In our data set shark teeth are all associated with large specimens (7-10 m long), thence all our evidence points to scavenging. The correlation between high degree of articulation and shark teeth (Figure 5C) suggests that in shallow waters the action of scavengers is not intense enough to disarticulate whale carcasses and disperse their bones, This datum is in accordance with knowledge from a modern shallow water study of a North Atlantic minke whale carcass, consumed by sharks and haghfishes within 6 months at 125 m depth without significant disarticulation (Dahlgren et al., 2006: Figure 5).

Low degree of preservation of the cortical bone tissue, together with the loss of vertebral processes, suggest bioerosion at the micro and mesoscale during exposition on the sea floor. At the microscale bioerosion can be caused by heterotrophic bacteria, cyanobacteria, algae or fungi consuming the bones, bioeroders considered only by palaeontologists (Amano and Little 2005, Kaim et al. 2008, Kiel 2008, Shapiro and Splanger 2009, Chapter 5: Danise et al. submitted) and for which actualistic data are badly needed. At the mesoscale, an active bioeroder could have been the siboglinid worm *Osedax*, the most famous among bone consumers in modern shallow

and deep water whale falls (Glover et al. 2005, Braby et al. 2007, Highs et al. 2010a), together with decapods, that can feed directly on fragile *Osedax*-laden lateral processes (Braby et al. 2007). Decapods are also among the more active scavengers at shallow sub-littoral, modern whale-fall sites (Glover et al. 2010) and are reported from three sites in our survey (W1, W16 and W17). *Osedax* trace fossils have been recognized only very recently in Oligocene whale bones (Kiel et al. 2010) and in one isolated Pliocene bone from Orciano Pisano, from an ancient collection housed at the MSNF (Higgs et al. 2010b). In conclusion, at all scales, bioerosion is an important biostratigraphic process of shallow water whale carcasses, allowing for significant exposition on the sea floor.

Encrusting epifauna on the bones, especially oysters and balanids, is a good paleoecological indicator for oxygenated bottom waters and low sedimentation rates, depending on their size and concentration (Martill 1985). Lack of correlation between bioencrustation and lithology (Figure 6C), does not help to relate biological and physical processes. Instead, a one by one analysis of well known encrusted skeletons and their associated sedimentary features, allows some important considerations. At W1 only one oyster was found attached to the bones (Figure 3B), but the occurrence of other vertebrate remains in the same outcrop, of a laterally continuous shell bed and glauconite grains (see Chapter 5) are all evidence of low sedimentation rates. Many encrusting oysters and a lateral continuous shell bed are also associated with W16. This shell bed is in the middle part of a small scale depositional sequence, corresponding to the maximum flooding interval (see Chapter 6), thence also this case points to low sedimentation rate at the whale carcass. Scanty data are available for the highly encrusted W14. Finally, the excellent report of Giuseppe Cortesi, despite the whale skeleton is no longer available (W7), leaves little doubt that the whale carcass had been deposited at a starved bottom: “... *picciole ostriche, parecchie delle quali veggonsi tuttavia incollate sulle ossa medesime... Morì questo cetaceo in un mare permanente e tranquillo; e perciò rimase lo scheletro nella sua naturale disposizione*” (Cortesi 1819). Finally the size of the ostreids attached to the studied whales, up to 10 cm long, suggests that some specimens lay on the sea floor at least for 6-10 years (Richardson 1993).

All of the above information helps framing the paucity of data concerning the chemosynthetic bivalves. As a conservative assumption we should not draw positive conclusions based on negative evidences, particularly knowing that chemosynthetic bivalves could have been present but overlooked. Large chemosynthetic bivalves, like at Orciano Pisano, must have been originally lacking in the best described cases of a fossil whale skeleton associated with molluscs (W3, W8, W14-W17). However this argument is no longer tenable in the case of very small bathymodiolins.

Among heterotrophic molluscs, the abundant suspension feeders were possibly exploiting flow enhancement, similarly to encrusting epibionts (Martill 1986, Smith et al. 2002). Pectinids were the most frequently recovered among suspension feeders in our dataset, and are found (*Pecten maximus*) even associated with shallow water artificially implanted carcasses at 23-30 m in the North Sea (Glover et al. 2010). The unusual abundance or size of *Glossus humanus* and

its proximity to large bones at two sites (W1, W8) might point to special adaptation to high sulphide concentrations. The only available study on the biology of this taxon (Owen 1953), adapted to very soft and calm mud bottoms, does not support this hypothesis. Nassarids, found at three sites (W1, W3, W20), and abundant in some cases, are scavengers that might have fed directly on the whale flesh, as observed in modern examples (Glover et al. 2010). They could also have been secondarily active predators on polychaetes and small crustaceans, as they are known to do in the present (Britton and Morton 1994). Naticid and fcid gastropods are active carnivores present or abundant at many whale falls (W1, W5, W14, W15, W20), they could have preyed on soft bodied biota living around the whale carcasses, or on bivalves and crustaceans (Taylor 1980).

#### 4.5.3 The fate of a whale carcass on the shelf

Building on previous experience (Dominici et al. 2009), the present study has shown that museum specimens can be used to understand the taphonomy of shallow water whale falls and that insights bring substantial knowledge of interest for both palaeontologists and marine biologists. Much of the paleobiological value of our research relies on knowledge gathered at Orciano, where an ecosystem-level approach was applied for the first time to the excavation of a large and articulated fossil whale, clearly implying that the same approach should be followed in all future excavations. Our taphonomic work concerns the fate of large cetacean carcasses sunken at shelf depths, with some degree of exportability to the taphonomy of Mesozoic large marine reptiles which are not explored here.

All natural occurrences of deep sea whale falls studied so far concern large and well-articulated carcasses which have undergone all stages of whale fall ecological succession and have been or are inhabited by large-sized shelled specialists, suggesting very similar taphonomic pathways (Allison et al. 1991, Naganuma et al. 1996, Goffredi et al. 2004, Lundsten et al. 2010). The ample variety of taphonomic states encountered in the Italian Neogene whale record suggests instead that in shallow marine bottoms the destiny of whale carcasses can be more variable than in the deep sea. Because of the wider ranges of variation of physical and biological factors, the way carcasses are recycled on the shelf can vary to a large degree. After a dead whale has sunk, its permanence on the sea floor will depend on the interplay between two main biological factors, i.e., the development of decompositional gasses and the rate of scavenging. If the process of soft tissue degradation is dominated by microbial decomposition and gas production, the carcass will easily resurface and become dismembered, leading to the final settlement of incomplete specimens. This has occurred in a minority of cases here under consideration, since the most studied specimens were complete (complete specimen here include those lacking the rostrum or the neurocranium, but with the two mandibles). This implies that most large whale falls that have made it to the fossil record, passed through an intense action of scavengers and rapid removal of abdominal soft tissues. Since gas production was not sufficient for buoyancy, the carcass had remained on the bottom where it had landed.

The following course of transformation depended on sedimentation rates. Each carcass, whether complete or not, might have been exposed on the sea floor interacting with the local ecosystem and subsequently buried at any stage of development of a whale fall community, if one was allowed to develop. Bioerosion and biota associated with our specimens suggest that most of them underwent an intense and prolonged biotic activity. We could recognize both the mobile scavenger stage and the enrichment opportunist stage on many shelf specimens, not differing from what occurs at deeper settings. Scavenging is marked by shark teeth or shelled predatory invertebrates, the opportunist stage by the general downgrading of the bones or by rare traces of the bone eating worm *Osedax*. Some specimens underwent a more prolonged exposure, testifying to sediment starvation, as testified by cemented epifauna resting on downgraded bones. Instances of bioincrustation on pristine bone suggests that successional stages can be intermingled. Benthic organisms associated with the bones and belonging to common taxa of the Neogene marine record, like many suspension feeding bivalves and carnivore gastropods, point to their general adaptation to exploit enhanced flow conditions (for example preferred by the pectinids) or large organic particles (preferred by the nassarids) which are much more frequent on the shelf than on the deep sea. The mature, sulphophilic stage of whale falls was recognized in one case, which coincided with the only excavation carried out on an ecosystem-level approach. This could mean that had all other recoveries dealt with the whole of the benthic fauna associated with the carcass, more instances of sulphophilic stage would have been found. Some evidences suggest however that this stage on the shelf seldom involves larger chemosymbiotic molluscs like in deep sea sites. These evidences include 1) the presence at Orciano of just large infaunal lucinids and very rare bathymodiolins, in the lack of larger chemosymbiotic bivalves like vesicomid clams and 2) the lack of chemosymbiotic taxa among all other shelled benthics reported at other sites.



## References

- Allison P.A., Smith C.R., Kukert H., Deming J.W. and Bennett B.A. 1991. Deep-water taphonomy of vertebrate carcasses: a whale skeleton in the bathyal Santa Catalina Basin. *Paleobiology* 17, 78–89.
- Amano K. and Little C.T.S. 2005. Miocene whale-fall community from Hokkaido, northern Japan. *Palaeogeography, Palaeoclimatology, Palaeoecology* 215, 345–356.
- Amano K., Little C.T.S. and Inoue K. 2007. A new Miocene whale-fall community from Japan. *Palaeogeography, Palaeoclimatology, Palaeoecology* 247, 236–242.
- Bellinzona G., Boni A., Braga G. and Marchetti G. 1971. Note illustrative della Carta Geologica d'Italia in scala 1:100.000, Foglio 71, Voghera. Servizio Geologico d'Italia, Roma, pp. 121.
- Bianucci G., Bisconti M., Landini W., Storai T., Zuffa M., Giuliani S. and Mojetta A. 2002. Mediterranean white shark-cetaceans interactions through time: a comparison between Pliocene and Recent data. In: Vacchi M., La Mesa G., Serena F. and Séret B. (Eds.), *Proceedings of the 4th European Elasmobranch Association Meeting*, Livorno, ICRAM, ARPAT & SFI, pp. 33–48.
- Bianucci G. and Landini W. 2005. I paleositi a vertebrati fossili della Provincia di Pisa. *Atti della Società Toscana di Scienze Naturali, Memorie, Serie A* 110, 1–21.
- Bisconti M. 2009. Taxonomy and evolution of the Italian Pliocene Mysticeti (Mammalia, Cetacea): a state of the art. *Bollettino della Società Paleontologica Italiana* 48, 147–156.
- Bossio A., Cerri R., Costantini A., Gandin A., Lazzarotto A., Magi M., Mazzanti R., Mazzei R., Sagri M., Salvatorini G. and Sandrelli F. 1992. I bacini distensivi neogenici e quaternari della Toscana. 76a Riunione estiva Società Geologica Italiana, Guida alle escursioni, Firenze, 199–227.
- Braby C.E., Rouse G.W., Johnson S.B., Jones W.J. and Vrijenhoek R.C. 2007. Bathymetric and temporal variation among *Osedax* boneworms and associated megafauna on whale-falls in Monterey Bay, California. *Deep-Sea Research I* 54, 1773–1791.
- Britton J.C. and Morton B. 1994. Marine carrion and scavengers. *Oceanography and Marine Biology: An Annual Review* 32, 369–434.
- Capellini G. 1865. Balenottere fossili del bolognese. *Memorie della Regia Accademia delle Scienze dell'Istituto di Bologna* 4, 3–24.
- Caretto P.G. 1970. La balenottera delle sabbie plioceniche di Valmontasca (Vigliano d'Asti). *Bollettino della Società Paleontologica Italiana* 9, 3–75.
- Carmignani L., Decandia F.A., Disperati L., Fantozzi P.L., Klingfield R., Lazzarotto A., Liotta D. and Meccheri M. 2001. Inner Northern Apennines. In: Vai G.B. and Martini I.P. (Eds.), *Anatomy of an Orogen: the Apennines and adjacent Mediterranean basins*. pp. 197–214.
- Chicchi S. and M. Scacchetti. 2001. *Valentina - Balena fossile del mare padano*. Civici Musei, Reggio Emilia, 31 pp.
- Coleman M.L. and Raiswell R. 1993. Microbial mineralization of organic matter: mechanisms of self-organization and inferred rates of precipitation of diagenetic minerals. *Philosophical Transactions: Physical Sciences and Engineering* 344, 69–87.

Cortesi G. 1819. Saggi geologici degli stati di Parma e Piacenza. Torchj del Majno, Piacenza, 165 pp.

Danise S., Cavalazzi B., Dominici S., Westall S., Monechi F., Guioli S. submitted. Fossil microbial ecosystem associated with a Miocene shallow-water whale-fall from Northern Italy. *Palaeogeography, Palaeoclimatology, Palaeoecology*.

Dahlgren T.G., Wiklund H., Källström B., Lundälv T., Smith C.R. and Glover A. 2006. A shallow-water whale-fall experiment in the north Atlantic. *Cahiers de Biologie Marine* 47, 385–389.

Danise S., Dominici S., Betocchi U. 2010. Mollusk species at a Pliocene shelf whale fall (Orciano Pisano, Tuscany). *Palaios* 25, 449–556.

Dominici S., Cioppi E., Danise S., Betocchi U., Gallai G., Tangocci F., Valleri G. and Monechi S. 2009. Mediterranean fossil whale falls and the adaptation of mollusks to extreme habitats. *Geology* 37, 815–818.

Dubilier N., Bergin C. and Lott C. 2008. Symbiotic diversity in marine animals: The art of harnessing chemosynthesis. *Nature Review* 6, 725–740.

Fergusson I.K. 1996. Distribution and autoecology of the white shark in the eastern North Atlantic Ocean and the Mediterranean Sea. In: Klimley A.P. and Ainley D.G. (Eds.), *Great White Sharks: The Biology of *Carcharodon carcharias**. San Diego, Academic Press, pp. 321–345.

Ferrero E. and Pavia G. 1996. La successione marina pre-villafranchiana. In: Carraro F. (Ed.), *Revisione del Villafranchiano nell'area-tipo di Villafranca d'Asti*. *Il Quaternario* 9, 36–38.

Fujiwara Y., Kawato M., Yamamoto T., Yamanaka T., Sato-Okoshi W., Noda C., Tsuchida S., Komai T., Cubelio S.S., Sasaki T., Jacobsen K., Kubokawa K., Fujikura K., Maruyama T., Furushima Y., Okoshi K., Miyake H., Miyazaki M., Nogi Y., Yatabe A., and Okutani T. 2007. Three-year investigations into sperm whale-fall ecosystems in Japan. *Marine Ecology* 28, 219–232.

Glover A.G., Kallstrom B., Smith C.R. and Dahlgren T.G. 2005. World-wide whale worms? A new species of *Osedax* from the shallow North Atlantic. *Proceedings of the Royal Society of London, Series B* 272, 2587–2592.

Glover A.G., Higgs N.D., Bagley P.M., Carlsson R., Davies A.G., Kemp K.M., Last K.S., Norling K., Rosenberg R., Wallin K., Källström B. and Dahlgren T.G. 2010. A live video observatory reveals temporal processes at a shelf-depth whale-fall. *Cahiers de Biologie Marine* 51, 375–381.

Goedert J.L., Squires R.L. and Barnes L.G. 1995. Paleoecology of whale-fall habitats from deep-water Oligocene rocks, Olympic Peninsula, Washington State. *Palaeogeography, Palaeoclimatology, Palaeoecology* 118, 151–158.

Goffredi S.K., Paull C.K., Fulton-Bennett K., Hurtado L.A. and Vrijenhoek R.C. 2004. Unusual benthic fauna associated with a whale fall in Monterey Canyon, California. *Deep-Sea Research I* 51, 1295–1306.

Goffredi S.K., Wilpiseski R., Lee R. and Orphan V.J. 2008. Temporal evolution of methane cycling and phylogenetic diversity of archaea in sediments from a deep-sea whale-fall in Monterey Canyon, California. *The International Society for Microbial Ecology Journal* 2, 204–220.

- Higgs N.D., Glover A.G., Dahlgren T.G. and Little C.T.S. 2010a. Using computed-tomography to document borings by *Osedax mucofloris* in whale bone. *Cahiers de Marine Biologie* 51, 401–405.
- Higgs N.D., Glover A.G., Dahlgren T.G. and Little C.T.S. 2010b. Identifying *Osedax* traces on fossil whale falls. Third International Palaeontological Congress, London, Abstract book, p. 199.
- Hogler J.A. 1994. Speculations on the role of marine reptile deadfalls in Mesozoic deep-sea paleoecology. *Palaios* 9, 42–47.
- Kaim A., Kobayashi Y., Echizenya H., Jenkins R.G. and Tanabe K. 2008. Chemosynthesis based associations on Cretaceous plesiosaurid carcasses. *Acta Palaeontologica Polonica* 53, 97–104.
- Kauffman. G. 1981. Ecological reappraisal of the German Posidonienscheifer (Toarcian) and the stagnant basin model. In: Gray J., Boucot A.J. and Berryw .B.N. (Eds.), *Communities of the Past*. Hutchison Ross, Stoudsberg, Pennsylvania, pp. 311–381.
- Kiel S. 2008. Fossil evidence for micro- and macrofaunal utilization of large nektonfalls: examples from early Cenozoic deep-water sediments in Washington State, USA. *Palaeogeography, Palaeoclimatology, Palaeoecology* 267, 161–174.
- Kiel S. and Goedert J.L. 2006. Deep-sea food bonanzas: Early Cenozoic whale-fall communities resemble wood-fall rather than seep communities. *Proceedings of the Royal Society B* 273, 2625–2631.
- Kiel S., Goedert J.L., Kahl W.-A., Rouse G.W. 2010 Fossil traces of the bone-eating worm *Osedax* in early Oligocene whale bones. *Proceedings of the National Academy of Science, USA* 107, 8656–8659.
- Kubodera T., Watanabe H. and Ichii T. 2007. Feeding habits of the blue shark, *Prionace glauca*, and salmon shark, *Lamna ditropis*, in the transition region of the western North Pacific. *Reviews in Fish Biology and Fisheries* 17, 111–124.
- Lancaster W.C. 1986. The taphonomy of an archaeocete skeleton and its associated fauna. *Proceedings of GCAGS Symposium*. Montgomery Landing Site, Marine Eocene of central LA, 119–131.
- Lundsten L., Paull C.K., Schlining K.L., Mc Gann M., Ussler III W. 2010. Biological characterization of a whale-fall near Vancouver Island, British Columbia, Canada. *Deep Sea Research I* 57, 918–922.
- Marshall J.T. 1900. On a British species of *Myrina*, with a note on the genus *Idas*. *Journal of Malacology* 7, 167–170.
- Martill D.M. 1985. The preservation of marine vertebrates in the Lower Oxford Clay (Jurassic) of central England. *Philosophical Transactions of the Royal Society B* 311, 155–165.
- Martill D.M. 1987. A taphonomic and diagenetic case study of a partially articulated ichthyosaur. *Palaeontology* 30, 543–555.
- Martill D.M., Cruickshank A.R.I. and Taylor M.A. 1995. Speculations on the role of marine reptile deadfalls in Mesozoic deep-sea paleoecology: comment. *Palaios* 10, 96–97.
- Mojetta A., Storai T. and Zuffa M. 1997. Segnalazioni di *Carcharodon carcharias* in acque

italiane. Quaderni della Civica Stazione Idrobiologica di Milano 22, 23–38.

Nesbitt E.A. 2005. A novel trophic relationship between cassid gastropods and mysticete whale carcasses. *Lethaia* 38, 17–25.

Pavlyuk O.N., Trebukhova Y.A. and Tarasov V.G. 2009. The impact of implanted whale carcass on Nematode communities in shallow water area of Peter the Great Bay (East Sea). *Ocean Science Journal* 44, 181–188.

Polino R. and Clari P.A. 2003. Carta Geologica d'Italia alla scala 1.50000, Foglio 157. Torino, Apat Dipartimento Difesa del Suolo.

Portis A. 1885. Catalogo descrittivo dei Talassoterii rinvenuti nei terreni terziari del Piemonte e della Liguria. *Memorie della Reale Accademia delle Scienze di Torino* 37, 247–365.

Pyenson N.D. and Haasl D.M. 2007. Miocene whale-fall from California demonstrates that cetacean size did not determine the evolution of modern whale-fall communities. *Biology Letters (Palaeontology)* 3, 709–711.

Ricci Lucchi F. 1987. Semi-allochthonous sedimentation in the Apenninic thrust belt. *Sedimentary Geology* 50, 119–134.

Richardson C.A., Collis S.A., Ekaratne K., Dare P. and Key D. 1993. The age determination and growth rate of the European flat oyster, *Ostrea edulis*, in British waters determined from acetate peels of umbo growth lines. *ICES Journal of Marine Science* 50, 493–500.

Rouse G.W., Goffredi S.K. and Vrijenhoek R.C. 2004. *Osedax*: Bone-eating marine worms with dwarf males. *Science* 305, 668–671.

Sarti C. and Gasparri F. 1996. La balenottera Pliocenica di Gorgognano (Pianoro, Bologna). *Bollettino della Società Paleontologica Italiana* 35, 331–347.

Schäfer W. 1972. Ecology and palaeoecology of marine environments. Chicago, University of Chicago Press.

Smith C.R. 2006. Bigger is better: The role of whales as detritus in marine ecosystems. In: Estes J. (Ed.), *Whales, Whaling and Ocean Ecosystems*. Berkeley, University of California Press, pp 284–299.

Smith C.R. and Baco A.R. 2003. Ecology of whale falls at the deep-sea floor. *Oceanography and Marine Biology: an Annual Review* 41, 311–354.

Smith C.R., Kukert H., Wheatcroft R.A., Jumars P.A. and Deming J.W. 1989. Vent fauna on whale remains. *Nature* 341, 27–28.

Smith C.R., Baco A.R. and Glover A. 2002. Faunal succession on replicate deep-sea whale falls: time scales and vent-seep affinities. *Cahiers de Marine Biologie* 43, 293–297.

Squires R.L., Goedert J.L. and Barnes L.G. 1991. Whale carcasses. *Nature* 349, 574.

Strobel P. 1881. *Iconografia comparata delle ossa fossili del gabinetto di Storia Naturale dell'Università di Parma*. Libreria Editrice Luigi Battei, Parma. 32 pp.

Taylor J.D. 1980. Diets and habitats of shallow water predatory gastropods around Tolo Channel, Hong Kong. In: Morton B. (Ed.), *The Malacofauna of Hong Kong and Southern China*.

Hong Kong University Press, Hong Kong, pp. 163–180.

Thorson G. 1957. Bottom communities (sublittoral or shallow shelf). Geological Society of America, Memoir 67, 461–534.

Vai G.B. 2001. Structure and stratigraphy: an overview. In: Vai F. and Martini I. P. (Eds.), *Anatomy of an Orogen: The Apennines and Adjacent Mediterranean Basins*. pp. 15-32.

Warén A. 1991. New and little known Mollusca from Iceland and Scandinavia. *Sarsia* 76, 53–124.

Williams S.T., Taylor J.D., and Glover E.A. 2004. Molecular phylogeny of the Lucinoidea (Bivalvia): Non-monophyly and separate acquisition of bacterial symbiosis. *The Journal of Molluscan Studies* 70, 187–202.

## Appendix

Information on the Pliocene whales here under study. Hosting institution abbreviation and taphonomic variables explained in the text. Among incomplete skeletons, \* indicates acephalous specimens, " indicates specimens that conserve only the skull.

LOCALITY	N°	HOSTING INSTITUTION	TAXON	LITOLGY	LENGTH (m)	BONE ARTICULATION	COMPLETENESS	CORTICAL BONE PRESERVATION	VERTERAL PROCESS PRESERVATION	BONE CEMENTATION	SHARK TEETH	CHEMOSYMBIOTIC RIVALVES	ENCRUSTING EPIBIONTS	OTHER INVERTEBRATES	REFERENCES
Orciano Pisano (PI)	W1	MSNF	<i>Mysticete</i>	Silty-fine grained sandstone	10	high	high	low	low	medium	yes	Lucinidae	yes	SEE CHAPTER 3	Dominici et al. 2009, Danise et al. 2010, CHAPTER 3
Vigliano d'Asti (AT)	W2	MGPT	<i>Balaenoptera acutorostrata</i>	Silty fine-grained sandstone	8	high	high	high	high	medium	no	n.d.	yes	n.d.	Caretto 1970, Dominici et al. 2009
San Marzanotto (AT)	W3	MPSC	<i>Balaenoptera acutorostrata</i>	Mudstone	8	low	low	high	high	low	yes	n.d.	yes	Carnivores ( <i>Nassarius italicus</i> ), suspension feeders ( <i>Amusium cristatum</i> , <i>Atrina pectinata</i> , <i>Anadara diluvii</i> , <i>Pelecycora brocchii</i> , <i>Neoplicnodonte cochlear</i> ), deposit feeders ( <i>Aporrhais uttingeriana</i> , <i>Tellina compressa</i> ) and browsing carnivores ( <i>Epitonium turtoni</i> )	Damarco 1995, Dominici et al. 2009
Portacomaro d'Asti (AT)	W4	MSNT	<i>Balaenula astensis</i>	Silty fine-grained sandstone	6	medium	low"	high	n.d.	medium	no	n.d.	no	n.d.	Trevisan 1941, Dominici et al. 2009
Castell'Arquato (PC)	W5	MPP	<i>Balaenoptera acutorostrata</i>	Mudstone	8	high	high	high	medium	high	no	n.d.	yes	Carnivores (Naticidae), suspension feeders (Mytilidae, Pectinidae)	Strobel 1881, Dominici et al. 2009
Rio dei Carbonari - Castell'Arquato (PC)	W6	MGC	<i>Archaeobalaenoptera castriarquati</i>	Silty fine-grained sandstone	7	high	low"	high	n.d.	low	yes	n.d.	yes	n.d.	Bisconti 2007, Dominici et al. 2009, Lo Russo and Miti pers. comm.

Rio Stramonte - Castell'Arquato (PC)	W7	No longer available	<i>Balaenoptera acutorostrata</i>	Mudstone	7	high	high	medium	high	medium	high	low	yes	n.d.	yes	n.d.	Cortesi 1819, Dominici et al. 2009
Rio Stramonte - Castell'Arquato (PC)	W8	MGC	<i>Mysticete</i>	Mudstone	n.d.	n.d.	low*	n.d.	n.d.	n.d.	n.d.	n.d.	no	n.d.	no	Suspension feeders ( <i>Glossus humanus</i> )	Lo Russo and Miti pers. comm.
Monte Falcone - Castell'Arquato (PC)	W9	MGC	<i>Balaenoptera acutorostrata</i>	Mudstone	n.d.	low	high	high	low	medium	low	medium	no	n.d.	no	n.d.	Francou 1994
Monte Falcone - Castell'Arquato (PC)	W10	MPP	<i>Cetotherium capellinii</i>	Sandstone	9	medium	low*	low	n.d.	low	n.d.	medium	no	n.d.	no	n.d.	Scabelli 1843
Monte La Ciocca - Castell'Arquato (PC)	W11	MGC	<i>Balaenoptera sp.</i>	Muddy sandstone	n.d.	low	low	medium	medium	medium	medium	low	no	n.d.	no	n.d.	Lo Russo and Miti pers. comm.
Monterzago, Luganano Val D'Arda (PC)	W12	MPP	<i>Megaptera sp.</i>	Sandstone	12	low	low*	medium	low	medium	low	low	no	n.d.	no	n.d.	Cortesi 1819
Monterzago, Luganano Val D'Arda (PC)	W13	MPP	<i>Balaenoptera acutorostrata</i>	Mudstone	4	medium	high	high	high	high	high	high	no	n.d.	no	n.d.	Cortesi 1819
Gorgignano (BO)	W14	MGCB	<i>Balaenoptera acutorostrata</i>	Mudstone	9	medium	high	low	medium	low	medium	medium	no	n.d.	yes	Suspension feeders ( <i>Mytilus sp.</i> ); deposit feeders ( <i>Antalis sp.</i> , <i>Aporrhais uttingeriana uttingeriana</i> ), carnivores ( <i>Ficus sp.</i> )	Sarti and Gasparri 1996, Dominici et al. 2009
San Lorenzo in Collina (BO)	W15	MGCB	<i>Balaenoptera acutorostrata</i>	Silty-fine grained sandstone	8	low	low	high	low	high	low	medium	yes	n.d.	yes	Suspension feeders ( <i>Pelecypora brocchi?</i> , <i>Venus multiamella?</i> ), carnivores (Naticidae)	Capellini 1865, Dominici et al. 2009
Castellarano (RE)	W16	MCRE	<i>Balaena sp.</i>	Silty fine grained sandstone	10	low	low	high	high	high	high	medium	yes	n.d.	yes	Suspension feeders ( <i>Glycymeris inflata</i> , <i>Modiolus sp.</i> , <i>Ostrea sp.</i> ), scavengers (decapods)	Chicchi and Scacchetti 2001, Dominici et al. 2009

Ponte a Elsa (PI)	W17	MSNF		<i>Balaena</i> sp.	Mudstone	10	high	high	high	n.d.	high	n.d.	high	yes	n.d.	no	Suspension feeders ( <i>Chlamys opercularis</i> ), deposit feeders ( <i>Aporrhais uttigeriana</i> , <i>Dentalium fossile</i> ), scavengers (decapods)	Borselli and Cozzini 1992, Dominici et al. 2009
Castel San Gimignano (PI)	W18	MSNF		<i>Balaenoptera</i> sp.	Sandstone	8	medium	low*	high	high	low	n.d.	low	no	n.d.	no	n.d.	Dominici et al. 2009
Montopoli (PI)	W19	MCPG		<i>Eubalena</i> sp.	Very fine-silty sandstone	n.d.	n.d.	low	medium	n.d.	n.d.	n.d.	yes	n.d.	no	no	n.d.	Bisconti 2002
Montopoli (PI)	W20	MSNF		<i>Idiocetus guicciardinii</i>	Sandy mudstone	n.d.	n.d.	high	high	high	low	low	no	n.d.	no	no	Carnivores (Naticidae, Nassaridae), suspension feeders (Pectinidae)	Capellini 1905
Castelfiorentino (FI)	W21	MSNF		<i>Balaenoptera</i> sp.	Mudstone	8	high	high	medium	medium	high	medium	yes	n.d.	yes	yes	Suspension feeders (Mytilidae, Pectinidae)	Dominici et al. 2009, this study
Montalcino (SI)	W22	CVB		<i>Balaenoptera</i> sp.	Silty-fine grained sandstones	10	low	high	high	high	low	low	yes	n.d.	no	no	n.d.	Dominici et al. 2009
Allerona (TR)	W23	MCGA		<i>Balaenula</i> sp. (juvenile)	Mudstone	2.5	low	high	medium	low	low	low	no	n.d.	no	no	n.d.	This study
Allerona (TR)	W24	MCGA		<i>Mysticete</i>	Mudstone	12	medium	high	high	medium	medium	medium	no	n.d.	yes	yes	Suspension feeders ( <i>Pelecyora brocchi</i> ?)	This study
Cà del Monte (PV)	W25	CMSNV		<i>Mysticete</i>	Fine grained sandstone	n.d.	low	low	high	medium	high	high	no	n.d.	no	no	n.d.	This study, CHAPTER 5



## REFERENCES

- Bisconti M. 2002. An early Late Pliocene right whale (genus *Eubalaena*) from Tuscany (Central Italy). *Bollettino della Società Paleontologica Italiana* 41, 83–91.
- Bisconti M. 2007. A new basal balaenopterid whale from the Pliocene of Northern Italy. *Palaeontology* 50, 1103–1122
- Borselli V. and Cozzini F. 1992. Il recupero di un cetaceo fossile in località Ponte a Elsa (Pisa). *Museologia Scientifica* 8, 9–22.
- Capellini G. 1865. Balenottere fossili del bolognese. *Memorie della Regia Accademia delle Scienze dell'Istituto di Bologna* 4, 3–24.
- Capellini G. 1905. Balene fossili toscane. III *Idiocetus guicciardinii*. *Atti della Reale Accademia delle Scienze dell'Istituto di Bologna*, Serie 68, 113–115.
- Caretto PG. 1970. La balenottera delle sabbie plioceniche di Valmontasca (Vigliano d'Asti). *Bollettino della Società Paleontologica Italiana* 9, 3–75.
- Chicchi S. and M. Scacchetti. 2001. Valentina - Balena fossile del mare padano. *Civici Musei, Reggio Emilia*, 31 pp.
- Cortesi G. 1819. Saggi geologici degli stati di Parma e Piacenza. *Torchj del Majno, Piacenza*, 165 pp.
- Damarco P. 1995. Una curiosa combinazione: la balena e le conchiglie fossili. *Word Shells* 15, 26–28.
- Danise S., Dominici S. and Betocchi U. 2010. Mollusk species at a Pliocene shelf whale fall (Orciano Pisano, Tuscany). *Palaios* 25, 449–556.
- Dominici S., Cioppi E., Danise S., Betocchi U., Gallai G., Tangocci F., Valleri G. and Monechi S. 2009. Mediterranean fossil whale falls and the adaptation of mollusks to extreme habitats. *Geology* 37, 815–818.
- Franco C. 1994. Nelle terre del Piacenziano. *Fondazione Cassa di Risparmio di Piacenza e Vigevano, Piacenza*, 126 pp.
- Strobel P. 1881. Iconografia comparata delle ossa fossili del gabinetto di Storia Naturale dell'Università di Parma. *Libreria Editrice Luigi Battei, Parma*. 32 pp.
- Scabelli 1843. Di una balena, di un delfino e molte conchiglie cavate dai colli del piacentino. *Tipografia vescovile tedeschi, Piacenza*.
- Sarti C. and Gasparri F. 1996. La balenottera Pliocenica di Gorgognano (Pianoro, Bologna). *Bollettino della Società Paleontologica Italiana* 35, 331–347.
- Trevisan L. 1941. Una nuova specie di *Balaenula* pliocenica. *Palaeontographia Italica* 40, 1–13.

# CHAPTER 5 — Fossil microbial ecosystems associated with Neogene Italian fossil whales

---

## *Fossil microbial ecosystem associated with a Miocene shallow-water whale fall from Northern Italy*

### 5. 1 Introduction\*

Microbial life occurs in, and seems to be adapted to, many different kinds of ecological niches, including unusual habitats, wherever chemical and physical conditions (*e.g.*, nutrient availability and energy sources) permit. The relatively poorly explored deep, dark biosphere is of great interest because it shows an high and still completely unknown biodiversity and continuously reveals evolutionary novelties, despite the scarcity of food sources (*e.g.*, Van Dover 2000, Rouse et al. 2004, Santelli et al. 2008, Cavalazzi 2007, Cavalazzi et al. submitted a). Several reports exist of diverse, well adapted, active macro- and micro-organisms recovered from submarine hydrothermal vents, hydrocarbon cold seeps and whale carcasses sunk in the deep sea (*e.g.*, Van Dover 2000, Smith and Baco 2003, Levin 2005). Modern submarine hydrothermal seep and hydrocarbon areas are known to support highly productive chemosynthesis-based ecosystems that are quite ecologically distinct from that of the surrounding sea floor and whose ancient counterparts are also increasingly recognized in the geological record (*e.g.*, Peckmann and Thiel 2004, Little and Vrijenhoek 2004, Campbell 2006). Sediments rich in organics on the seabed, including hydrocarbon seeps and mud volcanoes areas, are known to host consortia of anaerobic methane oxidizing archaea and sulphate-reducing bacteria that, as a consequence of their metabolism, bio-induce precipitation of carbonate minerals, thus favouring their accumulation as geological deposits (Orphan et al. 2001, Peckmann and Thiel 2004, Reitner et al. 2005). Modern deep water whale-falls represent symbiont-dominated oases that consist mainly of vesicomyids clams, bathymodioline mussels, and vestimentiferan tube worms (Smith et al. 1989, Smith and Baco 2003), together with their associated microbial consortia that are similar to those occurring at hydrocarbon cold seeps and that could be preserved in the geological record (Shapiro and Spangler 2009).

Whale bones contain up to 60% lipids by wet weight (Deming et al. 1997, Higgs et al. 2011) and anaerobic bacterial degradation of whale-bone lipids during the so-called sulfophilic stage of the ecological succession can provide hydrogen sulphide (H<sub>2</sub>S) to the chemoautotrophic

---

\* This part of the study consists of a paper by Danise S., Cavalazzi B., Dominici S., Westall , S. Monechi F. and Guioli S. "Fossil microbial ecosystem associated with a Miocene shallow-water whale-fall from Northern Italy" submitted to *Palaeogeography, Palaeoclimatology, Palaeoecology*."

community for periods of years to decades (Smith et al. 2002, Smith and Baco 2003, Lundsten et al. 2010). Chemosynthetic sulphide-oxidizing microorganisms found at whale falls include free-living bacteria (*e.g.*, *Beggiatoa* spp.) which cover bones and sediment surfaces, as well as endosymbionts in bivalves and tubeworms (Bennett et al. 1994, Deming et al. 1997, Goffredi et al. 2004). The sediments beneath and around whale carcasses, progressively enriched with lipids and other organic compounds (Naganuma et al. 1996, Smith et al. 1998), experience anoxic conditions due to high microbial oxygen consumption that, in turn, favours anaerobic processes such as sulphate reduction and methanogenesis (Allison et al. 1991). Thus, whale carcasses and the surrounding sediments represent a suitable habitat for sulphide-based chemosynthetic communities as well as sulphate-reducing and methane-producing microbial consortia (Goffredi et al. 2008, Treude et al. 2009).

Although significant advances have been made on the study of modern and fossil whale-falls, few studies have been made on bacterial degradation in ancient whale-falls. Positive evidence of fossil whale-falls, dating back to the late Eocene, is provided by the occurrence of chemosynthetic macro-invertebrates associated with fossil bones (Goedert et al. 1995, Amano and Little 2005, Kiel and Goedert 2006, Amano et al. 2007, Pyenson and Haasl 2007, Dominici et al. 2009, Danise et al. 2010). More recently, biosedimentological features such as botryoidal cements, microbial peloids, authigenic pyrite and microborings have been reported in association with fossil whale and marine reptile carcasses that could represent evidences of whale-fall community development (Kaim et al. 2008, Kiel 2008, Shapiro and Spangler 2009). However, the role played by depositional and diagenetic processes in preserving the traces left by microbial ecosystems related to whale-falls still remains to be elucidated (*e.g.*, Kiel 2008, Shapiro and Spangler 2009).

In this study we present the results of a detailed investigation of a fossil microbial ecosystem associated with the bones of a Miocene mysticete whale from shallow water sediments of Northern Italy. A combination of analytic techniques, such as optical and scanning electron microscopy, Raman spectroscopy and stable isotope geochemistry allowed us to investigate the fossil bones and enclosing concretions in order to i) reconstruct their taphonomic processes and diagenetic events, ii) recognize the distinguishing features of microbial activity, and iii) discuss the results in relation to the development of a whale-fall community.

## 5.2 Geological setting

The fossil whale investigated in this paper, hereafter called "*Voghera whale*" (W25: Chapter 4), was found in the lower member of the Monte Vallassa Formation, part of the Epiligurian succession cropping out in the northernmost part of the Northern Apennines (Figure 1). The Monte Vallassa Formation, ranging in age from the Serravallian to the Tortonian, is an approximately 400 m thick sequence consisting of a transgressive marine

cycle recording coastal to inner and outer shelf deposits (Bellinzona et al. 1971). The lower member is characterized by blue-grey sandy marls rich in macro-invertebrates, mainly terebratulids, and poorly preserved bivalves, gastropods, isolated corals and echinoids. Based on the occurrence of *Uvigerina barbatula* (Macfad), *Stilotomella vermeuili* (D'Orb.), *Orbulina universa* (D'Orb.) and *Globoquadrina dehiscens* (Chap., Parr., Coll.), to the lower member is assigned a Serravallian age (13.8-11.6 Ma) (Bellinzona et al. 1971).

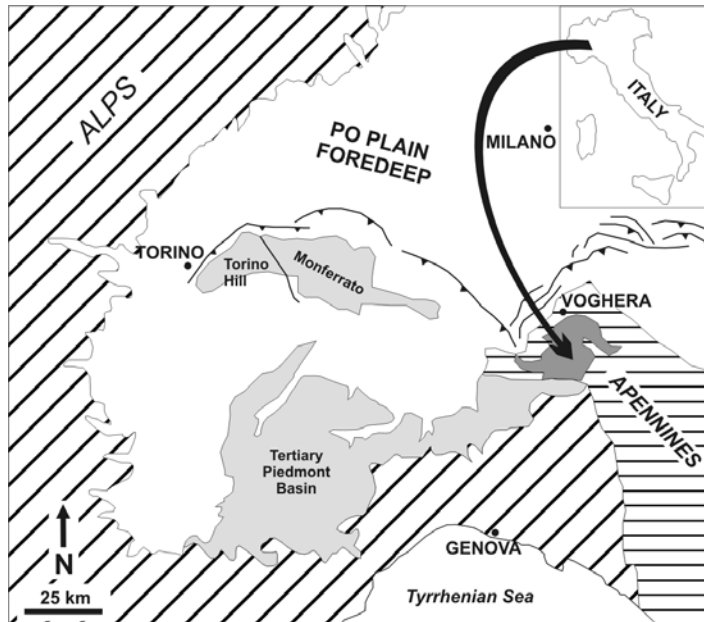


Figure 1. Schematic geological map of the Voghera whale site, Northern Italy. The Voghera whale was recovered within middle Miocene blue-grey sandy marls belonging to the Epiligurid Monte Vallassa Formation (arrow). Oblique lines: areas of outcrop of Alpine units; horizontal lines: areas of outcrop of Apennine units; light-grey : Oligo–Miocene sedimentary successions of Monferrato, Torino Hill and Tertiary Piedmont Basin; dark-grey: Epiligurids; unpatterned: Plio–Pleistocene sediments. Figure modified from Clari et al. 2009.

### 5.3 Materials and methods

The Voghera whale is curated in the Civico Museo di Scienze Naturali di Voghera (Pavia, Northern Italy) (specimen V658). The specimen, collected in 2007 at the Cà del Monte locality near to Cecima, Pavia (Figure 1), is an unidentified mysticaete consisting of three vertebrae, some ribs, one scapula and some undetermined fragments, partially enclosed in a carbonate concretion (Figure 2). Cemented fragmentary bones were selected for analysis. They were firstly characterized by optical microscopy examination of covered and uncovered standard petrographic thin sections (30  $\mu\text{m}$  thick) and polished surfaces. Optical analyses were performed in transmitted and reflected light by using a Zeiss Axioplan2 Imaging microscope equipped

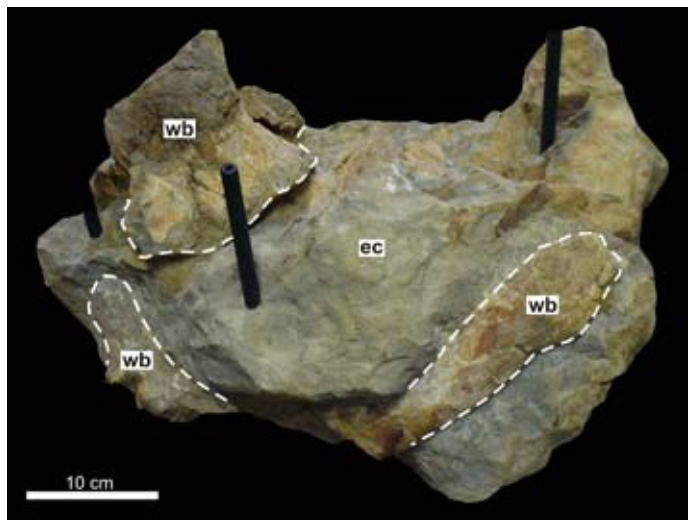


Figure 2. The Voghera whale, specimen V658, Civico Museo di Scienze Naturali di Voghera (Italy). Note the whale bones, such as vertebrae and ribs, enclosed in a carbonate concretion. wb: whale bone; ec: enclosing concretion.

with a Zeiss AxioCam digital camera and an Olympus BX51 TH-200 microscope equipped with an Olympus DP12 Digital Microscope Camera. Subsequently, the uncovered thin sections and polished surfaces were examined using a WITec Alpha500 AFM-confocal Raman microscope. Three objectives (Nikon 20x, 50x and 100x) and a frequency doubled Nd:YAG (532 nm) Ar-ion 20-mW monochromatic laser source were used to collect the Raman spectra. Beam centering and Raman spectra calibration were performed before spectra acquisition using a Si standard with a characteristic Si Raman peak at  $520.4\text{ cm}^{-1}$ . The optimum power for *in situ* analyses of different minerals was experimentally determined between 1.67 and 1.70 nW at the sample surface. Raman analyses and maps were recorded and treated using WITec Project 2.00® software. Finally, selected portions of the thin sections and freshly broken samples were etched in an aqueous solution of 1% HCl between 5 and 120 seconds, air dried and Au-coated for scanning electron microscope observations and element analysis (SEM-EDX). SEM-EDX imaging and analyses were performed using a Field Emission Gun-SEM (FEG-SEM) Hitachi S4200 and a ZEISS EVO MA 15, both equipped with an X-ray energy dispersive spectrometer system. The operating conditions of the scanning electron microscopes were 5 to 20 keV accelerating voltage for imaging, and 15-20 keV for elemental analyses.

$^{13}\text{C}$  and  $^{18}\text{O}$  stable isotope analyses were performed on carbonate cements inside whale bones and on the external matrix. Samples (3-5 milligrams) were hand drilled from polished slabs. The powdered samples were dissolved in vacuum in 100% phosphoric acid at  $25^{\circ}\text{C}$ , and analysed using a Finnigan-MAT 250 mass spectrometer. Reproducibility was checked by replicate analyses (10 identical samples) and the standard deviation was better than  $\pm 0.3\%$ . All results are reported in per mil (‰) deviations from the V-PDB (Vienna-Pee Dee Belemnite) standard.

The instruments used are located at the Dipartimento di Scienze della Terra and Centro Interdipartimentale di Microscopia Elettronica e Microanalisi, Università di Firenze (Italy), at the Centre de Biophysique Moléculaire, CNRS, Orléans (France), Centre de Microscopie Electronique, Université d'Orléans (France), and at the Stable Isotope Laboratory, Department of Geology, Copenhagen University (Denmark).

## 5.4 Results

### 5.4.1 Fossil bone preservation

The Voghera whale bones are enclosed in a grey, fine-grained host matrix, consisting of angular siliciclastic grains, such as quartz, feldspars and micas, and cemented with microcrystalline to small rhombohedral dolomite crystals (maximum size of the main axis  $10\text{ }\mu\text{m}$ ) (Figure 3A). Poorly preserved bioclasts of benthic foraminifera tests and concentrations of fecal pellets close to the fossil bones are also observed (Figure 3B).

The Voghera whale fossil bones are mineralized in carbonate-rich fluorapatite,

$\text{Ca}_5(\text{PO}_4, \text{CO}_3)_3\text{F}$  (Figure 4). The studied fossil bones preserve both the compact and the cancellous bone tissue (Figure 5A). They are light brown in colour in plane polarized and light black to light grey in cross polar, exhibiting a birefringence pattern (Figure 5B-C). Compact bones result in a relatively solid and dense bone texture, whereas cancellous bones are spongy and highly porous and consist of plates and struts called trabeculae that, in life, are filled with marrow (*sensu* Lyman 1994). The fossil bone structures are well preserved. Osteons, the major structural elements of bone tissue, and osteocytes, the bone cells, are clearly visible (Figure 5B-D). Osteons produce a roughly cylindrical structure of successive concentric lamellae surrounding a centrally located canal that contains blood vessel and nerves, the Haversian canal (Lyman 1994). In the Voghera whale, osteons show a radial system of microcracks (Figure 5C). In Figure 5A, the external part of cancellous bones appears to be highly enriched in dark iron sulphides. Optical microscopy and Raman spectroscopy show reddish, globular aggregates of lepidocrocite,  $\gamma\text{-FeO}(\text{OH})$ , intimately associated with the tissue of compact and cancellous bones (Figure 5E). The lepidocrocite grains have a diameter in between 4 and 8  $\mu\text{m}$ , however, rare larger diameter grains up to 40  $\mu\text{m}$  were also observed.

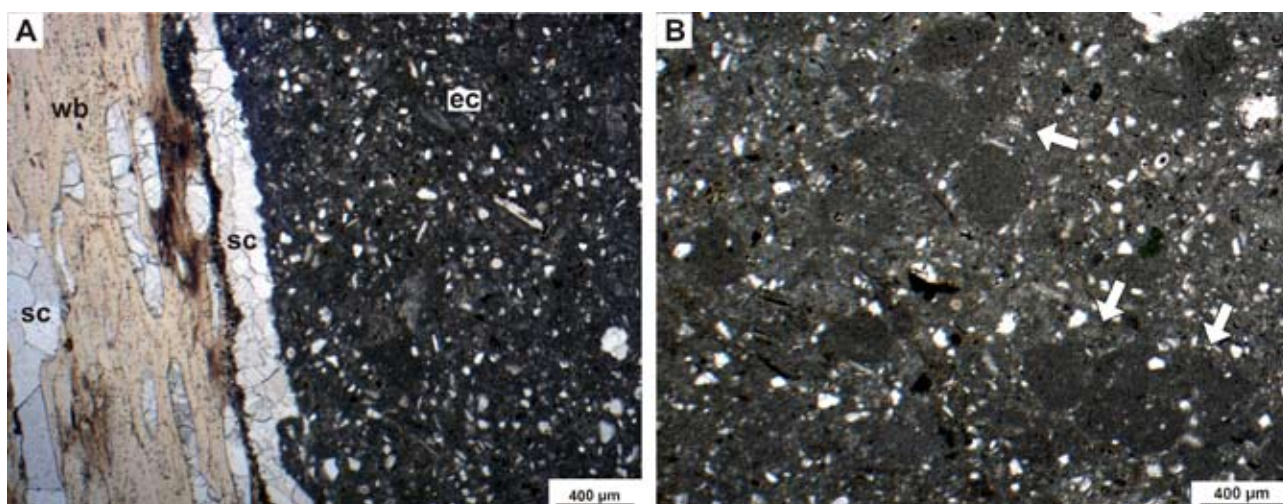


Figure 3. Transmitted light photomicrographs of petrographic thin sections of the Voghera whale bones and the enclosing carbonate concretion. A. Fossil whale bone (wb) and the enclosing concretion (ec). The enclosing concretion consists of a siliciclastic matrix cemented by microcrystalline dolomite. Note the canals of compact bones (wb) filled by sparry calcite (sc). B. Enclosing concretion with fecal pellets (arrows). Fecal pellets are ovoid or elliptical shape, are up to 420  $\mu\text{m}$  in length and contain minor amounts of iron sulphide.

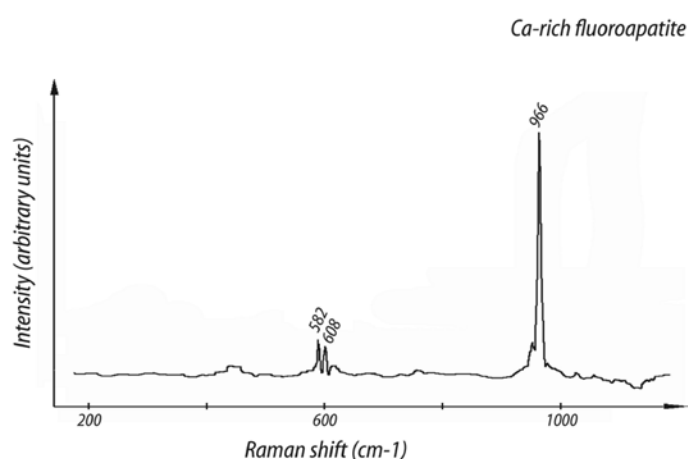


Figure 4. Raman spectrum of the Voghera whale fossil bones. The bones are preserved as Ca-rich fluoroapatite,  $\text{Ca}_5(\text{PO}_4, \text{CO}_3)_3\text{F}$ .

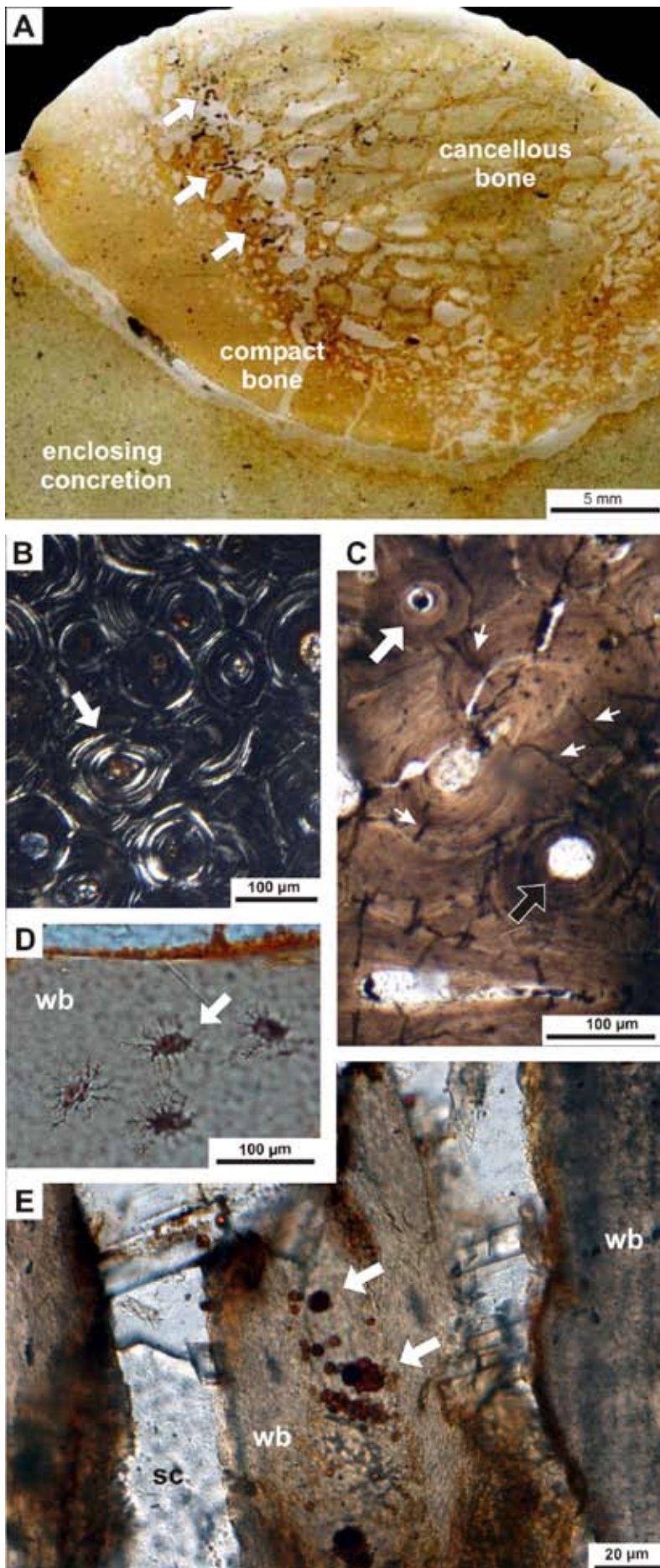
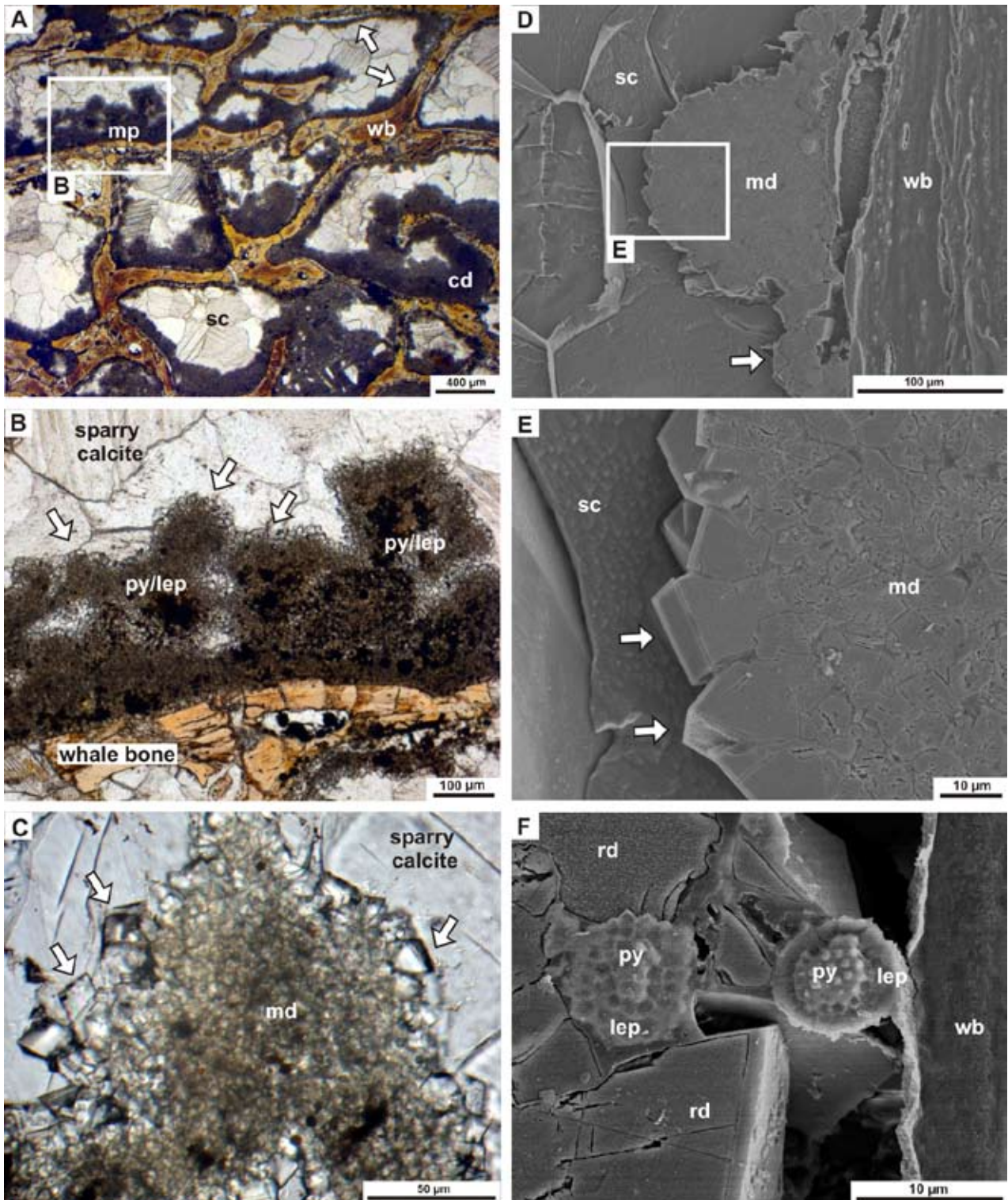


Figure 5. Transmitted light photomicrographs of petrographic thin sections of the Voghera whale bones. A. Bone structure with well preserved compact and cancellous bone tissue. Note black iron monosulphides especially concentrated at the compact-cancellous bone interface (arrows). B. Detail of compact bone as observed in cross polarized light. The birefringent pattern of the osteons emphasizes the concentric lamellar structures (arrow) surrounding the central Haversian canal. C. Detail of compact bone showing radial microcracks (small white arrows). The cavities of Haversian canals may be empty (black arrow) or filled with pyrite framboids (large white arrow). D. Well preserved osteocyte cells (arrow) within the carbonate-rich fluoroapatite fossil bone. E. Globular lepidocrocite (arrows) in the bone matrix. All figures in plane polarized light except C which is cross polarized.

### 5.4.2 Carbonate cements filling cancellous bones

Cancellous bones are filled with different carbonate phases, including microcrystalline and rhombohedral dolomite, and euhedral (sparry) calcite (Figure 6). In thin section, microcrystalline dolomite exhibits a clotted fabric, resulting in a dark, cloudy aggregate (Figure 6A). Locally microcrystalline dolomite forms well organized rounded to sub-rounded microbial peloids with an average radius of 57  $\mu\text{m}$  (min 37.8  $\mu\text{m}$ , max 116  $\mu\text{m}$ ) (Figure 6B-D). Microbial





Previous page:

**Figure 6.** Transmitted light photomicrographs and SEM images of petrographic thin sections showing different Ca-Mg-carbonate cements lining and filling cancellous bones. **A.** Whale bone trabeculae (wb) are lined and encrusted by thin rims (arrows) of microcrystalline dolomite and clotted dolomite (cd). Locally, microbial peloids (mp) are observed associated to clotted dolomite lining the trabecular bones (boxed area). Sparry calcite (sc) occludes the trabecular bone cavities. **B.** Detail (magnification of the boxed area in A) of an aggregate of microbial peloids (arrows). The peloids are stained by opaque Fe-sulphides (py: pyrite) and *-oxyhydroxide* (lep: lepidocrocite). **C.** High magnification of a microbial peloid. Microbial peloids consist of a microcrystalline dolomite nucleus (md) surrounded by small rhombohedral dolomite crystals (arrows). **D.** SEM image of microbial peloid with a rim of rhombohedral dolomite crystals (arrow) lining bone trabecula (wb), and cemented with sparry calcite (sc). **E.** Detail of the microbial peloid (high magnification of boxed area in D). Note the clotted (3-5  $\mu\text{m}$ ) microcrystalline dolomite (md) and the well developed rhombohedra on the external part (arrows). **F.** Pyrite framboids (py) partially oxidized into lepidocrocite (lep) and closely associated with small rhombohedral dolomite (rd). Note the internal area of framobids with still preserved pyrite microcrystallites. A, B, and C in plane polarized light.

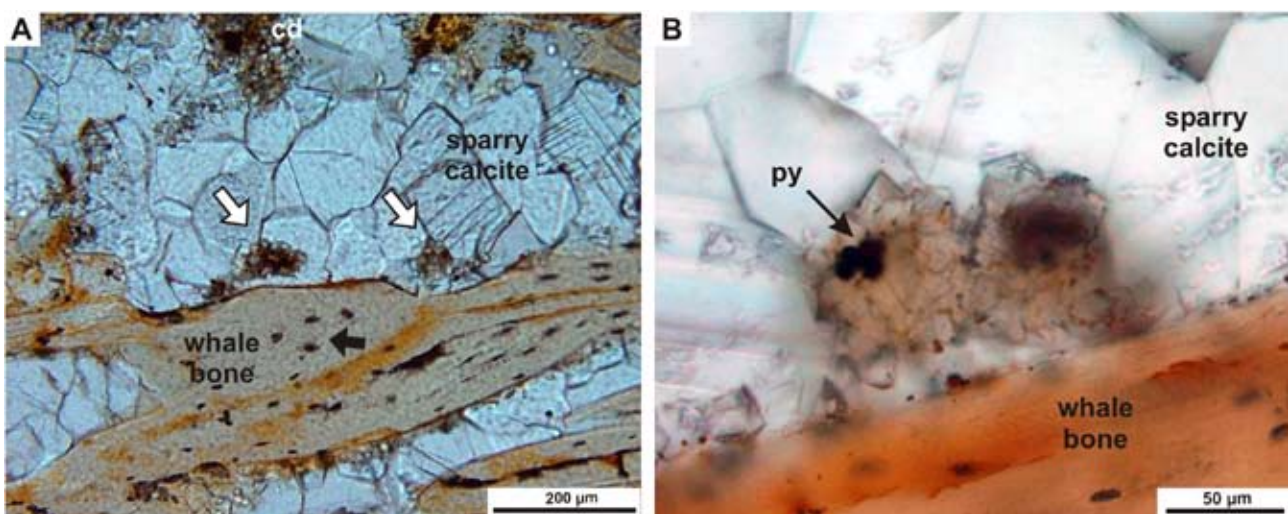


**Figure 7.** Transmitted light photomicrographs of petrographic thin sections showing flower-like cements lining whale bones. **A.** Flower-like structures (white arrows) close to bone trabeculae and embedded in sparry calcite. Flower-like structures occur typically as isolated and paired bodies, or in small aggregates. At the top note clotted microdolomite (cd) embedded in sparry calcite cement. Note also the osteocytes (black arrow) within the whale bone. **B.** Detail of flower-like structures formed by few small pyrite framboids (py) surrounded by rhombohedral dolomite crystals.

peloids show a characteristic internal organization. Their inner part consists of a dense aggregate of microcrystalline dolomite whereas their external portion shows a characteristic rim of rhombohedral dolomite crystals (Figure 6C). SEM observation of the microbial peloids shows a dense nucleus of microcrystalline dolomite, 3 to 5  $\mu\text{m}$  in size, and an external rim of rhombohedral dolomite with an average main axis size of 22  $\mu\text{m}$  (Figure 6E). Similar dolomite rhombohedra are also observed to line the surface of trabeculae bone (Figure 6A,D). Locally, dolomite rhombohedral crystals exhibit a particular habit of aggregates with a flower-like form and an average radius of 20  $\mu\text{m}$  (Figure 7). They can be solitary or coalescent (2-4 bodies) and are especially observed close to bone trabeculae and result embedded in the sparry calcite (Figure 7A). These flower-like structures are characterized by a dark, opaque nucleus of few pyrite framboids (Figure 7B). Raman analyses made on the peloids and flower-like structures show the presence of disordered carbonaceous matter (DCM) associated with the dolomite crystals

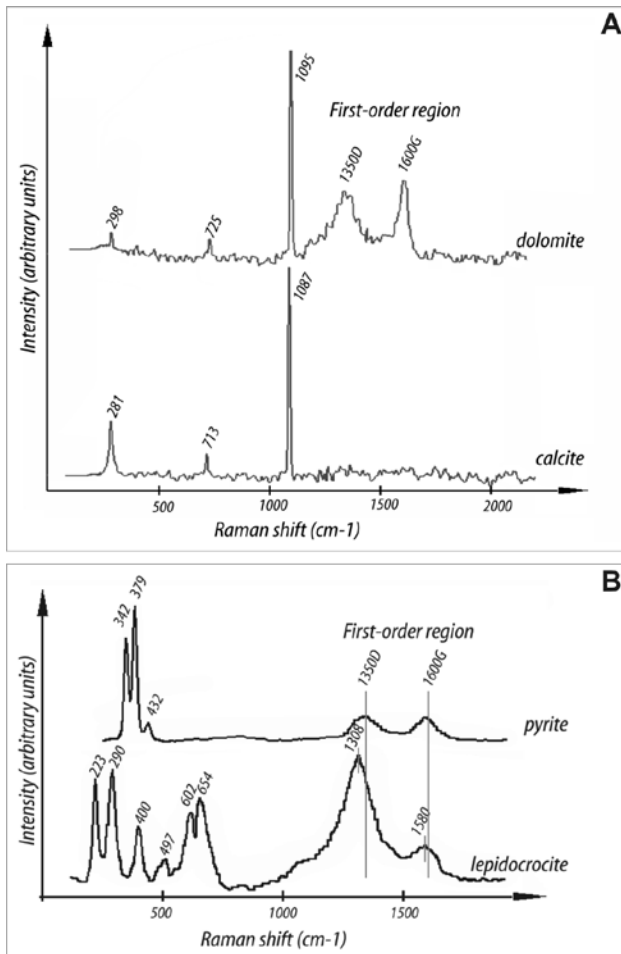


**Figure 8.** Raman spectra of the carbonate cements filling cancellous bones and of pyrite-lepidocrocite framboids. **A.** Raman spectral signature of rhombohedral dolomite crystals and sparry calcite. Note the presence of a well-defined D ( $1350\text{ cm}^{-1}$ ) and G ( $1600\text{ cm}^{-1}$ ) peaks associated with the dolomite crystals, indicating the presence of disordered carbonaceous matter (DCM). **B.** Raman spectral signature of pyrite and lepidocrocite minerals. Note the occurrence of D and G peaks associated with the framboidal pyrite, indicating the presence of disordered carbonaceous matter (DCM).

and the pyrite framboids, respectively (Figure 8A-B). Pyrite framboids, commonly associated with peloids and the flower-like structures, have an average diameter of  $6\text{ }\mu\text{m}$  and can be partially or totally oxidized to lepidocrocite (Figure 8B). SEM observations show zoned pyrite framboids with a pyritic nucleus and an external rim of lepidocrocite (Figure 6F).

### 5.4.3 Microborings

Two different microboring morphologies were observed in the Voghera whale samples (Figures 9-11). Type 1 microborings are the more abundant and occur both in the inner cancellous bones and in the outer compact bones (Figure 9). They have an average diameter size of  $3.8\text{ }\mu\text{m}$  (observed diameter between  $1.7$  and  $8.4\text{ }\mu\text{m}$ ) and a maximum measured length of  $37\text{ }\mu\text{m}$ . Optical microscope observations of type 1 microborings show that they are formed by not bifurcating, slightly curved microtunnels without any preferred orientation (Figure 9B,D). SEM-EDX analyses on type 1 microborings show microtunnels with the wall surface intensely encrusted by micron-sized iron-oxides (Figure 11B-C). On the external part of compact bones type 1 microborings form a  $300\text{ }\mu\text{m}$  thick densely tunnelled zone (Figures 9C-D, 11A). The bioeroded area is

to the bone surface by larger apertures (Figure 10D). Neither type 1 nor type 2 microboring developments are observed around post-mineralized fractures. In the same area in which the microborings occur, a 30  $\mu\text{m}$  thick barite coating encrusts the external surface of compact bones (Figure 11D). SEM and EDX analysis indicates that the barite crust is microcrystalline and is associated with a Sr-rich calcite cement (Figure 11E-F).

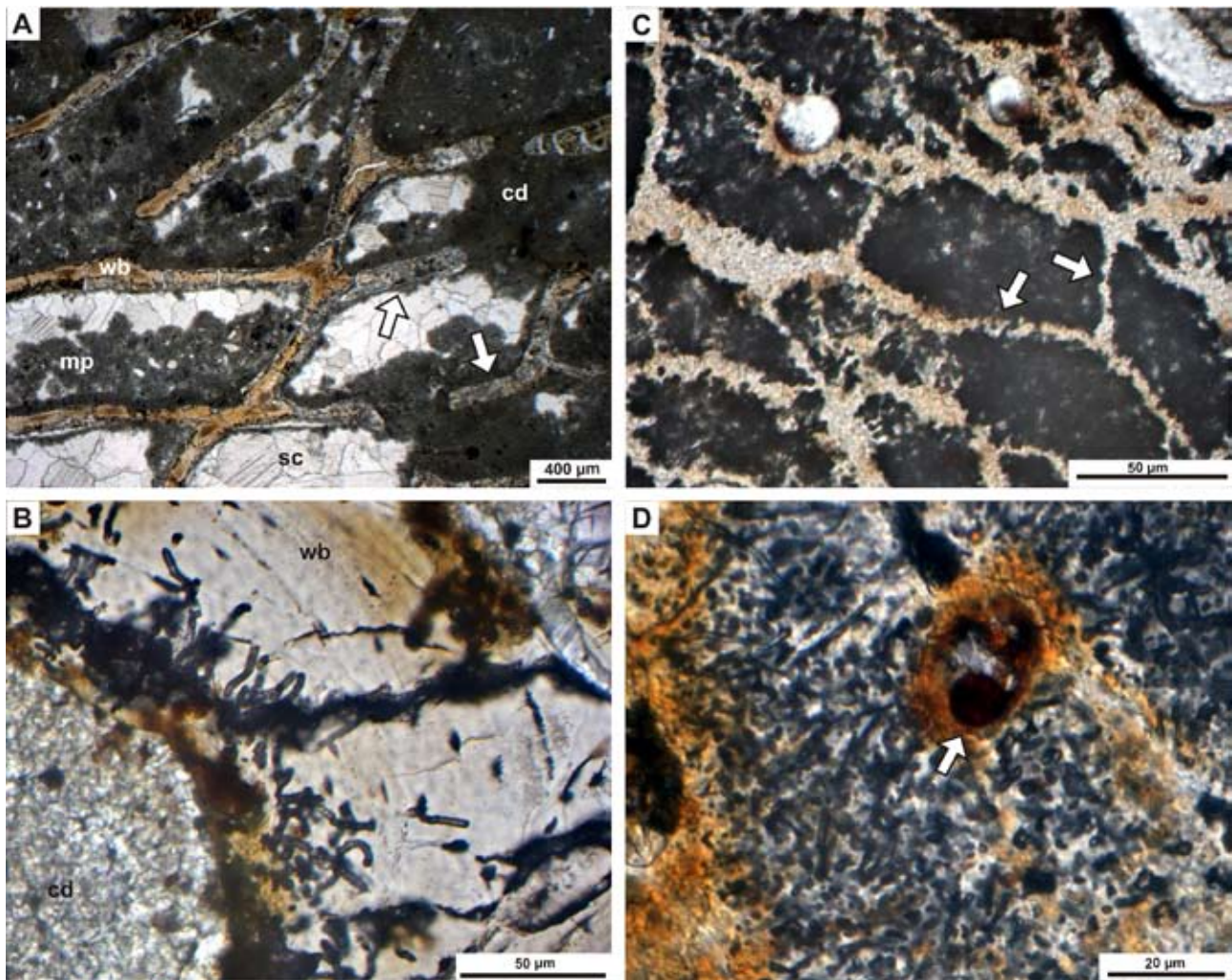


**Figure 9.** Transmitted light photomicrographs of petrographic thin sections showing type 1 microborings in cancellous and compact bones. **A.** Trabeculae of cancellous bones (wb) intensely bored by type 1 microborings (arrows). Note cancellous bones filled with clotted dolomite (cd), microbial peloids (mp) and sparry calcite (sc). **B.** Detail of type 1 microborings within trabecular bones. They do not show any preferential orientation. **C.** Type 1 microborings in compact bone. A 300  $\mu\text{m}$  thick intensely tunnelled zone is bored with a pattern that follows the micro-architecture of the bone tissue. Note in fact that the bioeroded area is delimited by bright cement lines (arrows) that mark the boundaries between the secondary osteons of the Haversian systems. **D.** Detail of the intensely bioeroded compact bone. The Haversian canal contains a reddish lepidocrocite grain (arrow). Note that the concentric lamellae typical of the osteons are totally obliterated by the microborings. All figures in plane polarized light.

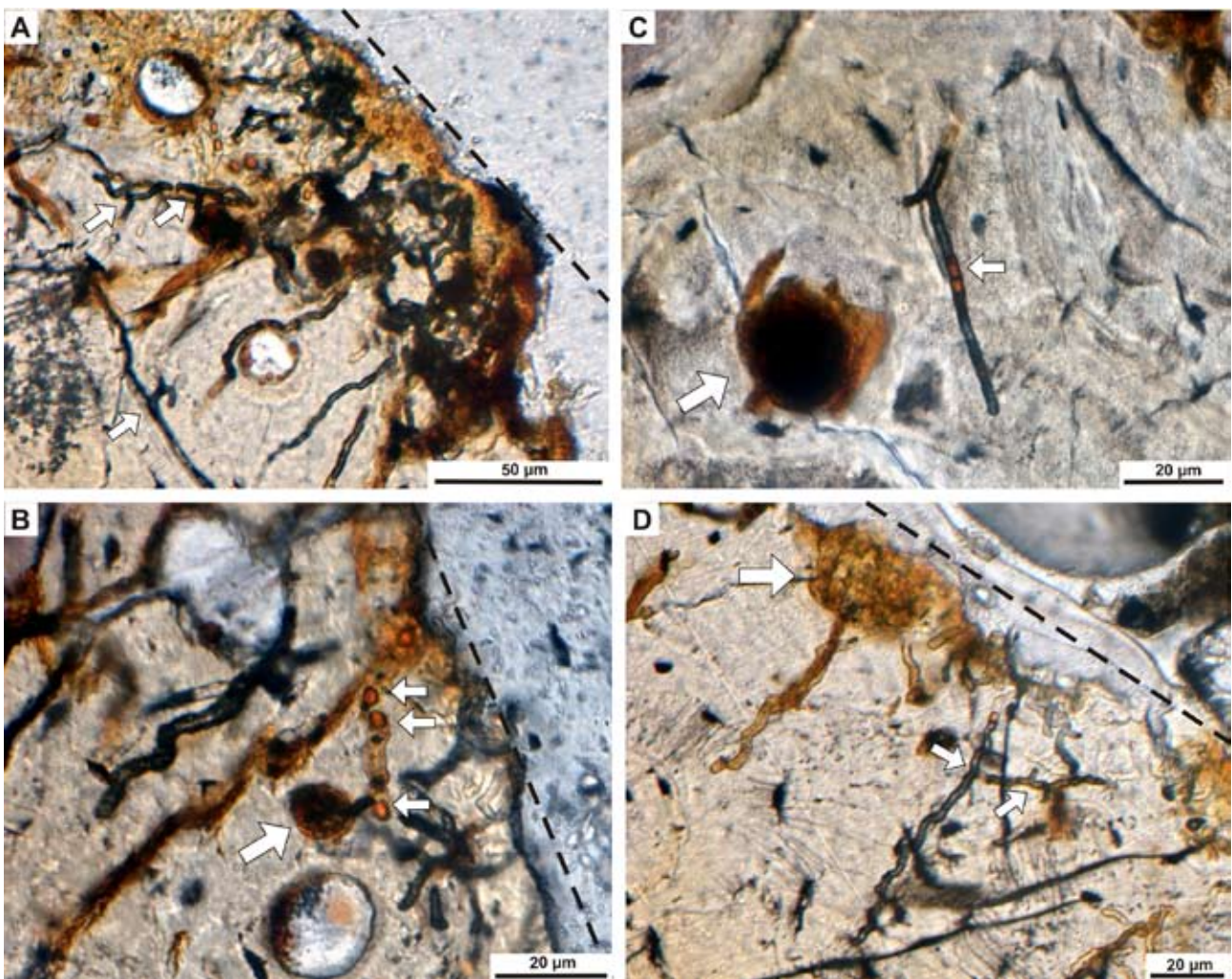


**Figure 10.** Transmitted light photomicrographs of petrographic thin sections showing type 2 microborings in compact bones. **A.** Type 2 microborings on the external side of the compact bone. Note the 90° bifurcations (arrows). **B.** Detail of type 2 microborings. Note the reddish lepidocrocite grains forming central swellings (small arrows) and a sack-shaped swelling at the tip of the same filament (large arrow). **C.** The large arrow points on an isolated sack-shaped swelling and the small arrow to a bifurcating microboring containing two small reddish lepidocrocite grains which highlight internal segmentation. **D.** Bifurcating type 2 microborings (small arrows). Note the large aperture linking one tunnel to the outside of the bone (large arrow). The black dotted line delimits the external side of the bone.

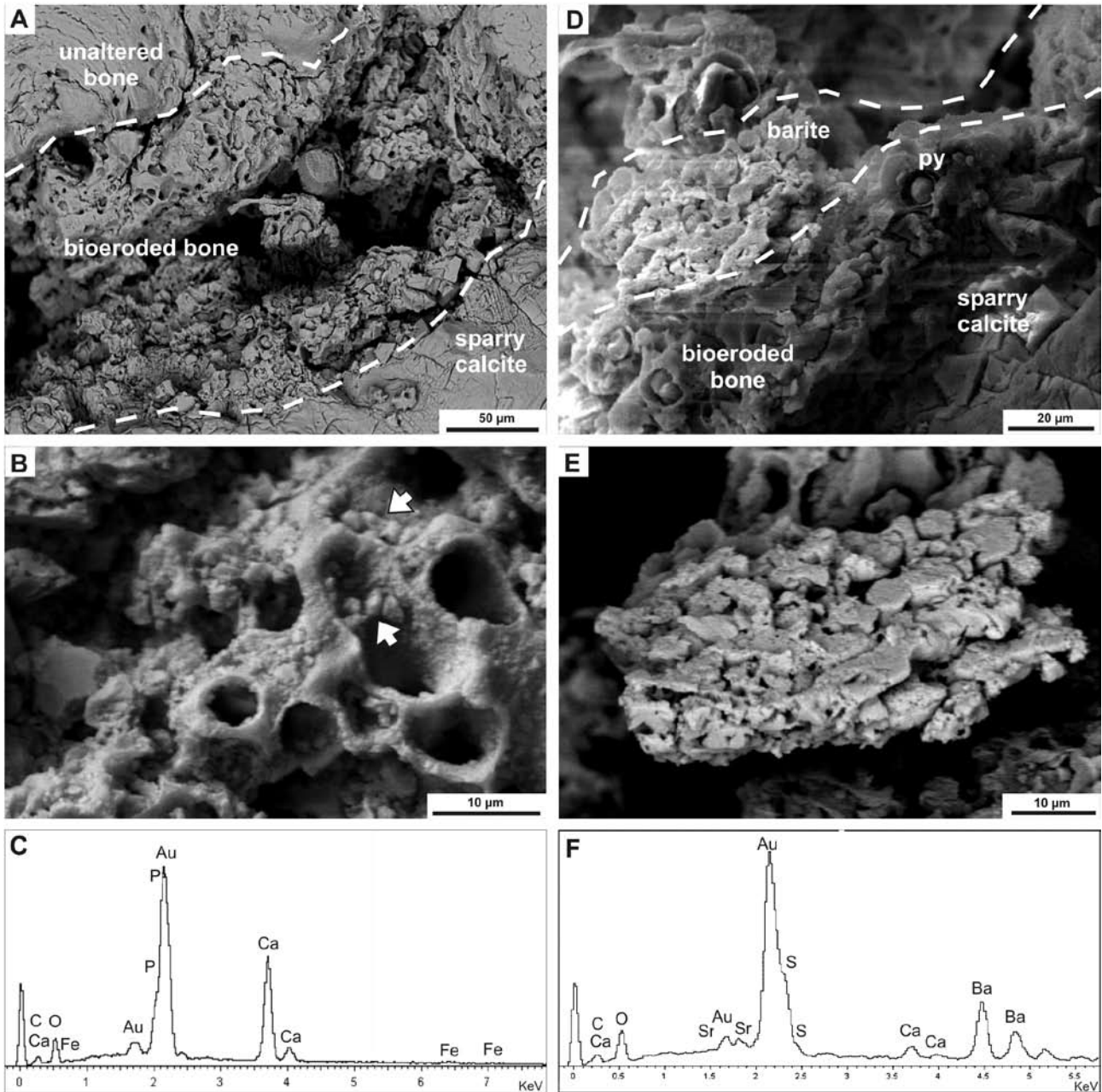


**Figure 11. SEM images of the bioeroded bones. A.** External surface of compact bones showing a 200 μm thick zone intensively bioeroded by type 1 microborings. **B.** Detail of type 1 microborings in cancellous bones. The microborings resemble empty tunnels with micron-sized mineral grains encrusting the walls (arrows). **C.** EDX analysis of the micron-sized Fe-oxide grains arrowed in B. Both apatite in the bone and the Fe-oxide were detected in this analysis. **D.** Barite crust covering the external surface of bones that are intensely bioeroded by type 1 microborings. **E.** Detail of the barite crust showing its massive microcrystalline habit. **F.** EDX analysis of the barite crust. Barite is associated with Sr-rich calcite. A and E were made in backscattered electron mode, C and D in secondary electron mode with an acceleration voltage of 15 kV.

### 5.4.4 Stable isotope analyses

Carbon and oxygen stable isotope values were obtained for the different carbonate mineral phases within our samples such as the dolomite cement of the enclosing concretion, the clotted microcrystalline dolomite and microbial peloids, and the sparry calcite (inside and outside the bones) (Figure 12). The  $\delta^{13}\text{C}$  and  $\delta^{18}\text{O}$  values of the microcrystalline dolomite sampled inside bone trabeculae range from  $-7.28\text{‰}$  to  $-7.15\text{‰}$ , and from  $+3.51\text{‰}$  to  $+3.54\text{‰}$  respectively. The dolomite cements of the enclosing concretion have  $\delta^{13}\text{C}$  values as low as  $-7.34\text{‰}$ , with  $\delta^{18}\text{O}$  values ranging from  $+3.86\text{‰}$  to  $+4.36\text{‰}$ . The sparry calcite occluding voids in- and outside bones has  $\delta^{13}\text{C}$  values between  $-1.33\text{‰}$  and  $+0.22\text{‰}$ , with  $\delta^{18}\text{O}$  values ranging between  $-1.67\text{‰}$  and  $-0.3\text{‰}$ .

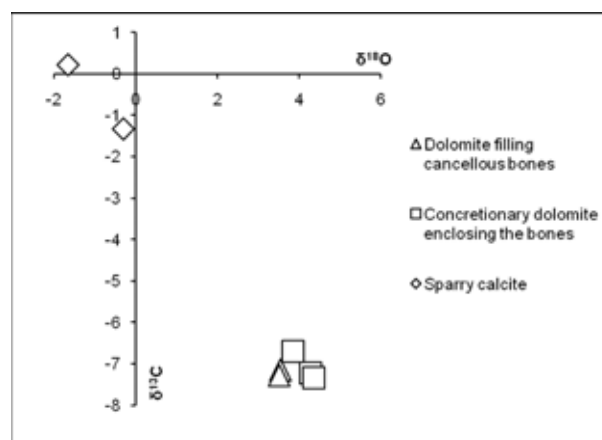


**Figure 12.** Stable isotope analyses of the carbonate cements inside and outside the Voghera whale fossil bones. Cross-plot of  $\delta^{13}\text{C}$  and  $\delta^{18}\text{O}$  values of dolomite filling cancellous bones (triangles), concretionary dolomite enclosing the bones (squares) and sparry calcite (rhombi).

## 5.5 Discussion

The Voghera whale fossil bones are preserved in Ca-rich fluorapatite, the mineral into which (hydroxyapatite) biogenic bones are commonly transformed during diagenesis (Allison and Briggs 1991). The birefringent pattern of the fossil bones investigated suggests that the bones retain the original alignment of apatite crystals that is typical of fresh, proteinated bones, despite the loss of the collagen fibres due to fossilization (Hubert et al. 1996). Iron oxide-hydroxide lepidocrocite is a common product of the diagenetic alteration of iron sulphides (Allison and Pye 1994, Bailey et al. 2010). The presence of iron sulphides within the bone matrix is presumably related to the early stages of bacterial bone decay. Sulphide produced by the bacterial degradation of bone collagen could have induced iron sulphide precipitation inside small void spaces within the bones, such as canaliculi, that are no longer visible because they have been occluded by diagenesis (Pfretzschner 2001). Similarly, iron monosulphides have been observed to form layers and fill in vertebrae micropores in modern deep-water whale-falls (see Figure 5 in Allison et al. 1991). In addition, radial microcracks in compact bones could be related to the degradation of collagen during early diagenetic processes as a consequence of the hydration of gelatinized collagen that swelled the bones (Pfretzschner 2004). Microcracks enhanced the exchange of fluids and chemicals between the bones and the surrounding water during bone decay (Pfretzschner 2004). The diffusion of oxygen and sulphates from the surrounding water into the bones presumably favoured the onset of the decay processes in the

inner part of the bones, where whales host large amounts of lipids (Higgs et al. 2011). Then, once oxygen was depleted by aerobic heterotrophic bacteria, sulphate reduction and methanogenesis could start (Allison et al. 1991). The concentric zone enriched in iron sulphide observed in the outer part of the Voghera cancellous bones may represent the boundary between an internal area in which sulphate reduction took place at the lipid-water interface and an outer zone where sulphide oxidation and aerobic decay were the dominant processes (Allison et al. 1991). A similar distribution of iron sulphides inside whale bones has been recognized in modern and fossil whales (Allison et al. 1991, Shapiro and Spangler 2009).

Clotted and peloidal structures similar to those described within Voghera fossil whale bones (Figure 6) occur in wide variety of different geological settings, such as in shallow water carbonates, coral reef crusts, mud mounds, hydrocarbon seep deposits, as well as in late Eocene-early Oligocene deep water whale-falls (Chafetz 1986, Cavagna et al. 1999, Campbell et al. 2002, Peckmann and Thiel 2004, Shapiro 2004, Barbieri and Cavalazzi 2005, Cavalazzi et al. 2007, Shapiro and Spangler 2009). The clotted fabric is related to small-scale variations in the chemical microenvironment during carbonate precipitation caused by the metabolic activities of microorganisms (Burne and Moore 1987). Peloids are interpreted as microbial bio-products or biominerals that are thought to be precipitated on the surface of bacterial clumps (Chafetz 1986). As observed in the Voghera whale bones, microbial peloids are characterized by richness of dark organic matter, indistinct margins, variable sizes, cloudy interiors, and sulphide minerals (Shapiro 2004). The flower-like structures floating within sparry calcite cement resemble small peloids although they lack the inner filling of microcrystalline dolomite (Figure 7). They could represent bacterially induced precipitates overgrown by single euhedral dolomite crystals instead of being completely lithified by microcrystalline calcite, as supposed for similar dolomite aggregates from a Miocene methane seep of northern Italy (Cavagna et al. 1999). A biogenic origin for the peloids and the flower-like structures is also supported by the presence of disordered carbonaceous matter in close association with them (Figure 8). In the Raman spectra the G and D bands represent a mixture of crystalline carbonaceous material (graphite, G) and poorly organized carbonaceous matter (D), respectively (Beissac et al. 2003) and the association with probable microbial structures, such as the peloids and the flower-like structures, may indicate that the carbon is of biological origin (Marshall et al. 2010).

Shapiro and Spangler (2009) suggested that the model presented by Riding and Tomás (2006) for the calcification of bacterial micropeloids in Cretaceous stromatolites may also be applicable to fossil whale bones. According to this model the clotted microcrystalline dolomite and the peloids of the Voghera whale would represent the product of the organic matter decay immediately below the sediment-water interface. During early diagenesis, microbial decay of whale bone lipids could have induced the dolomite precipitation, that potentially induced the calcification of bacterial aggregates forming the nuclei of peloids. The spatial distribution of aggregating bacterial colonies determined the spacing of the peloidal masses. When all the organic matter was consumed and the peloids overgrew, the sparry calcite cement occluded the water-filled voids.

The precipitation of dolomite in the peloids of the Voghera fossil whale bones was probably determined by the chemistry of the pore waters. Dolomite precipitation, in fact, is known to be inhibited by normal marine sulphate concentration, whereas is favoured when sulphates are removed from the pore waters by an intense reducing bacterial activity (Kastner 1984). In particular, the degradation of organic matter by sulphate reducing bacteria could promote early dolomite precipitation by simultaneously increasing the carbonate alkalinity and reducing near zero the sulphate ion concentration (Compton 1988). The sediment depth of early dolomite precipitation depends on the organic input, the rate of sulphate reduction and sedimentation rate, and already can start at less than 1 m below the sediment sea-water interface (Mazzullo 2000).

The common co-occurrence in the Voghera samples of pyrite framboids associated with dolomitic clots and rhomboedric dolomite cements suggests an intense sulphate reduction. Although diagenetic, microbially produced pyrite framboids and crystals are common in sedimentary rocks, especially in fine-grained lithologies (*e.g.*, Berner 1970), the association of framboidal pyrite with authigenic carbonates is less common, and in seep-related authigenic carbonates it is considered to be a paleoenvironmental indicator for bacteria sulphate reduction independent of burial diagenesis (Cavagna et al. 1999, Shapiro 2004, Cavalazzi et al. submitted b).

The similar carbon and oxygen isotopic signal obtained for the microcrystalline dolomite intimately associated with cancellous bone and for the dolomite in the enclosing concretion (average  $\delta^{13}\text{C}$ : -7.12 ‰; average  $\delta^{18}\text{O}$ : +3.81 ‰) suggests that they probably precipitated in similar geochemical conditions. The slightly depleted  $\delta^{13}\text{C}$  values are compatible with fractionation promoted by sulphate reduction processes during bacterial oxidation of the whale lipids (Irwin et al. 1977, Coleman et al. 1993, Mazzullo 2000). The slightly high  $\delta^{18}\text{O}$  values could be explained as a consequence of low bottom water temperatures on the shelf in addition to late diagenetic alteration (Mozley and Burns 1993). The carbon and oxygen stable isotope values of sparry calcite cement inside and outside the bones (avg  $\delta^{13}\text{C}$ : -0.55 ‰; avg  $\delta^{18}\text{O}$ : -0.98 ‰) are consistent with a (late) precipitation in chemical equilibrium with seawater (Mozley and Burns 1993).

Microborings in the Voghera fossil whale bones were generated prior to the fracturing and mineralization of the bones as they are not concentrated around post-mineralized fractures (Trueman and Martill 2002). Type 1 microborings are in the same range size of those described in previous studies on deep-water fossil whale-falls (Amano and Little 2005, Kiel 2008, Shapiro and Spangler 2009) and in plesiosaurid carcasses (Kaim et al. 2008), while type 2 microborings are smaller. The morphologies of the microborings are similar to the traces left by euendoliths, that is, endolithic microorganisms that actively penetrate into rocks or hard substrates and create microtubular cavities conform with the shapes of their bodies (Golubic et al. 1981). In the marine ecosystem such organisms include phototrophic cyanobacteria and algae and heterotrophic fungi and bacteria, all of which are capable of metabolizing collagen and dissolving the mineral matrix (Davis 1997, Trueman and Martill 2002). While phototrophic



euendoliths dominate within the sunlight-illuminated (euphotic) coastal ranges in the oceans, the light-independent heterotrophs follow the distribution of organic substrates for food and are found in all depths ranging from shallow coastal waters to the abyssal depths (Golubic et al. 2005 and references therein). As a consequence of convergent evolution of boring and reproductive behavior among unrelated organisms that exploit similar environments in shallow waters, the distinction between the borings of endolithic fungi, filamentous (and sometimes coccoid) cyanobacteria and eukaryotic algae is often difficult (Golubic et al. 2005, Jans 2008). The occurrence of the Voghera type 1 microborings along the internal walls of cancellous bones (Figure 9A) that is, in an environment not influenced by sunlight, suggests that the responsible organisms are heterotrophic rather than phototrophic. In addition, the absence of bifurcations, the presence of permineralized rims around the borings, and the destructive pattern of the bones support a prokaryotic origin (Turner-Walker 2008, Turner-Walker et al. 2002, Jans 2008). Type 2 microborings only occur on the external part of the bones (Figure 10). Here, the presence of dichotomously branched ramifications with internal segmentation and, especially, associated bag-shaped swellings support a fungal origin (Schumann et al. 2004, Golubic et al. 2005, Eickmann et al. 2009).

Barite ( $\text{BaSO}_4$ ) is known to form in numerous microbially colonized habitats, including marine cold seeps, white smokers, hot springs, and the upper water columns of lakes and oceans (Bonny and Jones 2008 and references therein). Barite deposits generally form as a result of mixing of soluble barium-containing fluids with sulphate-rich fluids. Deposits formed by direct precipitation from barium-enriched hydrothermal fluids are known as hydrothermal barite. They are restricted to the vicinity of seafloor vents and are commonly associated with anhydrite and sulphides (*e.g.*, Koski et al. 1985). At cold seeps, on the other hand, barite precipitation occurs when rising barium-rich fluids derived from the dissolution of biogenic barite deposits react with sulphate-rich, downwards-diffusing seawater or ascending brines (Torres et al. 2003, Aloisi et al. 2004). In the water column, barium sulphate is known to precipitate within microenvironments of decaying planktonic organisms, which may actively or passively accumulate barium and form barite in pelagic sediments underlying high productivity waters (Dehairs et al. 1980, Bishop 1988, Paytan and Griffith 2007). Authigenic barite has also been documented in biogenic calcareous rocks where barium is derived from the decomposition of organic matter, plankton and other organisms such as bacteria (Stamatakis and Hein 1993). Although the morphologies and sizes of marine barite crystals in the water column and in marine sediments indicate a possible biogenic origin, the living organisms which directly precipitate barite have not yet been identified in seawater (González-Munõz et al. 2003). Barite precipitation by living organisms (protozoa) has been, however, demonstrated in lacustrine freshwater environments, where sulphur-metabolizing microbes are capable of mediating barite saturation (*e.g.*, González-Munõz et al. 2003, Senko et al. 2004). Sulphur-oxidizing bacteria with affinities with the genus *Beggiatoa* can be suitable substrates for barite precipitation (Bonny and Jones 2008). Thus, microcrystalline barite on the external surface of the Voghera whale bones may be derived from the decomposition of organic

matter (plankton or bacteria), or may represent indirect evidence of sulphur-oxidizing bacterial mats encrusting the bones when they were lying on the sea floor.

## **5.6 Taphonomic model: an hypothesis**

After sinking on the sea floor in a shallow marine environment and the removal of fleshy tissue by scavengers, the dead whale underwent decay of the organic matter and the bone lipids. Organic matter decay started with bacterial degradation of bone collagen, as testified by the precipitation of iron sulphides in the bone matrix and by radial micro-cracks in compact bones. Saprophagous bone borers feeding on bone collagen created microscopic tunnels in the external surface of the bones, migrating progressively inward. These processes enhanced the inflow of seawater inside the bones, allowing the diffusion of sulphate. After the consumption of free oxygen by aerobic heterotrophic bacteria, the decay of bone lipids in the marrow cavities of cancellous bones was affected by anaerobic sulphate reduction. The whale-fall moved into the so-called sulfophilic stage during which elevated  $H_2S$  concentrations within the whale bone and the surrounding sediments led to a sulphide-based chemoautotrophic primary production. Microbial sulphide production induced the precipitation of iron sulphides in the external area of trabecular bones. Barite crusts on the surface of the bones could be linked to the oxidation of sulphide by sulphide-oxidizing bacteria. When the bones were just below the sediment-water interface, sulphate reduction processes promoted the precipitation of microcrystalline- and euhedral-dolomite cements inside bone trabeculae and in the bone-bearing concretion. The precipitation of early diagenetic cements could have been favoured by early burial of the bones, more desirable in a shallow marine depositional environment. High sedimentation rates caused rapid burial of the bones, hindering the onset of an epibiont "sulphur loving" stage of the ecological succession and the colonization of the bones by macro-invertebrates while at the same time favouring the preservation of the associated microbial processes in the fossil record.

## **5.7 Conclusions**

The detailed microfacies and geochemical analyses of the Voghera fossil whale-fall system provide fossil evidence of the intimate association of a microbial ecosystem with a decaying whale carcass on the sea floor. Traces were left by two different types of euendolith microorganisms, a prokaryote and a fungus, that intensely eroded the fossil bones. We also found evidence of the occurrence of microbial processes mediated by sulphate-reducing bacteria during the sulfophilic-stage that include diverse biofabrics and biominerals, such as microbial dolomite, microbial peloids, clotted textures, pyrite and barite. This evidence highlights how whale falls can create sulphidic conditions similar to other chemosynthetic habitats such as cold seeps and hydrothermal vents, and how their traces can be recognized in the fossil record. Finally, we illustrated the role of the depositional environment in the preservation of the microbially mediated structures.

## ***Two more case-studies: the Orciano Pisano and the Castelfiorentino fossil whales***

### **5.8 Introduction**

The same analytical methods applied to the study of the Voghera whale fossil bones were used for study the whale bones and the enclosing concretion of two Pliocene specimens. The Orciano Pisano whale is a 10 m long mysticete with associated chemosymbiotic bivalves (Figure 13A, Chapter 3, 4). The taphonomic study of the skeleton highlighted the presence of intense bioerosion on the higher side of the bones and cemented areas in the lower side, especially between vertebrae (Figure 13B). The Castelfiorentino whale (W21: Chapter 4), a very well preserved 8 m long balaenopterid, when excavated was intensively cemented in the thoracic region (Figure



**Figure 13.** The Orciano Pisano and the Castelfiorentino fossil whales. **A.** Field view of the 10 m long Orciano Pisano whale at the end of its excavation. **B.** Caudal vertebrae of the Orciano Pisano whale. Note the intense bioerosion on the upper side of the bones and the higher degree of cementation on the lower side (arrows). Note also the bivalve *Amusium cristatum* next to the bones. **C.** The articulated Castelfiorentino whale. **D.** Thoracic area of the Castelfiorentino whale bones soon after excavation. The arrows point on the diffuse carbonate concretion enclosing the bones. The concretion was totally removed during specimen preparation.

13D). During museum preparation carbonate concretions were totally removed from the bones (compare Figures 13C and D). No data are available on the presence of chemosymbiotic molluscs associated with the bones (Chapter 4: Appendix).

The Orciano Pisano whale comes from upper Piacentian-lower Gelasian marine sediments of

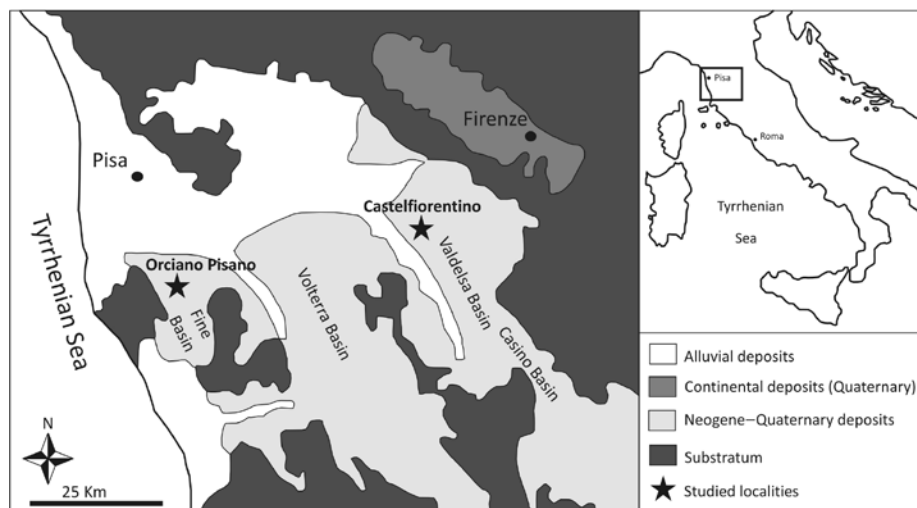


**Figure 14.** Schematic geological map (modified after Carnevale et al. 2008) and location of the two study sites.

the Fine Basin (Tuscany), and the Castelfiorentino whale from Piacentian marine sediments of the Valdelsa Basin (Tuscany) (Figure 14). The Fine Basin is situated on the Tyrrhenian side of the northern Apennines, and is filled by 1000 m of Tortonian-Pleistocene, mostly marine deposits. The depositional environment rapidly shifts

from deltaic to bathyal depths at the start of the Pliocene (Carnevale et al., 2008 and references therein), at the onset of deposition of grey-blue marls. The Orciano Pisano fossil whale was found in the middle part of the regressive deposits overlaying the grey-blue marls, within silty fine-grained sandstones marking the regression to shelf depths. The Valdelsa Basin is a post-collisional basin filled with more than 2000 m Neogene deposits, constituted by continental Miocene and Pliocene alluvial, coastal marine, and shelf sediments. The succession can be subdivided into large-scale sequences, previously referred to as synthem, where bounding unconformities are produced during major pulses of uplift of the Apennines (Benvenuti et al. 2007 and references therein). The whale was excavated from inner shelf muddy sediments (see Chapter 5).

Selected bone fragments and the enclosing concretion (Figure 15) were studied to find evidence of microbial processes associated with the degradation of whale bones and to reconstruct the burial and diagenetic history of the bones. Petrographic thin sections and polished slabs were analyzed at optical and scanning electron microscopes, and

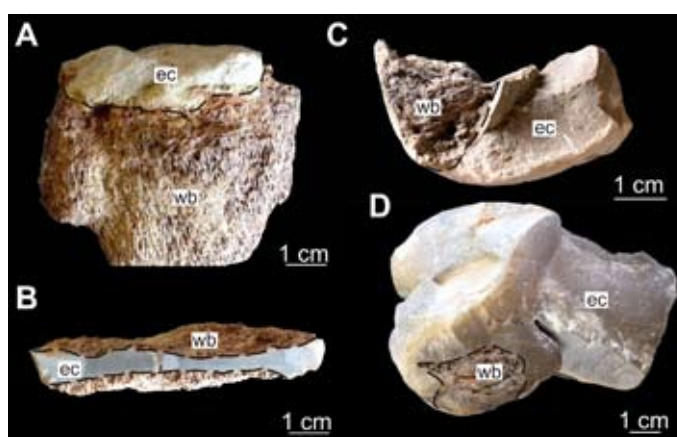


**Figure 15.** Studied samples. A and B. Selected bone fragments enclosed in the carbonate concretion of the Orciano Pisano whale. C and D. Selected bones and enclosing concretion of the Castelfiorentino whale. wb: whale bone; ec: enclosing concretion

powder samples were collected for  $^{13}\text{C}$  and  $^{18}\text{O}$  stable isotope analyses. For a detailed description of the methods see the Voghera whale method section, paragraph 5.3.

## 5.9 Results

### 5.9.1 The Orciano Pisano fossil whale

#### 5.9.1.1 Carbonate cements and fossil bone preservation

The Orciano whale bones are enclosed in a grey host matrix consisting of angular to subangular quartz grains, sparse pyrite framboids and abundant glauconite grains, cemented with dolomite crystals (Figures 16A-B, 17C). Glauconite grains are rounded to ovoidal in shape with an average size of  $76.2\ \mu\text{m}$  (min  $29.5\ \mu\text{m}$ , max  $128.7\ \mu\text{m}$ ), and are frequently stained by clusters of pyrite framboids (Figure 16C). Glauconite grains can also fill tests of benthic foraminifers (Figure 16C). The dolomite cement as observed at the optical microscope shows a clotted fabric, forming dark and cloudy aggregates of more densely packed crystals alternated with areas with less packed and larger crystals filling the voids (Figure 16B-C). SEM observations of the dolomite concretion allowed the distinction of areas with tightly packed anhedral to subhedral crystals and poorly distinct crystal boundaries (Figure 17A), from areas with loosely packed dolomite crystals, mostly euhedral in shape, floating in a fine argillous matrix (Figure 17B). Dolomite crystals range in size between  $4.7\ \mu\text{m}$  and  $18.4\ \mu\text{m}$ .

The fossil whale bones are preserved as carbonate apatite (Figure A,C). The external compact bone is missing and the internal, more porous cancellous bone, is directly in contact with the external dolomite concretion (Figure 16A). The bones are light brown in colour in plane polarized light and when observed in SEM backscattered electron mode they show densely de-mineralized areas with characteristic spongiform porosity (Figure 18A-B). This de-mineralization pattern is observed along the bone structure, and the resulting holes have an average diameter of  $2.2\ \mu\text{m}$ , with a minimum and maximum measured diameter of  $0.8\ \mu\text{m}$  and  $6.1\ \mu\text{m}$ , respectively. Locally, the holes are filled by spherules of calcium sulphate minerals with an average diameter of  $4.1\ \mu\text{m}$  (Figure 18B,D).

Cancellous bones are filled by the same dolomite cement forming the external carbonate concretion (Figure 19). The dolomite cement shows a clotted fabric and fills the trabecular cavities with a geopetal pattern (Figure 19A). Rare peloids are observed, with a medium diameter of  $90\ \mu\text{m}$  (Figure 19B). Locally, glauconite grains and benthic foraminifer tests are also observed (Figure 19A) as well as pyrite framboids (Figure 19C). Framboids are scattered within the dolomite cement, sometimes forming well defined clusters. They have a medium diameter of  $20.3\ \mu\text{m}$ , however, they are highly variable in size, with a minimum and maximum measured diameter of  $2.6\ \mu\text{m}$  and  $61.7\ \mu\text{m}$ , respectively. Rarely, a second carbonate cement is observed, consisting of banded fibrous calcite, also associated with euhedral or framboidal pyrite (Figure 19D-F).

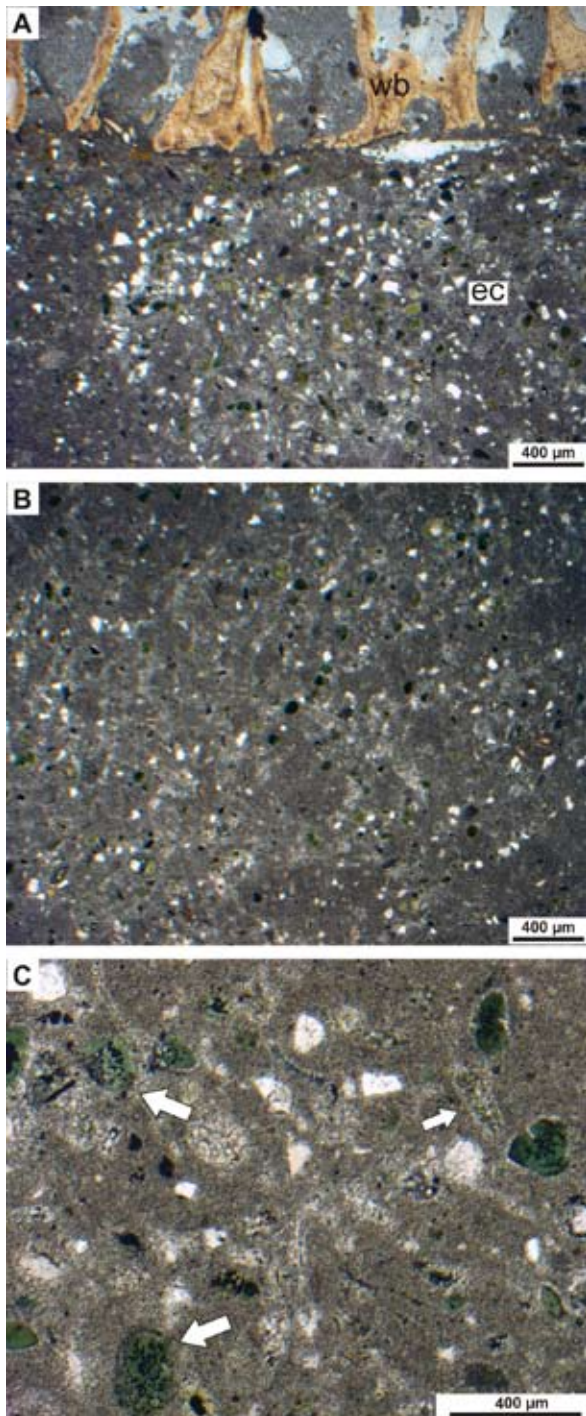


Figure 16. Transmitted light photomicrographs of petrographic thin sections of the Orciano Pisano whale bones and the enclosing carbonate concretion. A. The fossil whale bone (wb) and the enclosing concretion (ec). The enclosing concretion consists of angular to subangular quartz grains, sparse pyrite framboids and abundant glauconite grains, cemented with dolomite crystals. B. Detail of the enclosing concretion. Note the abundant, rounded, glauconite grains. C. Pyritized glauconite grains (large arrows) and glauconitized foraminifer test (small arrow).

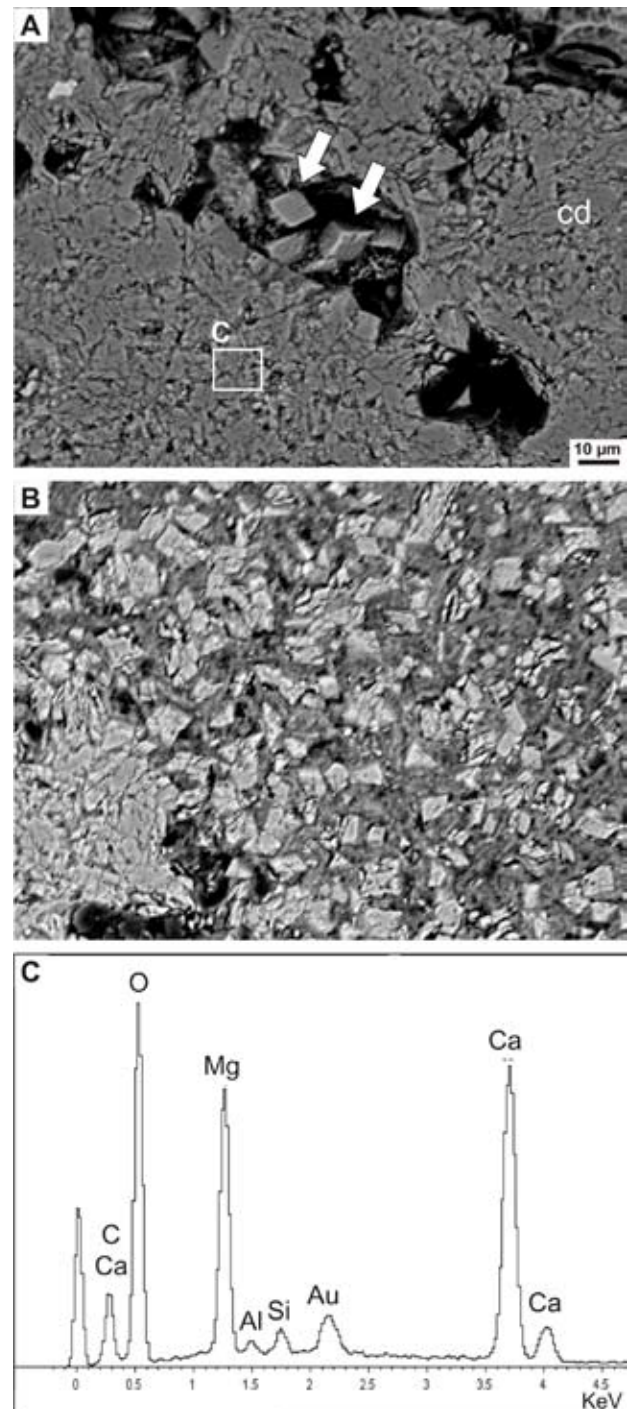


Figure 17. SEM images of petrographic thin sections of the dolomite concretion of the Orciano Pisano whale. A. Densely packed dolomite crystals (cd). Arrows point on euhedral dolomite crystals. B. loosely packed dolomite crystals, mostly euhedral in shape, floating in a fine argillous matrix. C. EDX analysis of the dolomite concretion. A and B were made in backscattered electron mode, C in secondary electron mode with an acceleration voltage of 15 kV.

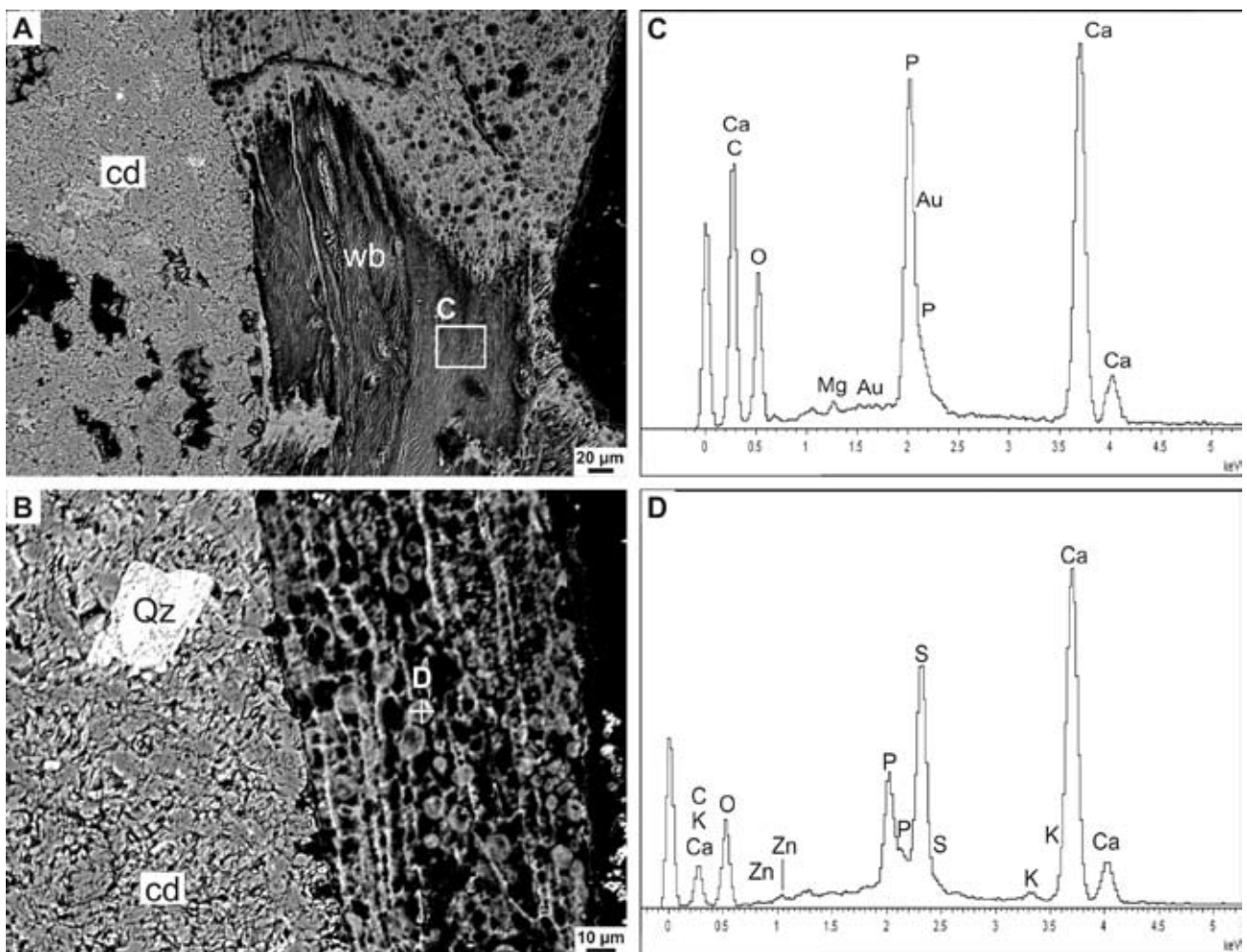


Figure 18. SEM images of petrographic thin sections of the Orciano Pisano whale bones. A. Contact between well preserved (bottom) and demineralised (top) bones. B. Detail of the demineralised area. Note the small calcium sulphate spheres filling the holes, analyzed in D. C. Areal EDX analysis of the fossil bone, preserved as carbonate apatite. D. Punctual EDX analysis of the small spheres filling demineralised bones. Calcium sulphate (gypsum? Anhydrite?) is associated with the carbonate apatite of the bone. A and B were made in backscattered electron mode, C and D in secondary electron mode with an acceleration voltage of 15 kV.

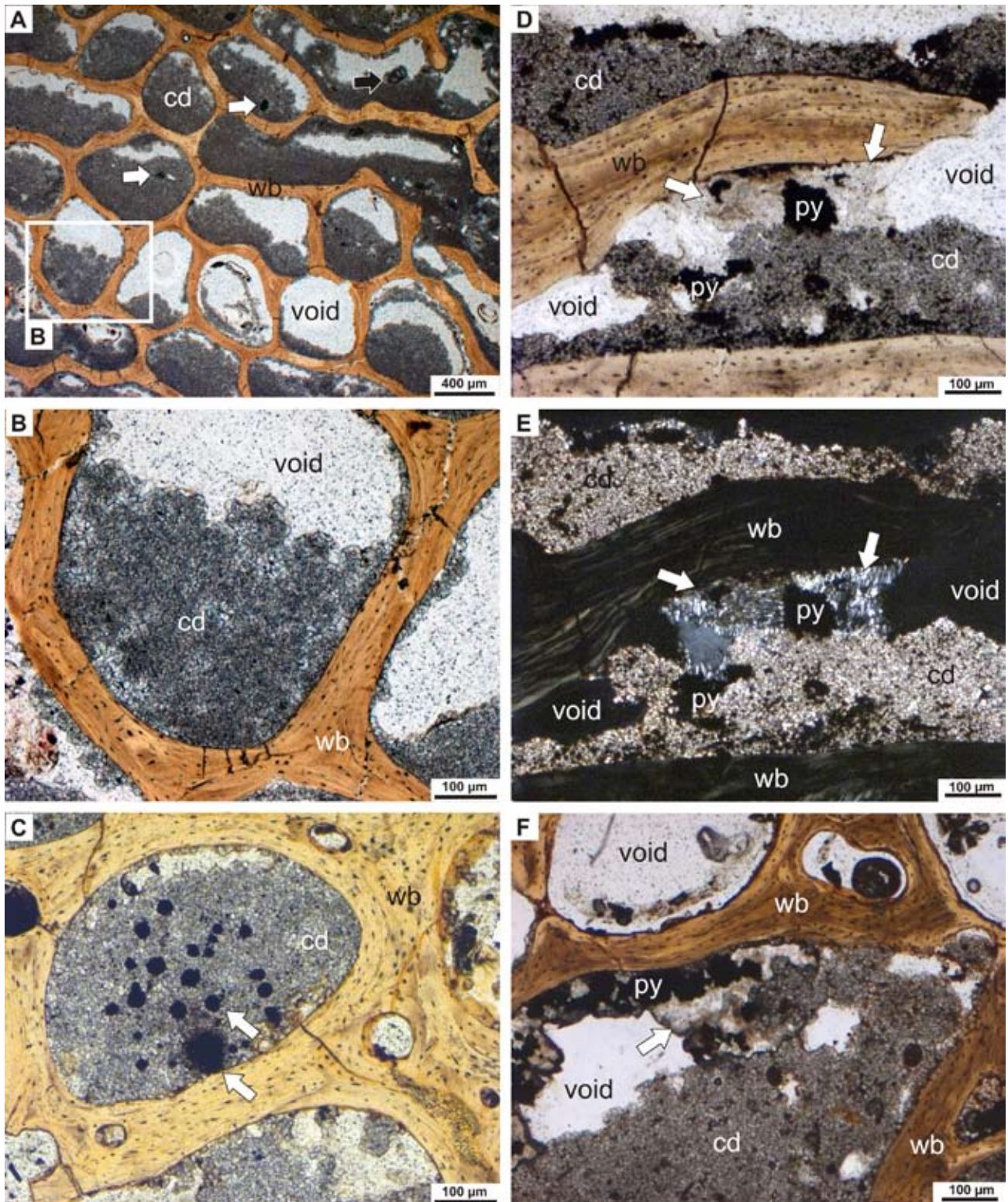
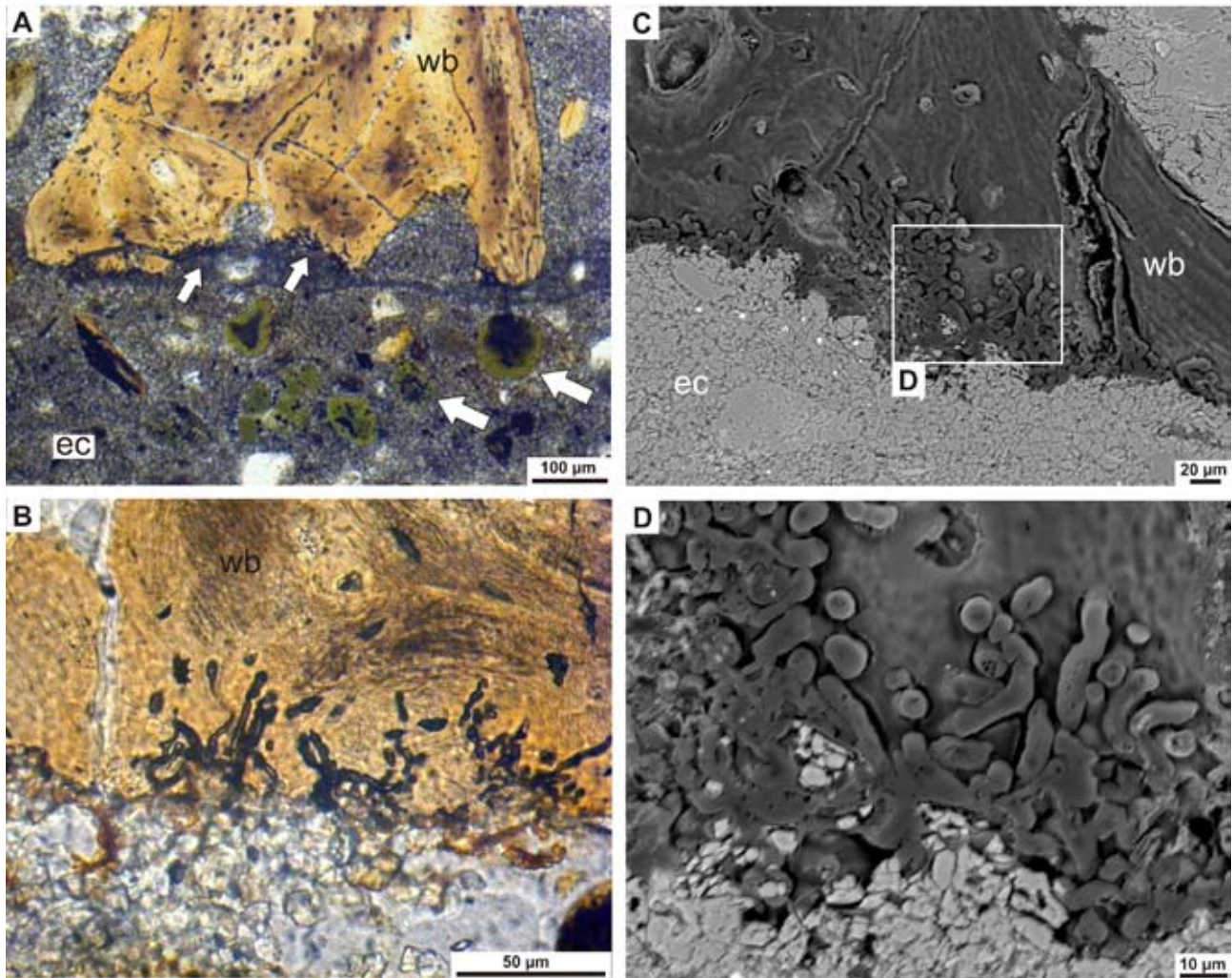


Figure 19. Transmitted light photomicrographs of petrographic thin sections of the Orciano Pisano whale bones. A. Clotted dolomite filling bone trabeculae. The remaining spaces are empty. Note the geopetal pattern with which dolomite fills the bones. Clotted dolomite hosts sparse glauconite grains (white arrows) and foraminifer tests (black arrow). B. Detail of the clotted dolomite in A. Badly preserved peloids occur. C. Pyrite framboids in the dolomite cement. D, E, F. Fibrous calcite secondary filling the voids, and associated with framboidal or euhedral pyrite grains. All figures in plane polarized light except E which is in cross polars.



### 5.9.1.2 Microborings

Microborings were observed in cancellous bones in contact with the external carbonate concretion (Figure 20). They are slightly- to highly-curved structures, not bifurcating, with a medium diameter of 4.4  $\mu\text{m}$  (min. 2.4  $\mu\text{m}$ , max. 7.1  $\mu\text{m}$ ) and a maximum measured length of 33.5  $\mu\text{m}$ . The microborings tunnel the bones without any preferred orientation and the eroded area have a maximum thickness of 64.2  $\mu\text{m}$ .



**Figure 20.** Transmitted light photomicrographs and SEM images of petrographic thin sections showing microborings tunnelling the external side of the bones. **A.** Bone trabecula in contact with the external concretion which is enriched in glauconite grains (large arrows). Small arrows point on the microtunnelled area. Note the well preserved osteocytes. **B.** Detail of the microborings which tunnel the bones for a maximum of 60  $\mu\text{m}$  towards the inside. **C and D.** SEM images of the microbored area. Microborings are slightly curved and do not bifurcate. **A and B** in plane polarized light, **C and D** in backscattered electron mode.

## 5.9.2 The Castelfiorentino whale

### 5.9.2.1 Carbonate cements and fossil bone preservation

The Castelfiorentino whale bones are enclosed in a dolomite concretion constituted by microcrystalline to larger dolomite crystals. Dolomite crystals are tightly packed, subhedral to anhedral in shape, have distinct straight crystal boundaries, and form a dense mosaic (Figure 21A,C). Dolomite crystals measure from 2.54 to 11.4  $\mu\text{m}$ , with a medium size of the main axis of 6.4  $\mu\text{m}$ . Subordinately voids are filled by a secondary cement of sparry calcite (Figure 21C). Rare siliciclastic grains, mainly quartz, occur in the dolomite cement, whereas pyrite framboids are abundant (Figure 21B-C). Pyrite framboids have an average diameter of 4.8  $\mu\text{m}$  (min. 0.9  $\mu\text{m}$ , max. 9.2  $\mu\text{m}$ ).

In most of the analyzed samples the outer compact bone is missing and the inner cancellous bone is directly in contact with the external concretion (Figure 21A). Cancellous bones are filled by the same cements of the enclosing concretion. Microcrystalline to larger dolomite crystals fill bone trabeculae, locally sparry calcite fills the remaining voids (Figure 22A-B). Bone trabeculae can be rimmed with equant calcite cement (12.3  $\mu\text{m}$  thick: Figure 22C). Cluster of pyrite framboids occur in the dolomite cement, and are more frequently distributed close to bone trabeculae (Figure 22D, 23B-C). Framboids have an average diameter of 3.4  $\mu\text{m}$ . The fossil bones, preserved as carbonate-apatite (Figure 23E) are cut by many secondary fractures (Figure 22D). The fractures can be empty or filled by massive pyrite (Figure 22E-F). Pyrite can also form thick crust covering large areas of the bones (Figure 23A,F).

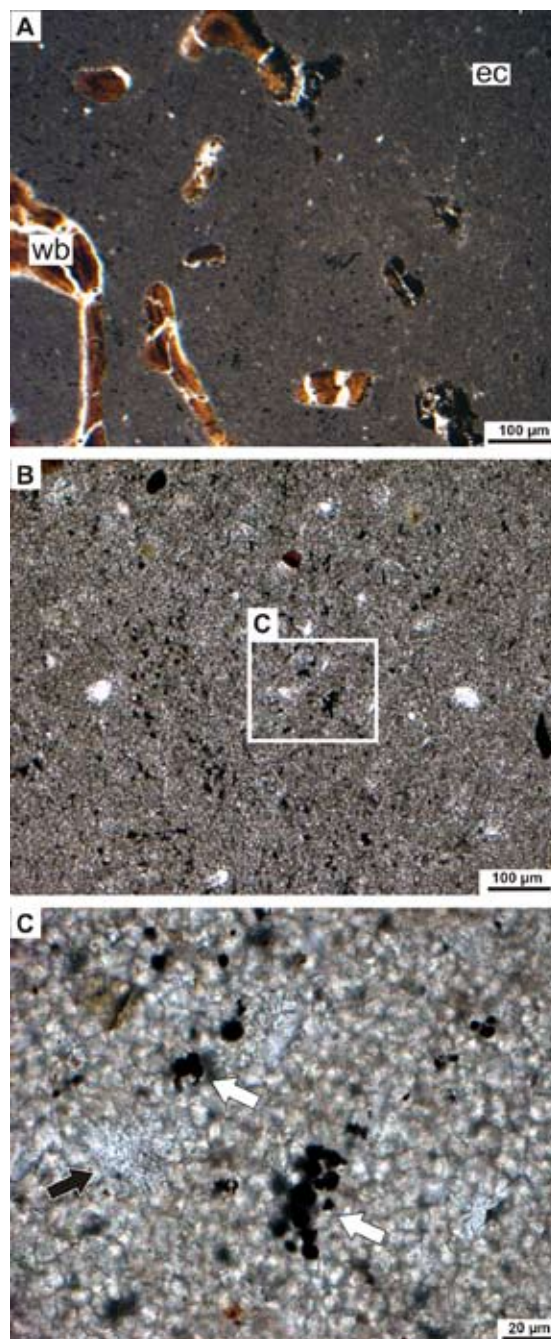


**Figure 21.** Transmitted light photomicrographs of the Castelfiorentino whale bones and the enclosing carbonate concretion. **A.** Trabecular bones directly in contact with the densely packed dolomite concretion. Bones are highly destroyed by microbial bioerosion. **B.** and **C.** Detail of the dolomite cement enclosing the bones. Note the abundant pyrite framboids (white arrows) and the secondary sparry calcite (black arrow). All figures in plane polarized light.

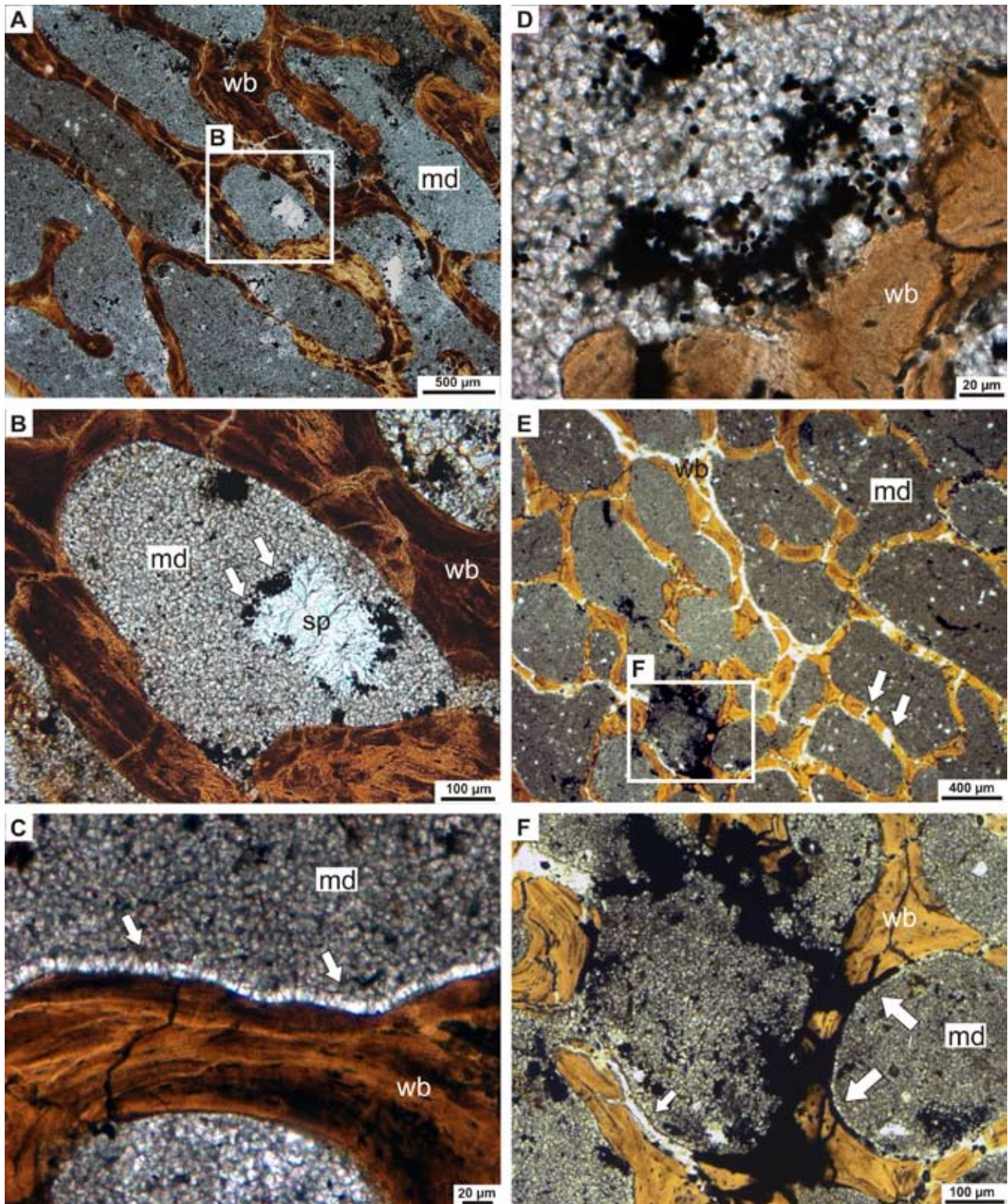


**Figure 22.** Transmitted light photomicrographs of the Castelfiorentino whale bones and cements filling bone trabeculae. A. Trabecular bones filled by a microcrystalline dolomite cement (md) with secondary sparry calcite (white box). B. Detail of figure A showing sparry calcite associated with framboidal pyrite (arrows). C. Bone trabecula rimmed with equant calcite cement. D. Area with high concentration of cluster of pyrite framboids next to the bones. E. Trabecular bones intensively cut by secondary fractures (arrows), which can be filled by massive pyrite crusts (white box). F. Detail of the pyrite crusts on trabecular bones. Large arrows point on pyrite crusts, the small arrow to an empty fracture. All figures in plane polarized light.

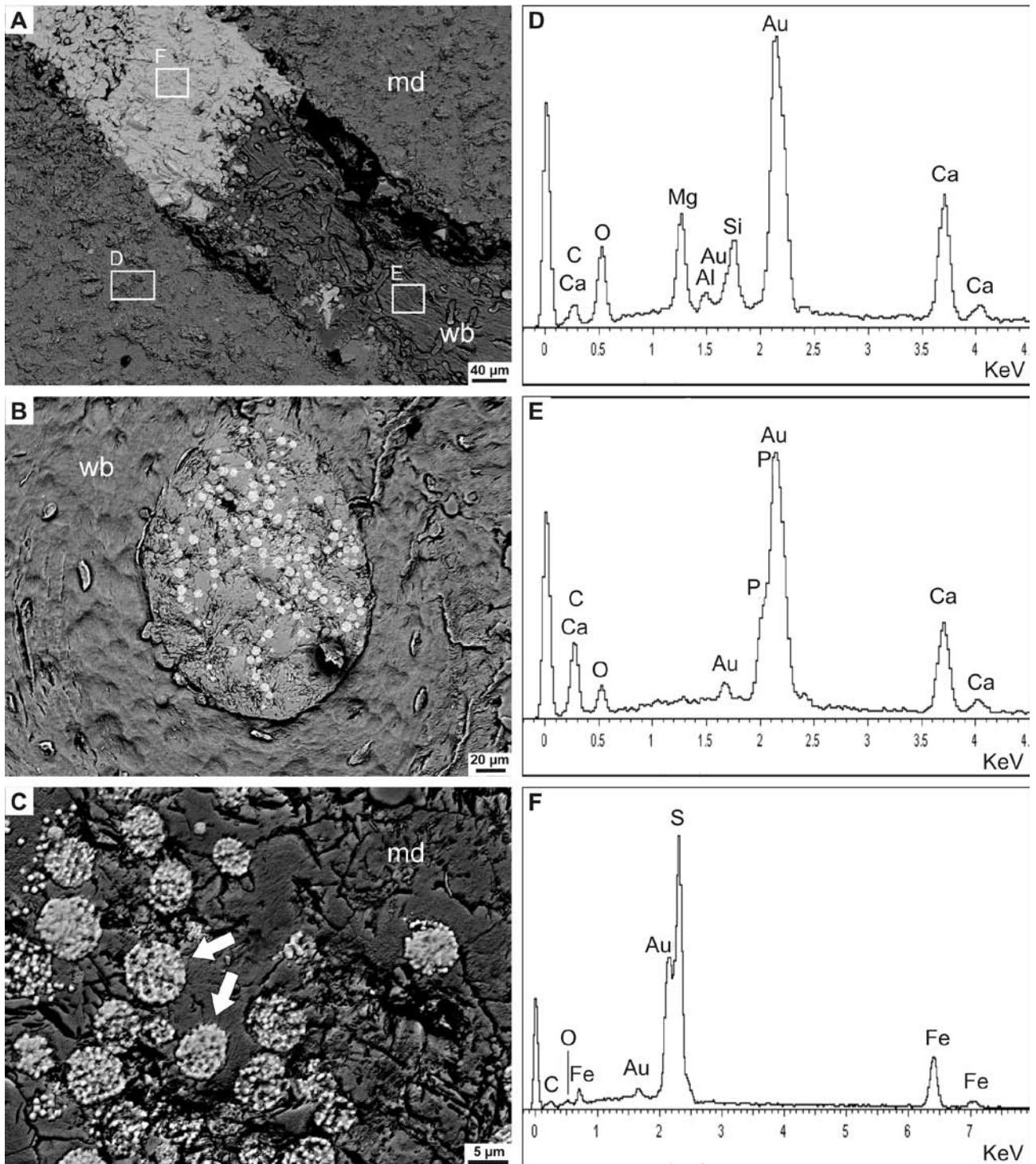


**Figure 23.** SEM images of petrographic thin sections of the Castelfiorentino whale bones. **A.** Well preserved bone trabecula in the lower part of the figure, pyritized bone in the upper part. **B.** Compact bone Haversian canal filled with pyrite framboids. **C.** Detail of pyrite framboids in the mosaic dolomite cement. **D.** Areal EDX analysis of the dolomite cement, hosting siliciclastic grains. **E.** Areal EDX analysis of the fossil bone, preserved as carbonate apatite. **F.** Areal analysis of the dense pyrite crust covering the bones. **A, B, C** figures in backscattered electron mode, **C, D, F** analyses in secondary electron mode with an acceleration voltage of 15 kV.

### 5.9.2.2 Microborings

The outer part of cancellous bones is intensively eroded by micron-sized microborings. The microborings do not show any preferred orientation respect to the bone structure, they tunnel progressively the bones from the surface toward the internal part (Figure 24A-B). The eroded area has a maximum thickness of 450  $\mu\text{m}$ . In heavily tunnelled area the bone shows a dark and cloudy habit (Figure 24B). The microborings have a maximum measured length of 103  $\mu\text{m}$  and a diameter between 3.9  $\mu\text{m}$  and 10.7  $\mu\text{m}$  (medium value 6.6  $\mu\text{m}$ ). They are straight or slightly curved and preferentially do not bifurcate (Figures 24C-D, 25). The microborings are empty or filled by pyrite framboids (Figure 25A-B). In the same area where microborings occur, on the external side of the bones, euhedral pyrite crystals are observed (average size 9.7  $\mu\text{m}$ : Figure 24C).

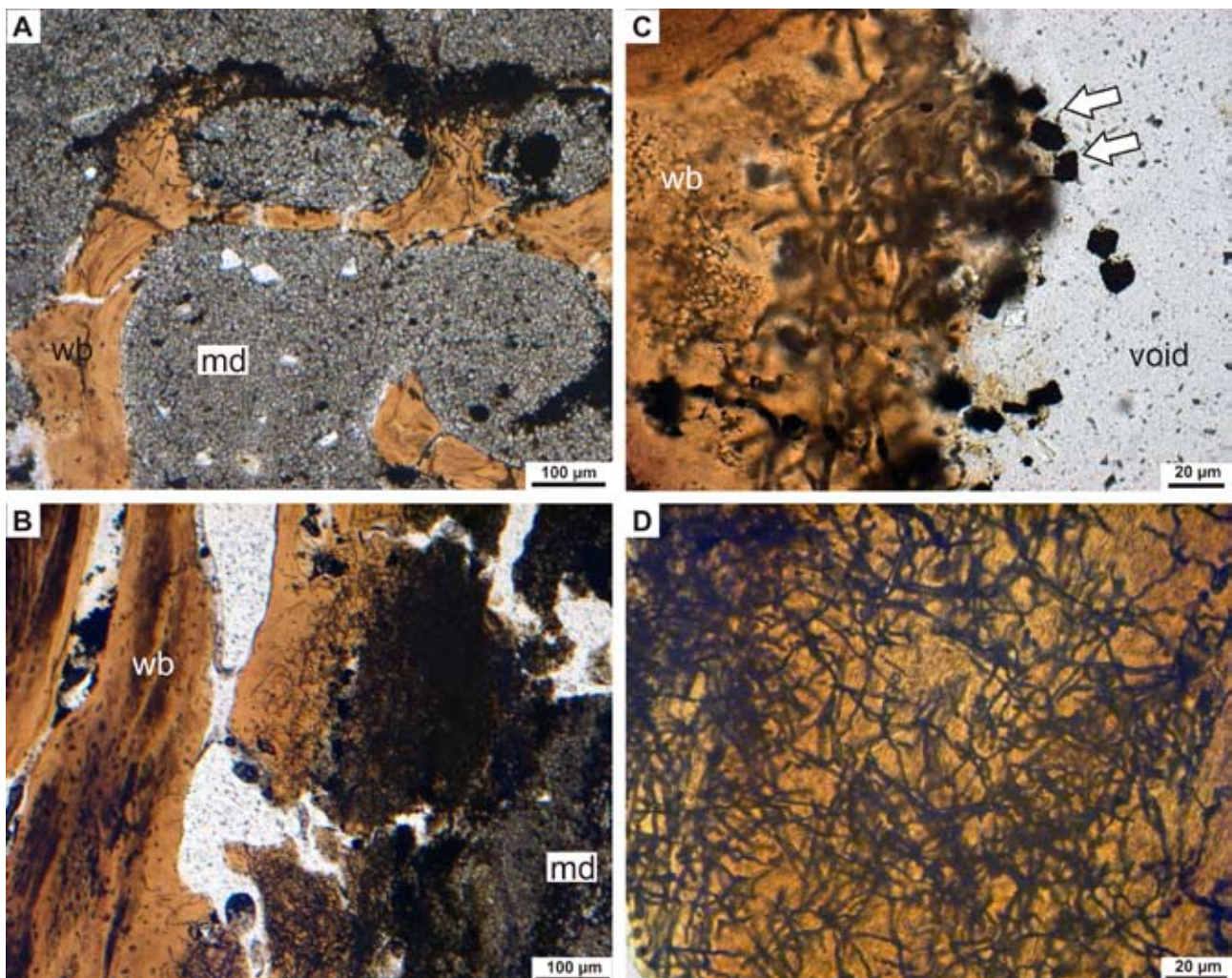


Figure 24. Bioerosion on Castelfiorentino fossil bones. A. Trabecular bone intensively bioeroded by micron-sized microborings. The density of microborings decrease toward the internal part of the bones; they do not show any preferred orientation. B. Dark and cloudy 300  $\mu\text{m}$  thick bioeroded area. C. Detail of microborings. They can be empty or filled by pyrite. Note euhedral pyrite on the external side of the bones next to the bioeroded area. D. Detail of microborings. They are straight or slightly curved and preferentially do not bifurcate. All figures in plane polarized light.

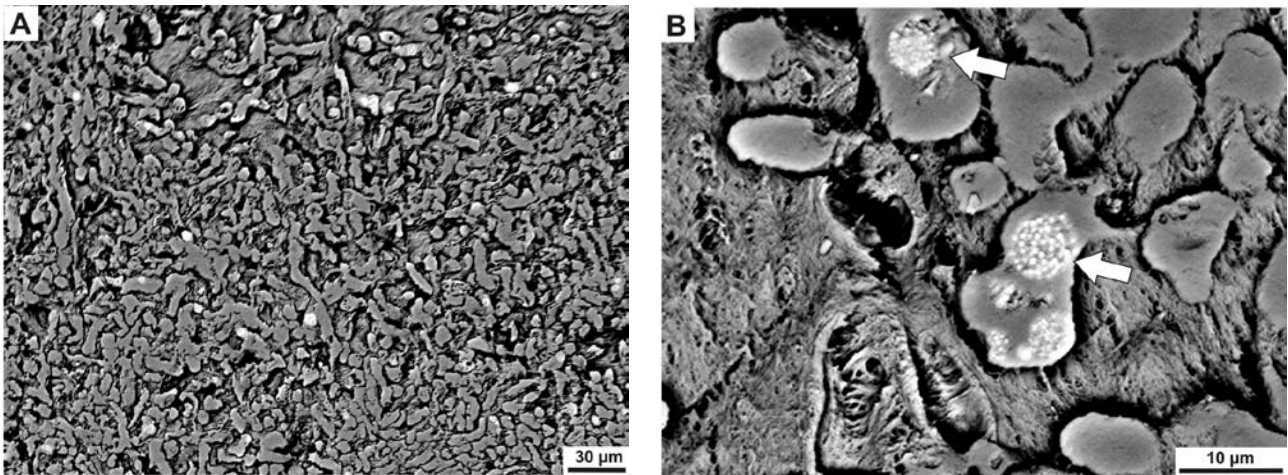
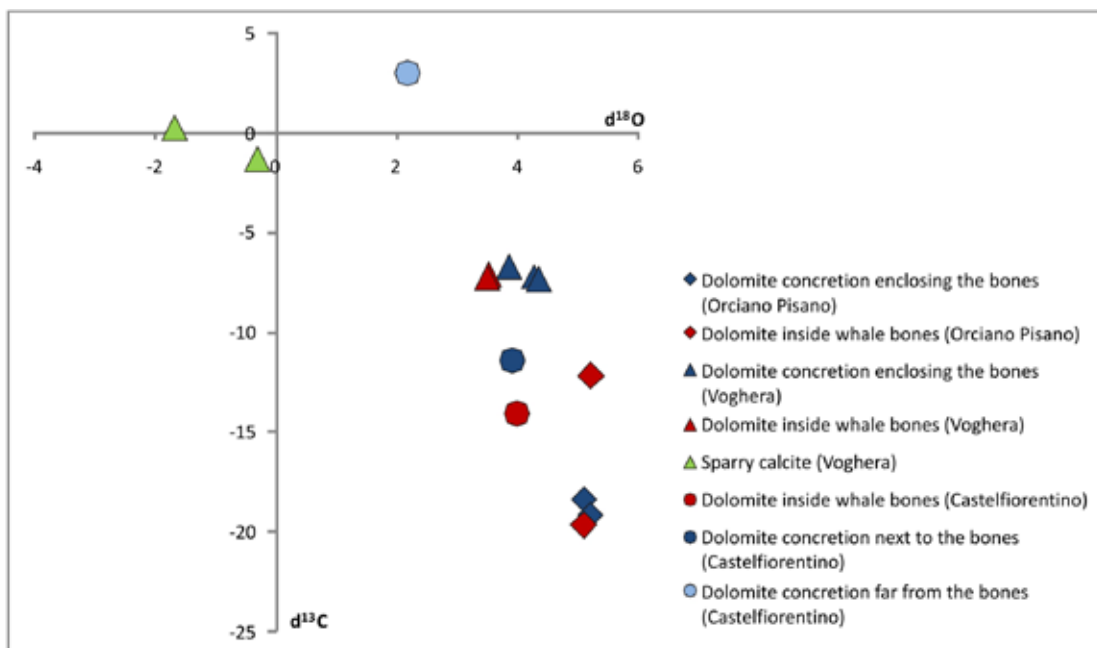


Figure 25. SEM images of petrographic thin sections on bioeroded bones of the Castelfiorentino whale. A. Microborings. Note the absence of bifurcations and sparse pyrite framboids inside the holes. B. Microborings partially filled by pyrite framboids (arrows). All figures in backscattered electron mode.

### 5.10 Isotope analyses

Carbon and oxygen stable isotope analyses have been performed on the dolomite concretions enclosing the bones and on the dolomite cement filling cancellous bones (Table 1, Figure 26). The dolomite concretion outside the Orciano Pisano whale bones has  $\delta^{13}\text{C}$  values between -12.18 ‰ and -19,23 ‰, and  $\delta^{18}\text{O}$  medium values of between +5.10 ‰ and +5.23 ‰. Dolomite cements inside the bones have similar values, with  $\delta^{13}\text{C}$  between -18.4‰ and -19.69 ‰ and  $\delta^{18}\text{O}$  values between +5.10 ‰ and +5.21 ‰. The concretion outside the Castelfiorentino fossil bones has  $\delta^{13}\text{C}$  values of -11.41 ‰ close to the bones, and +2.98 ‰, 2.2 cm far from the bones.  $\delta^{13}\text{C}$  inside bone trabeculae has a value of -14.12 ‰.  $\delta^{18}\text{O}$  outside and inside the bones has values of +3.05‰ (on average) and +3.99‰, respectively.



Previous page:

**Figure 26.** Stable isotope analyses of the carbonate cements inside and outside the Castelfiorentino and the Orciano Pisano whales. Also data on the Voghera whale bones are reported (see Figure 12). The Orciano Pisano dolomite cement inside bone trabeculae and in the surrounding concretion has the lowest  $\delta^{13}\text{C}$  values, as low as  $-19.23\text{‰}$ .

**Table 1.** Stable isotope analysis of the carbonate cements inside and outside the fossil bones. Data on the Orciano Pisano, Castelfiorentino and Voghera whales are summarized.

	$\delta^{13}\text{C}$ (‰)	$\delta^{18}\text{O}$ (‰)
Dolomite inside whale bones (Orciano Pisano)	-18.4 / -19.23	+5.10 / +5.21
Dolomite concretion enclosing the bones (Orciano Pisano)	-12.18 / -19.69	+5.10 / +5.23
Dolomite inside bone trabeculae (Castelfiorentino)	-14.22	+ 3.99
Dolomite concretion next to the bones (Castelfiorentino)	-11.41	+ 3.92
Dolomite concretion far from the bones (Castelfiorentino)	+ 2.98	+ 2.18
Dolomite inside whale bones (Voghera)	-6.71 / -7.34	+3.86 / +4.36
Dolomite concretion enclosing the bones (Voghera)	-7.15 / -7.28	+3.51 / +3.54
Sparry calcite (Voghera)	+0.22 / -1.33	-1.67 / - 0.30

## 5.11 Discussion

The abundant glauconite grains in the Orciano Pisano enclosing concretion are indicative of a relatively shallow marine deposition and slow sedimentation rates. Glauconite is often concentrated at discontinuity surfaces indicating depositional breaks (Flügel 2010), and it is also associated with marine bone beds, stratigraphic levels where vertebrate bioclast concentration is high (Esperante 2009 et al and references therein), like at the Orciano Pisano site (Bianucci and Landini 2005).

As for the Voghera whale, for the Orciano Pisano and the Castelfiorentino fossil whales carbon and oxygen stable isotope values of the dolomite cement are similar inside the bones and in the enclosing concretion, suggesting that they precipitated under similar geochemical conditions. The  $\delta^{18}\text{O}$  positive values could be result from precipitation in cold pore fluids (Raiswell and Fisher 2000). The negative  $\delta^{13}\text{C}$  values, as low as  $-19.69\text{‰}$  for the Orciano Pisano whale and  $-14.22\text{‰}$  for the Castelfiorentino whale, suggest that dolomite cements precipitated from the microbial oxidation of organic matter by sulphate reduction (Kiriakoulakis et al. 2000, Raiswell and Fisher 2000). The positive  $\delta^{13}\text{C}$  value for the dolomite sampled far from the bones, in the Castelfiorentino whale concretion, suggests a possible significant methanogenic influence during later stages of organic matter oxidation (Raiswell and Fisher 2000).

Dolomite carbonate concretions form preferably when the rate of organic-carbon oxidation is rapid and when sediments contain highly reactive organic matter (Mozley and Burns 1993). Dolomite precipitation is also favoured by the simultaneous reduction of dissolved seawater sulphate to near zero and by a large increase in carbonate alkalinity from the bacterial degradation of organic matter (Compton 1988). The presence of a carbonate precursor, as a

whalebone, would promote dolomite precipitation by providing a source of Ca and  $\text{CO}_3^{2-}$  ions (Compton 1988). The microbial oxidation of the whale organic matter by sulphate reduction, once the bones were buried below the sediment-water interface, would have thus favoured the precipitation of dolomite. The pervasive distribution of pyrite framboids in the dolomite cement of both of the studied fossil whales, sometimes localized in well defined clusters, suggests that also pyrite formed as a consequence of the production of hydrogen sulphide by sulphate reduction processes (Coleman and Raiswell 1993, Mazzullo 2000). Secondary cements as fibrous calcite in the Orciano Pisano whale and sparry calcite in the Castelfiorentino whale could have precipitated in equilibrium with sea-water, once the whale organic carbon was totally consumed.

The clotted fabric of the dolomite cement filling the Orciano Pisano whale bones might have a microbial origin (Peckmann and Thiel 2004). It could have been originated by the whale organic matter decay immediately below the sediment-water interface, during early diagenesis (cf. paragraph 5.5). The Castelfiorentino whale bones are instead exclusively filled by massive, mosaic, hypidiotopic-like dolomite cements that could have formed once the bones were deeply buried in the sulphate reduction zone (see Kiel 2008). The fractures observed in the Castelfiorentino whale bones indicate that the bones underwent physical compaction due to burial diagenesis (Scholle and Ulmer-Scholle 2003). The pyrite crusts closely associated with the fractures presumably formed during late diagenetic processes.

As discussed in the Voghera whale section (cf. paragraph 5.5), endolithic microorganisms that actively penetrate into rocks or hard substrates in the marine ecosystem include phototrophic cyanobacteria and algae, and heterotrophic fungi and bacteria, all of which are able to metabolize collagen and dissolve mineral matrix (Davis 1997; Trueman and Martill 2002). Microborings occurring on the external side of both the Orciano Pisano and Castelfiorentino fossil bones, tunnel progressively inwards. They show a destruction pattern frequently described as “wedl tunnelling” and typically ascribed to the action of fungi or cyanobacteria (Davis 1997, Turner-Walker and Jans 2008). On the contrary the intensively demineralized area of the Orciano Pisano whale bones (Figure 18) shows a very distinct pattern that could be interpreted as bacterial degradation (Turner-Walker 2008, Jans 2008). The preferred orientation of the holes suggests that bacterial degradation followed the orientation of the collagen fibres in different parts of the bone (Turner-Walker 2008). The presence of sulphate minerals in the same area, closely related to the bone tissue, could be linked to late changes in the burial environment from reducing to more oxidizing conditions. Pyrite, precipitated under reducing conditions, could in fact have undergone oxidation with the consequent release of sulphate and hydrogen ions. The resulting fall in pH could have caused local dissolution of bone apatite giving rise to the deposition of gypsum ( $\text{CaSO}_4 \cdot 2\text{H}_2\text{O}$ ) (Turner-Walker 2008).



## 5.12 Conclusions

The results of microfacies analysis on the Orciano Pisano fossil whale are consistent with what observed during the macro-scale taphonomic analysis of the bones (Chapter 4). At the macro-scale the bones are intensively bioeroded, suggesting a prolonged exposure of the skeleton on the sea bottom together with an intense biotic activity on the bone surface. A prolonged permanence on the sea floor is confirmed by the high amount of glauconite in the host concretion. At the microscale the bioerosion of the bones is testified both by the absence of the outer compact bone tissue in thin sectioned samples and by the occurrence of two different traces left by euhendolitic microorganisms. The  $\delta^{13}\text{C}$  negative values of the dolomite cement, together with the microbial clotted fabric, indicate that dolomite precipitated from the microbial oxidation of organic matter by sulphate reduction. The enrichment with hydrogen sulphide of the sediments around the bones is further supported by the occurrence of chemosymbiont-bearing lucinid bivalves in life position closely associated with the bones (Chapter 3, 4).

The intense bioerosion on the Castelfiorentino whale bones, due to a fungal or a prokaryote (cyanobacteria) trace maker, testifies a period of exposure of the bones on the sea floor, before burial. Differently from the other two-case studies, the microfacies analysis suggests that the dolomite concretion enclosing the bones formed when the bones were deeply buried in the sulphate reduction zone, and that originated during late diagenetic processes.

In sum, microfacies and biosedimentological analysis of fossil bones can be a very useful tool to integrate taphonomic data collected during a macro-scale study of the bones. The application of a multidisciplinary approach allows to reconstruct in detail most of the main taphonomic processes that occur after the death of a large whale, from biostratinomy to bone diagenesis. Our study increases general knowledge of taphonomic processes linked to microbial degradation of organic matter in a poorly investigated habitat and contributes to better understanding of the ecological and evolutionary relationships between whale-fall microbial ecosystems and other localized reducing ecosystems on the sea floor. In particular, future studies should focus on the analysis of older marine carcasses, which may have supported similar chemoautotrophic communities before the evolution whales.

## References

- Allison P.A. and Briggs D.E.G. 1991. The taphonomy of soft-bodied animals: In: Donovan S.K. (Ed). *Fossilization: the process of taphonomy*. Belhaven Press, London, pp. 120–140.
- Allison P.A. and Pye K. 1994. Early diagenetic mineralization and fossil preservation in modern carbonate concretions. *Palaios* 9, 561–575.
- Allison P.A., Smith C.R., Kukert H., Deming J.W. and Bennett B.A. 1991. Deep-water taphonomy of vertebrate carcasses: a whale skeleton in the bathyal Santa Catalina Basin. *Paleobiology* 17, 78–89.
- Aloisi G., Wallmann K., Bollwerk S.M., Derkachev A., Bohrmann G. and Suess E. 2004. The effect of dissolved barium on biogeochemical processes at cold seeps. *Geochimica et Cosmochimica Acta* 68, 1735–1748.
- Amano K. and Little C.T.S. 2005. Miocene whale-fall community from Hokkaido, northern Japan. *Palaeogeography, Palaeoclimatology, Palaeoecology* 215, 345–356.
- Amano K., Little C.T.S. and Inoue K. 2007. A new Miocene whale-fall community from Japan. *Palaeogeography, Palaeoclimatology, Palaeoecology* 247, 236–242.
- Bailey J.V., Raub T.D., Meckler A.N., Harrison B.K., Raub T.M.D., Green A.M. and Orphan V.J. 2010. Pseudofossils in relict methane seep carbonates resemble endemic microbial consortia. *Palaeogeography, Palaeoclimatology, Palaeoecology* 285, 131–142.
- Barbieri R. and Cavalazzi B. 2005. Microbial fabrics from Neogene cold seep carbonates, Northern Apennine, Italy. *Palaeogeography, Palaeoclimatology, Palaeoecology* 227, 143–155.
- Bellinzona G., Boni A., Braga G. and Marchetti G. 1971. Note illustrative della Carta Geologica d'Italia in scala 1:100.000, Foglio 71, Voghera. Servizio Geologico d'Italia, Roma, pp. 121.
- Bennett B.A., Smith C.R., Glaser B. and Maybaum H.L. 1994. Faunal community structure of a chemoautotrophic assemblage on whale bones in the deep northeast Pacific Ocean. *Marine Ecology Progress Series* 108, 205–223.
- Benvenuti M., Bertini A., Conti C. and Dominici S. 2007. Integrated analyses of litho- and biofacies in a Pliocene cyclothemic, alluvial to shallow marine succession (Tuscany, Italy). *Geobios* 40, 143–158.
- Berner R.A. 1970. Sedimentary pyrite formation. *American Journal of Science* 268, 1–23.
- Beyssac O., Goffé B., Petit J., Froigneux E., Moreau M. and Rouzaud J.N. 2003. On the characterization of disordered and heterogeneous carbonaceous materials by Raman spectroscopy. *Spectrochimica Acta Part A* 59, 2267–2276.
- Bianucci G. and Landini W. 2005. I paleositi a vertebrati fossili della Provincia di Pisa. *Atti della Società toscana di Scienze naturali, Memorie, Serie A* 110, 1–21.
- Bishop J.K.B. 1988. The barite-opal-organic carbon association in oceanic particulate matter. *Nature* 332, 341–343.
- Bonny S.M. and Jones B. 2008. Experimental precipitation of barite ( $\text{BaSO}_4$ ) among streamers of sulfur-oxidizing bacteria. *Journal of Sedimentary Research* 78, 357–365.

Burne R.V. and Moore L.S. 1987. Microbialites: organosedimentary deposits of benthic microbial communities. *Palaios* 2, 241–254.

Campbell K.A. 2006. Hydrocarbon seep and hydrothermal vent paleoenvironments and paleontology: Past developments and future research directions. *Palaeogeography, Palaeoclimatology, Palaeoecology* 232, 362–407.

Campbell K.A., Farmer J.D. and Des Marais D. 2002. Ancient hydrocarbon seeps from the Mesozoic convergent margin of California: carbonate geochemistry, fluids and palaeoenvironments. *Geofluids* 2, 63–94.

Carnevale G., Longinelli A., Caputo D., Barbieri M. and Landini W. 2008. Did the Mediterranean marine reflooding precede the Mio–Pliocene boundary? Paleontological and geochemical evidence from upper Messinian sequences of Tuscany, Italy. *Palaeogeography, Palaeoclimatology, Palaeoecology* 257, 81–105.

Cavagna S., Clari P. and Martire L. 1999. The role of bacteria in the formation of cold seep carbonates: geological evidence from Monferrato (Tertiary NW Italy). *Sedimentary Geology* 126, 253–270.

Cavalazzi B. 2007. Chemotrophic filamentous microfossils from the Hollard Mound (Devonian, Morocco) as investigated by focused ion beam. *Astrobiology* 7, 402–415.

Cavalazzi B., Barbieri R. and Ori G.G. 2007. Chemosynthetic microbialites in the Devonian carbonate mounds of Hamar Laghdad (Anti-Atlas, Morocco). *Sedimentary Geology* 200, 73–88.

Cavalazzi B., Westall F., Barbieri R. and Frédéric F. (submitted a). Endolithic fossil microbes in a vesicular pillow basalt, Coral Patch Seamount, eastern North Atlantic Ocean. *Palaeogeography, Palaeoclimatology, Palaeoecology*.

Cavalazzi B., Barbieri R., Cady S.L., Gennaro S., Westall F., Lui A. and Rossi A.P. (submitted b). Iron-rich framboids from a hydrocarbon-related Devonian mound (Anti-Atlas, Morocco): fossil or pseudofossils of fossil bacterial colonies? *Sedimentary Geology*.

Chafetz H.S. 1986. Marine peloids; a product of bacterially induced precipitation of calcite. *Journal of Sedimentary Research* 56, 812–817.

Coleman M.L. and Raiswell R. 1993. Microbial mineralization of organic matter: mechanisms of self-organization and inferred rates of precipitation of diagenetic minerals. *Philosophical Transactions: Physical Sciences and Engineering* 344, 69–87.

Compton J.S. 1988. Degree of supersaturation and precipitation of organogenic dolomite. *Geology* 16, 318–321.

Danise S., Dominici S. and Betocchi U. 2010. Mollusk species at a Pliocene shelf whale fall (Orciano Pisano, Tuscany). *Palaios* 25, 449–556.

Davis P.G. 1997. The bioerosion of bird bones, *International Journal of Osteoarchaeology* 7, 388–401.

Dehairs F., Chesselet R. and Jedwab J. 1980. Discrete suspended particles of barite and the barium cycle in the open Ocean. *Earth and Planetary Science Letters* 49, 528–550.

Deming J.W., Reysenbach A.L., Macko S.A. and Smith C.R. 1997. Evidence for the microbial basis of a chemoautotrophic invertebrate community at a whale fall on the deep seafloor: bone-

colonizing bacteria and invertebrate endosymbionts. *Microscopy Research and Technique* 37, 162–170.

Dominici S., Cioppi E., Danise S., Betocchi U., Gallai G., Tangocci F., Valleri G. and Monechi S. 2009. Mediterranean fossil whale falls and the adaptation of mollusks to extreme habitats. *Geology* 37, 815–818.

Eickmann B., Bach W., Kiel S., Reitner J. and Peckmann J. 2009. Evidence for cryptoendolithic life in Devonian pillow basalts of Variscan orogens, Germany. *Palaeogeography, Palaeoclimatology, Palaeoecology* 283, 120–125.

Esperante R., Muniz Guinea F. and Nick K.E. 2009. Taphonomy of a mysticeti whale in the lower Pliocene Huelva Sands Formation (Southern Spain). *Geologica acta* 7, 489–505.

Flügel E. 2010. *Microfacies of carbonate rocks: analysis, interpretation and application*. Springer-Verlag, 984 pp.

Goedert J.L., Squires R.L. and Barnes L.G. 1995. Paleocology of whale-fall habitats from deep-water Oligocene rocks, Olympic Peninsula, Washington state. *Palaeogeography, Palaeoclimatology, Palaeoecology* 118, 151–158.

Goffredi S.K., Paull C.K., Fulton-Bennett K., Hurtado L.A. and Vrijenhoek R.C. 2004. Unusual benthic fauna associated with a whale fall in Monterey Canyon, California. *Deep-Sea Research I*, 51, 1295–1306.

Goffredi S.K., Wilpiseski R., Lee R. and Orphan V.J. 2008. Temporal evolution of methane cycling and phylogenetic diversity of archaea in sediments from a deep-sea whale-fall in Monterey Canyon, California. *The International Society for Microbial Ecology Journal* 2, 204–220.

Golubic S., Friedmann I. and Schneider J. 1981. The lithobiontic ecological niche, with special reference to microorganisms. *Journal of Sedimentary Petrology* 51, 475–478.

Golubic S., Radtke G. and Le Campion-Alsumard T. 2005. Endolithic fungi in marine ecosystems. *Trends in Microbiology* 13, 229–235.

González-Munoz M.T., Fernández-Luque B., Martínez-Ruiz F., Chekroun K.B., Arias J.M., Rodríguez-Gallego M., Martínez-Canamero M., De Linares C. and Paytan, A. 2003. Precipitation of Barite by *Myxococcus xanthus*: Possible implications for the biogeochemical cycle of Barium. *Applied and Environmental Microbiology* 69, 5722–5725.

Higgs N.D., Little C.T.S and Glover A.G. 2011. Bones as biofuel: a review of whale bone composition with implications for deep-sea biology and palaeoanthropology. *Proceedings of the Royal Society B* 278, 9–17.

Hubert J.F., Panish P.T., Probst K.S. and Chure D.J. 1996. Chemistry, microstructure, petrology, and diagenetic model of Jurassic dinosaur bones, Dinosaur National Monument, Utah. *Journal of Sedimentary Research* 66, 531–547.

Irwin H., Curtis C. and Coleman M. 1977. Isotopic evidence for source of diagenetic carbonates formed during burial of organic-rich sediments. *Nature* 269, 209–213.

Jans M.M.E. 2008. Microbial bioerosion of bone – a review, in: Wisshak, M., Tapanila L. (Eds.), *Current development in Bioerosion*. Erlangen Earth Conference Series, pp. 397–413.

Kaim A., Kobayashi Y., Echizenya H., Jenkins R.G. and Tanabe K. 2008. Chemosynthesis based associations on Cretaceous plesiosaurid carcasses. *Acta Palaeontologica Polonica* 53, 97–104.

Kastner, M. 1984. Control of dolomite formation. *Nature* 311, 410–411.

Kiel S. 2008. Fossil evidence for micro- and macrofaunal utilization of large nektonfalls: examples from early Cenozoic deep-water sediments in Washington State, USA. *Palaeogeography, Palaeoclimatology, Palaeoecology* 267, 161–174.

Kiel S. and Goedert J.L. 2006. Deep-sea food bonanzas: early Cenozoic whale-fall communities resemble wood-fall rather than seep communities. *Proceedings of the Royal Society of London B* 273, 2625–2631.

Kiriakoulakis K., Marschall J.D. and Wolff G.A. 2000. Biomarkers in a lower Jurassic concretion from Dorset (UK). *Journal of the Royal Society of London* 157, 207–220.

Koski R.A., Lonsdale P.F., Shanks W.C., Vemdt M.E. and Howe S.S. 1985. Mineralogy and geochemistry of a sediment hosted hydrothermal sulfide deposits from the southern trough of the Guaymas Basin, Gulf of California. *Journal of Geophysical Research* 90, 6695–6707.

Levin L.A. 2005. Ecology of cold seep sediments: interactions of fauna with flow, chemistry and microbes. *Oceanography and Marine Biology: An Annual Review* 43, 1–46.

Little C.T.S. and Vrijenhoek R.C. 2003. Are hydrothermal vent animals living fossils? *Trends in Ecology and Evolution* 18, 582–588.

Lundsten L., Paull C.K., Schlining K.L., McGann M. and Ussler W. 2010. Biological characterization of a whale-fall near Vancouver Island, British Columbia, Canada. *Deep-Sea Research I* 57, 918–922.

Lyman R.L. 1994. *Vertebrate taphonomy*. Cambridge University Press, Cambridge.

Marshall C.P., Edwards H.G.M. and Jehlicka J. 2010. Understanding the application of Raman spectroscopy to the detection of traces of life. *Astrobiology* 10, 229–243.

Mazzullo S.J. 2000. Organogenic dolomitization in peritidal to deep-sea sediments. *Journal of Sedimentary Research* 70, 10–23.

Mozley P.S. and Buns S.J. 1993. Oxygen and carbon isotopic composition of marine carbonate concretions: an overview. *Journal of Sedimentary Petrology* 63, 73–83.

Naganuma T., Wada H. and Fujioka K. 1996. Biological community and sediment fatty acids associated with the deep-sea whale skeleton at the Torishima Seamount. *Journal of Oceanography* 52, 1–15.

Orphan V.J., Hinrichs K.U., Ussler W., Paull C.K., Taylor L.T., Sylva S.P., Hayes J.M. and De Long E.F. 2001. Comparative analysis of methane-oxidizing archaea and sulfate-reducing bacteria in anoxic marine sediments. *Applied Environmental Microbiology* 67, 1922–1934.

Paytan A. and Griffith E.M. 2007. Marine barite: Recorder of variations in ocean export productivity. *Deep-Sea Research II* 54, 687–705.

Peckmann J. and Thiel V. 2004. Carbon cycling at ancient methane-seeps. *Chemical Geology* 205, 443–467.

Pfretzschner H.U. 2001. Pyrite in fossil bone, Neues Jahrbuch für Geologie und Paläontologie Abhandlungen 220, 1–23.

Pfretzschner H.U. 2004. Fossilization of Haversian bone in aquatic environments. *Comptes Rendus Palevol* 3, 605–616.

Pyenson N.D. and Haasl D.M. 2007. Miocene whale-fall from California demonstrates that cetacean size did not determine the evolution of modern whale-fall communities. *Biology Letters (Palaeontology)* 3, 709–711.

Raiswell R. and Fisher Q.J. 2000. Mudrock hosted carbonate concretions: a review of growth mechanisms and their influence on chemical and isotopic composition. *Journal of the Geological Society of London* 157, 239–251.

Reitner J., Peckmann J., Blumenberg M., Michaelis W., Reimer A. and Thiel V. 2005. Anatomy of methane-derived carbonates and associated microbial communities in Black Sea sediments. *Palaeogeography, Palaeoclimatology, Palaeoecology* 227, 18–30.

Riding R. and Tomás S. 2006. Stromatolite reef crusts, Early Cretaceous, Spain; bacterial origin of in situ-precipitated peloid microspar? *Sedimentology* 53, 23–34.

Rouse G.W., Goffredi S.K. and Vrijenhoek R.C. 2004. *Osedax*: bone-eating marine worms with dwarf males. *Science* 305, 668–671.

Santelli C.M., Orcutt B.N., Banning E., Bach W., Moyer C.L., Sogin M.L., Staudige H. and Edwards K.J. 2008. Abundance and diversity of microbial life in ocean crust. *Nature* 453, 653–656.

Scholle P.A. and Ulmer-Scholle D.S. 2003. *A Color Guide to the Petrography of Carbonate Rocks: Grains, textures, porosity, diagenesis*: Tulsa, OK, American Association of Petroleum Geologists Memoir 77, 474 pp.

Schumann G., Manz W., Reitner J. and Lustrino M. 2004. Ancient fungal life in North Pacific Eocene oceanic crust. *Geomicrobiology Journal* 21, 241–246.

Senko J.M., Campbell B.S., Henriksen J.R., Elshahed M.S., Dewers T.A. and Krumholz L.R. 2004. Barite deposition resulting from phototrophic sulfide-oxidizing bacterial activity. *Geochimica et Cosmochimica Acta* 68, 773–780.

Shapiro R.S. 2004. Recognition of Fossil Prokaryotes in Cretaceous Methane Seep Carbonates: Relevance to Astrobiology. *Astrobiology* 4, 438–449.

Shapiro R.S. and Spangler E. 2009. Bacterial fossil record in whale-falls: Petrographic evidence of microbial sulfate reduction. *Palaeogeography, Palaeoclimatology, Palaeoecology* 274, 196–203.

Smith C.R. and Baco A.R. 2003. Ecology of whale falls at the deep-sea floor. *Oceanography and Marine Biology: an Annual Review* 41, 311–354.

Smith C.R., Kukert H., Wheatcroft R.A., Jumars P.A. and Deming J.W. 1989. Vent fauna on whale remains. *Nature* 341, 27–28.

Smith C.R., Maybaum H.L., Baco A.R., Pope R.H., Carpenter S.D., Yager P.L., Macko S.A. and Deming J.W. 1998. Sediment community structure around a whale skeleton in the deep Northeast Pacific: macrofaunal, microbial and bioturbation effects. *Deep-Sea Research II* 45, 335–364.

Smith C.R., Baco A.R. and Glover A. 2002. Faunal succession on replicate deep-sea whale falls: time scales and vent-seep affinities. *Cahiers de Marine Biologie* 43, 293–297.

Stamatakis M.G. and Hein J.R. 1993. Origin in tertiary marine sedimentary rocks from Lefkas Island, Greece. *Economic Geology* 88, 91–103.

Torres M.E., Bohrmann G., Dubé T.E. and Poole F.G. 2003 Formation of modern and Paleozoic stratiform barite at cold methane seeps on continental margins. *Geology* 31, 897–900.

Treude T., Smith C.R., Wenzhöfer F., Carney E., Bernardino A.F., Hannides A.K., Krüger M. and Boetius A. 2009. Biogeochemistry of a deep-sea whale fall: sulphate reduction, sulfide efflux and methanogenesis. *Marine Ecology Progress Series* 382, 1–21.

Trueman C.N. and Martill D.M. 2002. The long-term survival of bone: the role of bioerosion. *Archaeometry* 44, 371–382.

Turner-Walker G. 2008. The chemical and microbial degradation of bones and teeth. In: Pinhasi R. and Mays S. (Eds.), *Advances in human paleopathology*, pp. 1–29.

Turner-Walker G., Nielsen-Marsh C.M., Syversen U., Kars H. and Collins M.J. 2002. Sub-micron spongiform porosity is the major ultra-structural alteration occurring in archaeological bone. *International Journal of Osteoarchaeology* 12, 407–414.

Van Dover C.L. 2000. *The ecology of deep sea hydrothermal vents*. Princeton University Press, Princeton.

# CHAPTER 6 — Whale fall communities, background communities and their controlling factors in the Neogene of Italy

---

## 6.1 Introduction

Water depth is usually interpreted as the single most important factor controlling the distribution of marine benthic organisms. Many key factors controlling the structure and taxonomic composition of base level communities, like pressure, salinity, energy, oxygen content, seasonality and grain size, are directly correlated with water depth (Holland et al. 2001). These parameters control also the distribution of chemosynthetic communities, whose composition varies following a depth gradient (Tarasov et al. 2005, Dando 2010). One of the key physical factors which matters more than others on the structure of base level communities in extreme, reducing environments is light penetration. Benthic communities of the photic zone, roughly ending at the shelf break, are dependent on photosynthesis, have a higher biomass and are stronger competitors than typical deep water species at cold seeps and hydrothermal vents, which on the opposite rely on chemical compounds not directly derived from photosynthesis. Shallow water reducing communities at vents and seeps are sharply different from those of the deep sea. Such communities at deep sites are characterized by specialists that have not been found yet on the shelf (Sahling et al. 2003, Tarasov et al. 2005, Dando 2010) and that evolved from coastal ancestors (Distel et al. 2000, Jones et al. 2006). The transition between the euphotic zone and the bathyal is the belt where speciation most probably occur (Dominici et al. 2009). Knowledge on the absolute depth of deposition of the fossil whale falls here under study can help to understand the ecological role of benthic islands in extreme reducing conditions, such as whale and wood falls, their role as stepping stones, and can bring clues to macroevolutionary theory (Smith 1989, Distell et al. 2000, Kiel and Little 2006). The taphonomic analysis of Neogene shallow marine whale-falls (Chapter 4) has given some clues as to the physical factors controlling the distribution of fossil whale falls on the shelf, suggesting a relationship with depth. To test this possibility, we carried out a paleobathymetric analysis in term of absolute depths based on quantitative data on fossil benthos, after calculating average life depth of their modern relatives. Taxonomic composition of fossil assemblages can be an indirect measure of environmental gradients in the geological past (Olszewski and Patzkowsky 2001, Hohenegger 2005). Previous studies have shown how ordination can extract high resolution paleoenvironmental signals from high-quality, quantitative data (Holland et al. 2001, Scarponi and Kowalewski 2004, Dominici et al. 2008, Bush and Brame 2010). All studies based on quantitative data on benthic species in



stratigraphical samples prove a primary control from depth-related factors. The best results are obtained from abundance data analyzed through multidimensional statistics, where taxonomic units are the variables with which samples are ordered in the multidimensional space. Holland et al. (2001) used detrended correspondence analysis (DCA) to calculate the relative water depth preferences and depth ranges of fossil taxa from the late Ordovician of the Cinchinnati region, Ohio. Scarponi and Kowalewski (2004) performed a similar analysis on Quaternary molluscs from the Po Plain, Italy, verifying that ordination recovered a bathymetric signal that they could quantify by comparing score along the main axis of distribution of DCA (DC1) with the known depth preferences of extant genera. They showed how ecologically understood molluscs provide viable quantitative estimates of bathymetry and related environmental parameters, based on DC1 score. Successively Dominici et al. (2008) applied a similar approach at the species-level to foraminifer assemblages from a Pliocene alluvial and marine succession in Tuscany, Italy.

Here the approach of Scarponi and Kowalewski (2004) and Dominici et al. (2008) was adopted for the multivariate analysis of a large data set of mollusc abundances. This set includes quantitative bulk samples collected along seven sedimentary successions where fossil nearly-complete large skeletons have been previously recovered. Bulk samples were collected at both the bone beds and the sediments immediately above and below. These new data were merged with published abundances previously used by Dominici et al. 2009 at the family level, where an intertidal to bathyal gradient based on Italian Pliocene to early-Pleistocene samples was presented. The same database was here used at the genus-level. To interpret the ordination in terms of absolute depth we calculated the average life depth of extant mollusc genera which were also particularly abundant and characterizing in our dataset. Data on modern depths derive from the European Register of Marine Species (Costello et al. 2008). All previous quantitative studies have tried to approach environmental control other than depth by interpreting score along the second axis of distribution in the multivariate ordination (Holland et al. 2001, Scarponi and Kowaleski 2004, Dominici et al. 2008). The same analysis was performed here, finally comparing the results of our study with those of the above authors.

## 6.2 Materials and methods

The seven Pliocene successions where fossil whales were recovered (W1, W14, W15, W16, W21, W22, W23; Figure 1) belong to different geological settings described in Chapter 4 (paragraph 4.2). Each succession was studied in detail to put in context the seven whale-falls with the respective sedimentary and stratigraphic setting. Bulk samples were collected for the analysis of the mollusc content along those successions, with reference to the conditions immediately above, around and below whale-falls. 33 bulk samples, ranging from 0.5 to 3.5 litres, were wet sieved through a 1 mm screen and the residue was sorted under a binocular microscope for all

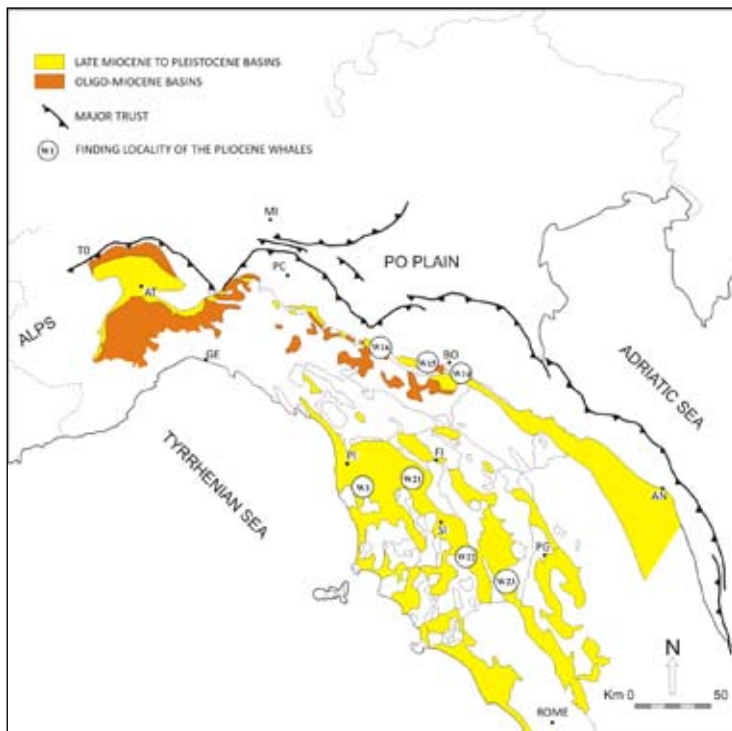


**Figure 1. Location map of the localities of recovery of the studied fossil whales (W1, W14, W15, W16, W21, W22, W23) and schematic geological map. Modified from Vai (2001).**

recognizable biogenic components. The latter includes molluscs, polychaetes, echinoids and decapods. Molluscs were determined at the species level. Bivalve abundance was equated to the highest number of right or left valves and half of the remaining, the latter roughly corresponding to the number of unmatched valves. Gastropods were equated to the number of apices. A total of 4,639 mollusc specimens were thus computed and used for subsequent analyses (Appendix 1: p. 143).

To reach a meaningful ordination, the new data related to the whale fall sites, expressed as abundances of genera, were added with comparable data from the Pliocene (Zanclean, Piacentian) and lower Pleistocene (Gelasian) of Italy (Appendix 2, 3: pp. 149, 173). These consist of 303,460 individuals from 94 samples, and belong to the Paleo-Tyrrhenian domain (22 samples), the Paleo-Adriatic domain (53 samples) and Southern Italy (19 samples). These new abundance data were gathered from the literature or are unpublished (Appendix 3: p. 173). Independent information on their stratigraphic context, lithology and sedimentary structures allowed us to make general interpretations on the relative position of each site with respect to mean sea level (Appendix 3: p. 173). The total dataset, consisting of whale fall sites and all the other Plio-Pleistocene sites, includes 312,904 individuals belonging to 330 genera, and formed the basis for the multivariate ordination. Genera occurring in only one sample were removed, resulting in a data set constituted by the 99.9% of the original specimens. Since the comparison concerned varying volumes of sediment, the raw abundances were normalized and square-root transformed to de-emphasize the influence of most abundant taxa (Clarke and Warwick 1994). Data were elaborated through detrended correspondence analysis (DCA), a multivariate statistical technique widely used with ecological data to ordinate taxa along underlying ecological gradients (Hill and Gauch 1980). In DCA plot, axis 1 reflects the primary source of ecological variation in the composition of faunas, axes 2 and 3 reflect additional sources of variation beyond the principal gradient.

Bivariate analysis was based on average depths expressed in meters (Table 1), and calculated from independent bathymetric estimates for extant genera recorded in the European Register of Marine Species (ERMS) for the Mediterranean and the North Atlantic (Costello et al. 2008). 47 genera were chosen for their abundance in our dataset, providing a continuous

coverage along DC1 axis (see Scarponi and Kowalewski 2004).

Finally a similarity percentage analysis (SIMPER; see Clarke and Warwick 1994) was performed to determine which genera were primarily responsible for differences between three selected group of samples of the total dataset. DCA and SIMPER analyses were performed with the program PAST (Hammer et al. 2001).

## 6.3 Results

### 6.3.1 Outcrop evidences at whale-fall sites

The local succession at Orciano Pisano (W1; Chapter 3) is formed, from bottom to top by: (i) bioturbated grey-colored siltstones (thickness 50 cm) with sparse macrofauna; (ii) a 4-5 cm thick, densely-packed *Archimediella spirata* shell pavement regularly continuous in all the area; bivalves are typically articulated, *Archimediella* shells are empty or partially filled with clay; fragments of fossil wood are abundant and up to 15 cm long; remains of marine vertebrates are abundant (sharks, teleosts, marine mammals, chelonids); (iii) massive silty fine-grained sandstones, more than 1 m thick, with sparse to loosely-packed macrofauna; adults of the highly mobile epifaunal *Amusium cristatum* and other bivalves (e.g., *Anadara diluvii*, *Corbula gibba*, *Tellina planata*) are in life position. *Archimediella spirata*, *Aporrhais uttingeriana uttingeriana*, spatangoid echinoderms, trace fossils (Ophiomorpha, Thalassinoides) and vegetal debris are abundant throughout the outcrop. The whale was lying in unit (iii) about 20 cm above the *Archimediella* bed and parallel to it. For the position of collected samples see Chapter 3, Figure 2.

The sampled Gorgognano (W14) outcrop is situated about 50 m from the site where the fossil whale was excavated (Figure 2A). The studied succession consists of 5 m of grey, massive, fine-grained sandy mudstones. Sparse specimens in life position of *Venus multilamella*, *Amusium cristatum* and the gastropods *Nassarius semistriatus* and *Natica* sp. were recovered. The serpulid *Ditrupa cornea* is abundant; well preserved decapods and sparse wood fragments occur (Figure 3).

The site where the S. Lorenzo in Collina whale (W15) was excavated is exactly 14 meters stratigraphically below the base of the church with the same name (see Capellini 1865) (Figure 2B). The succession shows a general coarsening upward trend and, from bottom to top, is made by: (i) 9 m of blue-grey, massive mudstones with abundant carbonate concretions up to 1 m large and sparse macrofauna; (ii) 4 m of massive blue-gray mudstones with scarce macrofauna and intensively bioturbated; (iii) 3 m of yellow, horizontal-plane stratified, fine to medium grained sandstones. Three laterally continuous, about 40 cm thick shell beds were recognized in the first unit, and quantitatively sampled for molluscs content (Figure 3). The lowest shell bed is presumably the bone bed and is characterized by abundant *Amusium cristatum* and *Pelecycora islandicoides* in life position. The middle bed is particularly rich in ostreids, and the upper shell bed is characterized by *Glans intermedia* and *Modiolus* sp. in life position.

The Castellarano whale (W16) comes from an outcrop up to 100 m thick. The overall succession consists of basal, tabular, fine grained sandstones, about 30 m thick, passing with a fining upward trend to massive, silty mudstones intercalated with silty mudstones, about 50 m thick, and overlaid by a second facies of tabular, medium grained sandstones. This succession represents a small scale depositional sequence, the fossil whale coming from the middle part, corresponding to the maximum flooding interval (Figure 2C). The sampled succession is 8 m thick and includes the exact place of recovery of the fossil whale (Figure 3, see Chicchi and Scacchetti 2001). The succession is made by massive, grey silty-sandstones intercalated with 40-60 cm thick silty-mudstone horizons rich in molluscs. From bottom to top, the (i) first shell bed is characterized by numerous glycymerids; (ii) the second, where the fossil whale comes from, by pectinids in life position (*Aequipecten scabrella* and *Amusium cristatum*) and (iii) the third bears many mytilids (*Modiolus cf. barbatus*) in life position and fragments of fossil wood.

The studied succession at Castelfiorentino (ex SILAP quarry) comprises the area of excavation of the W21 fossil whale (Figure 2D). The succession was described in a nearby outcrop by Landini et al (1990). This is about a 50 m thick succession mainly consisting of massive gray silstone and mudstones with sparse shell beds. The outcrop below the whale excavation site consists of 1 m of grey mudstones with sparse fauna dominated by *Petaloconchus* sp., and abundant *Venus multilamella*, *Chlamys varia*, *Modiolus* sp., *Nassarius semistriatus* and solitary corals; former mudstones are overlaid by a 60 cm thick shell bed with loosely packed, articulated specimens, in life position or perpendicular to their original position, with many *Ostrea edulis* and wood fragments (Figure 2E). The fossil whale comes from a grey mudstone facies with sparse molluscs. Shells are articulated, oblique or perpendicular from the original life position or nested. *Anadara pectinata*, *Modiolus* sp., *Ostrea edulis*, *Pelecypora brocchii* and *Neverita josephina* occur. Two meters above the whale outcrop there is a third horizon consisting of massive mudstones with a 50 cm thick shell bed. Molluscs are highly packed and ostreids, modiolids and arcids dominate (Figure 4).

The Montalcino (W22) was excavated at locality Poggio alle Mura. The skeleton was lying on a 40 cm shell bed made by densely-packed molluscs (Figure 2F, 4). *Venus multilamella* and *Pelecypora brocchi* are disarticulated and nested. *Haustator vermicularis* and *Dentalium* sp. are abundant. Large fossil woods were found during the excavation.

The badly outcropping succession of the Allerona (W23) whale was measured and sampled (Figure 2G, 4). Additional fragmentary vertebrate remains were recovered at the excavation site characterized by a 60-80 cm thick shell bed in grey-blue massive mudstones. The shells are loosely packed and mostly in life positions. Solitary corals are abundant (Figure 2I), as well as *Glans aculeata* (Figure 2H), *Venus multilamella* and *Pelecypora islandicoides*.



**Figure 2.** The sampled sedimentary successions where the seven fossil whales come from. **A.** The Gorgognano whale (W14) site; the arrow points on the studied outcrop about 50 m far from the exact excavation area where a monument was placed. **B.** The San Lorenzo in Collina (W15) sedimentary succession. The arrows point on the site of excavation of the fossil whale about 14 m stratigraphically below the church (see Capellini 1865). **C.** The Castellarano succession (W16); The arrow points on the stratigraphic level of excavation of the fossil whale (see Campanini 1998).

Next pages:

**D.** The Castelfiorentino whale (W21); area of excavation marked by the arrow. **E.** Outcrop of the Castelfiorentino succession a few metres below the excavation site. Blue-grey mudstones with sparse macrofauna; articulated specimens in the upper part. **F.** Shell bed at Montalcino, Poggio alle Mure locality (W22). Note nested bivalves and abundant turritellid gastropods. **G.** Excavation site of the Allerona fossil whale (W23). Excavation was carried out in 2007 and the outline of the site is still recognizable (arrows). **H, I.** Cardiids and solitary corals at the Allerona shell bed.





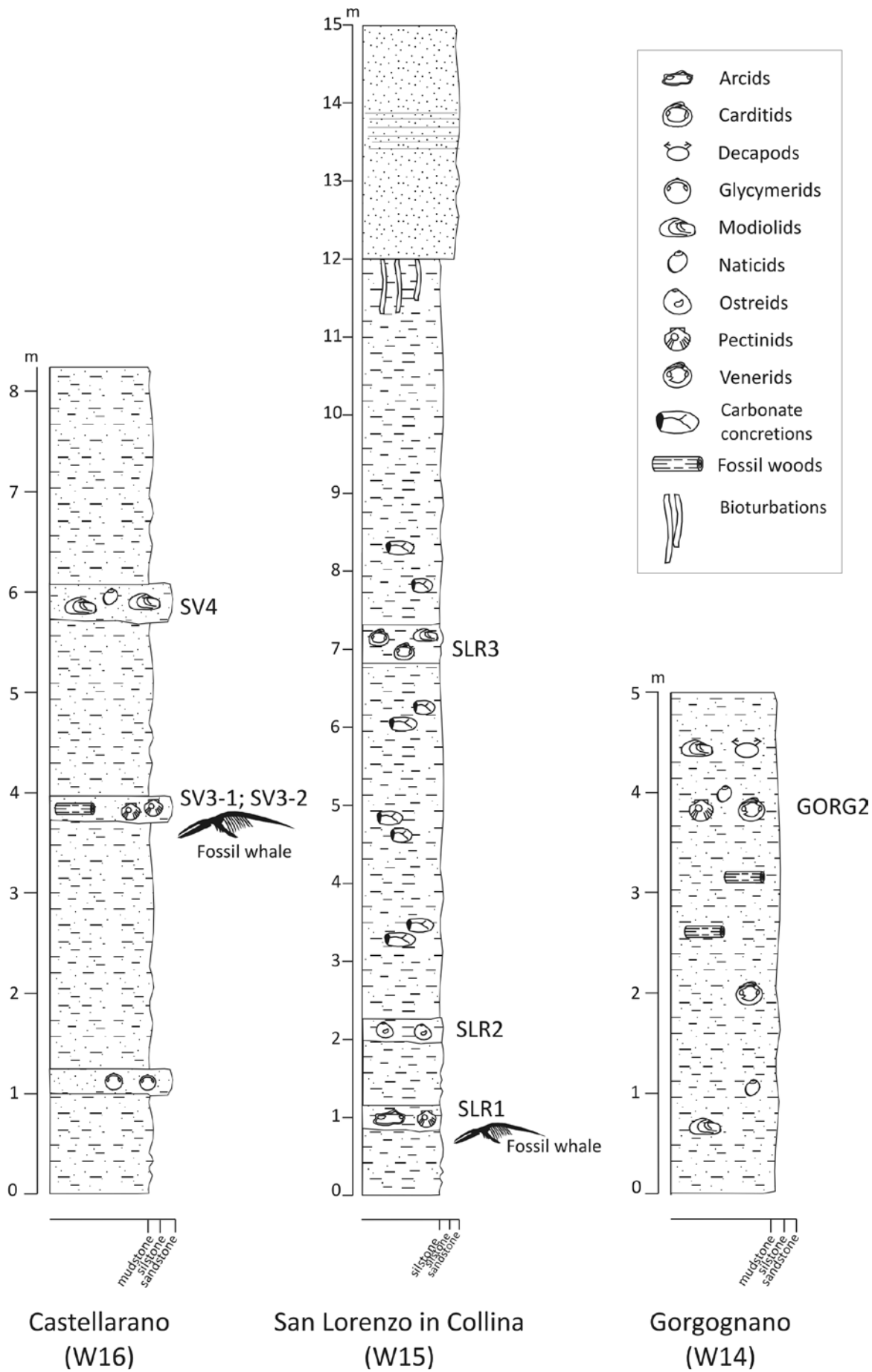


Figure 3. Detail of the sedimentary successions of the studied fossil whales. Paleo-Adriatic fossil whales (W14, W15, W16). The exact bone bed and the point where bulk samples were collected are shown.



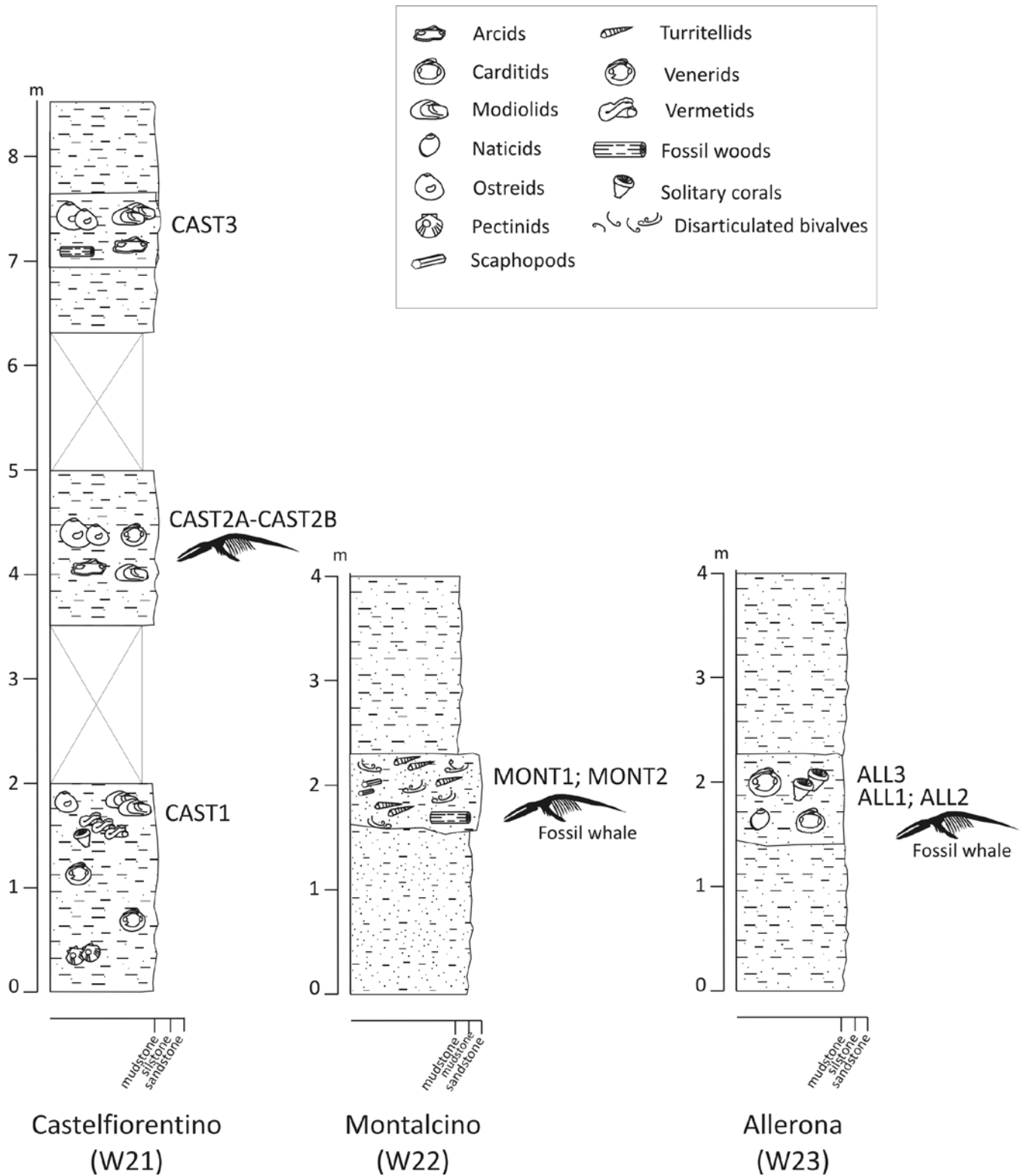


Figure 4. Detail of the sedimentary successions of the studied fossil whales. Paleo-Tyrrhenian fossil whales (W21, W22, W23). The exact bone bed and the point where bulk samples were collected are shown.

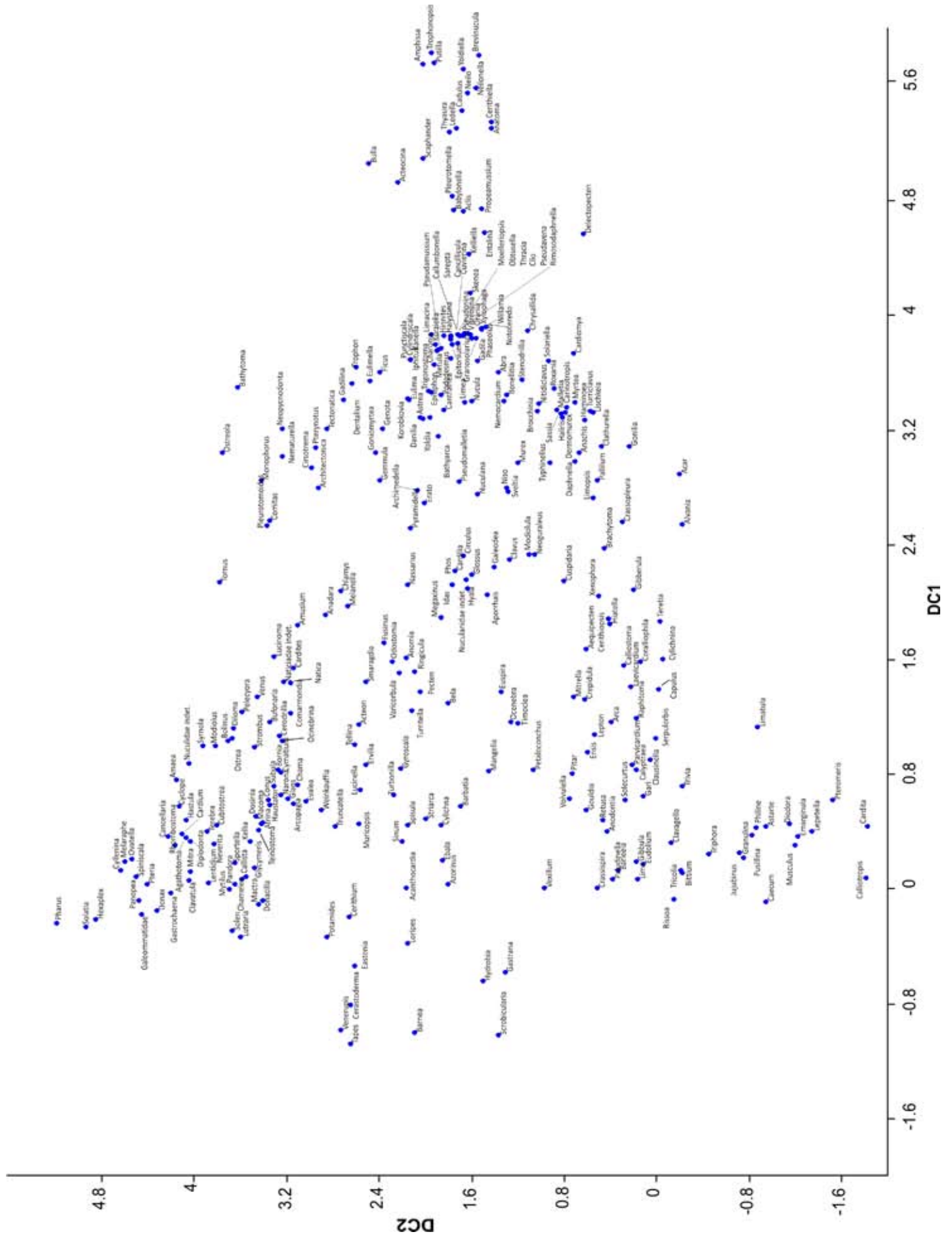
### 6.3.2 Multivariate analysis of bulk samples

The DCA multivariate analysis was performed on the total dataset, including abundance data on the fossil whale successions and the other Pliocene and Pleistocene sites of Italy. In the resulting diagram the first two axes (DC1 and DC2) are well representative of the full distribution of data, explaining 94.5 % of their variance (DC1 = 63.9 %, DC2 = 30.6 %). The r-mode diagram, plotting genera after using samples as variables, shows a continuous distribution of taxa along axis 1 of the ordination (DC1: Figure 5). A qualitative analysis of the present-day distribution of the main genera suggests that DC1 expresses a bathymetric gradient, with shallow water genera on the left-side of the diagram and bathyal genera on the right-side. This interpretation of DC1 was quantitatively verified using present-day preferred depths of 47 genera well-represented in the dataset. Preferred depths were estimated using data of ERMS database, resulting in values ranging from 1.1 to 4208 m depth below sea level (Table 1). Number of observations on which ERMS is based ranges from 8 (*Smaragdia*) to 4451 (*Hydrobia*). Extreme depth values range from -2 m for some intertidal molluscs to 4829 m for deep water deposit- and detritus-feeders. Deeper genera also tended to show the widest depth ranges. In the bivariate diagram each genera is represented by a point expressed by DC1 score in axis x and average depth on axis y (Figure 6). Points in the diagram were fitted with an exponential regression curve, which covers the depth distribution of the selected genera along the DC1 axis up to bathyal depth (about 1980m depth below sea level). The bivariate analysis indicates that DC1 scores are very good predictors of average depth of mollusc genera ( $R = 0.91$ ;  $R^2 = 0.82$ : Figure 6). If DC1 of genera is a very good predictor of depth, then q-mode DC1 can be used to estimate absolute depth of each sample using the regression curve. In the q-mode plot mollusc genera are used as variables and samples are distributed more or less continuously along DC1 (Figure 7). The sedimentary information for each sample allow an independent test of the validity of the bathymetric meaning assigned to DC1 (Figure 7). These a priori data are consistently arranged as to display intertidal samples on the left part of the diagram, in correspondence of the lowest DC1 scores, bathyal sample on the far right side, all other a priori groups in between. To definitely resolve the depth of final deposition of the seven whale falls here under consideration, absolute paleodepths (m) are given according to DC1 scores (Figure 8). The Orciano Pisano whale settled on a sea bottom of about  $93.4 \pm 1.2$  m and the others, on average, between 47 and 68 m depth, Castelfiorentino coming from shallower waters than all other whale-falls here under scrutiny (Table 2).

Samples coming from inner-outer shelf conditions are widely scattered along axis 2 of DCA ordination, whereas all other a priori groups, aligned along the main axis, have a narrow range of scores on the second axis (Figure 7). All whale sites have medium to high DC2 scores, irrespective of geographic setting (Figure 8, Appendix 4: p. 178). Samples from the paleo-Adriatic have the widest range of DC2 values, among which very low values in correspondence

**Next page:**

**Figure 5. DCA r-mode diagram. Each point correspond to one genus of the mollusc dataset (n=308). Genera are continuously distributed along axis 1 (DC1) of the ordination.**



of samples from cool-water carbonates of the Stirone calcarenite. To understand what secondary factors, other than those related to depth, control the distribution of molluscs of offshore samples, a SIMPER analysis on a selected database limited to inner and outer shelf conditions was performed. Three a priori groups were selected (a) siliciclastic samples from whale-fall sites, (b) all the other siliciclastic samples and (c) samples from cool-water carbonates. SIMPER allowed to cast out what genera contribute to the differentiation of the three a priori groups (Table 3). Since the three groups are in their turn distributed around different DC2 values, those genera can help to discriminate what factors are behind DC2. The taxa contributing most are the suspension feeding bivalves of genus *Varicorbula* and the herbivore gastropods of genus *Bittium*. *Varicorbula* increases in importance from (c) to (a), in inverse relationship with *Bittium*. *Varicorbula gibba* (the only species of this genus in our dataset) is a well-studied, small-sized opportunist present at all depths from intertidal to deep sea. In particular it thrives at conditions prohibiting for other suspension feeders, like extremely turbid waters (Hrs-Brenco 2006). On the opposite, macrophytes-dwelling, herbivores like *Bittium* can occur in offshore settings only under extremely clear-water conditions required for photosynthesis at those depths. This trend is confirmed by the importance of other herbivores like *Alvania* in discriminating cool-water carbonates, face to face with an increasing contribution of other suspension-feeders (*Venus*, *Archimediella*, *Chlamys*, *Amusium*) and deposit feeders (*Nucula*, *Nuculana*) in the other direction.

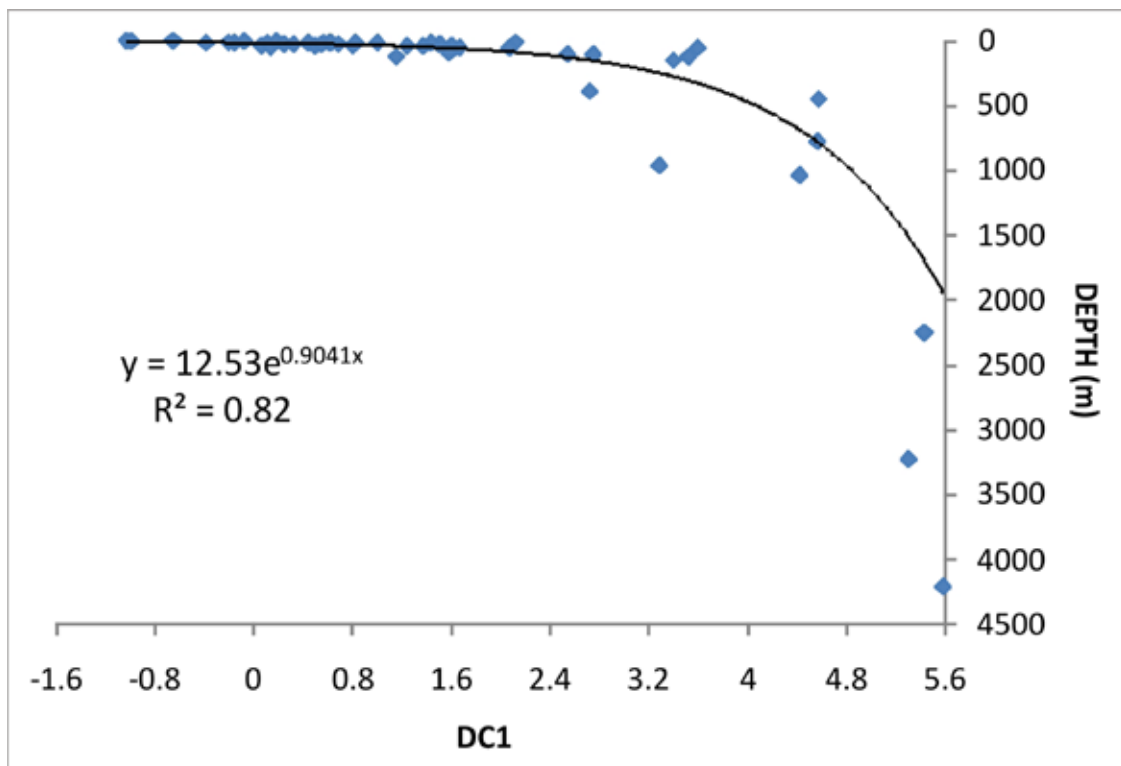


Figure 6. Bivariate plot correlating DC1 values of the 47 selected genera of the dataset (axis x) with the average depth, expressed in meters, of the corresponding modern counterparts (axis y). The exponential regression curve is a good predictor of the distribution of points up to bathyal depths (about 1980 m below sea level).

**Table 1. Summary of bathymetric data and multivariate scores used for environmental calibration of the DCA ordination. Abundance (%): genera abundance in the Pliocene dataset; Obs: number of observation (sampling sites) in the ERMS Database; Max (m): maximum depth of recurrence recovered in the ERMS database; Median (m): most frequent class of recurrences recovered in the ERMS database; Min (m): minimum depth of recurrence recovered in the ERMS database; Range (m): depth range; MEAN: mean genus depth distribution; DC1: score of detrended correspondence analysis axis 1 (DC1).**

n°	Abundance (%)	Genera	Obs	Max (m)	Median (m)	Min (m)	Range (m)	MEAN (m)	DC1
1	29.70	<i>Donax</i>	326	37.0	17.5	0.0	37.0	17.1	-0.14
2	12.73	<i>Varicorbula</i>	661	110.0	36.0	0.0	110.0	32.9	1.51
3	4.04	<i>Nassarius</i>	417	1940.0	4.5	0.0	1940.0	13.9	2.13
4	3.69	<i>Ringicula</i>	13	36.0	35.0	6.5	29.5	33.0	1.52
5	3.18	<i>Spisula</i>	2164	375.0	9.7	-1.4	376.4	20.7	0.45
6	3.07	<i>Bittium</i>	173	80.0	15.0	0.0	80.0	21.6	0.12
7	2.33	<i>Chamelea</i>	845	145.0	38.0	0.0	145.0	37.1	0.07
8	2.16	<i>Smaragdia</i>	8	30.4	20.0	3.0	27.4	18.1	1.45
9	1.58	<i>Nuculana</i>	191	800.0	79.0	0.0	800.0	107.1	2.76
10	1.55	<i>Anomia</i>	177	496.0	4.0	0.0	496.0	37.8	1.61
11	1.51	<i>Timoclea</i>	748	330.0	115.0	0.0	330.0	123.2	1.16
12	1.23	<i>Euspira</i>	1518	355.0	30.0	0.0	355.0	43.5	1.38
13	1.17	<i>Rissoa</i>	70	71.0	0.0	0.0	71.0	7.9	-0.07
14	0.97	<i>Delectopecten</i>	41	3850.0	374.0	6.0	3844.0	780.3	4.57
15	0.96	<i>Neilonella</i>	40	4829.0	4291.5	2034.0	2795.0	4208.3	5.59
16	0.87	<i>Tricolia</i>	54	260.0	10.5	0.0	260.0	18.8	0.62
17	0.83	<i>Glycymeris</i>	115	270.0	47.5	6.0	264.0	48.0	0.15
18	0.74	<i>Cyclope</i>	54	102.0	15.0	4.0	98.0	22.4	0.58
19	0.66	<i>Aequipecten</i>	345	1726.0	30.0	0.0	1726.0	53.3	1.68
20	0.65	<i>Entalina</i>	296	1557.0	316.0	190.0	1367.0	451.3	4.58
21	0.62	<i>Odostomia</i>	81	1072.0	31.0	0.0	1072.0	93.5	1.59
22	0.57	<i>Scrobicularia</i>	981	36.0	0.0	-1.1	37.1	1.1	-1.02
23	0.56	<i>Nucula</i>	1435	4268.0	41.3	0.0	4268.0	151.7	3.40
24	0.52	<i>Turritella</i>	316	290.9	38.0	0.0	290.9	41.5	1.25
25	0.50	<i>Glans</i>	15	40.0	15.0	3.0	37.0	16.5	0.63
26	0.49	<i>Tellina</i>	2896	257.0	10.9	0.0	257.0	16.7	1.01
27	0.46	<i>Limopsis</i>	504	4829.0	311.0	30.0	4799.0	392.7	2.73
28	0.44	<i>Pitar</i>	99	165.0	20.0	3.0	162.0	36.9	0.81
29	0.42	<i>Dentalium</i>	240	3264.0	86.0	0.0	3264.0	124.6	3.53
30	0.39	<i>Loripes</i>	25	85.0	15.0	6.0	79.0	19.0	-0.38
31	0.38	<i>Ledella</i>	162	4829.0	2906.0	450.0	4379.0	3227.1	5.31
32	0.37	<i>Alvania</i>	208	1606.0	30.0	0.0	1606.0	105.9	2.55
33	0.33	<i>Cerithium</i>	139	71.0	9.0	0.0	71.0	14.4	-0.19
34	0.33	<i>Abra</i>	3214	512.1	21.2	-1.4	513.5	59.9	3.60
35	0.31	<i>Cadulus</i>	128	4829.0	2165.5	136.0	4693.0	2247.3	5.43
36	0.28	<i>Dosinia</i>	516	141.0	37.0	0.0	141.0	37.5	0.51
37	0.27	<i>Lucinella</i>	21	40.0	30.0	3.0	37.0	23.7	0.69
38	0.24	<i>Calyptreaea</i>	55	64.0	19.0	6.0	58.0	22.4	0.83
39	0.20	<i>Gouldia</i>	105	130.0	19.0	6.0	124.0	27.4	0.55
40	0.19	<i>Diplodonta</i>	31	90.0	18.0	4.7	85.3	29.6	0.33
41	0.18	<i>Hydrobia</i>	4451	89.0	0.0	-2.0	91.0	2.5	-0.64
42	0.17	<i>Kelliella</i>	442	4829.0	347.0	10.0	4819.0	1040.7	4.43
43	0.17	<i>Yoldia</i>	32	1557.0	1337.0	53.0	1504.0	963.4	3.29
44	0.13	<i>Venerupis</i>	500	90.0	4.8	0.0	90.0	6.9	-0.98
45	0.12	<i>Gibbula</i>	1086	142.0	4.0	0.0	142.0	8.2	0.19
46	0.11	<i>Chlamys</i>	294	2081.0	15.0	0.0	2081.0	56.6	2.08
47	0.11	<i>Jujubinus</i>	82	160.0	30.0	0.0	160.0	26.6	0.25

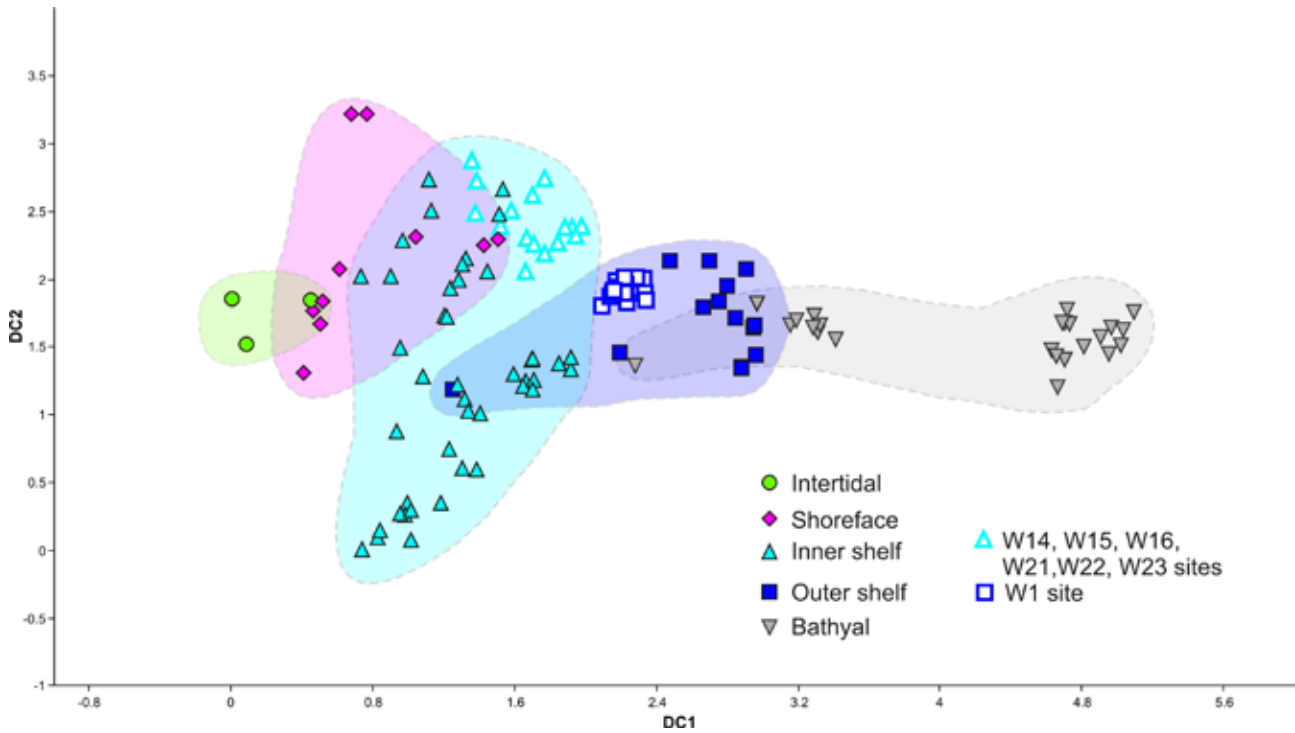


Figure 7. DCA q-mode diagram. Each point on the diagram correspond to one sample of the dataset (n=127). Samples are grouped following the a priori determination of their original paleoenvironment (see Appendix 3: p. 173). Samples are more or less continuously distributed along axis 1. Inner shelf samples have the widest range of DC2 scores.

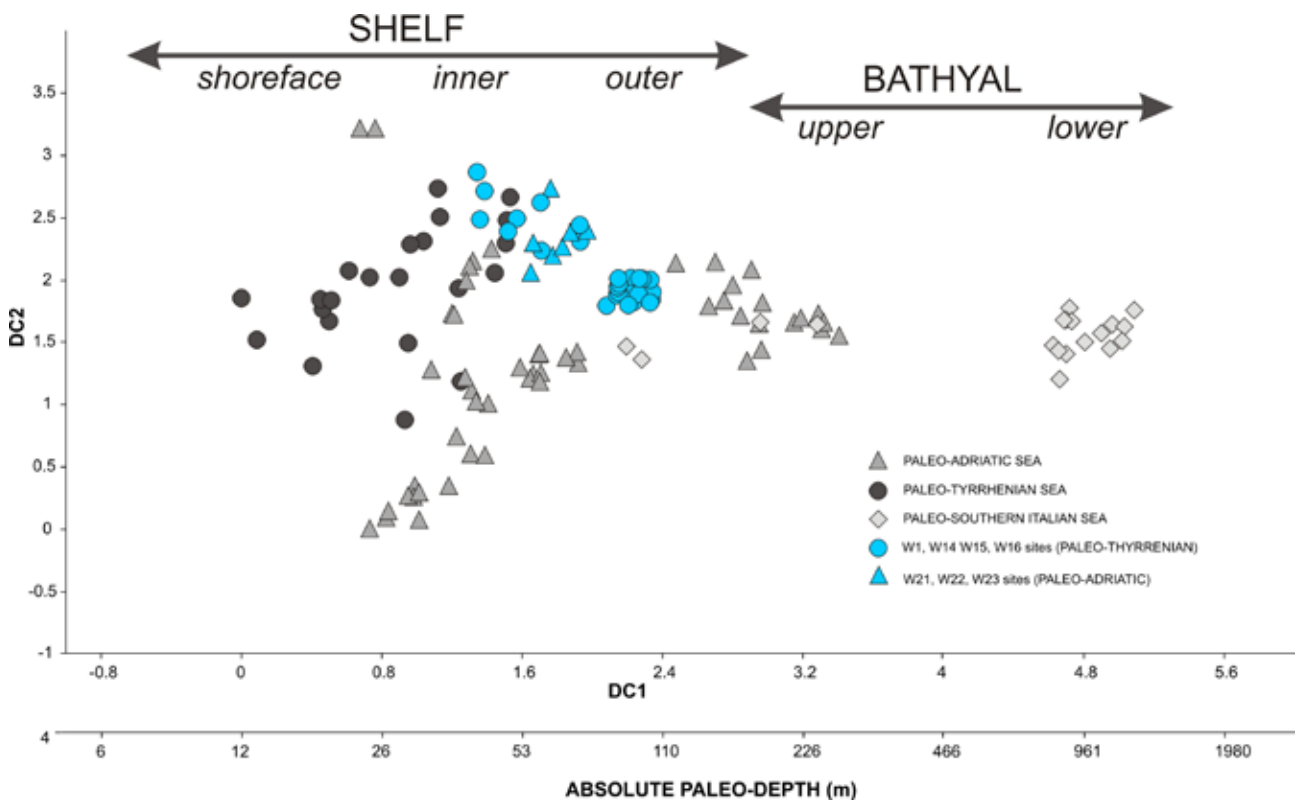


Figure 8. DCA q-mode diagram. Samples are grouped following the Paleogeographic domain of provenance. After bivariate analysis, together with DC1 values, in axis x also the absolute paleodepth for each DC1 score are reported. This allowed to distinguish along DC1 shelf depth samples (shoreface, inner shelf, outer shelf) and bathyal samples (upper and lower).

Table 2. Average depth distribution of the fossil whale sites.

FOSSIL WHALE	SAMPLES	PALEODEPTH (m)	MEAN PALEODEPTH (m)
Gorgognano (W14)	GORG2	61.7	61.7
San Lorenzo in Collina (W15)	SLR1	62.1	61.5 ± 1.2
	SLR2	66.3	
	SLR3	56.0	
Castellarano (W16)	SV3-1	71.2	67.5 ± 2.2
	SV3-2	74.8	
	SV4	56.4	
	OP8	82.9	
Orciano Pisano (W1)	OP9	92.6	93.4 ± 1.2
	OP10	86.9	
	OP11	89.7	
	OP12	103.4	
	OP13	102.6	
	OP14	99.1	
	OP15	103.8	
	OP16	94.6	
	OP17	93.8	
	OP1	89.4	
	OP2	92.1	
	OP3	88.0	
	OP4	93.1	
	OP5	93.4	
	OP6	93.5	
OP7	88.3		
Castelfiorentino (W21)	CAST1	43.4	47.1 ± 2.2
	CAST2A	43.8	
	CAST2B	42.7	
	CAST3	58.3	
Montalcino (W22)	MONT1	49.5	50.8 ± 0.5
	MONT2	52.2	
Allerona (W23)	ALL1	72.4	66.5 ± 1.8
	ALL2	58.5	
	ALL3	68.6	

Table 3. Results of SIMPER analysis. In the table genera contributing up to the 50% of dissimilarity among the three a priori groups of samples are shown. The three a priori groups are: (a) samples from the whale fall sites; (b) all the remaining samples from siliclastic offshore settings; (c) samples from the Stirone cool water carbonates.

Taxon	Contribution	Cumulative %	Mean abundance (a)	Mean abundance (b)	Mean abundance (c)
<i>Varicorbula</i>	2.915	3.923	4.31	3.29	1.94
<i>Bittium</i>	2.693	7.547	0.0247	1.41	5.59
<i>Timoclea</i>	2.028	10.28	1.56	1.67	2.17
<i>Venus</i>	1.826	12.73	1.72	0.4	0.118
<i>Nuculana</i>	1.608	14.9	1.92	2.3	0.872
<i>Archimedeella</i>	1.485	16.9	1.37	0.522	0
<i>Nassarius</i>	1.437	18.83	1.35	1.46	0.486
<i>Alvania</i>	1.433	20.76	0.0388	0.917	2.36
<i>Aequipecten</i>	1.396	22.64	0.514	1.01	1.07
<i>Parvicardium</i>	1.302	24.39	0.309	1.12	1.3
<i>Amusium</i>	1.295	26.13	1.33	0.0842	0
<i>Chlamys</i>	1.293	27.87	1.33	0.555	0
<i>Ringicula</i>	1.235	29.53	1.31	0.712	0.717
<i>Dentalium</i>	1.212	31.16	1.35	0.787	0.0821
<i>Limopsis</i>	1.186	32.76	0.551	0.773	1.41
<i>Anomia</i>	1.169	34.33	0.669	0.915	0
<i>Nucula</i>	1.166	35.9	1.16	0.959	0.575
<i>Ostrea</i>	1.156	37.46	0.882	0.472	0.0821
<i>Pseudomalletia</i>	1.152	39.01	1.2	0	0
<i>Tellina</i>	1.147	40.55	0.924	0.791	0.164
<i>Yoldia</i>	1.129	42.07	0.82	0.765	0
<i>Anadara</i>	1.085	43.53	1.19	0.35	0
<i>Spisula</i>	1.079	44.98	0.0204	1.02	0.359
<i>Euspira</i>	1.024	46.36	0.571	0.841	0.61
<i>Turritella</i>	1.021	47.73	0.931	0.548	0.34
<i>Odostomia</i>	0.9214	48.97	0.915	0.447	0.405
<i>Limea</i>	0.9028	50.19	0.421	0.629	0

## 6.4 Discussion

### 6.4.1 Clues from sedimentary geology

Whale-fall sedimentary successions show analogous tracts. With the exception of W22, which was recovered from a shell bed with highly disarticulated and nestled bivalves, indicating sediment reworking by bottom currents, all the other fossil whales were associated with shell beds with sparse molluscs, in life position or however articulated, suggesting low energy conditions and low sedimentation rates. On the outcrop, also the mollusc fauna showed similarities, with the recurrence of suspension feeding bivalves, like the epifaunal *Amusium cristatum*, *Modiolus* sp. and *Ostrea* sp. and the infaunal *Venus multilamella*, *Pelecyora brocchii* and *P. islandicoides*. Molluscs from the bottoms immediately below, around and above the whale falls can be compared with those found directly associated with the bones during their excavation (Chapter 4, Appendix), with the exclusion of W22 and W23 for which no data are available on the associated biota. All taxa associated with the bones of W15 (*Pelecyora brocchii*, *Venus multilamella*, naticids), W16 (*Glycimeris inflata*, *Modiolus* sp., *Ostrea* sp.) and W21 (mytilids, pectinids) are common also in the surrounding soft bottoms. Even the detailed study of W1 whale-fall and background communities has shown very similar faunal compositions and has further shown that the trophic nucleus of whale-falls and background communities are the same (Chapter 3). Albeit local faunal characters exist, there is a general constancy within- and between- whale-fall sites, disregarding of geographical setting, but consistently with a constancy in sedimentary conditions, that suggests that more or less complete whale skeletons preferentially sink and develop at particular environmental conditions on the shelf. A common denominator is depth (inner or outer shelf), low- to medium sedimentation rates, nutrient levels and types consistent with a fauna dominated by epifaunal and infaunal suspension feeders. On these bottoms, whale falls don't form effective trophic and structural islands as their deep water counterparts.

### 6.4.2 Environmental factors at whale-fall sites

Consistently with all previous applications of DCA to shallow marine benthic faunas, from Ordovician (Holland et al. 2001) to Pleistocene (Scarponi and Kowaleski 2004), our study of Plio-Pleistocene molluscs has shown that depth controls score along the main axis of ordination. Bivariate plots based on preferred depths of modern genera, allowed to estimate absolute depths of all samples used in the ordination, which range from intertidal to bathyal, and comprise those collected in proximity of seven whale-falls. The large fossil vertebrates could thus be interpreted as having sunken at depths of 46-93 m, corresponding to inner to outer shelf bottoms. This result confirms incomplete knowledge based on taphonomy (Chapter 4) and sedimentary geology (paragraph 6.4.1). Within this rather narrow depth range, the Orciano Pisano whale is the deepest.



Samples coming from inner-outer shelf conditions are also widely scattered along axis 2 of DCA ordination. The DCA plot, coupled with SIMPER analysis, gives us the opportunity to interpret what environmental factors are behind DC2 score. The a priori groups are ordered according to the hypothesis that from whale-fall offshore sites to molluscs of cool-water carbonates nutrient level decreases. Whale-fall bottoms are under relatively eutrophic conditions and cool-water carbonates under (relatively) oligotrophic waters. At high DC2 scores, samples are dominated by opportunist suspension-feeders, organisms of small size that can rapidly exploit resources which are abundant at unpredictable times. On the opposite side, benthic communities living on cool-water carbonates point to clear waters down to inner-mid shelf depths. This suggests that DC2 is controlled by nutrient levels, as in a previous similar study (Dominici et al. 2008). Eutrophic conditions under turbid waters could be linked to phytoplankton blooms, for the advantage of opportunist suspension feeders, whereas relatively oligotrophic conditions could develop under clear waters. This result implies that all whale falls considered in the multivariate analysis are typical of high nutrient offshore bottoms. The filter-feeding habit of large mysticetes, which obtain enormous amounts of small prey by filtering vast quantities of water, implies that the ecosystems exploited by cetaceans must be extremely productive (Ryther 1969). The concentration of cetacean populations in localized regions characterized by eutrophic conditions, like feeding and breeding areas, could then increase the possibility for whales to become part of the fossil record. As a matter of fact, cetacean paleodiversity during the Neogene is strongly directly related to diatom diversity, among the dominant marine primary producers (Marx and Uhen 2010). Furthermore exceptional accumulations of fossil whales in the Miocene–Pliocene Pisco Formation are associated with diatomaceous sediments, suggesting nutrient enrichment by ocean upwelling (Brand et al. 2004). Coastal upwelling and an abundant and diverse cetacean fauna are found in the modern northern Tyrrhenian sea (Notarbartolo Di Sciara et al. 2008). The same environmental conditions could thus explain the abundance of marine vertebrates in the Pliocene of Italy and their high biodiversity (Bisconti 2009).

## References

- Bisconti M. 2009. Taxonomy and evolution of the Italian Pliocene Mysticeti (Mammalia, Cetacea): a state of the art. *Bollettino della Società Paleontologica Italiana* 48, 147–156.
- Brand L.R., Esperante R., Chadwick A.V., Poma Porras O. and Alomia M. 2004. Fossil whale preservation implies high diatom accumulation rate in the Miocene–Pliocene Pisco Formation of Peru. *Geology* 32, 165–168.
- Bush A.M. and Brame R.I. 2010. Multiple paleoecological controls on the composition of marine fossil assemblages from the Frasnian (Late Devonian) of Virginia, with a comparison of ordination methods. *Paleobiology* 36, 573–591.
- Capellini G. 1865. Balenottere fossili del bolognese. *Memorie della Regia Accademia delle Scienze dell'Istituto di Bologna* 4, 3–24.
- Chicchi S. and M. Scacchetti. 2001. Valentina - Balena fossile del mare padano. *Civici Musei, Reggio Emilia*, 31 pp.
- Clarke K.R. and Warwick R.M. 1994. Changes in marine communities: An approach to statistical analysis and interpretation: Plymouth Marine Laboratory, Plymouth, UK, 144 pp.
- Costello M.J., Bouchet P., Boxshall G., Arvantidis C. and Appeltans W. 2008. European Register of Marine Species. <http://www.marbef.org/data/erms.php>. Consulted on 2010-10-20.
- Dando P.R. 2010. Biological communities at marine shallow-water vent and seep sites. In: S. Kiel (Ed.), *The Vent and Seep Biota*, Springer, p.333–378.
- Distel D.L., Baco A.R., Chuang E., Morrill W., Cavanaugh C. and Smith C.R. 2000. Do mussels take wooden steps to deep-sea vents? *Nature* 403, 725–726.
- Dominici S., Conti C. and Benvenuti M. 2008. Foraminifer communities and environmental change in marginal marine sequences (Pliocene, Tuscany, Italy). *Lethaia* 41, 447–460.
- Dominici S., Cioppi E., Danise S., Betocchi U., Gallai G., Tangocci F., Valleri G. and Monechi S. 2009. Mediterranean fossil whale falls and the adaptation of mollusks to extreme habitats. *Geology* 37, 815–818.
- Hill M.O. and H.G. Gauch Jr. 1980. Detrended correspondence analysis: an improved ordination technique. *Vegetatio* 42, 47–58.
- Hohenegger J. 2005. Estimation of environmental paleogradient values based on presence/absence data: a case study based on benthic foraminifera for paleodepth estimation. *Palaeogeography, Palaeoclimatology, Palaeoecology* 217, 115–130.
- Holland S.M., Miller A.I., Meyer D.L. and Dattilo B.F. 2001. The detection and importance of subtle biofacies change within a single lithofacies: The upper Ordovician Kope Formation of the Cincinnati, Ohio, region. *Palaios* 16, 205–217.
- Hrs-Brenco M. 2006. The basket shell, *Corbula gibba* Olivi, 1792 (Bivalve Mollusks) as a species resistant to environmental disturbances: A review. *Acta Adriatica* 47, 49–64.
- Jones W.J., Won Y.J., Maas P.A.Y., Smith P.J., Lutz R.A. and Vrijenhoek R.C. 2006. Evolution of habitat use by deep-sea mussels. *Marine Biology* 148, 841–851.

Kiel S. and Little C.T.S. 2006. Cold-seep mollusks are older than the general marine mollusk fauna. *Science* 313, 1429–1431.

Landini W., Menesini E. and Ragaini L. (1990) Paleocomunità a molluschi ed otoliti nel Pliocene di Castelfiorentino (Firenze, Italia). *Atti Società Toscana di Scienze Naturali, Memorie, Serie A* 97, 175–202.

Marx F.G. and Uhen M.D. 2010. Climate, Critters, and Cetaceans: cenozoic drivers of the evolution of modern whales. *Science* 327, 993–996.

Notarbartolo di Sciarra G., Agardy T., Hyrenbach D., Scovazzi T. and Van Klaveren P. 2008. The Pelagos sanctuary for Mediterranean marine mammals. *Aquatic Conservation. Marine and Freshwater Ecosystems* 18, 367–391.

Olszewski T.D. and Patzkowsky M.E. 2001. Measuring recurrence of marine biotic gradients: a case study from the Pennsylvanian-Permian Midcontinent. *Palaios* 16, 444–460.

Ryther J.H. 1969. Photosynthesis and Fish Production in the Sea. *Science* 166, 72–76.

Scarponi D. and Kowalewski M. 2004. Stratigraphic paleoecology: bathymetric signatures and sequence overprint of mollusk associations from upper Quaternary sequences of the Po Plain, Italy. *Geology* 32, 989–992

Sahling H., Galkin S.V., Salyuk A., Greinert J., Foerstel H., Piepenburg D., Suess E. 2003. Depth-related structure and ecological significance of cold-seep communities—a case study from the Sea of Okhotsk. *Deep Sea Research I* 50, 1391–1409.

Smith C.R., Kukert H., Wheatcroft R.A., Jumars P.A. and Deming J.W. 1989. Vent fauna on whale remains. *Nature* 341, 27–28.

Tarasov V.G., Gebruk A.V., Mironov A.N. and Moskalev L.I. 2005. Deep-sea and shallow-water hydrothermal vent communities: Two different phenomena? *Chemical Geology* 224, 5–39.

Vai G.B. 2001. Structure and stratigraphy: an overview. In: Vai F. and Martini I. P. (Eds.), *Anatomy of an Orogen: The Apennines and Adjacent Mediterranean Basins*. pp. 15-32.

# SHORT NOTE — Modern and fossil bathymodiolin mussels from the Mediterranean

Mytilid bivalves of the subfamily Bathymodiolinae live around chimneys emitting hot fluids at deep sea hydrothermal vents, as well as at cold seeps and on sunken organic debris (sunken wood, whale falls). Despite the absence of light-driven primary production in these deep-sea ecosystems, mussels succeed reaching high biomasses in these harsh conditions thanks to chemosynthetic, carbon-fixing bacterial symbionts located in their gill tissue (Duperron et al. 2009). Mussels attach by their byssal threads to hard substrates just above the interface between bottom seawater and sediment or rocks. Most species harbor sulphur oxidizing bacteria, but other symbionts such as methanotrophs and methylotrophs were also identified. This variability could explain the abilities of host species to adapt to various substrates (Duperron et al. 2008).

Here two new findings of bathymodiolin mussels of the genus *Idas* are reported from whale bones. One is from the modern southern Tyrrhenian sea, the other from Late Oligocene?-early Miocene sediments of northern Italy. These discoveries testify the presence of bathymodiolin mussels of the genus *Idas* in the Mediterranean at least from 25 Ma.

## ***Idas simpsoni* from Marettimo island**

Five individual of the bathymodiolin mussel *Idas simpsoni* (MARSHALL, 1900) were collected from the skull of a fin whale *Balaenoptera physalus* (LINNAEUS,1758). The skull was trawled up in 1998 from a depth of about 200m near Marettimo Island, in the south Tyrrhenian Sea (Figure 1). The bivalves were nestled in the bone crevices of the 280 cm long jawbone (Figure 2). The size-distribution of the measured specimens ranges from 12.5 X 6 mm (Figure 3) to 2.8 X 1.5mm.

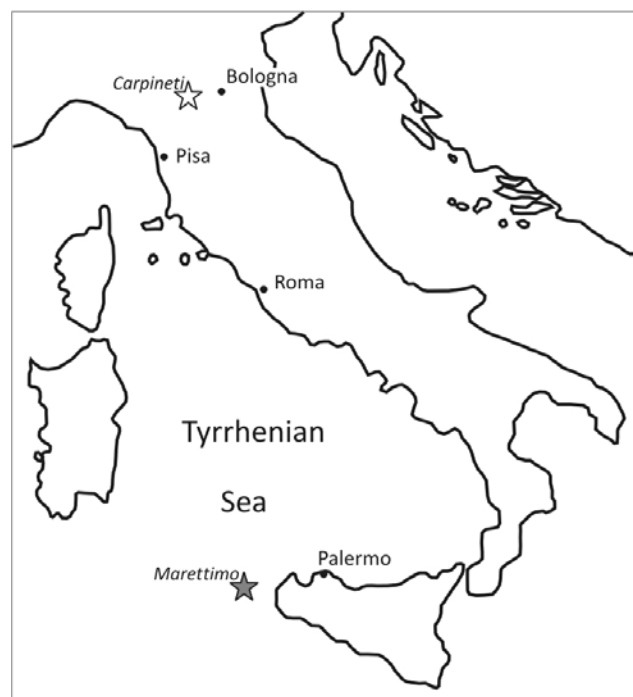


Figure 1. Location map of the two study sites. The late Oligocene?-early Miocene toothed whale comes from Carpineti, Reggio Emilia (white star), while the modern whale fall comes from waters off the Marettimo island, Trapani (grey star).

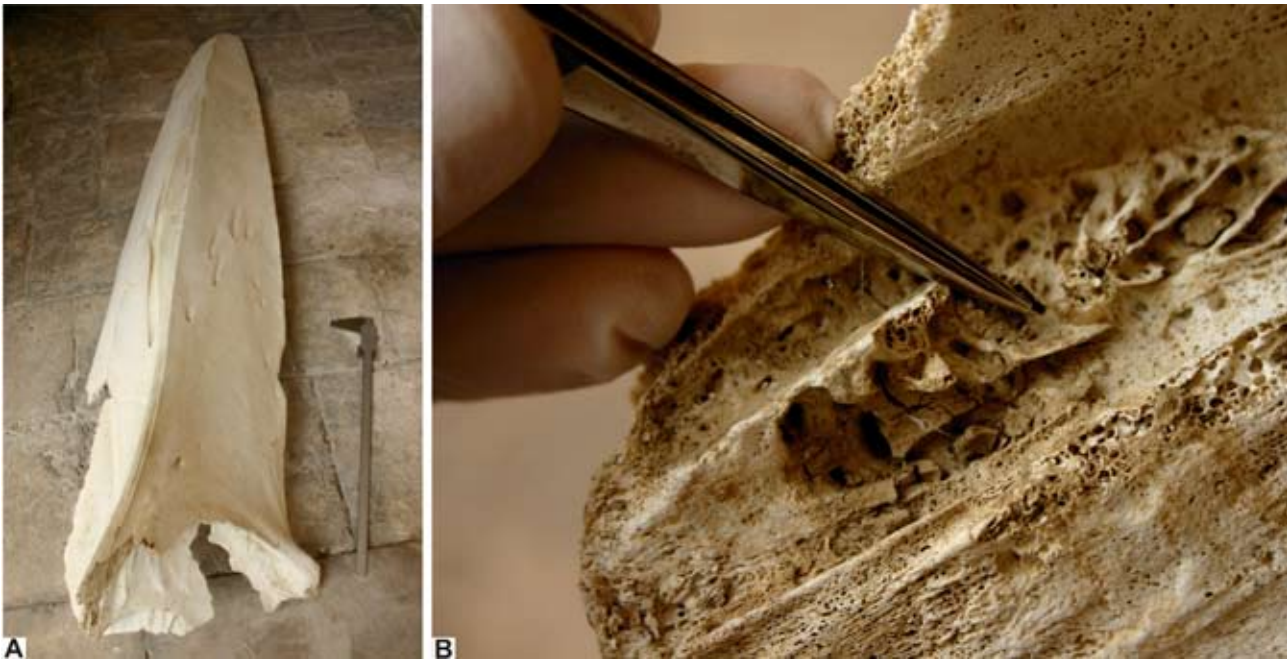


Figure 2. The skull of the fin whale *Balaenoptera physalus* (A) with one specimen of the bivalve *Idas simpsoni* in the bone crevices (B). Photographs by Gianni Insacco (Museo Civico di Storia natural di Comiso).

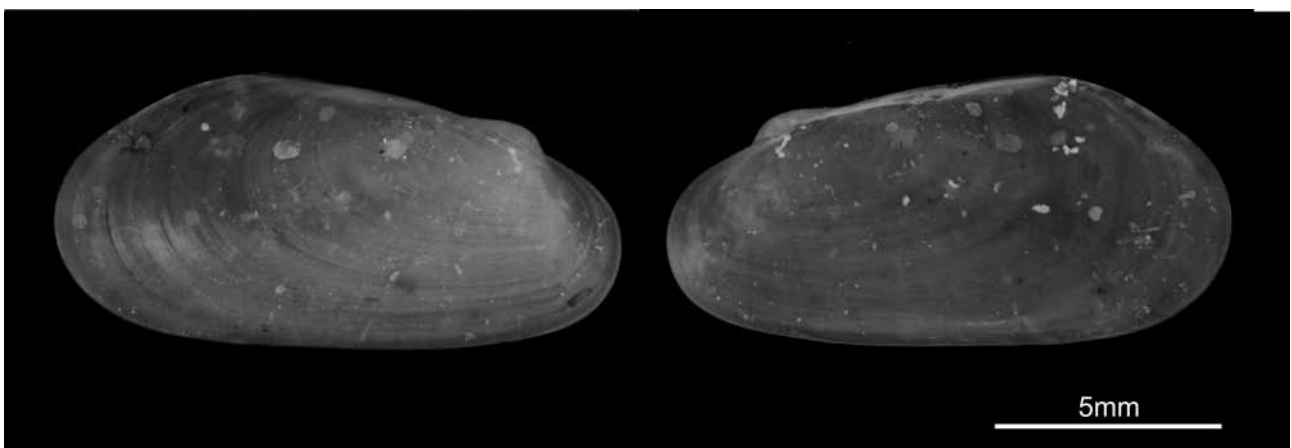


Figure 3. Specimen of *Idas simpsoni* associated with the fin whale.

### General distribution and habitat

The species *Idas simpsoni* is found on whale skeletons, including dolphins, and occasionally on wood falls. It is known from Southern Iceland, from 100-200 m depth, and from the North Sea in a few hundred metres depth (Warén 1991). In the Mediterranean Sea specimens of *Idas simpsoni* were previously found at 170 m depth off Capraia Island (Tuscan Archipelago), attached on sunken wood and trawled whale bones (Barsotti 1972, Barsotti and Giannini 1974). In the Adriatic sea more than one hundred specimens were recovered at 430 m depth from the skull of a fin whale (Bolotin et al. 2005).

## Trophism

Recent studies on bacterial symbionts on *Idas simpsoni* specimens from a whale skull in the North Sea, confirm the presence of thiotrophic (sulphur oxidizing) bacteria in their gills (Southward 2008).

### **Idas sp. from Carpineti (Northern Italy)**

More than 250 individuals of the bathymodiolin mussel *Idas* sp. were found associated with the bones of an unidentified odontocete from upper Oligocene?-lower Miocene sediments of northern Italy (Carpineti, Reggio Emilia) (Figure 1). The bones come from a sedimentary succession of hemipelagic siltstones and marls belonging to the Epiligurid Antognola Formation (Figure 4). The bathymodiolin mussels, preserved as external moulds, are mainly articulated. They can be directly in contact with whale bones or teeth, or concentrated in the nearest sediments (Figure 5).



Figure 4. The hemipelagic succession with which the lower Oligocene?-lower Miocene whale fall comes from. Photograph by Stefano Dominici.

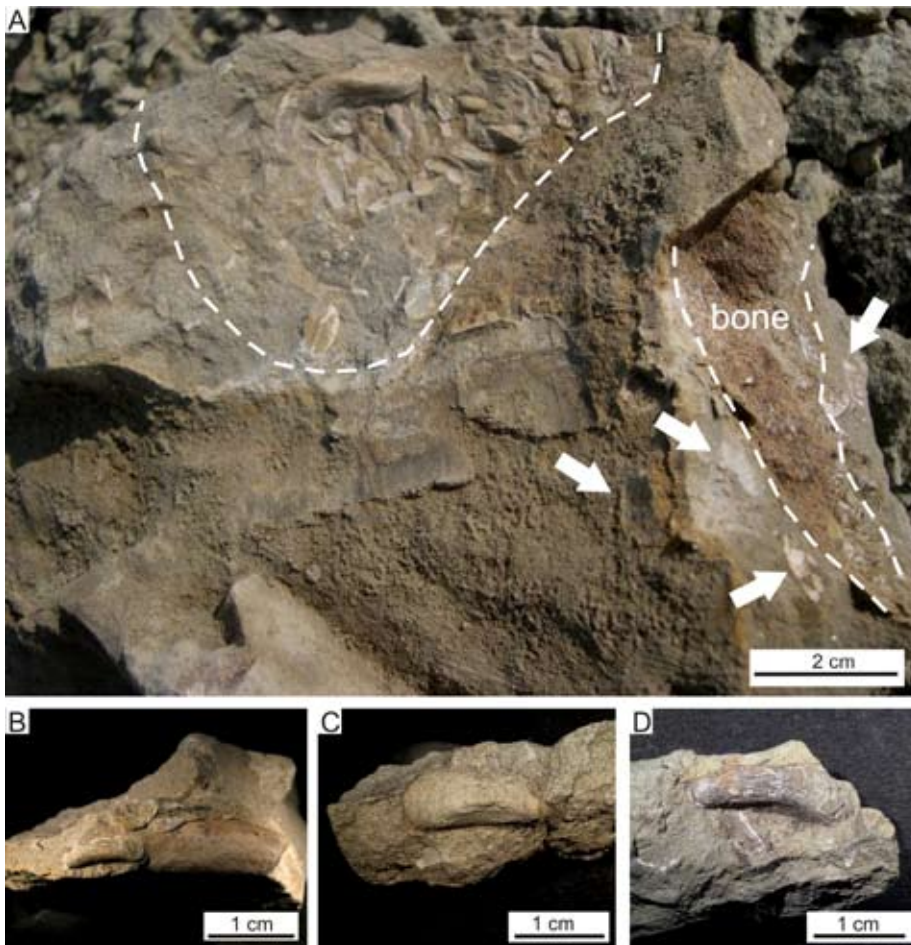


Figure 5. The Late Oligocene?-early Miocene toothed-whale with bathymodioline mussels. A. Bone fragment surrounded by sparse *Idas* sp. (white arrows). Note the large area with an high concentration of specimens on the left. B. Tooth in close association with one specimen of *Idas* sp. C and D. Respectively left and right valve.

## General distribution

Fossil bathymodiolin mussels in the Mediterranean area were previously found associated with the bones of a 10 m long mysticete from the Pliocene of central Italy (see Chapter 3), and on a Pliocene? deep water wood-fall (Bertolaso and Palazzi 1993). The genus *Idas* associated with fossil whales has a worldwide distribution. It was recovered from Early Oligocene whale- and wood-falls from the Washington State, USA (Kiel and Goedert 2006, 2007, Kiel 2008) and from the lower middle Miocene of Japan (Amano and Little 2005, Amano et al. 2007). In the latter examples, following Warèn (1991), the genus *Idas* and *Adipicola* are considered the same.

## Trophism

At modern whale falls, species of the genus *Idas*, like *Idas washingtonia*, are extremely abundant, and are known to harbour chemoautotrophic endosymbionts (Bennett et al. 1994, Deming et al. 1997). On the contrary, isotopic analyses on specimens living on small skeletons, suggest that most of the macrofaunal biomass (including the dominant *Idas washingtonia*) is not derived from sulphide-based chemoautotrophic production of endosymbionts. Thus, in contrast with large whale skeletons, the macrofaunal communities on small skeletons are sulphide tolerant but do not appear to be predominantly chemoautotrophic (Smith and Baco 2003).

## References

- Amano K. and Little C.T.S. 2005. Miocene whale-fall community from Hokkaido, northern Japan. *Palaeogeography, Palaeoclimatology, Palaeoecology* 215, 345–356.
- Amano K., Little C.T.S. and Inoue K. 2007. A new Miocene whale-fall community from Japan. *Palaeogeography, Palaeoclimatology, Palaeoecology* 247, 236–242.
- Barsotti G. 1972. *La Conchiglia*, rivista mensile delle meraviglie del mare 7-8, pp. 7.
- Barsotti G. and Giannini F. 1974. Primo ritrovamento di *Delectopecten vitreus* (GMELIN, 1789) e nuova segnalazione di *Adula simpsoni* (Marshall, 1900) nelle acque dell'Alto Tirreno. (Mollusca, lamellibranchiata). *La Conchiglia* 6, 10–11, 15.
- Bennett B.A., Smith C.R., Glaser B. and Maybaum H.L., 1994. Faunal community structure of a chemoautotrophic assemblage on whale bones in the deep northeast Pacific Ocean. *Marine Ecology Progress Series* 108, 205–223.
- Bertolaso L. and Palazzi S. 1993. La posizione sistematica di *Delphinula bellardii* Michelotti, 1847. *Bolletino Malacologico* 29, 291–302.
- Bolotin J., Hrs-Brenko M., Tutman P., Glavic N., Kožul V., Skaramuca B., Lucic D. and Lucic J. 2005. First record of *Idas simpsoni* (Mollusca: Bivalvia: Mytilidae) in the Adriatic Sea. *Journal of the Marine Biological Association of the UK* 85, 977–978.
- Deming J.W., Reysenbach A.L., Macko S.A. and Smith C.R. 1997. Evidence for the microbial basis of a chemoautotrophic invertebrate community at a whale fall on the deep seafloor: bone-colonizing bacteria and invertebrate endosymbionts. *Microscopy Research and Technique* 37, 162–170.
- Duperron S., Halary S., Lorion J., Sibuet M. and Gaill F. 2008. Unexpected co-occurrence of six bacterial symbionts in the gills of the cold seep mussel *Idas* sp. (Bivalvia: Mytilidae). *Environmental Microbiology* 10, 433–445.
- Duperron S., Lorion J., Samadi S., Gros O. and F. Gaill. 2009. Symbioses between deep-sea mussels (Mytilidae: Bathymodiolinae) and chemosynthetic bacteria: diversity, function and evolution. *Comptes Rendus Biologies* 332, 298–310.
- Kiel S. and Goedert J.L. 2006. Deep-sea food bonanzas: Early Cenozoic whale-fall communities resemble wood-fall rather than seep communities. *Proceedings of the Royal Society of London, Series B* 273, 2625–2631.
- Kiel S. and Goedert J.L. 2007. Six new mollusk species associated with biogenic substrates in Cenozoic deep-water sediments in Washington State, USA. *Acta Palaeontologica Polonica* 52, 41–52.
- Kiel S. 2008. Fossil evidence for micro- and macrofaunal utilization of large nektonfalls: examples from early Cenozoic deep-water sediments in Washington State, USA. *Palaeogeography, Palaeoclimatology, Palaeoecology* 267, 161–174.
- Pyenson N.D. and Haasl D.M. 2007. Miocene whale-fall from California demonstrates that cetacean size did not determine the evolution of modern whale-fall communities. *Biology Letters (Palaeontology)* 3, 709–711.
- Smith C.R. and Baco A.R. 2003. Ecology of whale falls at the deep-sea floor. *Oceanography and Marine Biology Annual Review* 41, 311–354.



Southward E.C. 2008. The morphology of bacterial symbioses in the gills of mussels of the genera *Adipicola* and *Idas* (Bivalvia: Mytilidae), *The Journal of Shellfish Research* 27, 139–146.

Warén A. 1991. New and little known Mollusca from Iceland and Scandinavia. *Sarsia* 76, 53–124.

# GENERAL CONCLUSIONS — An ecosystem approach to the fossil record of whale falls

---

The first part of the study concerned shallow marine modern and fossil mollusc communities associated with whale carcasses. Mollusc species collected at the Kosterfjord whale fall – the first study on a complete skeleton at depths shallower than the shelf break – indicate that 5 years after deployment the community reached the sulphophilic stage of the ecological succession. Sediments below whale bones were dominated by the bivalve *Thyasira sarsi*, which is known to contain endosymbiotic sulphur-oxidizing bacteria and usually lives in organic rich sediments with high total sulphide concentrations, like sewage-polluted fjords and active methane seeps. On the contrary the surrounding soft bottoms were inhabited by another species of the same genus, *T. equalis*, which is less dependent on the bacterial carbon for its nutrition and lives in less organic-rich sediments than *T. sarsi*. These data on modern mollusc communities living at a shallow water whale fall suggest that the sulphophilic stage of the ecological succession is characterized by more generalist, chemosynthetic bivalves compared with the specialists found at deep sea sites. The somehow similar paleoecological study carried out at species-level on the 10 m long, fossil baleen whale from the Pliocene of Tuscany (Italy) gave consistent results with the above hypothesis. Although the bulk of the fauna associated with the Orciano fossil bones was dominated by the same heterotrophs as found in the surrounding community, whale-fall samples were distinguishable primarily by the presence of chemosymbiotic bivalves and a greater richness of carnivores and parasites. Large specimens of the lucinid clam *Megaxinus incrassatus* and very rare small mussels of genus *Idas* testify to the occurrence of a sulphophilic stage, but large chemosymbiotic obligates related to vesicomid clams, common at deep-sea whale falls, are absent. The picture that emerges from both the modern and fossil large organic falls considered at Kosterfjord and at Orciano Pisano is in accordance with data from other extreme reducing habitats in shallow marine settings. Hydrothermal vent and hydrocarbon seeps at shelf depths are in fact also inhabited by a subset of the fauna commonly living in the surrounding bottoms and obligate taxa are absent. The occurrence of the obligate mussels of the genus *Idas* even at shallow water whale falls could derive from the high adaptability of this taxa to different substrata and its feeding strategies. Some species are in fact mixotrophs, being able to filter particles as well as harbouring chemosynthetic bacteria.

In the second part a multi-level ecosystem approach was applied to the study of fossil whale falls. Information from taphonomy, microfacies and geochemical analyses on fossil bones, paleoecology of the associated biota and helped to better understand biostratigraphic processes occurring at shallow water whale falls. The taphonomic pathways of a whale carcass

on a relatively shallow marine bottom is much more variable than in the deep sea, where large carcasses rest articulated on the sea floor and pass through all stages of the ecological succession. Notwithstanding resurfacing, disarticulation and early burial hinder the onset of whale fall communities on the shelf, we found multiple evidence of the development of the mobile scavenger stage, the enrichment opportunist stage - possibly including *Osedax*-like polychaetes - and the reef stage. Orciano Pisano remains so far the only fossil whale carcass where signs of the sulphophilic stage were found, possibly as an effect of insufficient sampling during recovery of vertebrate bones. However evidences of the production of sulphide by bacterial degradation of whale bones, the process triggering the onset of the sulphophilic stage, coupled with the possible traces of sulphur-oxidizing bacteria on the surface of whale bones, were found even in specimens where chemosymbiotic bivalves are absent. This implies that even on the shelf whale carcasses can create reducing conditions favourable to the development of a sulphophilic stage, although they are differently exploited respect to the deep sea. All the other ecological stages are characterized by unspecialized taxa commonly living in the surrounding environment, from pelagic sharks to benthic suspension and deposit feeders, predatory and browsing carnivores. The only exception are organisms specifically adapted to the whalebone ecological niche. The bone eating worm *Osedax*, hosting heterotrophic bacteria to exploit the bone organic matter, is found both at shallow and deep water whale falls. Microborings very similar in size and shape, originated by microbial euhendoliths like fungi or bacteria tunnelling inside whale bones, are also common to both settings. Although microborings are widely documented in the fossil record, no data are available from their modern counterpart, which could help to better understand their trophic behaviour.

Finally data collected from the sedimentary successions where some of the studied fossil whales were excavated helped to reconstruct paleoenvironmental conditions at the bottom where carcasses sank prior to final burial and fossilization. All the fossil whales come from similar inner to outer shelf settings, the deepest depth corresponding to the Orciano Pisano fossil whale. These settings were accomanated by characterizing elements of the molluscan fauna which have been related to high-nutrient conditions, in accordance with the fact that eutrophic, productive waters are known to be the best place for large cetaceans to thrive because of their filter feeding habit. We thus hypothesize that the rich and diverse record of fossil cetaceans in the Pliocene of Italy is partly controlled by eutrophic conditions in the water column, at particular depths and particular geographic settings, favouring large cetacean populations and an higher probability of carcasses to become part of the fossil record.

The multidisciplinary synoptical approach to the study of modern and fossil whale fall ecosystems confers additional value to results based on a series of single-group or single-discipline approaches. On the shelf the course of the ecological succession is dependent on such a large variety of factors that a coherent picture can stem only by considering multilpe evidences at once. This approach can be extended back in time to the study of fossil communities associated with large marine Mesozoic reptiles, in search for possible evolutionary routes followed from coastal ancestors to deep sea obligates of extreme reducing conditions.



## Acknowledgments

First at all thanks to my supervisor Simonetta Monechi who supported me unconditionally at any moment of the PhD. Thanks for your enthusiasm for whale fall studies, for your very good advices, and for trying always to provide me all necessary tools to perform this research in the best way. A special thank goes to my co-supervisor Stefano Dominici, for many reasons. Thanks for introducing me to the world of dead whales and for every single thing you taught me in these three years. Thanks for your patience, for trying to let me improve my English (mission impossible!), for sharing office and for the infinite meals and teas we shared. Thanks for the lively discussions, both when we were in agreement or not. Thanks to Barbara Cavalazzi, my external-supervisor. Thanks for your help with microfacies analysis, for everything you taught me on the world at the micro-scale, and for phone calls late in the night to discuss data! Thomas Dahlgren and Adrian Glover, thanks for the opportunity you gave me to work not only with dead things but also with living and smelling animals! Visiting Tjärno is one of the unforgettable experience of my PhD. Thanks to Elisabetta Cioppi for providing me everything I need to feel home at the Museo di Storia Naturale, for her enthusiasm, and for discussions on Tai Chi! Thanks to Francesco Landucci for sharing office and for his attempts to teach me basic knowledge of restoration of vertebrate bones. Thanks to many other people who help me during these three years, to Frances Westall who hosted me in her lab at Orleans, thanks to Birger Schmitz for isotope analysis and for help in interpreting results. Thanks to Steffen Kiel for inviting me to Göttingen. Thanks to Helena Wiklund for helping me sampling muddy sediments at Tjärno, a rather easy practice for marine biologists but not for a paleontologist! At Tjärno also Tomas Lundälv assisted during ROV operations and video documentations, Ingemar Adolfsson, Anders Billing helped with RV *Nereus*. Anders Warén, Rafael La Perna, Simone Marsili, Michelangelo Bisconti, Enrico Ulivi helped me in different stages of the thesis for specimen identification. Cris Little gave me good insights reading part of the manuscript, Stuart Wallace helped with the English, Nicola Cipriani and Marta Marcucci helped me with petrographic and micropaleontological thin sections, Maurizio Ulivi assisted me during the endless but exciting SEM sessions. Thanks to Moreno Pacini for trying the best way to get better thin sections, Laura Balestrieri and Francesca Tangocci were very good roommates in the paleo-invertebrate lab. During this thesis I met many museum curators and amateur paleontologists with which I shared many information, thanks to Daniele Ormezzano, Silvia Chicchi (thanks for sampling together!), Piero Damarco, Mino Lo Russo and Mario Miti, Vittorio Borselli, Simone Casati, Stefano Bulla, Enrico Sguazzini, Maria Cristina Peparello, Carlo Sarti, Maria Grazia Mezzadri, Cristina De Angelis and Barberi Gabriella. A special thank also to Simona Guioli who provided bone samples for microfacies analysis, to Gianni Insacco for specimens of *Idas simponi* and to Luca Bertolaso for the very nice field trip at the toothed-whale site.

Thanks to all other people I met at conferences and meetings or wherever during these intense three years of PhD.

Many many thanks to my parents, who always supported be in any choice, also when I had the “crazy” idea to leave a safe and boring job to get involved in this adventure. Thanks to my friends Claudia and Veronica for the time passed together speaking about life, future, projects.... Veronica thanks for helping me with the final layout of the manuscript!

To Francesco, thank you, for all the time you spent listening to me speaking about whales, dead or alive, molluscs and bacteria, and for encouraging me in bad moments. Thank you for your patient in the last months when I moved from home into my PC! Thanks for cheering me up with your wonderful cooking and for taking care of the wooden stove (“la stouva”!).



**APPENDIX 1. Mollusc samples from the fossil whale outcrops.****Mollusc identified at the species level**Gorgognano whale (W14)

<b>FAMILY</b>	<b>SPECIES</b>	<b>GORG2</b>
Nassaridae	<i>Nassarius semistriatus</i>	1
Nuculanidae	<i>Nucula sulcata</i>	10
Arcidae	<i>Anadara diluvii</i>	2
Pectinidae	<i>Amusium cristatum</i>	8
Anomiidae	<i>Anomia ehippium</i>	1
Tellinidae	<i>Tellina</i> sp.	1
Veneridae	<i>Venus multilamella</i>	44
Veneridae	<i>Timoclea ovata</i>	2
Veneridae	<i>Pelecypora brocchii</i>	5
Corbulidae	<i>Corbula gibba</i>	1
	<b>TOTAL</b>	<b>75</b>
	<b>OTHERS</b>	
Serpulidae	<i>Ditrupa cornea</i>	89
	Decapods	1

San Lorenzo in Collina whale (W15)

<b>FAMILY</b>	<b>SPECIES</b>	<b>SLR1</b>	<b>SLR2</b>	<b>SLR3</b>
Turritellidae	<i>Turritella tricarinata</i>	4	3	5
Aporrhaidae	<i>Aporrhais uttingeriana</i>	3	0	0
Naticidae	<i>Euspira</i> sp.	1	0	8
Naticidae	<i>Natica pseudoepiglottina</i>	14	10	0
Bursidae	<i>Bufoaria (Aspa) marginatum</i>	1	0	0
Epitoniidae	<i>Epitonium cf. frondiculoides</i>	3	0	0
Epitoniidae	<i>Epitonium</i> sp.	0	1	0
Eulimidae	<i>Eulima glabra</i>	0	1	0
Columbelliidae	<i>Mitrella</i> sp.	2	0	0
Nassaridae	<i>Nassarius semistriatus</i>	1	0	2
Nassaridae	<i>Nassarius fontanensi</i>	0	1	4
Nassaridae	<i>Nassarius cf. libasi</i>	0	0	3
Fasciolariidae	<i>Fusinus</i> sp.	1	0	0
Mitridae	<i>Cancilla</i> sp.	1	0	0
Turridae	<i>Cerodrillia sigmoidea</i>	0	0	1
Turridae	<i>Comitas dimidiata</i>	0	0	1
Conidae	<i>Clathromangelia clathrata</i>	0	0	1
Conidae	<i>Comarmondia cf. gracilis</i>	0	1	0
Terebridae	<i>Conus antidiluvianus</i>	1	0	0
Pyramidellidae	<i>Odostomia</i> sp.	6	1	0
Pyramidellidae	<i>Turbonilla</i> sp.	0	1	1
Ringiculidae	<i>Ringicula (Ringiculina) auriculata</i>	3	4	2
Nuculanidae	<i>Nucula placentina</i>	1	0	0
Nuculanidae	<i>Nucula (lamellinucula) jeffreysi</i>	0	1	0
Nuculanidae	<i>Nucula</i> sp.	0	2	0
Nuculanidae	<i>Nuculana pella</i>	0	0	1
Nuculanidae	<i>Nuculana fragilis</i>	46	24	30
Yoldiidae	<i>Yoldia sp.1</i>	16	3	6
Arcidae	<i>Anadara diluvii</i>	4	1	2
Glycymeridae	<i>Glycymeris</i> sp.	1	0	0
Mytilidae	<i>Modiolus</i> sp.	0	2	0
Ostreidae	<i>Ostrea edulis</i>	4	2	2
Pectinidae	<i>Chlamys varia</i>	0	1	0

APPENDIX

Pectinidae	<i>Aequipecten opercularis</i>	2	0	0
Pectinidae	<i>Amusium cristatum</i>	5	3	1
Pectinidae	<i>Pecten sp.</i>	1	0	0
Lucinidae	<i>Myrtea spinifera</i>	1	0	0
Chamidae	<i>Chama cf. gryphoides</i>	0	1	0
Carditidae	<i>Glans intermedia</i>	1	0	6
Cardiidae	<i>Acanthocardia sp.</i>	3	0	1
Cardiidae	<i>Parvicardium papillosum</i>	4	2	3
Tellinidae	<i>Tellina sp.</i>	3	0	4
Psammobiidae	<i>Gari fervensis</i>	1	2	0
Veneridae	<i>Venus multilamella</i>	16	12	3
Veneridae	<i>Venus sp.</i>	0	0	6
Veneridae	<i>Timoclea ovata</i>	40	24	80
Veneridae	<i>Pelecypora islandicoides</i>	12	5	
Corbulidae	<i>Varicorbula gibba</i>	42	26	19
Hiatellidae	<i>Hiatella arctica</i>	0	0	1
Cuspidariidae	<i>Cuspidaria cuspidata</i>	0	1	0
Dentaliidae	<i>Dentalium sexangulum</i>	1	0	0
Dentaliidae	<i>Dentalium fossile</i>	1	2	0
Dentaliidae	<i>Dentalium sp.</i>	2	1	0
Gadiliniidae	<i>Gadilina jani</i>	3	3	5
	<b>TOTAL</b>	<b>251</b>	<b>141</b>	<b>198</b>
	<b>OTHERS</b>			
Serpulidae	<i>Ditrupa cornea</i>	31	3	53
	Balanid plates	1	0	0
	Briozoa	3	2	8
	Wood fragments	0	10	2

Castellarano whale (W16)

FAMILY	SPECIES	SV3-1	SV3-2	SV4
Trochidae	indet.	0	0	1
Trochidae	<i>Calliostoma sp.</i>	0	0	1
Rissoidae	<i>Alvania cf. discors</i>	0	0	1
Turritellidae	<i>Turritella tricarinata</i>	0	0	8
Turritellidae	<i>Archimediella spirata</i>	0	0	2
Turritellidae	<i>Turritella sp.</i>	1	1	0
Eratoidea	<i>Erato voluta</i>	0	0	1
Naticidae	<i>Natica tigrina</i>	0	0	17
Naticidae	<i>Tectonatica astensis</i>	4	3	0
Cassidae	<i>Phalium intermedium</i>	0	0	1
Bursidae	<i>Bufo naria (Aspa) marginata</i>	0	0	3
Triphoridae	<i>Monophorus cf. perversus</i>	0	0	1
Nassaridae	<i>Nassarius semistriatus</i>	3	0	0
Nassaridae	<i>Nassarius clathratus</i>	0	0	1
Nassaridae	<i>Nassarius cf. lingusticus</i>	0	0	10
Nassaridae	<i>Nassarius serraticosta</i>	0	0	4
Nassaridae	<i>Nassarius sp.</i>	0	0	1
Fasciolaridae	<i>Fusinus lamellosus</i>	0	0	1
Cancellaridae	<i>Calcarata calcarata</i>	0	0	2
Turridae	<i>Cerodrillia sigmoidea</i>	0	0	2
Conidae	<i>Bela brachystoma</i>	0	0	1
Pyramidellidae	<i>Eulimella pyramidata</i>	0	0	1
Pyramidellidae	<i>Turbinilla lactea</i>	0	0	5
Pyramidellidae	<i>Turbonilla sp.</i>	1	0	0
Rinigculidae	<i>Ringicula auriculata</i>	0	0	1
Nuculanidae	<i>Nucula placentina</i>	4	3	0
Nuculanidae	<i>Nuculana fragilis</i>	0	0	25



Yoldiidae	<i>Yoldia sp.1</i>	5	2	0
Yoldiidae	<i>Yoldia sp.2</i>	4	2	0
Arcidae	<i>Anadara diluvii</i>	0	1	4
Limopsidae	<i>Limopsis aurita</i>	0	0	4
Glycymeridae	<i>Glycymeris inflata</i>	0	0	2
Mytilidae	<i>Modiolus cf. barbatus</i>	0	3	0
Mytilidae	<i>Modiolus sp.</i>	0	0	18
Ostreidae	<i>Ostrea edulis</i>	0	0	36
Pectinidae	<i>Amusium cristatum</i>	4	5	0
Pectinidae	<i>Aequipecten scabrella</i>	8	6	41
Anomiidae	<i>Anomia ehippium</i>	0	0	13
Anomiidae	<i>Pododesmus squamula</i>	0	0	2
Cardiidae	<i>Plagiocardium papillosum</i>	0	0	1
Tellinidae	<i>Tellina donacina</i>	0	0	4
Veneridae	<i>Venus multilamella</i>	12	10	6
Veneridae	<i>Timoclea ovata</i>	18	8	23
Veneridae	<i>Pelecypora broccchii</i>	6	2	7
Veneridae	<i>Dosinia cf. exoleta</i>	15	0	1
Corbulidae	<i>Varicorbula gibba</i>	8	5	18
Dentaliidae	<i>Dentalium sexangulum</i>	1	0	6
Dentaliidae	<i>Dentalium (Antalis) vulgare</i>	6	3	0
Gadiliniidae	<i>Gadilina jani</i>	2	0	0
	<b>TOTAL</b>	<b>102</b>	<b>54</b>	<b>276</b>

**OTHERS**

Serpulidae	<i>Ditrupa cornea</i>	28	13	7
	Foraminifers	8	1	8
	Fish otoliths	4	0	1
	Fish teeth	1	0	1
	Briozoa	5	0	2
	Regular echinoid plates	0	0	2
	Balanid plates	0	0	2

Castelfiorentino whale (W21)

FAMILY	SPECIES	CAST1	CAST2A	CAST2B	CAST3
Turritellidae	<i>Turritella tricarinata</i>	2	2	6	2
Vermetidae	<i>Petalococonchus sp.</i>	100	0	2	8
Naticidae	<i>Euspira catena</i>	7	1	0	6
Naticidae	<i>Neverita josephina</i>	0	0	1	0
Triphoridae	<i>Monophorus perversus</i>	2	0	0	1
Muricidae	<i>Bolinus brandaris</i>	1	0	1	0
Nassaridae	<i>Nassarius semistriatus</i>	0	3	2	0
Nassaridae	<i>Nassarius cf. libasi</i>	1	0	0	0
Fasciolaridae	<i>Fusinus lamellosus</i>	1	0	0	0
Fasciolaridae	<i>Fusinus rostratus</i>	1	0	0	0
Fasciolaridae	<i>Fusinus sp.</i>	0	1	0	0
Cancellariidae	<i>Babylonella costellifera</i>	0	0	0	1
Turridae	<i>Comitas dimidiata</i>	0	0	0	1
Conidae	<i>Comarmondia gracilis</i>	0	0	0	1
Pyramidellidae	<i>Odostomia conoidea</i>	3	0	0	1
Pyramidellidae	<i>Odostomia sp.</i>	0	1	0	0
Pyramidellidae	<i>Chrysallida sp.</i>	0	0	0	1
Pyramidellidae	<i>Turbonilla cf. lactea</i>	1	0	0	0
Nuculidae	<i>Nucula sulcata</i>	0	0	1	0
Nuculidae	indet.	0	2	0	1
Nuculanidae	<i>Sacella sp.</i>	4	0	0	0
Nuculanidae	<i>Nuculana fragilis</i>	0	1	2	0
Nuculanidae	indet.	1	0	0	0

APPENDIX

Yoldiidae	<i>Yoldia nitida</i>	0	0	0	1
Arcidae	<i>Barbatia barbata</i>	2	0	0	0
Arcidae	<i>Anadara diluvii</i>	0	5	6	5
Arcidae	<i>Anadara pectinata</i>	0	0	1	0
Arcidae	indet.	6	0	0	0
Mytilidae	<i>Modiolus sp.</i>	16	4	10	6
Mytilidae	indet.	0	0	1	0
Ostreidae	<i>Ostrea edulis</i>	48	8	20	19
Pectinidae	<i>Chlamys multistriata</i>	5	0	0	12
Pectinidae	<i>Amusium cristatum</i>	0	2	6	0
Anomiidae	<i>Anomia ehippium</i>	0	1	1	0
Carditidae	<i>Glans intermedia</i>	0	0	1	0
Cardiidae	<i>Acanthocardia echinata</i>	0	0	1	0
Cardiidae	<i>Parvicardiun minimum</i>	0	1	0	0
Tellinidae	<i>Tellina cf. pulchella</i>	5	2	4	1
Veneridae	<i>Venus multilamella</i>	9	12	9	1
Veneridae	<i>Timoclea ovata</i>	6	3	1	1
Veneridae	<i>Pelecypora brocchii</i>	4	0	6	2
Corbulidae	<i>Varicorbula gibba</i>	1	3	3	4
Dentaliidae	<i>Dentalium fossile</i>	5	0	0	0
Dentaliidae	<i>Dentalium sp.</i>	0	0	0	1
Gadiliniidae	<i>Gadilina jani</i>	4	0	0	0
	<b>TOTAL</b>	<b>235</b>	<b>52</b>	<b>85</b>	<b>76</b>
	<b>OTHERS</b>				
Serpulidae	Ditrupa cornea	2	2	4	3
	Regula echinoid plates	1	0	0	0
	Balanid plates	4	0	0	12
	Decapod chelae	1	0	0	1
	Fish otoliths	1	0	0	0
	Briozoa	0	2	0	1
	Corals	12	0	0	2

Montalcino whale (W22)

FAMILY	SPECIES	MONT1	MONT2
Trochidae	<i>Jujubinus sp.</i>	1	0
Trochidae	<i>Calliostoma cf. miliaris</i>	1	0
Rissoidae	<i>Rissoa sp.</i>	1	0
Rissoidae	<i>Alvania cf. discors</i>	0	1
Turritellidae	<i>Haustator vermicularis</i>	96	59
Vermetidae	indet.	2	0
Aporrhaidae	<i>Aporrhais uttingeriana uttingeriana</i>	0	3
Naticidae	<i>Euspira cf. catena</i>	8	9
Naticidae	<i>Natica cf. plicatula</i>	1	2
Muricidae	<i>Ocinebrina aciculata</i>	0	1
Columbellidae	<i>Columbella sp.</i>	0	1
Nassaridae	<i>Nassarius semistriatus</i>	6	4
Pyramidellidae	<i>Odostomia sp.</i>	5	0
Pyramidellidae	<i>Turbonilla cf. lactea</i>	1	0
Ringiculidae	<i>Ringicula (Ringiculina) ventricosa</i>	2	0
Ringiculidae	<i>Ringicula sp.</i>	0	1
Nuculanidae	<i>Nucula placentina</i>	1	2
Nuculanidae	<i>Nuculana pella</i>	1	0
Nuculanidae	<i>Nuculana fragilis</i>	15	8
Arcidae	<i>Anadara diluvii</i>	1	2
Mytilidae	<i>Modiolula phaseolina</i>	1	0
Ostreidae	<i>Ostrea edulis</i>	9	7
Pectinidae	<i>Chlamys varia</i>	2	1

Pectinidae	<i>Chlamys multistriata</i>	3	2
Pectinidae	<i>Aequipecten cf. scabrella</i>	0	2
Pectinidae	<i>Amusium cristatum</i>	2	1
Pectinidae	<i>Hyalopecten (Similpecten) similis</i>	1	0
Anomiidae	<i>Anomia ephippium</i>	1	0
Lucinidae	<i>Myrtea spinifera</i>	4	3
Lucinidae	<i>Lucinoma boreale</i>	3	2
Lucinidae	<i>Lucinella divaricata</i>	3	2
Cardiidae	<i>Cardium hians</i>	0	5
Cardiidae	<i>Acanthocardia echinata</i>	1	0
Cardiidae	<i>Plagiocardium papaillosum</i>	1	1
Mactridae	<i>Spisula subtruncata</i>	0	1
Tellinidae	<i>Tellina sp.1</i>	7	10
Tellinidae	<i>Tellina sp. 2</i>	0	3
Semelidae	<i>Abra longicallus</i>	1	0
Semelidae	<i>Abra sp.</i>	0	1
Veneridae	<i>Venus multilamella</i>	47	50
Veneridae	<i>Timoclea ovata</i>	3	9
Veneridae	<i>Pitar rudis</i>	1	0
Veneridae	<i>Pelecypora brocchii</i>	4	3
Veneridae	<i>Dosinia exoleta</i>	0	1
Myidae	<i>Sphenia sp.</i>	0	5
Corbulidae	<i>Varicorbula gibba</i>	8	11
Dentaliidae	<i>Dentalium fossile</i>	3	7
Dentaliidae	<i>Dentalium inaequicostatum</i>	4	6
		<b>251</b>	<b>226</b>

**OTHERS**

	Iregular echinoid spines	7	0
	Iregular echinoid plates	0	2
	Regula echinoids spines	0	2
Serpulidae	<i>Ditrupa cornea</i>	1	0
	Foraminifers	6	0
	Decapod chelae	3	2
	Balanid plates	0	2
	Wood fragments	4	0
	Fish otoliths	6	10
	Fish teeth	4	2
	Briozoa	1	0

Allerona whale (W23)

<b>FAMILY</b>	<b>SPECIES</b>	<b>ALL1</b>	<b>ALL2</b>	<b>ALL3</b>
Trochidae	<i>Gibbula sp.</i>	0	1	0
Trochidae	<i>Callistoma sp.</i>	0	1	0
Turritellidae	<i>Archimedella spirata</i>	1	11	1
Naticidae	indet.	1	5	0
Pyramidellidae	<i>Odostomia conoidea</i>	1	2	0
Nuculanidae	<i>Nucula sulcata</i>	0	1	0
Nuculanidae	<i>Nuculana fragilis</i>	3	2	4
Yoldiidae	<i>Yoldia nitida</i>	1	1	1
Limopsidae	<i>Limopsis minuta</i>	2	1	0
Pectinidae	<i>Chlamys varia</i>	1	1	2
Pectinidae	<i>Aequipecten scabrella</i>	0	2	2
Pectinidae	<i>Amusium cristatum</i>	1	4	5
Pectinidae	<i>cf. Korobkovia oblonga</i>	2	0	0
Pectinidae	<i>Pecten sp.</i>	0	1	0
Anomiidae	<i>Anomia ephippium</i>	3	2	0
Carditidae	<i>Glans aculeata</i>	4	16	6

APPENDIX

---

Chamidae	<i>Chama sp.</i>	0	1	0
Cardiidae	<i>Parvicardium minimum</i>	0	1	0
Tellinidae	<i>Tellina planata</i>	0	1	0
Tellinidae	<i>Tellina sp.</i>	1	0	0
Veneridae	<i>Venus multilamella</i>	3	10	8
Veneridae	<i>Timoclea ovata</i>	4	5	9
Veneridae	<i>Pelecypora brocchii</i>	3	2	3
Corbulidae	<i>Varicorbula gibba</i>	3	6	1
Dentaliidae	<i>Dentalium sexangulum</i>	0	3	6
Entalinidae	<i>Entalina tetragona</i>	1	0	0
		<b>35</b>	<b>80</b>	<b>48</b>
	<b>OTHERS</b>			
Serpulidae	<i>Ditrupa cornea</i>	1	0	1
	Regular echinoid spines	1	2	0
	Irregula echinoid spines	0	1	0
	Foraminifers	31	13	7
	Decapod chelae	2	1	0
	Solitary corals	1	3	6
	Fish otoliths	9	8	4
	Briozoa	3	5	0















FAMILY	GENUS	ALL3	TTA	TTB	TTIC	TTD	TTIE	TTA	TTB	TT2B	TT3A	TT3B	TT3C	TT3D	TT5A	TT5B	TT5C	TT5D	TT5E	TT6	TT7A	TT7B	TT8A	TT8B	TT8C	A1A	A1B	A1C	A1D	A1E	A1F	A1G	A2A	A2B					
Lepetellidae	<i>Lepetella</i>	0	0	0	0	0	0	0	0	0	0	0	0	0	0	0	0	0	0	0	0	0	0	0	0	0	0	0	0	0	0	0	0	0	0	0			
Fissurellidae	<i>Enarginula</i>	0	0	0	0	0	0	0	0	0	0	0	0	0	0	0	0	0	0	0	0	0	0	0	0	0	0	0	0	0	0	0	0	0	0	0			
Fissurellidae	<i>Diodora</i>	0	0	0	0	0	0	0	0	0	0	0	0	0	0	0	0	0	0	0	0	0	0	0	0	0	0	0	0	0	0	0	0	0	0	0	0		
Scissurellidae	<i>Anatoma</i>	0	0	0	0	0	0	0	0	0	0	0	0	0	0	0	0	0	0	0	0	0	0	0	0	0	0	0	0	0	0	0	0	0	0	0	0		
Turbinidae	<i>Contrainea</i>	0	0	0	0	0	0	0	0	0	0	0	0	0	0	0	0	0	0	0	0	0	0	0	0	0	0	0	0	0	0	0	0	0	0	0	0		
Turbinidae	<i>Astrea</i>	0	0	0	0	0	0	0	0	0	0	0	0	0	0	0	0	0	0	0	0	0	0	0	0	0	0	0	0	0	0	0	0	0	0	0	0	0	
Turbinidae	<i>Tricolia</i>	0	0	0	27	0	0	0	0	0	0	0	0	0	0	0	0	0	0	0	0	0	0	0	0	0	0	0	0	0	0	0	0	0	0	0	0		
Trochidae	<i>Danilia</i>	0	0	0	0	0	0	0	0	0	0	0	0	0	0	0	0	0	0	0	0	0	0	0	0	0	0	0	0	0	0	0	0	0	0	0	0	0	
Trochidae	<i>Calliactropis</i>	0	0	0	0	0	0	0	0	0	0	0	0	0	0	0	0	0	0	0	0	0	0	0	0	0	0	0	0	0	0	0	0	0	0	0	0	0	
Trochidae	<i>Lischkeia</i>	0	0	0	0	0	0	0	0	0	0	0	0	0	0	0	0	0	0	0	0	0	0	0	0	0	0	0	0	0	0	0	0	0	0	0	0	0	
Trochidae	<i>Gibbula</i>	0	33	26	12	8	0	0	0	0	0	0	0	0	0	0	0	0	0	0	0	0	0	0	0	0	0	0	0	0	0	0	0	0	0	0	0	0	
Trochidae	<i>Diloma</i>	0	0	0	0	0	0	0	0	0	0	0	0	0	0	0	0	0	0	0	0	0	0	0	0	0	0	0	0	0	0	0	0	0	0	0	0	0	0
Trochidae	<i>Jujubinus</i>	0	0	0	0	0	0	0	0	0	0	0	0	0	0	0	0	0	0	0	0	0	0	0	0	0	0	0	0	0	0	0	0	0	0	0	0	0	0
Trochidae	<i>Calliastoma</i>	0	0	0	0	0	0	0	0	0	0	0	0	0	0	0	0	0	0	0	0	0	0	0	0	0	0	0	0	0	0	0	0	0	0	0	0	0	0
Trochidae	<i>Callumbornella</i>	0	0	0	0	0	0	0	0	0	0	0	0	0	0	0	0	0	0	0	0	0	0	0	0	0	0	0	0	0	0	0	0	0	0	0	0	0	0
Trochidae	indet. 1	0	0	0	0	0	0	0	0	0	0	0	0	0	0	0	0	0	0	0	0	0	0	0	0	0	0	0	0	0	0	0	0	0	0	0	0	0	0
Trochidae	indet. 2	0	0	0	0	0	0	0	0	0	0	0	0	0	0	0	0	0	0	0	0	0	0	0	0	0	0	0	0	0	0	0	0	0	0	0	0	0	0
Sequeziidae	<i>Halystina</i>	0	0	0	0	0	0	0	0	0	0	0	0	0	0	0	0	0	0	0	0	0	0	0	0	0	0	0	0	0	0	0	0	0	0	0	0	0	0
Trochidae	<i>Solaria</i>	0	0	0	0	0	0	0	0	0	0	0	0	0	0	0	0	0	0	0	0	0	0	0	0	0	0	0	0	0	0	0	0	0	0	0	0	0	0
Trochidae	<i>Solaria</i>	0	0	0	0	0	0	0	0	0	0	0	0	0	0	0	0	0	0	0	0	0	0	0	0	0	0	0	0	0	0	0	0	0	0	0	0	0	0
Skeneidae	<i>Skenea</i>	0	0	0	0	0	0	0	0	0	0	0	0	0	0	0	0	0	0	0	0	0	0	0	0	0	0	0	0	0	0	0	0	0	0	0	0	0	0
Skeneidae	<i>Purilla</i>	0	0	0	0	0	0	0	0	0	0	0	0	0	0	0	0	0	0	0	0	0	0	0	0	0	0	0	0	0	0	0	0	0	0	0	0	0	0
Lissospiridae	<i>Malleriopsis</i>	0	0	0	0	0	0	0	0	0	0	0	0	0	0	0	0	0	0	0	0	0	0	0	0	0	0	0	0	0	0	0	0	0	0	0	0	0	0
Neeritidae	<i>Smaragdia</i>	0	0	0	0	0	0	0	0	0	0	0	0	0	0	0	0	0	0	0	0	0	0	0	0	0	0	0	0	0	0	0	0	0	0	0	0	0	0
Rissoidae	<i>Rissoa</i>	0	0	0	0	0	0	0	0	0	72	1721	381	192	0	0	0	0	0	0	0	0	0	0	0	0	0	0	0	0	0	0	0	0	0	0	0	0	0
Rissoidae	<i>Alvania</i>	0	0	0	0	0	0	0	0	0	0	0	0	0	0	0	0	0	0	0	0	0	0	0	0	0	0	0	0	0	0	0	0	0	0	0	0	0	
Rissoidae	<i>Obolusella</i>	0	0	0	0	0	0	0	0	0	0	0	0	0	0	0	0	0	0	0	0	0	0	0	0	0	0	0	0	0	0	0	0	0	0	0	0	0	0
Rissoidae	<i>Pusillina</i>	0	0	0	0	0	0	0	0	0	0	0	0	0	0	0	0	0	0	0	0	0	0	0	0	0	0	0	0	0	0	0	0	0	0	0	0	0	0
Rissoidae	<i>Circulus</i>	0	0	0	0	0	0	0	0	0	0	0	0	0	0	0	0	0	0	0	0	0	0	0	0	0	0	0	0	0	0	0	0	0	0	0	0	0	0
Adeorbidae	<i>Adeorbis</i>	0	0	0	0	0	0	0	0	0	0	0	0	0	0	0	0	0	0	0	0	0	0	0	0	0	0	0	0	0	0	0	0	0	0	0	0	0	0
Barleeidae	<i>Barleia</i>	0	0	0	0	0	0	0	0	0	0	0	0	0	0	0	0	0	0	0	0	0	0	0	0	0	0	0	0	0	0	0	0	0	0	0	0	0	0
Barleeidae	<i>Tetrasoma</i>	0	0	0	0	0	0	0	0	0	0	0	0	0	0	0	0	0	0	0	0	0	0	0	0	0	0	0	0	0	0	0	0	0	0	0	0	0	0
Barleeidae	<i>Caecum</i>	0	0	0	0	0	0	0	0	0	39	0	0	0	0	0	0	0	0	0	0	0	0	0	0	0	0	0	0	0	0	0	0	0	0	0	0	0	
Assimineidae	<i>Palulinella</i>	0	0	0	0	0	0	0	0	0	0	0	0	0	0	0	0	0	0	0	0	0	0	0	0	0	0	0	0	0	0	0	0	0	0	0	0	0	
Hydrobiidae	<i>Hydrobia</i>	0	51	32	16	1	0	0	0	0	0	0	0	0	0	0	0	0	0	0	0	0	0	0	0	0	0	0	0	0	0	0	0	0	0	0	0	0	
Micromelaniidae	<i>Nematurella</i>	0	0	0	0	0	0	0	0	0	0	0	0	0	0	0	0	0	0	0	0	0	0	0	0	0	0	0	0	0	0	0	0	0	0	0	0	0	0
Iravadiidae	<i>Hyala</i>	0	0	0	0	0	0	0	0	0	0	0	0	0	0	0	0	0	0	0	0	0	0	0	0	0	0	0	0	0	0	0	0	0	0	0	0	0	0
Iravadiidae	<i>Rhombostoma</i>	0	0	0	0	0	0	0	0	0	0	0	0	0	0	0	0	0	0	0	0	0	0	0	0	0	0	0	0	0	0	0	0	0	0	0	0	0	0
Citloceratidae	<i>Pseudomina</i>	0	0	0	0	0	0	0	0	0	0	0	0	0	0	0	0	0	0	0	0	0	0	0	0	0	0	0	0	0	0	0	0	0	0	0	0	0	0
Tornidae	<i>Tornus</i>	0	0	0	0	0	0	0	0	0	0	0	0	0	0	0	0	0	0	0	0	0	0	0	0	0	0	0	0	0	0	0	0	0	0	0	0	0	0
Cerithiidae	<i>Cerithium</i>	0	0	29	11	67	0	0	0	0	0	0	0	0	0	0	0	0	0	0	0	0	0	0	0	0	0	0	0	0	0	0	0	0	0	0	0	0	
Cerithiidae	<i>Bitium</i>	0	185	299	147</																																		

APPENDIX

	A2B	A2A	A2Abis	A1G	A1F	A1E	A1D	A1C	A1B	A1A	T8C	T8B	T8A	T7B	T7A	T6	T5E	T5D	T5C	T5B	T5A	T3D	T3C	T3B	T3A	T2B	T2A	T1E	T1D	T1C	T1B	T1A	A13			
<i>Tectonatica</i>	0	0	0	0	0	0	0	0	0	0	0	0	0	0	0	0	0	0	0	0	0	0	0	0	0	0	0	0	0	0	0	0	0			
<i>indet.</i>	0	0	0	0	0	0	0	0	0	0	0	0	0	0	0	0	0	0	0	0	0	0	0	0	0	0	0	0	0	0	0	0	0			
<i>Sinum</i>	0	0	0	0	0	0	0	0	0	0	0	0	0	0	0	0	0	0	0	0	0	0	0	0	0	0	0	0	0	0	0	0	0	0		
<i>Eudalum</i>	0	0	0	0	0	0	0	0	0	0	0	0	0	0	0	0	0	0	0	0	0	0	0	0	0	0	0	0	0	0	0	0	0	0		
<i>Tonnidae</i>	0	0	0	0	0	0	0	0	0	0	0	0	0	0	0	0	0	0	0	0	0	0	0	0	0	0	0	0	0	0	0	0	0	0		
<i>Malea</i>	0	0	0	0	0	0	0	0	0	0	0	0	0	0	0	0	0	0	0	0	0	0	0	0	0	0	0	0	0	0	0	0	0	0		
<i>Ficus</i>	0	0	0	0	0	0	0	0	0	0	0	0	0	0	0	0	0	0	0	0	0	0	0	0	0	0	0	0	0	0	0	0	0	0	0	
<i>Galeodea</i>	0	0	0	0	0	0	0	0	0	0	0	0	0	0	0	0	0	0	0	0	0	0	0	0	0	0	0	0	0	0	0	0	0	0	0	
<i>Cassidae</i>	0	0	0	0	0	0	0	0	0	0	0	0	0	0	0	0	0	0	0	0	0	0	0	0	0	0	0	0	0	0	0	0	0	0	0	
<i>Phalum</i>	0	0	0	0	0	0	0	0	0	0	0	0	0	0	0	0	0	0	0	0	0	0	0	0	0	0	0	0	0	0	0	0	0	0	0	
<i>Cymactium</i>	0	0	0	0	0	0	0	0	0	0	0	0	0	0	0	0	0	0	0	0	0	0	0	0	0	0	0	0	0	0	0	0	0	0	0	
<i>Charonia</i>	0	0	0	0	0	0	0	0	0	0	0	0	0	0	0	0	0	0	0	0	0	0	0	0	0	0	0	0	0	0	0	0	0	0	0	
<i>Ranelidae</i>	0	0	0	0	0	0	0	0	0	0	0	0	0	0	0	0	0	0	0	0	0	0	0	0	0	0	0	0	0	0	0	0	0	0	0	
<i>Ranelidae</i>	0	0	0	0	0	0	0	0	0	0	0	0	0	0	0	0	0	0	0	0	0	0	0	0	0	0	0	0	0	0	0	0	0	0	0	
<i>Ranelidae</i>	0	0	0	0	0	0	0	0	0	0	0	0	0	0	0	0	0	0	0	0	0	0	0	0	0	0	0	0	0	0	0	0	0	0	0	
<i>Bursidae</i>	0	0	0	0	0	0	0	0	0	0	0	0	0	0	0	0	0	0	0	0	0	0	0	0	0	0	0	0	0	0	0	0	0	0	0	
<i>Bufonaria</i>	0	0	0	0	0	0	0	0	0	0	0	0	0	0	0	0	0	0	0	0	0	0	0	0	0	0	0	0	0	0	0	0	0	0	0	
<i>Cerithiopsis</i>	0	0	0	0	0	0	0	0	0	0	0	0	0	0	0	0	0	0	0	0	0	0	0	0	0	0	0	0	0	0	0	0	0	0	0	
<i>Cerithiopsidae</i>	0	0	0	0	0	0	0	0	0	0	0	0	0	0	0	0	0	0	0	0	0	0	0	0	0	0	0	0	0	0	0	0	0	0	0	
<i>Triphoridae</i>	0	0	0	0	0	0	0	0	0	0	0	0	0	0	0	0	0	0	0	0	0	0	0	0	0	0	0	0	0	0	0	0	0	0	0	
<i>Monophorus</i>	0	0	0	0	0	0	0	0	0	0	0	0	0	0	0	0	0	0	0	0	0	0	0	0	0	0	0	0	0	0	0	0	0	0	0	
<i>Epitonium</i>	0	0	0	0	0	0	0	0	0	0	0	0	0	0	0	0	0	0	0	0	0	0	0	0	0	0	0	0	0	0	0	0	0	0	0	
<i>Amoeba</i>	0	0	0	0	0	0	0	0	0	0	0	0	0	0	0	0	0	0	0	0	0	0	0	0	0	0	0	0	0	0	0	0	0	0	0	
<i>Cirsorena</i>	0	0	0	0	0	0	0	0	0	0	0	0	0	0	0	0	0	0	0	0	0	0	0	0	0	0	0	0	0	0	0	0	0	0	0	
<i>Cylindriscala</i>	0	0	0	0	0	0	0	0	0	0	0	0	0	0	0	0	0	0	0	0	0	0	0	0	0	0	0	0	0	0	0	0	0	0	0	0
<i>Gyrascala</i>	0	0	0	0	0	0	0	0	0	0	0	0	0	0	0	0	0	0	0	0	0	0	0	0	0	0	0	0	0	0	0	0	0	0	0	0
<i>Punctiscula</i>	0	0	0	0	0	0	0	0	0	0	0	0	0	0	0	0	0	0	0	0	0	0	0	0	0	0	0	0	0	0	0	0	0	0	0	0
<i>Iphitus</i>	0	0	0	0	0	0	0	0	0	0	0	0	0	0	0	0	0	0	0	0	0	0	0	0	0	0	0	0	0	0	0	0	0	0	0	0
<i>Epitonidae</i>	0	0	0	0	0	0	0	0	0	0	0	0	0	0	0	0	0	0	0	0	0	0	0	0	0	0	0	0	0	0	0	0	0	0	0	0
<i>Spiniscalia</i>	0	0	0	0	0	0	0	0	0	0	0	0	0	0	0	0	0	0	0	0	0	0	0	0	0	0	0	0	0	0	0	0	0	0	0	0
<i>Eulima</i>	0	0	0	0	0	0	0	0	0	0	0	0	0	0	0	0	0	0	0	0	0	0	0	0	0	0	0	0	0	0	0	0	0	0	0	0
<i>Eulimidae</i>	0	0	0	0	0	0	0	0	0	0	0	0	0	0	0	0	0	0	0	0	0	0	0	0	0	0	0	0	0	0	0	0	0	0	0	0
<i>Eulimidae</i>	0	0	0	0	0	0	0	0	0	0	0	0	0	0	0	0	0	0	0	0	0	0	0	0	0	0	0	0	0	0	0	0	0	0	0	0
<i>Eulimidae</i>	0	0	0	0	0	0	0	0	0	0	0	0	0	0	0	0	0	0	0	0	0	0	0	0	0	0	0	0	0	0	0	0	0	0	0	0
<i>Melanella</i>	0	0	0	0	0	0	0	0	0	0	0	0	0	0	0	0	0	0	0	0	0	0	0	0	0	0	0	0	0	0	0	0	0	0	0	0
<i>Niso</i>	0	0	0	0	0	0	0	0	0	0	0	0	0	0	0	0	0	0	0	0	0	0	0	0	0	0	0	0	0	0	0	0	0	0	0	0
<i>Vitreolina</i>	0	0	0	0	0	0	0	0	0	0	0	0	0	0	0	0	0	0	0	0	0	0	0	0	0	0	0	0	0	0	0	0	0	0	0	0
<i>Vitreolina</i>	0	0	0	0	0	0	0	0	0	0	0	0	0	0	0	0	0	0	0	0	0	0	0	0	0	0	0	0	0	0	0	0	0	0	0	0
<i>Acilis</i>	0	0	0	0	0	0	0	0	0	0	0	0	0	0	0	0	0	0	0	0	0	0	0	0	0	0	0	0	0	0	0	0	0	0	0	0
<i>Murex</i>	0	0	0	0	0	0	0	0	0	0	0	0	0	0	0	0	0	0	0	0	0	0	0	0	0	0	0	0	0	0	0	0	0	0	0	0
<i>Muricidae</i>	0	0	0	0	0	0	0	0	0	0	0	0	0	0	0	0	0	0	0	0	0	0	0	0	0	0	0	0	0	0	0	0	0	0	0	0
<i>Muricidae</i>	0	0	0	0	0	0	0	0	0	0	0	0	0	0	0	0	0	0	0	0	0	0	0	0	0	0	0	0	0	0	0	0	0	0	0	0
<i>Muricidae</i>	0	0	0	0	0	0	0	0	0	0	0	0	0	0	0	0	0	0	0	0	0	0	0	0	0	0	0	0	0	0	0	0	0	0	0	0
<i>Muricidae</i>	0	0	0	0	0	0	0	0	0	0	0	0	0	0	0	0	0	0	0	0	0	0	0	0	0	0	0	0	0	0	0	0	0	0	0	0
<i>Muricidae</i>	0	0	0	0	0	0	0	0	0	0	0	0	0	0	0	0	0	0	0	0	0	0	0	0	0	0	0	0	0	0	0	0	0	0	0	0
<i>Muricidae</i>	0	0																																		







	ALLS	T1A	T1B	T1C	T1D	T1E	T2A	T2B	T3A	T3B	T3C	T3D	T5A	T5B	T5C	T5D	T5E	T6	T7A	T7B	T8A	T8B	T8C	A1A	A1B	A1C	A1D	A1E	A1F	A1G	A2Abis	A2A	A2B						
Veneridae	1	0	0	0	0	0	1	0	0	0	0	0	0	0	0	0	0	0	2	0	0	0	0	0	0	0	0	0	0	0	0	0	0						
Veneridae	0	0	0	0	0	0	0	1	0	0	349	0	0	0	0	0	0	0	0	0	0	0	0	0	0	0	0	0	0	0	0	0	0						
Veneridae	0	0	0	0	0	0	0	0	0	0	323	41	0	0	0	0	0	0	0	0	0	0	0	0	0	0	0	0	0	0	0	0	0	0					
Veneridae	0	2	3	6	5	1	23	0	0	0	0	28	0	0	0	0	0	1	3	1	1	1	0	0	0	0	0	0	0	0	0	0	0	0					
Myidae	0	0	0	0	0	0	0	0	0	0	0	0	0	0	0	0	0	0	0	0	0	0	0	0	0	0	0	0	0	0	0	0	0	0					
Corbidae	3	0	0	3	0	0	133	1345	0	152	13438	77	716	62	306	70	81	8	3	129	27	307	27	1	34	2	15	0	8	6	65	42	22	82					
Corbidae	0	0	0	0	0	0	0	0	0	0	0	0	0	0	0	0	0	0	0	0	0	0	0	0	0	0	0	0	0	0	0	0	0	0					
Gastrochaenidae	0	0	0	0	0	0	0	0	0	0	0	3	4	7	2	7	0	0	0	0	0	1	0	0	0	0	0	0	0	0	0	0	0	0	0				
Hiatellidae	0	0	0	0	0	0	0	0	0	0	0	0	0	0	0	0	0	0	0	0	0	1	0	0	0	0	0	0	0	0	0	0	0	0	0				
Hiatellidae	0	0	0	0	0	0	0	0	0	0	0	0	0	0	0	0	0	0	0	0	0	1	0	0	0	0	0	0	0	0	0	0	0	0	0				
Pholadidae	0	0	0	0	0	0	0	2	2	0	59	72	0	0	1	0	0	0	0	0	0	0	0	0	0	0	0	0	0	0	0	0	0	0	0				
Pholadidae	0	0	0	0	0	0	0	0	0	0	0	0	0	0	0	0	0	0	0	0	0	0	0	0	0	0	0	0	0	0	0	0	0	0	0	0			
Xylophagidae	0	0	0	0	0	0	0	0	0	0	0	0	0	0	0	0	0	0	0	0	0	0	0	0	0	0	0	0	0	0	0	0	0	0	0	0			
Terenidae	0	0	0	0	0	0	0	0	0	0	0	0	0	0	0	0	0	0	0	0	0	0	0	0	0	0	0	0	0	0	0	0	0	0	0	0			
Terenidae	0	0	0	0	0	0	0	0	0	0	0	0	0	0	0	0	0	0	0	0	0	0	0	0	0	0	0	0	0	0	0	0	0	0	0	0	0		
Thracidae	0	0	0	0	0	0	0	0	0	0	0	0	0	0	0	0	0	0	0	0	0	0	0	0	0	0	0	0	0	0	0	0	0	0	0	0	0		
Thracidae	0	0	0	0	0	0	0	0	0	0	0	0	0	0	0	0	0	0	0	0	0	0	0	0	0	0	0	0	0	0	0	0	0	0	0	0	0		
Pandoridae	0	0	0	0	0	0	0	0	0	0	0	0	0	0	0	1	0	0	0	0	0	0	0	0	0	0	0	0	0	0	0	0	0	0	0	0	0		
Pandoridae	0	0	0	0	0	0	0	0	0	0	0	0	0	0	0	0	0	0	0	0	0	0	0	0	0	0	0	0	0	0	0	0	0	0	0	0	0	0	
Clavagellidae	0	0	0	0	0	0	0	0	0	0	0	0	0	0	0	0	0	0	0	0	0	0	0	0	0	0	0	0	0	0	0	0	0	0	0	0	0	0	
Cuspidariidae	0	0	0	0	0	0	0	0	0	0	0	0	0	0	0	0	0	0	0	0	0	0	0	0	0	0	0	0	0	0	0	0	0	0	0	0	0	0	
Cuspidariidae	0	0	0	0	0	0	0	0	0	0	0	0	0	0	0	0	0	0	0	0	0	0	0	0	0	0	0	0	0	0	0	0	0	0	0	0	0	0	0
Verticordidae	0	0	0	0	0	0	0	0	0	0	0	0	0	0	0	0	0	0	0	0	0	0	0	0	0	0	0	0	0	0	0	0	0	0	0	0	0	0	
Dentalidae	6	7	9	24	0	1	27	0	0	23	0	0	14	2	6	40	6	1	0	15	5	1	14	3	4	0	0	0	0	0	0	0	0	0	0	0	0		
Dentalidae	0	0	0	0	0	0	0	0	0	0	0	0	0	0	0	0	0	0	0	0	0	0	0	0	0	0	0	0	0	0	0	0	0	0	0	0	0		
Siphonodentalidae	0	0	0	0	0	0	0	0	0	0	0	0	0	0	0	0	0	0	0	0	0	0	0	0	0	0	0	0	0	0	0	0	0	0	0	0	0		
Siphonodentalidae	0	0	0	0	0	0	0	0	0	0	0	0	0	0	0	0	0	0	0	0	0	0	0	0	0	0	0	0	0	0	0	0	0	0	0	0	0	0	
Gadlinidae	0	0	0	0	0	0	0	0	0	0	0	0	0	0	0	0	0	0	0	0	0	0	0	0	0	0	0	0	0	0	0	0	0	0	0	0	0	0	
Gadlinidae	0	0	0	0	0	0	0	0	0	0	0	0	0	0	0	0	0	0	0	0	0	0	0	0	0	0	0	0	0	0	0	0	0	0	0	0	0	0	0
Gadlinidae	0	0	0	0	0	0	0	0	0	0	0	0	0	0	0	0	0	0	0	0	0	0	0	0	0	0	0	0	0	0	0	0	0	0	0	0	0	0	0
Entalinidae	0	0	0	0	0	0	0	0	0	0	0	0	0	0	0	0	0	0	0	0	0	0	0	0	0	0	0	0	0	0	0	0	0	0	0	0	0	0	
Gadlinidae	0	0	0	0	0	0	0	0	0	0	0	0	0	0	0	0	0	0	0	0	0	0	0	0	0	0	0	0	0	0	0	0	0	0	0	0	0	0	0
Gadlinidae	0	0	0	0	0	0	0	0	0	0	0	0	0	0	0	0	0	0	0	0	0	0	0	0	0	0	0	0	0	0	0	0	0	0	0	0	0	0	0
TOTAL	48	470	601	391	1184	304	6219	1775	7068	20679	2335	4776	737	1279	573	428	70	312	175	63	932	251	800	832	244	493	143	318	421	2407	972	899	1026						



FAMILY	GENUS	A2C	A2D	A2E	A2F	A2G	A2H	A2I	A3A	A3B	A3C	A3D	A3E	A3F	A3G	A3H	A3I	A3L	A3M	A3N	A3O	A3P	A3Q	A3R	A3S	A4A	A4B	A4C	A4D	A4E	A5A	A5B	A6A	A6B	A6C	A6D			
Lepetellidae	<i>Lepetella</i>	0	0	0	0	0	0	0	0	0	0	0	0	0	0	0	0	0	0	0	0	0	0	0	0	0	0	0	0	0	0	0	0	0	0	0	0		
Fissurellidae	<i>Emarginula</i>	0	0	0	0	0	0	0	0	0	0	0	0	0	0	0	0	0	0	0	0	0	0	0	0	0	0	0	0	0	0	0	0	0	0	0	0		
Fissurellidae	<i>Diadara</i>	0	0	0	0	0	0	0	0	0	0	0	0	0	0	0	0	0	0	0	0	0	0	0	0	0	0	0	0	0	0	0	0	0	0	0	0	0	
Scissurellidae	<i>Anatoma</i>	0	0	0	0	0	0	0	0	0	0	0	0	0	0	0	0	0	0	0	0	0	0	0	0	0	0	0	0	0	0	0	0	0	0	0	0	0	
Turbinidae	<i>Contrainaea</i>	0	0	0	0	0	0	0	0	0	0	0	0	0	0	0	0	0	0	0	0	0	0	0	0	0	0	0	0	0	0	0	0	0	0	0	0	0	
Turbinidae	<i>Astrea</i>	0	0	0	0	0	0	0	0	0	0	0	0	0	0	0	0	0	0	0	0	0	0	0	0	0	0	0	0	0	0	0	0	0	0	0	0	0	
Turbinidae	<i>Tricola</i>	0	0	0	0	0	0	0	0	0	0	0	0	0	0	0	0	0	0	0	0	0	0	0	0	0	0	0	0	0	0	0	0	0	0	0	0	0	
Trochidae	<i>Danilia</i>	0	0	0	0	0	0	0	0	0	0	0	0	0	0	0	0	0	0	0	0	0	0	0	0	0	0	0	0	0	0	0	0	0	0	0	0	0	
Trochidae	<i>Callitropis</i>	0	0	0	0	0	0	0	0	0	0	0	0	0	0	0	0	0	0	0	0	0	0	0	0	0	0	0	0	0	0	0	0	0	0	0	0	0	
Trochidae	<i>Lischkeia</i>	0	0	0	0	0	0	0	0	0	0	0	0	0	0	0	0	0	0	0	0	0	0	0	0	0	0	0	0	0	0	0	0	0	0	0	0	0	
Trochidae	<i>Gibbula</i>	0	0	0	0	0	0	0	0	0	0	0	0	0	0	0	0	0	0	0	0	0	0	0	0	0	0	0	0	0	0	0	0	0	0	0	0	0	0
Trochidae	<i>Diloma</i>	0	0	0	0	0	0	0	0	0	0	0	0	0	0	0	0	0	0	0	0	0	0	0	0	0	0	0	0	0	0	0	0	0	0	0	0	0	0
Trochidae	<i>Jujubinus</i>	0	0	0	0	0	0	0	0	0	0	0	0	0	0	0	0	0	0	0	0	0	0	0	0	0	0	0	0	0	0	0	0	0	0	0	0	0	0
Trochidae	<i>Calliostoma</i>	2	10	0	0	20	20	18	1	2	0	0	0	0	0	0	0	0	0	0	0	0	0	0	0	0	0	0	0	0	0	0	0	0	0	0	0	0	
Trochidae	<i>Callumbonella</i>	0	0	0	0	0	0	0	0	0	0	0	0	0	0	0	0	0	0	0	0	0	0	0	0	0	0	0	0	0	0	0	0	0	0	0	0	0	
Trochidae	indet. 1	0	0	0	0	0	0	0	0	0	0	0	0	0	0	0	0	0	0	0	0	0	0	0	0	0	0	0	0	0	0	0	0	0	0	0	0	0	
Trochidae	indet. 2	0	0	0	0	0	0	0	0	0	0	0	0	0	0	0	0	0	0	0	0	0	0	0	0	0	0	0	0	0	0	0	0	0	0	0	0	0	
Sequeziidae	<i>Halystitina</i>	0	0	0	0	0	0	0	0	0	0	0	0	0	0	0	0	0	0	0	0	0	0	0	0	0	0	0	0	0	0	0	0	0	0	0	0	0	
Trochidae	<i>Solarella</i>	0	0	0	0	0	0	0	0	0	0	0	0	0	0	0	0	0	0	0	0	0	0	0	0	0	0	0	0	0	0	0	0	0	0	0	0	0	
Skeneidae	<i>Skenea</i>	0	0	0	0	0	0	0	0	0	0	0	0	0	0	0	0	0	0	0	0	0	0	0	0	0	0	0	0	0	0	0	0	0	0	0	0	0	
Skeneidae	<i>Putilla</i>	0	0	0	0	0	0	0	0	0	0	0	0	0	0	0	0	0	0	0	0	0	0	0	0	0	0	0	0	0	0	0	0	0	0	0	0	0	
Lissospiridae	<i>Maelleriopsis</i>	0	0	0	0	0	0	0	0	0	0	0	0	0	0	0	0	0	0	0	0	0	0	0	0	0	0	0	0	0	0	0	0	0	0	0	0	0	0
Neritidae	<i>Smarragalia</i>	0	0	0	0	0	0	0	0	0	0	0	0	0	0	0	0	0	0	0	0	0	0	0	0	0	0	0	0	0	0	0	0	0	0	0	0	0	0
Rissoidae	<i>Rissoa</i>	0	0	0	0	0	0	0	0	0	0	0	0	0	0	0	0	0	0	0	0	0	0	0	0	0	0	0	0	0	0	0	0	0	0	0	0	0	
Rissoidae	<i>Alvaria</i>	0	0	0	0	0	0	0	0	0	0	0	0	0	0	0	0	0	0	0	0	0	0	0	0	0	0	0	0	0	0	0	0	0	0	0	0	0	
Rissoidae	<i>Obtusella</i>	0	0	0	0	0	0	0	0	0	0	0	0	0	0	0	0	0	0	0	0	0	0	0	0	0	0	0	0	0	0	0	0	0	0	0	0	0	
Rissoidae	<i>Pusillina</i>	0	0	0	0	0	0	0	0	0	0	0	0	0	0	0	0	0	0	0	0	0	0	0	0	0	0	0	0	0	0	0	0	0	0	0	0	0	
Adeorbidae	<i>Circulus</i>	0	0	0	0	0	0	0	0	0	0	0	0	0	0	0	0	0	0	0	0	0	0	0	0	0	0	0	0	0	0	0	0	0	0	0	0	0	
Barleidae	<i>Barleia</i>	0	0	0	0	0	0	0	0	0	0	0	0	0	0	0	0	0	0	0	0	0	0	0	0	0	0	0	0	0	0	0	0	0	0	0	0	0	0
Barleidae	<i>Teinostoma</i>	0	0	0	0	0	0	0	0	0	0	0	0	0	0	0	0	0	0	0	0	0	0	0	0	0	0	0	0	0	0	0	0	0	0	0	0	0	0
Caecidae	<i>Caecum</i>	0	0	0	0	0	0	0	0	0	0	0	0	0	0	0	0	0	0	0	0	0	0	0	0	0	0	0	0	0	0	0	0	0	0	0	0	0	0
Paludineidae	<i>Paludinea</i>	0	0	0	0	0	0	0	0	0	0	0	0	0	0	0	0	0	0	0	0	0	0	0	0	0	0	0	0	0	0	0	0	0	0	0	0	0	0
Hydrobiidae	<i>Hydrobia</i>	0	0	0	0	0	0	0	0	0	0	0	0	0	0	0	0	0	0	0	0	0	0	0	0	0	0	0	0	0	0	0	0	0	0	0	0	0	0
Micromelaniidae	<i>Nematurella</i>	0	0	0	0	0	0	0	0	0	0	0	0	0	0	0	0	0	0	0	0	0	0	0	0	0	0	0	0	0	0	0	0	0	0	0	0	0	0
Iravadiidae	<i>Hyalia</i>	0	0	0	0	0	0	0	0	0	0	0	0	0	0	0	0	0	0	0	0	0	0	0	0	0	0	0	0	0	0	0	0	0	0	0	0	0	0
Iravadiidae	<i>Rhombostoma</i>	0	0	0	0	0	0	0	0	0	0	0	0	0	0	0	0	0	0	0	0	0	0	0	0	0	0	0	0	0	0	0	0	0	0	0	0	0	0
Clitocerotidae	<i>Pseudovina</i>	0	0	0	0	0	0	0	0	0	0	0	0	0	0	0	0	0	0	0	0	0	0	0	0	0	0	0	0	0	0	0	0	0	0	0	0	0	0
Tornidae	<i>Tornus</i>	0	0	0	0	0	0	0	0	0	0	0	0	0	0	0	0	0	0	0	0	0	0	0	0	0	0	0	0	0	0	0	0	0	0	0	0	0	
Cerithiidae	<i>Cerithium</i>	0	0	0	0	0	0	0	0	0	0	0	0	0	0	0	0	0	0	0	0	0	0	0	0	0	0	0	0	0	0	0	0	0	0	0	0	0	0
Cerithiidae	<i>Bitium</i>	0	0	0	0	0	0	0	0	0	0	0	0	0	0	0	0	0	0	0	0	0	0	0	0	0	0	0	0	0	0	0	0	0	0	0	0	0	0
Potamidae	<i>Potamides</i>	0	0	0	0	0	0	0	0	0	0	0	0	0	0	0	0	0	0	0	0	0	0	0	0	0	0	0	0	0	0	0	0	0	0	0	0	0	0
Turritellidae	<i>Turritella</i>	4	60	10	0	0	0	0	0																														









APPENDIX

	A2C	A2D	A2E	A2F	A2G	A2H	A2I	A3A	A3B	A3C	A3D	A3E	A3F	A3G	A3H	A3I	A3L	A3M	A3N	A3O	A3P	A3Q	A3R	A3S	A4A	A4B	A4C	A4D	A4E	A5A	A5B	A6A	A6B	A6C	A6D				
Veneridae	0	0	0	0	0	0	0	0	0	0	0	0	0	0	0	0	0	0	0	0	0	0	0	0	0	0	0	0	0	0	0	0	0	0	0	0	0		
Veneridae	0	0	0	0	0	0	0	0	0	0	0	0	0	0	0	0	0	0	0	0	0	0	0	0	0	0	0	0	0	0	0	0	0	0	0	0	0	0	
Veneridae	0	0	0	0	0	0	0	0	0	0	0	0	0	0	0	0	0	0	0	0	0	0	0	0	0	0	0	0	0	0	0	0	0	0	0	0	0	0	
Veneridae	0	0	0	0	0	0	0	0	0	0	0	0	0	0	0	0	0	0	0	0	0	0	0	0	0	0	0	0	0	0	0	0	0	0	0	0	0	0	0
Myidae	0	0	0	0	0	0	0	0	0	0	0	0	0	0	0	0	0	0	0	0	0	0	0	0	0	0	0	0	0	0	0	0	0	0	0	0	0	0	0
Corbidae	76	180	280	140	138	75	45	3	28	29	11	15	3	0	3	1	3	0	0	0	6	17	0	43	136	4	5	40	17	2	300	556	0	0	0	34	0		
Lentidium	0	0	0	0	0	0	0	0	0	0	0	0	0	0	0	0	0	0	0	0	0	0	0	0	0	0	0	0	0	203	71	0	0	0	0	0	0		
Gastrochaenidae	0	0	0	0	0	0	0	0	0	0	0	0	0	0	0	0	0	0	0	0	0	0	0	0	0	0	0	0	0	0	0	0	0	0	0	0	0	0	0
Hiattellidae	0	5	2	10	8	8	18	2	0	2	4	2	3	4	11	0	0	0	2	1	0	0	2	12	3	1	3	2	2	0	6	0	0	0	0	0	0		
Pholadidae	0	0	0	0	0	0	0	0	0	0	0	0	0	0	0	0	0	0	0	0	0	0	0	0	0	0	0	0	0	0	0	0	0	0	0	0	0	0	0
Pholadidae	0	0	0	0	0	0	0	0	0	0	0	0	0	0	0	0	0	0	0	0	0	0	0	0	0	0	0	0	0	0	0	0	0	0	0	0	0	0	0
Xylophagidae	0	0	0	0	0	0	0	0	0	0	0	0	0	0	0	0	0	0	0	0	0	0	0	0	0	0	0	0	0	0	0	0	0	0	0	0	0	0	0
Terenidae	0	0	0	0	0	0	0	0	0	0	0	0	0	0	0	0	0	0	0	0	0	0	0	0	0	0	0	0	0	0	0	0	0	0	0	0	0	0	0
Thracia	0	0	0	0	0	0	0	0	0	0	0	0	0	0	0	0	0	0	0	0	0	0	0	0	0	0	0	0	0	0	0	0	0	0	0	0	0	0	0
Pandoridae	0	0	0	0	0	0	0	0	0	0	0	0	0	0	0	0	0	0	0	0	0	0	0	0	0	0	0	0	0	0	0	0	0	0	0	0	0	0	0
Clavagellidae	0	0	0	0	0	0	0	0	0	1	0	0	0	0	0	0	0	0	0	0	0	0	0	0	0	0	0	0	0	0	0	0	0	0	0	0	0	0	0
Cuspidariidae	0	0	0	0	0	0	0	0	0	0	1	0	0	0	0	0	0	0	0	0	0	0	0	0	0	0	0	0	0	0	0	0	0	0	0	0	0	0	0
Cuspidariidae	0	5	0	0	0	0	0	0	0	0	0	0	0	0	0	0	0	0	0	0	0	0	0	0	0	0	0	0	0	0	0	0	0	0	0	0	0	0	0
Verticordiidae	0	0	0	0	0	0	0	0	0	0	0	0	0	0	0	0	0	0	0	0	0	0	0	0	0	0	0	0	0	0	0	0	0	0	0	0	0	0	0
Dentalidae	0	0	4	0	8	0	0	0	0	0	3	0	0	0	0	0	0	0	0	0	0	0	0	0	0	0	0	0	0	0	0	0	0	0	0	0	0	0	0
Siphonodentaliidae	0	0	0	0	0	0	0	0	0	0	0	0	0	0	0	0	0	0	0	0	0	0	0	0	0	0	0	0	0	0	0	0	0	0	0	0	0	0	0
Gadilinae	0	0	0	0	0	0	0	0	0	0	0	2	0	0	0	0	0	0	0	0	0	0	0	0	0	0	0	0	0	0	0	0	0	0	0	0	0	0	0
Gadilinae	0	0	0	0	0	0	0	0	0	0	0	0	0	0	0	0	0	0	0	0	0	0	0	0	0	0	0	0	0	0	0	0	0	0	0	0	0	0	0
Gadilinae	0	0	0	0	0	0	0	0	0	0	0	0	0	0	0	0	0	0	0	0	0	0	0	0	0	0	0	0	0	0	0	0	0	0	0	0	0	0	0
Entaliniidae	0	0	0	0	0	0	0	0	0	0	0	0	0	0	0	0	0	0	0	0	0	0	0	0	0	0	0	0	0	0	0	0	0	0	0	0	0	0	0
Gadilidae	0	0	0	0	0	0	0	0	0	0	0	0	0	0	0	0	0	0	0	0	0	0	0	0	0	0	0	0	0	0	0	0	0	0	0	0	0	0	0

TOTAL	846	836	686	757	991	813	564	30	104	267	151	291	127	234	261	103	288	857	781	636	174	60	454	605	38	25	281	234	299	43434	64702	523	450	590	261
-------	-----	-----	-----	-----	-----	-----	-----	----	-----	-----	-----	-----	-----	-----	-----	-----	-----	-----	-----	-----	-----	----	-----	-----	----	----	-----	-----	-----	-------	-------	-----	-----	-----	-----















## APPENDIX 3.

External information on mollusc samples analyzed in the study and relative sources.

SAMPLE NAME	n	AGE	ENVIRONMENT	LOCALITY	LITOLGY	SAMPLE NAME (Auct.)	REFERENCE
OP8	56	Piacentian	Outer shelf	Orciano Pisano	Siltstone	OP8	Chapter 3, Danise et al. 2010 (1)
OP9	61	Piacentian	Outer shelf	Orciano Pisano	Siltstone	OP9	Chapter 3, Danise et al. 2010 (1)
OP10	92	Piacentian	Outer shelf	Orciano Pisano	Siltstone	OP10	Chapter 3, Danise et al. 2010 (1)
OP11	61	Piacentian	Outer shelf	Orciano Pisano	Siltstone	OP11	Chapter 3, Danise et al. 2010 (1)
OP12	282	Piacentian	Outer shelf	Orciano Pisano	Silty fine-grained sandstone	OP12	Chapter 3, Danise et al. 2010 (1)
OP13	172	Piacentian	Outer shelf	Orciano Pisano	Silty fine-grained sandstone	OP13	Chapter 3, Danise et al. 2010 (1)
OP14	188	Piacentian	Outer shelf	Orciano Pisano	Silty fine-grained sandstone	OP14	Chapter 3, Danise et al. 2010 (1)
OP15	54	Piacentian	Outer shelf	Orciano Pisano	Silty fine-grained sandstone	OP15	Chapter 3, Danise et al. 2010 (1)
OP16	75	Piacentian	Outer shelf	Orciano Pisano	Silty fine-grained sandstone	OP16	Chapter 3, Danise et al. 2010 (1)
OP17	140	Piacentian	Outer shelf	Orciano Pisano	Silty fine-grained sandstone	OP17	Chapter 3, Danise et al. 2010 (1)
OP1	257	Piacentian	Outer shelf	Orciano Pisano	Silty fine-grained sandstone	OP1	Chapter 3, Danise et al. 2010 (1)
OP2	228	Piacentian	Outer shelf	Orciano Pisano	Silty fine-grained sandstone	OP2	Chapter 3, Danise et al. 2010 (1)
OP3	241	Piacentian	Outer shelf	Orciano Pisano	Silty fine-grained sandstone	OP3	Chapter 3, Danise et al. 2010 (1)
OP4	116	Piacentian	Outer shelf	Orciano Pisano	Silty fine-grained sandstone	OP4	Chapter 3, Danise et al. 2010 (1)
OP5	150	Piacentian	Outer shelf	Orciano Pisano	Silty fine-grained sandstone	OP5	Chapter 3, Danise et al. 2010 (1)
OP6	204	Piacentian	Outer shelf	Orciano Pisano	Silty fine-grained sandstone	OP6	Chapter 3, Danise et al. 2010 (1)
OP7	72	Piacentian	Outer shelf	Orciano Pisano	Silty fine-grained sandstone	OP7	Chapter 3, Danise et al. 2010 (1)
GORG2	75	Piacentian	Inner shelf	Gorgognano	Mudstone	GORG2	This work
SLR1	251	Piacentian	Inner shelf	San Lorenzo In Collina	Silty fine-grained sandstone	SLR1	This work
SLR2	141	Piacentian	Inner shelf	San Lorenzo In Collina	Silty fine-grained sandstone	SLR2	This work
SLR3	198	Piacentian	Inner shelf	San Lorenzo In Collina	Silty fine-grained sandstone	SLR3	This work
SV3-1	102	Zanclean	Inner shelf	Castellarano	Silty fine-grained sandstone	SV3-1	This work
SV3-2	54	Zanclean	Inner shelf	Castellarano	Silty fine-grained sandstone	SV3-2	This work
SV4	276	Zanclean	Inner shelf	Castellarano	Silty fine-grained sandstone	SV4	This work
CAST1	238	Piacentian	Inner shelf	Castelfiorentino	Mudstone	CAST1	This work
CAST2A	54	Piacentian	Inner shelf	Castelfiorentino	Mudstone	CAST2A	This work
CAST2B	85	Piacentian	Inner shelf	Castelfiorentino	Mudstone	CAST2B	This work
CAST3	76	Piacentian	Inner shelf	Castelfiorentino	Mudstone	CAST3	This work
MONT1	251	Zanclean	Inner shelf	Montalcino	Silty sandstone	MONT1	This work
MONT2	226	Zanclean	Inner shelf	Montalcino	Silty sandstone	MONT2	This work

SAMPLE NAME	n	AGE	ENVIRONMENT	LOCALITY	LITOLGY	SAMPLE NAME (Auct.)	REFERENCE
ALL1	35	Zanclean	Inner shelf	Allerona	Mudstone	ALL1	This work
ALL2	80	Zanclean	Inner shelf	Allerona	Mudstone	ALL2	This work
ALL3	48	Zanclean	Inner shelf	Allerona	Mudstone	ALL3	This work
T1A	470	Piacenzian	Shoreface	Pastine	Sandstone	PST0	Dominici unpublished
T1B	601	Piacenzian	Shoreface	Pastine	Sandstone	PST1	Dominici unpublished
T1C	391	Piacenzian	Shoreface	Pastine	Sandstone	PST2	Dominici unpublished
T1D	1184	Piacenzian	Shoreface	Pastine	Sandstone	PST3	Dominici unpublished
T1E	304	Piacenzian	Shoreface	La Foce	Sandstone	FC1bis	Dominici unpublished
T2A	6219	Piacenzian	Shoreface	San Lorenzo	Coarse-grained sandstone	CSL0	Dominici 1994 (2)
T2B	1775	Piacenzian	Intertidal	San Lorenzo	Mudstone	CSL1	Dominici 1994 (2)
T3A	7068	Piacenzian	Inner shelf	Catena	Silty sandstone	C1	Benvenuti and Dominici 1992 (3)
T3B	20679	Piacenzian	Intertidal	Catena	Silty fine-grained sandstone	C3	Benvenuti and Dominici 1992 (3)
T3C	2335	Piacenzian	Intertidal	Catena	Siltstone	C4	Benvenuti and Dominici 1992 (3)
T3D	4776	Piacenzian	Shoreface	Catena	Sandstone	C6	Benvenuti and Dominici 1992 (3)
T5A	737	Piacenzian	Inner shelf	Cappuccini	Muddy sandstone	CP6	Dominici unpublished Master thesis
T5B	1279	Piacenzian	Inner shelf	Cappuccini	Muddy sandstone	CP4III	Dominici unpublished Master thesis
T5C	573	Piacenzian	Inner shelf	Cappuccini	Sandstone	TB	Dominici unpublished Master thesis
T5D	428	Piacenzian	Inner shelf	Cappuccini	Sandstone	CP2a	Dominici unpublished Master thesis
T5E	70	Piacenzian	Outersheif	Cappuccini	Mudstone	CP2	Dominici unpublished Master thesis
T6	312	Piacenzian	Inner shelf	Castelfiorentino	Mudstone	SLP33	Dominici unpublished
T7A	175	Piacenzian	Inner shelf	LaFoce	Muddy sandstone	FC4	Dominici unpublished
T7B	63	Piacenzian	Inner shelf	LaFoce	Muddy sandstone	FC3	Dominici unpublished
T8A	932	Piacenzian	Inner shelf	Ullignano	Muddy sandstone	ULI 2	Dominici unpublished
T8B	251	Piacenzian	Inner shelf	Ullignano	Muddy sandstone	YLL	Dominici unpublished
T8C	800	Piacenzian	Inner shelf	Ullignano	Muddy sandstone	SB	Dominici unpublished
A1A	832	Piacenzian	Bathyal	Campore	Muddy siltstone	5,6,8,10	Ceregato et al. 2007 (4)
A1B	244	Piacenzian	Bathyal	Campore	Muddy siltstone	3,12	Ceregato et al. 2007 (4)
A1C	493	Piacenzian	Bathyal	Campore	Muddy siltstone	11	Ceregato et al. 2007 (4)
A1D	143	Piacenzian	Bathyal	Campore	Muddy siltstone	7	Ceregato et al. 2007 (4)
A1E	318	Piacenzian	Bathyal	Campore	Muddy siltstone	1	Ceregato et al. 2007 (4)
A1F	421	Piacenzian	Bathyal	Campore	Muddy siltstone	2	Ceregato et al. 2007 (4)
A1G	2407	Piacenzian	Bathyal	Campore	Muddy siltstone	10-12	Ceregato et al. 2007 (4)
A2A	972	Piacenzian	Inner shelf	Monte Falcone	Sandy siltstone	MF1	Monegatti et al. 1997 (5)
A2Abis	899	Piacenzian	Inner shelf	Monte Falcone	Sandy siltstone	MF2	Monegatti et al. 1997 (5)

SAMPLE NAME	n	AGE	ENVIRONMENT	LOCALITY	LITOLGY	SAMPLE NAME (Auct.)	REFERENCE
A2B	1026	Piacentian	Inner shelf	Monte Falcone	Sandy siltstone	MF3	Monegatti et al. 1997 (5)
A2C	846	Piacentian	Inner shelf	Monte Falcone	Sandy siltstone	MF4	Monegatti et al. 1997 (5)
A2D	836	Gelasian	Inner shelf	Monte Falcone	Sandy siltstone	MF5	Monegatti et al. 1997 (5)
A2E	686	Gelasian	Inner shelf	Monte Falcone	Sandy siltstone	MF6	Monegatti et al. 1997 (5)
A2F	757	Gelasian	Inner shelf	Monte Falcone	Sandy siltstone	MF7	Monegatti et al. 1997 (5)
A2G	991	Gelasian	Inner shelf	Monte Falcone	Sandy siltstone	MF8	Monegatti et al. 1997 (5)
A2H	813	Gelasian	Inner shelf	Arda	Silty sandstone	RR1	Monegatti et al. 1997 (5)
A2I	564	Gelasian	Inner shelf	Arda	sandstone	RR2	Monegatti et al. 1997 (5)
A3A	30	Gelasian	Inner shelf	Stirone	Mudstone	N1	Dominici 2001 (6)
A3B	104	Gelasian	Inner shelf	Stirone	Mudstone	N0	Dominici 2001 (6)
A3C	267	Gelasian	Inner shelf	Stirone	Mudstone	N1bis	Dominici 2001 (6)
A3D	151	Gelasian	Inner shelf	Stirone	Mudstone	N0.1	Dominici 2001 (6)
A3E	291	Gelasian	Inner shelf	Stirone	Mudstone	N1.2	Dominici 2001 (6)
A3F	127	Gelasian	Inner shelf	Stirone	Mudstone	N2.1	Dominici 2001 (6)
A3G	234	Gelasian	Inner shelf	Stirone	Fine-grained sandstone	N3	Dominici 2001 (6)
A3H	261	Gelasian	Inner shelf	Stirone	Fine-grained sandstone	N2bis	Dominici 2001 (6)
A3I	103	Gelasian	Inner shelf	Stirone	Fine-grained sandstone	N3	Dominici 2001 (6)
A3L	288	Gelasian	Inner shelf	Stirone	Carbonates	N4	Dominici 2001 (6)
A3M	857	Gelasian	Inner shelf	Stirone	Carbonates	N5	Dominici 2001 (6)
A3N	781	Gelasian	Inner shelf	Stirone	Carbonates	N6	Dominici 2001 (6)
A3O	636	Gelasian	Inner shelf	Stirone	Carbonates	N7	Dominici 2001 (6)
A3P	174	Gelasian	Inner shelf	Stirone	Carbonates	N8	Dominici 2001 (6)
A3Q	60	Gelasian	Inner shelf	Stirone	Mudstone	N9	Dominici 2001 (6)
A3R	454	Gelasian	Inner shelf	Arda	Sandstone	AO	Dominici 2001 (6)
A3S	605	Gelasian	Inner shelf	Arda	Sandstone	A1	Dominici 2001 (6)
A4A	38	Zanclean	Outer shelf	Zinola	Very fine-grained sandy mudstone	SV4	Bernasconi 1989 (7)
A4B	25	Zanclean	Outer shelf	Zinola	Very fine-grained sandy mudstone	SV3b	Bernasconi 1989 (7)
A4C	281	Zanclean	Outer shelf	Zinola	Very fine-grained sandy mudstone	SV5	Bernasconi 1989 (7)
A4D	234	Zanclean	Outer shelf	Zinola	Very fine-grained sandy mudstone	SV4b	Bernasconi 1989 (7)
A4E	299	Zanclean	Outer shelf	Zinola	Very fine-grained sandy mudstone	SV5b	Bernasconi 1989 (7)
A5A	43434	Piacentian	Shoreface	S. Anna	Fine grained sandstone	A	Ferrero and Merlino 1998 (8)
A5B	64702	Piacentian	Shoreface	S. Anna	Fine grained sandstone	B	Ferrero and Merlino 1998 (8)
A6A	523	Piacentian	Outer shelf	Breolungi	Muddy siltstone	BP1	Pavia et al. 1989 (9)
A6B	450	Piacentian	Outer shelf	Breolungi	Muddy siltstone	BP2	Pavia et al. 1989 (9)
A6C	590	Piacentian	Outer shelf	Breolungi	Muddy siltstone	BP3	Pavia et al. 1989 (9)

SAMPLE NAME	n	AGE	ENVIRONMENT	LOCALITY	LITOLGY	SAMPLE NAME (Auct.)	REFERENCE
A6D	261	Piacentian	Outer shelf	Breolungi	Muddy siltstone	BP4	Pavia et al. 1989 (9)
A6E	104	Piacentian	Outer shelf	Breolungi	Muddy siltstone	BP5	Pavia et al. 1989 (9)
A6F	194	Piacentian	Outer shelf	Breolungi	Muddy siltstone	BP6	Pavia et al. 1989 (9)
A7	58268	Piacentian	Shoreface	Monteu Roero	Sandstone	MR3	Pavia 1975 (10)
A8A	10256	Piacentian	Inner shelf	Volpedo	Silty sandstone	VCB1	Benigni and Corselli 1982 (11)
A8B	14466	Piacentian	Inner shelf	Volpedo	Sandy siltstone	VCB2	Benigni and Corselli 1982 (11)
A8C	5191	Piacentian	Inner shelf	Volpedo	Silty sandstone	VCB4	Benigni and Corselli 1982 (11)
A8D	6900	Piacentian	Inner shelf	Volpedo	Silty sandstone	VCB6	Benigni and Corselli 1982 (11)
A8E	12078	Piacentian	Inner shelf	Volpedo	Silty sandstone	VCB8	Benigni and Corselli 1982 (11)
S1A	786	Zandclean	Bathyal	Nocella	Sandy-muddy siltstone	1	Greco and Buccheri 1988 (12)
S1B	5305	Zandclean	Bathyal	Nocella	Muddy Sandstone	2	Greco and Buccheri 1988 (12)
S1C	398	Zandclean	Outer shelf	Nocella	Silty sandstone	3	Greco and Buccheri 1988 (12)
S1D	88	Zandclean	Outer shelf	Nocella	Silty sandstone	4	Greco and Buccheri 1988 (12)
S2A	949	Gelasian	Bathyal	Peschiera	Muddy siltstone	Ca2	D'Alessandro and De Marco 1993 (13)
S2B	908	Gelasian	Bathyal	Peschiera	Muddy siltstone	Cb2	D'Alessandro and De Marco 1993 (13)
S2C	852	Gelasian	Bathyal	Peschiera	Muddy siltstone	Cc2	D'Alessandro and De Marco 1993 (13)
S2D	992	Gelasian	Bathyal	Peschiera	Sandy siltstone	Ca3	D'Alessandro and De Marco 1993 (13)
S2E	974	Gelasian	Bathyal	Peschiera	Sandy siltstone	Cb3	D'Alessandro and De Marco 1993 (13)
S2F	880	Gelasian	Bathyal	Peschiera	Silty sandstone	Cc3	D'Alessandro and De Marco 1993 (13)
S2G	889	Gelasian	Bathyal	Peschiera	Muddy siltstone	Ca4	D'Alessandro and De Marco 1993 (13)
S2H	948	Gelasian	Bathyal	Peschiera	Muddy siltstone	Cb4	D'Alessandro and De Marco 1993 (13)
S2I	937	Gelasian	Bathyal	Peschiera	Silty sandstone	Cc4	D'Alessandro and De Marco 1993 (13)
S2L	843	Gelasian	Bathyal	Granatella	Muddy siltstone	MT3	D'Alessandro and De Marco 1993 (13)
S2M	656	Gelasian	Bathyal	Granatella	Muddy siltstone	MT4	D'Alessandro and De Marco 1993 (13)
S2N	908	Gelasian	Bathyal	Granatella	Muddy siltstone	MT7	D'Alessandro and De Marco 1993 (13)
S2O	866	Gelasian	Bathyal	Granatella	Muddy siltstone	MT8	D'Alessandro and De Marco 1993 (13)
S2P	850	Gelasian	Bathyal	Granatella	Muddy siltstone	MT9	D'Alessandro and De Marco 1993 (13)
S2Q	849	Gelasian	Bathyal	Granatella	Muddy siltstone	MT10	D'Alessandro and De Marco 1993 (13)



## REFERENCES

- (1) Danise S., Dominici S. and Betocchi U. 2010. Mollusk species at a Pliocene shelf whale fall (Orciano Pisano, Tuscany). *Palaios* 25, 449–456.
- (2) Dominici S. 1994. Regressive–transgressive cycles from the Pliocene of the San Miniato area (Tuscany, Italy): paleoecology and sequence stratigraphy. *Bollettino della Società Paleontologica Italiana*, Supplemento 2, 117–126.
- (3) Benvenuti M. and Dominici S. 1992. Facies analysis, paleoecology and sequence stratigraphy in a Pliocene siliciclastic succession, San Miniato (Pisa, Italy). *Bollettino della Società Paleontologica Italiana* 31, 241–259.
- (4) Ceregato A., Raffi S. and Scarponi D. 2007. The circalittoral/bathyal paleocommunities in the Middle Pliocene of Northern Italy: The case of the *Korabkovia oblonga*–*Jupiteria concava* paleocommunity type. *Geobios* 40, 555–572.
- (5) Monegatti P., Raffi S., and Raineri G., 1997, The Monte Falcone-Rio Riorzo section: biostratigraphic and ecobiostratigraphic remarks. *Bollettino della Società paleontologica Italiana* 36.
- (6) Dominici S. 2001. Taphonomy and Paleoecology of Shallow Marine Macrofossil Assemblages in a Collisional Setting (Late Pliocene–Early Pleistocene, Western Emilia, Italy). *Palaios* 16, 336–353.
- (7) Bernasconi M.P., 1989, *Studi paleoecologici sul Pliocene ligure*. V. Il Pliocene di Savona. *Bollettino del Museo regionale di Scienze Naturali*, Torino, 7, 49-116.
- (9) Pavia G., Chiambretto L. and Oreggia G. 1989. Paleocomunità a molluschi nel Pliocene Inferiore di Breolungi (Mondovì, Italia). *Atti Quinto Simposio di Ecologia e Paleoecologia delle Comunità Bentoniche*, Taormina, 521–569.
- (10) Pavia G. 1975. I Molluschi del Pliocene inferiore in Monte Roero (Alba, Italia NW). *Bollettino della Società Paleontologica Italiana* 14, 99–175.
- (11) Benigni C. and Corselli C. 1982. Paleocomunità a molluschi bentonici del Pliocene di Volpedo (AL): *Rivista italiana di Paleontologia e Stratigrafia* 87, 637–702.
- (12) Greco A. and Buccheri G. 1988. Considerazioni paleoecologiche e stratigrafiche sulla malacofauna del Pliocene inferiore della foce del Nocella (Partinico, Palermo). *Atti Quarto Simposio di Ecologia e Paleoecologia delle Comunità Bentoniche*, Sorrento, 397–427.
- (13) D'Alessandro A. and De Marco A. 1993. Bionomic analysis of two Upper Pliocene communities from southern Italy. *Beringeria* 8, 109-137.

Appendix 4. DCA q-mode diagram in which the name of each samples is reported.

